STEAM AIR EJECTOR PERFORMANCE AND ITS DIMENSIONAL PARAMETERS

By

JABER MOHAMAD ADNAN DANDACHI

BSc (Mosul), MSc (Loughborough)

A DOCTORAL THESIS

Submitted in Partial Fulfilment of the Requirements

for the Award of

DOCTOR OF PHILOSOPHY

of the

LOUGHBOROUGH UNIVERSITY OF TECHNOLOGY

October 1990

Supervisor : Dr. P. Rice

Department of Chemical Engineering

Loughborough University of Technology

بِسْمِ اللَّهِ الرَّحْمَٰنِ الرَّحِيمِ

In the name of Allah,
Most Gracious, Most Merciful.

وَقُل رَّبِّ زِدْنِي عِلْمًا

"O my Lord! Advance me
in Knowledge".

To my mum, dad, wife, and Iman

ABSTRACT

This thesis reports a two part investigation of single- and two-stage ejector systems in which the primary fluid is steam and the secondary fluid is air.

The first part is an experimental investigation. The vacuum created by the ejector is strongly affected by the distance between the steam nozzle outlet and the diffuser throat section. The relation between this distance, which is called in this thesis "the nozzle optimum distance (L_{op})", and the geometrical and operating parameters of the nozzle and the diffuser were investigated and forms the object of this part of the thesis.

The second part is a theoretical approach. The exit Mach number for the nozzle was found by using the one-dimensional gas dynamic equations together with the first law of thermodynamics. Also a two-dimensional approach using the Method of Characteristics was used to find the exit Mach number and the characteristic net of the flow from the throat to the outlet of the nozzle. Two computer programmes were written on the basis of these two different theoretical techniques and the comparison between the results for the exit Mach number found to be 95% in agreement over the pressure range of the experimental work. A computer programme was also written using the Method of Characteristics to find the shape i.e. the characteristic net and the constant density lines within the flow of the steam jet leaving the nozzle and entering the diffuser. It is believed that the jet diameter at the point where it meets the diffuser wall, which is called in this work "the optimum jet diameter (D_{op})", is strongly related to the nozzle optimum distance (L_{op}). When the characteristic net for the jet is drawn, its point of interception with the diffuser wall can be found and then (D_{op}) can be measured. This diameter (D_{op}) was then related to the ejector dimensional parameters and the ejector operating conditions; an equation was found to predict the optimum jet diameter from this equation $(D_{op})_e$. Then the predicted optimum nozzles distance $(L_{op})_e$ was determined by using this computer program where the characteristic net meets the diffuser wall at the calculated optimum jet diameter $(D_{op})_e$. Finally, the experimentally determined value of the nozzle optimum distance (L_{op}) was compared to the theoretically predicted value, and the average error was found to be 1.23%.

DECLARATION

This is to certify that I am responsible for the work submitted in this thesis and the original work is my own except where due reference to previous work has been noted. I also certify that neither the thesis nor the original work contained therein has been submitted to this or any other institution for a higher degree.

JABER M. A. DANDACHI

ACKNOWLEDGEMENTS

The author is particularly indebted to Dr Peter Rice for his invaluable, constructive and unlimited advice, criticism and discussions which made possible to complete this work.

The author would like to acknowledge Dr A. Khan and Dr S. Mahmoud for their help and moral support through this work, to Mr H. Peters the laboratory supervisor for his help. Sincere thanks to the staff of the computer centre reception for their help in the computer work.

The author also would like to acknowledge Hariri Foundation for the financial support of this work.

The author would further like to thank the members of his family for their moral help and encouragement throughout this work and especially his wife who suffered the hard days of this work with patience and with no complaints.

Finally, I take this opportunity to thank all my friends for the pleasant time I have had with them at Loughborough.

LIST OF CONTENTS

LIST OF FIGURES

CHAPTER EIGHT

LIST OF TABLES

LIST OF SYMBOLS

A	Area
a	Velocity of air
bI	Average slope of physical characteristics curve I
bII	Average slope of physical characteristics curve II
C1,....,C7	Combination number
c_p	Specific heat at constant pressure
c_v	Specific heat at constant volume
D	Diffuser diameter
	Jet diameter
d	Nozzle diameter
D1,....,D5	Diffuser number
E	Degree of expansion
E1,....,E20	Ejector number
G1,....,G3	Pressure gauge number
h	Enthalpy
I	Right running characteristic wave
II	Left running characteristic wave
K	Degree of compression
L	Distance between the nozzle outlet and the start of the diffuser throat
	Diffuser length
L_w	Distance between the nozzle outlet and the inlet of the diffuser
l (small L)	Nozzle length
M	Mach number
m	Mass flowrate
N1,....,N8	Nozzle number
n	Pressure ratio (P_e/P_s)
nw	The number of waves in the Prandtl-Meyer
P	Pressure
R	Gas constant
S	Entropy
T	Temperature
t	Time
U	Velocity
	Coefficient of injection

u	Velocity component in the x-direction
V1,....V5	Valve number
v	Velocity component in the y-direction
w	Velocity component in the z-direction
X	Relative length of the jet
x,y	Cartesian coordinate in the x- and y-axes

Greek Symbols

α	Local Mach angle
β	Total convergence angle of the diffuser
γ	Total divergence angle of the diffuser
	Ratio of specific heats (c_p/c_v)
δ	Angle of deflecion of the stream line after meeting the diffuser wall
ϕ	Angle between the stream line and the shock wave after meeting the diffuser wall
θ	Angle of the velocity vector with the u-axis
ρ	Density
ν	Prandtl-Meyer angle
ζ	Total divergence angle of the nozzle

Suffixes

a	Air
at	Atmospheric
c	Critical
	Divergence part of the nozzle
	Convergence part of the diffuser
d	Discharge
	Divergence part of the diffuser
e	Exit nozzle section
g	Saturated vapour
i	Inlet diffuser section
m	Motive
max	Maximum
o	Diffuser outlet section
	Nozzle outlet section
	Stagnation
	Nozzle corner
op	Optimum condition

p	Primary
s	Suction
	Secondary
	Isentropic state
t	Nozzle throat section
th	Diffuser throat section
T	Overall length
w	From the nozzle outlet to the first point where the jet meets the diffuser wall
1 (one)	Upstream of the nozzle throat

o	
1	
2	
3	
.	
.	
.	
nw	Particular mesh points in the characteristics net
(nw+1)	
(nw+2)	
.	
.	
.	
(2nw+1)	
2(nw+1)	

CHAPTER ONE

INTRODUCTION

1.1. Applications of Steam Ejectors :

In general, ejectors, exhausters or jet pumps, as they are called sometimes, are widely used in many industrial fields. Steam ejectors are employed in the power generation, chemical processing, nuclear industries, exhausting air from condensers, vacuum evaporation, distillation, and crystallization, refrigeration, drying, air conditioning, and for pumping large volumes of vapour and gas at low pressure. The main advantage of steam ejectors is that they have no pistons, valves, rotors, or any other moving parts, no lubrication or oil problems, nor extremely close tolerances and hence require little maintenance.They are, mechanically, the simplest of all of the present-day type of vacuum pumps. Figure (1.1.) illustrates a steam ejector.

Compared with mechanical pumps, steam ejectors have very low efficiencies when used in normal pumping applications but when a source of waste or low grade steam is available, a steam ejector may be cheaper to operate than a mechanical pump. Steam ejectors have many applications, such as heating, humidifying and pumping toxic and solids-bearing fluids, where a mechanical pump may be unsuitable.

1.2. Principle of Operation :

A single stage steam ejector depends for its pumping action on an expanding motive nozzle discharging a supersonic velocity jet at low pressure across a converging chamber, which is connected to the equipment to be evacuated, and so bringing the suction fluid into intimate contact with the high-velocity motive steam. The suction fluid is then entrained by the steam and mixed with it in a parallel section. Then passing through a diffuser the velocity is reduced and discharge pressure recovered.

1.2.1. Multi-Stage Steam Ejectors :

A single stage ejector has an operating limit to the attainable compression ratio which is usually about 8:1. The compression ratio is the ratio of the discharge pressure to the suction pressure (P_d/P_s). So, attempting to produce a vacuum of more than about 100 torr, means that the ejector is using steam uneconomically. Thus, to have progressively higher vacua more stages are added as indicated in Figure (1.2.) (after Frumerman), a satisfactory number being chosen to improve the work stability and to use the steam more economically. In other words, the number of stages required is dependent upon the vacuum required, and upon which the more is important to the user, the operational cost or the equipment cost. One must bear in mind that, when using a two-stage steam ejector, the second stage has to be large enough in capacity to handle the initial

suction load plus the motive steam from the first stage unless an interstage condenser is used.

1.3. Ejector Terminology :

Functionally, as mentioned earlier, a steam ejector is a device in which :

(a) The motive steam, discharges from a high pressure region through a nozzle into a low pressure zone, developing a high velocity jet at low pressure for moving the fluid into the mixing chamber, (i.e. the convergent section of the diffuser).
(b) The motive steam mixes with the second flow entering the mixing chamber (i.e. the parallel sections of the diffuser).
(c) The mixture flows through the divergent part of the diffuser to be discharged at a higher pressure than in the mixing chamber.

Considering the entrainment process it can be described by several stages :

(i) Expansion of the jet to a pressure lower than that of the entrained fluid flow pressure around the axis of the jet.
(ii) Entrainment and diffusion action of the molecule of the entrained fluid by the viscous friction at the mating surface boundaries of the jet.
(iii) Acceleration of the particles of the entrained fluid by impact with the particles from the motive steam.

From what has been mentioned in this paragraph it is clear that the dimensional parameters of the ejector play a major role on its performance.

1.4. Layout of this Thesis :

The thesis can be mainly divided into two parts :

(i) Experimental studies for finding out the optimum nozzle distance (L_{op}) for the ejectors used in the experimental work, and finding how some of the dimensional parameters of the ejector affect this distance. Also, presenting how some of the dimensional parameters affect the ejector performance.

(ii) The development of three computer programs :

(a) The first program used the first law of thermodynamics together with the equations of properties of steam to predict the exit Mach number (M_e) for the steam flow .

(b) The second program predicts the shape of the characteristic net of the steam flow, by the use of the method of characteristics, inside the nozzle and, finally, it calculates its exit Mach number (M_e) as well.

(c) The third program also used the method of characteristics to predict the shape of the steam jet leaving the nozzle and entering the diffuser inside the ejector.

The theoretical studies enabled a comparison between the one-dimensional thermodynamic approach and the two-dimensional on their results, i.e. the exit Mach number (M_e) of the nozzles. And secondly to find out the optimum jet diameter (D_{op}) for the steam flow at the point were it meets the diffuser wall. Also, an empirical equation was found between the optimum nozzle distance (D_{op}) and the area ratio (A_o/A_{th}), which was used with the third computer program to predict the optimum nozzle distance (L_{op}). A design procedure for a single stage steam ejector is presented based on the experimental and theoretical work carried out and on the previous related work.

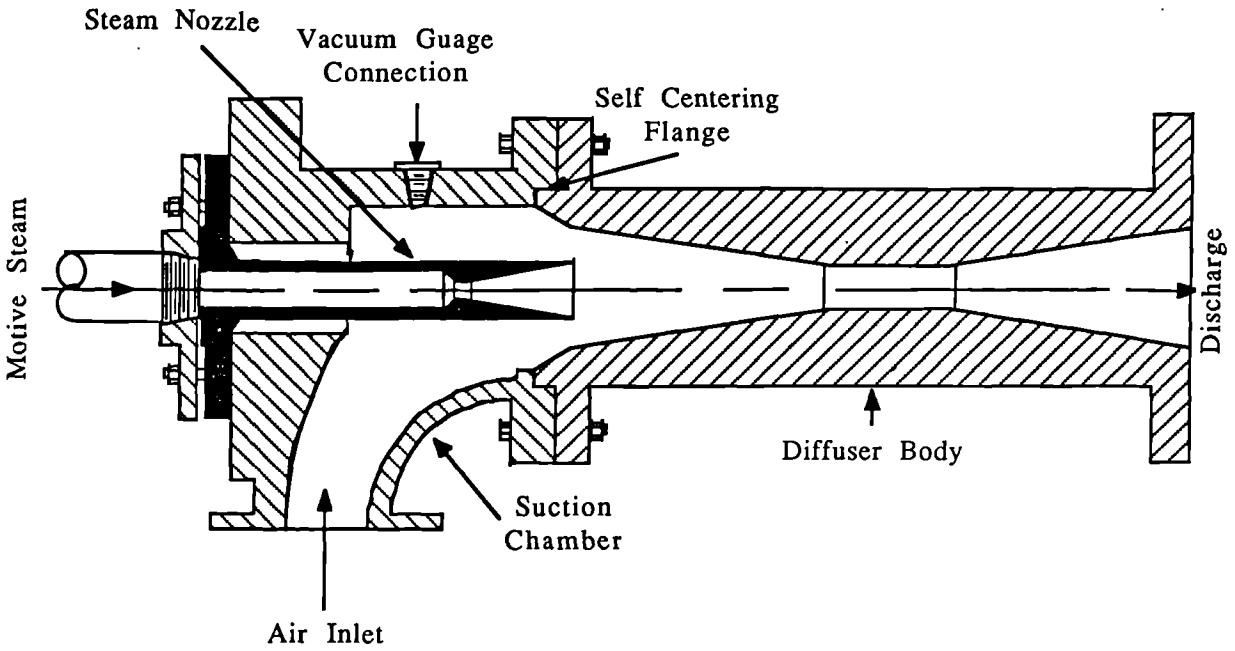

Figure 1.1. A Typical Single-Stage Steam Ejector.

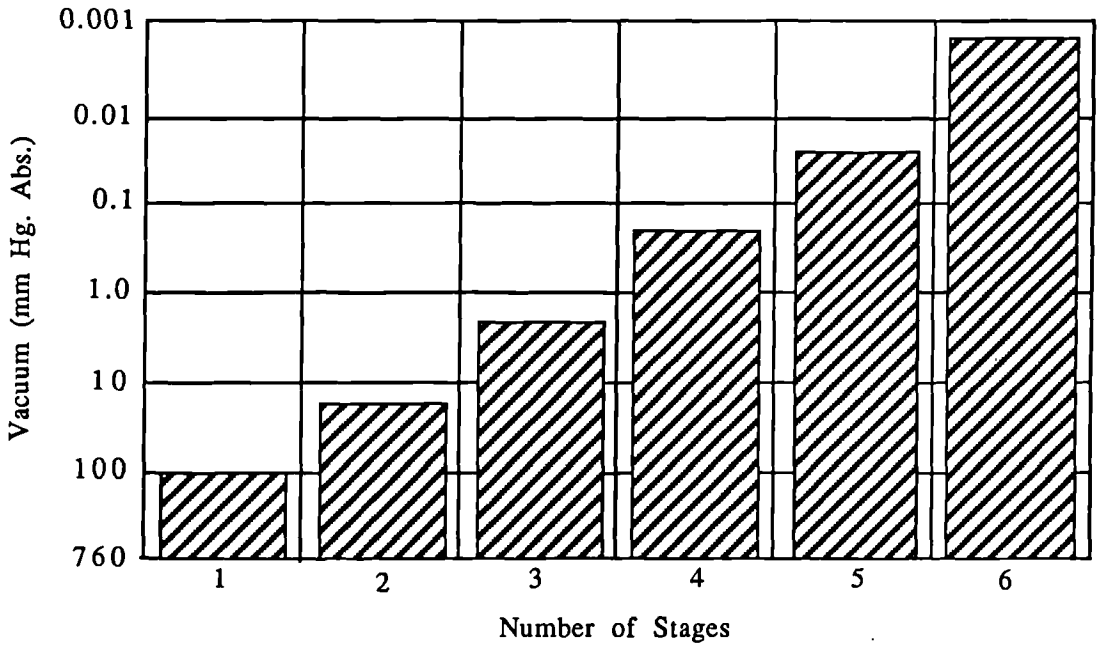

Figure 1.2. Range of Ejector Suction Pressures, (after Frumerman).

CHAPTER TWO

LITERATURE SURVEY

2.1. Historical Background :

2.1.1. Steam Nozzles :

The study of jet action has, of late years, assumed greater importance owing to the large extent to which it is now employed in engineering process. The steam-jet ejector is a device known for a long time in the chemical industry under the name of "ejector". It is a pump which uses the action of steam to entrain the air.

From the experimental point of view, the subject appears to have been examined first by Napier in 1867, when passing steam at constant pressure through an orifice into a chamber maintained at some lower pressure. He found that the amount of steam passing through the orifice was a maximum when the pressure in the chamber was about half the value of the pressure at admission to the orifice. Any lowering of this back pressure produced no increase in the steam flow (Mellanby, 1928).

In 1886, Osborne Reynolds showed that in a nozzle of varying section the velocity at the minimum section could not exceed the velocity of sound in the fluid, hence, the lowest possible pressure at

the exit of the orifice itself would be equal to that at which the pressure drop would produce a gas speed equal to the velocity of sound in the gas (Mellanby, 1928).

2.1.2. Steam Ejectors :

The first successful application of the ejector as a vacuum producer was for surface condensers in the arrangement patented by Parsons, where the ejector worked in series with a reciprocating pump. In actual fact, steam ejectors find wide application in industry as a vacuum source because of their moderate investment, ease of operation, reasonable maintenance requirement, and dependability.

Dependability is most essential, since an inoperative vacuum source can result in a severe yield penalty or even a plant shutdown. In spite of their wide application, until the late forties, usable design data were not available in the literature, and when an engineer had to design an ejector, most of the time, he resorted to trial and error, which may result in unsatisfactory performance or a waste of power, material, and labour.

Robert B. Power (1963) wrote " A great need exists for the release of steam-jet air ejector estimating data by manufacturers ". This quotation shows how rare[is] the design data, in the literature, of the steam ejectors.

2.2. The Effect of Dimensional Parameters on Performance Characteristics :

It was early recognised that the most serious obstacle to the development of the ejector was the design of the diffuser, which shape has the most suitable form, that is, the length and angle of convergence, the length, if any, of the section of minimum area, and the length and angle of divergence. Apart from the diffuser design, there was a need, also, to find the optimum distance from the outlet of the nozzle to the beginning of the diffuser throat, which was believed to be the most important distance in the ejector design (Kroll (1947)).

Nowadays, most design factors of a steam ejector are known, and there are definite ways, either by empirical formulae or by graphical relations, for determining these factors. However, these methods are perfect only for any ejector having the rest of its factors the same as those used in the experimental work from which data was used for the design. As noted above, the important factor which can greatly affect the performance of the ejector is the position of the nozzle exit with respect to the diffuser throat, i.e. the optimum nozzle distance (L_{op}).

This factor and other important aspects in the design of the ejector, as found in the literature, are discussed in the following paragraphs.

2.2.1. Distance from Nozzle Outlet to Diffuser Throat (L):

The length (L) was found to affect considerably the performance of an ejector, however, few researchers have investigated this point. Some recommended that nozzle position should be made variable so that adjustment for best performance could be made readily in the field. Others found some empirical formulae useful for their particular kind of ejector as mentioned before.

Third (1927) stated that the optimum nozzle distance (L_{op}) was dependent on the diffuser throat diameter (D_{th}). He did not give any explanation how it varied with increasing or decreasing the diffuser throat diameter (D_{th}).

Mellanby (1928) suggested that the factors upon which this distance depends are :

1 - The throat and outlet area of the nozzle,
2 - the pressure of nozzle supply, i.e. the motive steam pressure (P_m),
3 - the suction pressure (P_s),
4 - and the form of the diffuser.

From the experimental work, he pointed out that an increase in the nozzle motive pressure (P_m), leads to an increase in the dimensions of the jet, and so requires an increase in the nozzle

distance (L). The results of the investigation had been combined in a calculation chart which gave the nozzle distance (L), based on the motive steam pressure (P_m), the vacuum required (P_s), and the diffuser throat diameter (D_{th}).

Later, Watson (1933) conducted experimental investigation on two lengths, (L) and (L_w), where (L_w) is the length from the nozzle outlet to the inlet of the diffuser. The reason for this was that, when (L) is changing, the setting of the diffuser throat with respect to the wave sections in the core of the jet is changing, while with the latter, the circumferential area of the jet in contact with the entering air is altered. Also, he noted, that these two lengths are probably connected respectively with two entirely different functions which the ejector has to perform; the first, the admission and entrainment of the air, and the second a partial sealing of the diffuser throat (by a portion of a wave in the jet) as well as a pumping action between the regions of low and high pressure.

To make this clear, he compared the change in vacuum with the change of (L) and (L_w). He found that the predominant length which greatly affected the vacuum was apparently the length (L_w). Reaching this point, Watson went on to find out the effect of this length on producing vacuum. By plotting (L_w) against the vacuum produced by different motive steam pressures , he found that :

1 - The distance (L_w) is related to the motive steam pressure (P_m), that the lower the motive steam pressure (P_m) the lower is the value of (L_w) for maximum vacuum at that pressure.

2 - The distance (L_w) is evidently some function of the wavelength in the jet outside the nozzle.

Dowson (1937) published some very basic ideas of ejector design and emphasised the inadequacy of any conventional theoretical treatment for a complete solution of the problem. But, in answer to his paper, Keown (1937) wrote that the "wave form" has an important influence on the optimum distance. This distance is one wave length and in some cases it is one wave and a half length. He stated that it depends on the steam to air ratio as well.

Royds and Johnson (1941) found that the optimum position of the nozzle is nearly independent of the dimensions of the ejector, the weight of steam, and the air flow. They recommended that the nozzle should be placed at a distance of 3 to 3.5 inches from the point where the pressure in the diffuser reaches the adiabatic critical value, i.e. $P_c = 0.55\ P_d$, where (P_d) is the ejector discharge pressure.

Keenan and Neumann (1942) were principally concerned in selecting the simplest form of ejector which would perform in a useful way, and to analyse its performance independent of

published data on ejectors. So, they recommended that the best position of the nozzle outlet is only a short distance upstream from the beginning of the diffuser throat.

Keenan et al (1950) conducted an investigation on the ejector design. They used the one-dimensional analysis of the mixing of two gas streams. For the determination of the optimum distance, they constructed a graph connecting the ratio of the distance from the nozzle outlet to the end of the diffuser throat to the diffuser throat diameter, i.e. $((L+L_{th})/D_{th})$ and the ratio of the motive to suction pressure, i.e. (P_m/P_s).

In the same year, Kastner and Spooner (1950) had run an investigation on the performance and design of an ejector employing low pressure air as the driving fluid. They used with their experimental work two ranges of area ratio (i.e. the ratio of the diffuser throat area to the nozzle throat area (A_{th}/A_t)). The first, termed the "small-area-ratio apparatus", covered area ratios between 1.44 and 40.7 in seven steps, and the second, or the "large-area-ratio apparatus", covered area ratios between 76.0 and 1110.0 in five steps. They concluded that, where the maximum suction air-flow is desired at a given degree of compression; the optimum projection ratio, defined as the distance from the nozzle outlet to the diffuser throat divided by the diffuser throat diameter (L/D_{th}), should be about 1.5 for ejectors of small-area-ratio, and between zero and one for large-area-ratio ejectors.

In addition, it was found that this projection ratio becomes larger than 1.5 when (L_{th}/D_{th}) becomes too small. For other cases where the requirement is just the largest pressure ratio (P_m/P_s) with zero mass flow, no simple relation was given.

Johanneson (1951) suggested how the optimum nozzle distance would be changing with varying the working conditions :

1 - The optimum nozzle distance (L_{op}) increases with increasing the motive steam pressure (P_m) at fixed air load (m_a).
2 - The optimum nozzle distance (L_{op}) increases with increasing the air load (m_a) at fixed motive steam pressure (P_m).

Medici (1953) pointed out that the optimum nozzle distance (L_{op}) was a function of the pressure ratio (P_m/P_s) and the diffuser throat diameter (D_{th}). The following equation was presented:

$$\frac{P_m}{P_s} = \frac{L_{op}}{D_{th}} \qquad 2.1.$$

Cunningham et al (1957) had conducted an experimental work on the theory and performance of the jet-pump working with fluids of high viscosity. With respect to the optimum distance,

a graph was presented between the optimum nozzle distance divided by the nozzle throat diameter (L_{op}/d_t) and the area ratio of the nozzle throat area to the diffuser throat area (A_t/A_{th}). The ratio (L_{op}/d_t) reveals a consistent decrease with increase in this area ratio (A_t/A_{th}), and it is approximated by the empirical relation :

$$\frac{L_{op}}{d_t} = \frac{1 - \left[\frac{A_t}{A_{th}}\right]}{2\left[\frac{d_t}{A_{th}}\right]} \qquad 2.2.$$

His comment on the validity of this equation was that it gives a good agreement between theory and experiments only in the range of the area ratio (A_t/A_{th}) from (0.1 to 0.4).

Harris and Fisher (1964) examined the characteristics of the steam ejector. With their experimental work, they found that the pumping characteristics for any given size unit can be varied considerably by varying the position of the nozzle outlet with respect to the diffuser throat. They presented a graph relating the air capacity (m_a) with the suction pressure (P_s) for different nozzle locations. In short, the curves reveal that as the nozzle position is moved farther away from the diffuser throat, the mass of air (m_a)at any given suction pressure (P_s) increases while the discharge

pressure (P_d) and compression ratio (P_m/P_s) decrease. When the nozzle position is moved too far into the diffuser, decreases in the mass of air (m_a) occur without any increase in discharge pressure (P_d) or compression ratio (P_m/P_s). At the other extreme, when the nozzle is far from the diffuser the jet becomes unstable at pressures near shutoff. No empirical formula or any graphical aid was given to calculate this optimum nozzle distance (L_{op}).

Robozev (1965) presented an equation relating the optimum nozzle distance (L_{op}) to the injection coefficient (U) of the ejector and the nozzle outlet diameter (d_o). The successful use of the equation relies on the fact that the nozzle to be used in the experimental work should have the angle (Zeta) equal to 24° as an angle of divergence (this angle was recommended with an injection coefficient (U) of 0.5). In actual fact his definition of the optimum nozzle distance (L_{op}) was from the nozzle exit to the first point where the jet hits the diffuser wall (L_{opw}).
The empirical equation he presented was :

$$L_{opw} = 3.5\ d_o \sqrt{U} \qquad 2.3.$$

Shklover et al (1966) found the optimum nozzle distance relative to the diffuser was determined as the point on a curve plotted between the suction pressure (P_s) and the nozzle distance (L). By generalising the data on the optimum nozzle distance,

they presented two functions relating the optimum nozzle distance (L_{op}) with the ratio of the diffuser throat to the nozzle throat area (D_{th}/A_t). These two functions were approximately described by the following empirical equations :

for the first stage of a two stage ejector,

$$\frac{L_{op}}{D_{th}} = 0.019 \left(\frac{D_{th}^2}{A_t^2} + 50\right) \qquad 2.4.$$

while for the second stage,

$$\frac{L_{op}}{D_{th}} = 0.25 \left(\frac{D_{th}^2}{A_t^2} - 8\right) \qquad 2.5.$$

Putilov (1967(a)) used the criteria of the dimensionless flow of an incompressible liquid, and the theory of turbulent jets to calculate the optimum nozzle distance (L_{op}). He obtained a formula for calculating the relative length of the jet ($\bar{X}$) within the limits of its initial sector, with a given injection coefficient (U) :

$$\bar{X} = \frac{\sqrt{0.072 + 0.104\ U} - 0.268}{0.052\ C} \qquad 2.6.$$

where C is an experimental constant (for the main sector of the jet) he set equal to (0.27).

On the basis of the conclusions drawn by Sokolov (1948) that with constant geometrical jet dimensions the nozzle distance (L) depends only slightly on the operating conditions and that this distance is a function of the area ratio (A_{th}/A_o), Putilov, took the optimum nozzle distance (L_{op}) equal to ($\overline{X}$) and divided the left and right sides by the diameter of the diffuser throat (D_{th}), then Equation (2.6.), after simple conversion, he brought it to the form :

$$\frac{L_{op}}{D_{th}} = \frac{\sqrt{0.072 + 0.104\,U} - 0.268}{0.104\,C} \sqrt{\frac{A_o}{A_{th}}} \qquad 2.7.$$

Using Equation (2.7.), Putilov constructed a nomogram; with the aid of which, it is possible from the injection coefficient (U), and the geometrical parameters of the nozzle and the unit, to select the optimum relative distance of the nozzle (L_{op}/D_{th}) without resorting to calculations using Equation (2.7.).

Putilov found that this type of theoretical equation does not solve either the problem of selecting the optimum nozzle distance when the temperatures of the motive and the suction flows are variable and quite distinct from one another, or that of a unit working on wet steam. In a further investigation (1967(b)), he studied the effect of changing the temperatures of the supply and injected flow.

The following conclusions could be drawn from the results of

the investigations :

1 - The optimum distance of the nozzle does not depend on the temperatures and conditions of the supply and injected steam.

2 - Equation (2.6.) can satisfactorily be used to calculate the optimum distance at any temperature and states of the motive steam and the suction flow.

In the same year, Kuznestor and Uspenskii (1967) stated that the optimum nozzle distance (L_{op}) was the distance from the nozzle outlet to the end of the parallel section of the diffuser throat ($L+L_{th}$), and it should be between 8 and 10 times the diffuser throat diameter (D_{th}).

Zinger (1968), proposed a method for calculating the optimum nozzle distance (L_{op}). His method was based on two requirements. The first that it uses an experimental constant for the free jet and the injection coefficient. And the second, was that the convergent angle of the diffuser had to be 90°. He proposed that the optimum nozzle distance (L_{op}) is equal to the length of the free jet plus the diffuser throat diameter divided by 10 ($D_{th}/10$).

Although not directly relevant to steam ejectors Watanabe (1972) conducted his investigation on an air-ejector. He presented a graph showing the relation between pressure ratio (P_s/P_{at}) and

(L), with the mass flow ratio m_{as}/m_{ap} as parameter, for three different motive air pressures (P_{ma}). The minimum pressure ratio was obtained at a definite point for the predominant ranges of the mass flow ratio and the motive pressure (P_{ma}). Thus, the optimum ratio was $(L_{op}/D_{th})=1.57$ and $(L_{op}/d_o)=2.56$. But, with further experimental work, he found that the optimum projection ratio $(L_{op}/D_{th})=0.7$ - 0.9 and $(L_{op}/d_o)=1.5$.

2.2.2. Length of the Parallel Part of the diffuser Throat (L_{th}) :

Early work indicated that diffusers with parallel throats produced a higher maximum vacuum than diffusers which had a gradual constriction tapering off to the outlet without having any parallel length. In 1928, Mellanby was trying to optimise the rate of divergent taper immediately following the throat section. The design of the experimental diffusers was based on the belief that an extension of the throat section, or a very gradual preliminary taper, would provide the ideal form.

Four experimental diffusers were made to investigate this point. Diffuser "F" was of the type most generally used throughout the general tests i.e. convergent section followed by a parallel part, and then the divergent part; in the diffuser "Q" the parallel section was extended to the outlet i.e. the divergent section had been eliminated; diffuser "R" had the same outlet area as "F", but a much

smaller length of the parallel section; while "T" with a similar short parallel section as "R", but with a greater divergent angle. From the results it was found that the diffuser "F" was the best of the four types. It seemed clear from the results that, for the ideal diffuser; divergence should not follow rapidly after convergence. This condition may be fulfilled by having a parallel extension of the throat, which was in Mellanby's case L_{th}=4.17 D_{th}.

The importance of this length, was also recognised by Watson (1933) during his experimental work. He found that a throat with a considerable length tends to give a more uniform vacuum and a higher maximum value for every motive steam pressure (P_m). The length (L_{th}) for the best performance diffuser was (2 D_{th}).

Royds and Johnson (1941) recommended that the diffuser throat should be situated at or near the point where the critical adiabatic pressure (P_c) occurs, and they stated that a short parallel part in the diffuser behind the throat, and one of moderate length in front, would not affect the efficiency appreciably.

However Keenan and Neumann (1942) stated that a throat length of five to ten times the throat diameter (D_{th}) gave 3 per cent variation of optimum performance, and although the optimum length increased slightly with pressure and throat diameter (D_{th}), the increase was less than one diameter even when these factors

were doubled. Neumann stated that after the convergence section of the diffuser, the throat length (L_{th}) should be made slightly greater than seven times the diffuser throat diameter (D_{th}).

An optimum throat length (L_{th}) of 7.5 times the throat diameter (D_{th}) was found by Engdahl and Holton (1943) while Kroll (1947) reported seven to be the optimum.

Kastner and Spooner (1950) stated that the value (L_{th}) was a significant factor which should be 7 to 8 times (D_{th}) for pneumatic ejectors.

Shklover et al (1966) recommended a length of 4 to 6 times the diffuser throat diameter (D_{th}).

Kuznestor and Uspenskii (1967) stated that this length (L_{th}) should be around two times the diffuser throat diameter (D_{th}).

Watanabe (1972) fixed the throat diameter (D_{th}) and changed the length of the parallel part of the diffuser (L_{th}). It was found that the optimum length (L_{th}) was between 6 to 8.5 times the (D_{th}). But at a later experimental stage he found that (L_{th}) is 5 times the diffuser throat diameter (D_{th}).

2.2.3. Diffuser Throat Diameter (D_{th}) :

The correct throat area is important. A comparatively small change in the throat area makes a large difference in the amount of air entrained i.e. it will affect the vacuum produced. If the throat is too small choking will occur and if it is too large a leakage of air back into the system occurs.

Mellanby (1928) during his experimental work, fixed the suction pressure (P_s) and changed the diffuser throat area (A_{th}). He concluded that this area depends upon the mass of air (m_a) and the suction pressure (P_s) as well as upon the nozzle throat diameter (d_t) and the motive pressure (P_m).

Vil'der (1964) found a simplified method of calculating the throat diameter (D_{th}) in relation with the mass flow rate and the output pressure of the ejector, by the use of the equation below :

$$D_{th} = 1.6 \sqrt{\frac{\frac{18}{29}\,(m_a) + m_s \quad (kg/hr)}{P_d \quad (kgf/cm^2)}} \qquad 2.8.$$

He used Equation (2.9.) which is used to determine the nozzle throat diameter (d_t), since the diffuser is a supersonic diffuser i.e. a supersonic nozzle in reverse. The air flow having been converted to an equivalent steam flow using the molecular weight ratio (18/29).

The theoretical predictions of Kastner and Spooner (1950) showed that the maximum vacuum is obtained with no secondary flow, and the pressure ratio (P_s/P_d) decreases as the area ratio of the diffuser throat to the nozzle outlet (A_{th}/A_o) becomes smaller.

Watanabe (1972) showed by experimental work, that the maximum vacuum is obtained with zero secondary flow. But, showed that the pressure ratio (P_s/P_d) tends initially to decrease, as the area ratio (A_{th}/A_o) decreases until it reaches a minimum, then increasing again. This phenomenon may be due to the choking phenomena within ranges of smaller values of the area ratio (A_{th}/A_o).

2.2.4. Diffuser Entrance and Outlet :

The best form for the entrance to the diffuser throat parallel part was found to be a circular, conical shape entry. This was stated by Mellanby (1928), Watson (1933), and Engdahl and Holton (1943). This conical entry has an angle (Beta), which was in the early experimental work to be around 20°.

But later, Kastner and Spooner (1950) stated that for the small-area ratio ejectors (A_{th}/A_t) the diffuser inlet angle should be of a value of about 5° to 10°, and for the big-area ratio ejectors (A_{th}/A_t) they suggested to eliminate this convergent section.

Shklover et al (1966) also recommended a small convergence angle with their work, from 5° to 6°, and the length was 6 times the diffuser throat diameter (D_{th}). After the parallel section, a divergent section having an angle (Gamma), of from 4° to 10° is normally used. It was found that a parallel section without the divergent tail piece caused a reduction in the mass ratio of air to steam (m_a/m_s) of about 20 per cent.

It was suggested by some investigators that the length should be from around 7 to 9 throat diameter (D_{th}) for best performance (Kroll (1947)), and other from 4 to 6 times the throat diameter (D_{th}) with an angle of 10° to 12° (Kastner and Spooner (1950)).

2.2.5. The Suction Chamber :

During his experimental work, Mellanby (1928) conducted four tests in which he had changed the entrance and the position of the induced air to the suction chamber. It can be concluded that, for all practical purposes, the capacity of a jet for entraining the fluid is independent of the position in which the entrained fluid enters.

This may be taken to indicate that the ejector action depends very little upon the design of the suction chamber or the position of the motive nozzle.

2.2.6. The Nozzle :

It is known that poorly shaped nozzles cause unnecessary losses and useless lateral expansion. However, Engdahl and Holton (1943) found, for the steam-jet pump, that nozzles designed by the conventional method for specific pressures performed only slightly better than simple straight-hole nozzles at pressures up to 170 (psig.). Also, they noted that a machined nozzle with a convergent approach and a 10° angle of divergence was only 3 to 6 per cent better above 100 (psig.) than a simple pipe-cap nozzle made by drilling a hole in a standard pipe cap.

Watson (1933) conducted his experimental work with two different nozzles with different divergent angles (Zeta) 9.5° and 13.1° respectively. He found that the one which had a bigger angle created a better vacuum.

It is sometimes stated that over-expansion is an effect which contributes to the production of a good and steady vacuum in an air ejector. This was shown with Watson's experience as the over-expanded jet was better suited to the conditions over the wide range of pressure used.

On the contrary, Royds and Johnson (1943) made comparison between the over-expansion and under-expansion nozzles. The general results of their experiments showed that nozzles having a moderate degree of under-expansion were efficient in operation,

and usually gave stable conditions of performance when in a good position. They stated that under-expansion in the nozzle seems to be a prerequisite to good entrainment capacity.

Kastner and Spooner (1950) relied on what had been stated by Watson (1933) that over-expansion is advantageous and results in a very steady vacuum; they attempted to use "over-expanding" nozzle. But, their experiences were discouraging, indicating that over-expansion had no advantages. For their subsequent experiments they used a nozzle which was designed to give no expansion in the nozzle beyond the throat, and proved successful.

Vil'der (1964) derived a very simple equation, based on the one dimensional flow theory to calculate the nozzle throat diameter (d_t) and, also, the outlet diameter (d_o). This, he did by means of a graph. The equation for the nozzle throat diameter (d_t) is :

$$d_t = 1.6 \sqrt{\frac{m_s \ (kg/hr)}{P_m \ (kgf/cm^2 \ Abs.)}} \qquad 2.9.$$

and for the nozzle outlet diameter (d_o) :

$$d_o = I \, d_t \qquad 2.10.$$

where,

$$I = 0.54 \ (2.64)^{Log(E)} \qquad 2.11.$$

2.3. Conclusions :

From what it has been presented in this chapter it was found that it is necessary :

1_ To study how some of the dimensional parameters of the ejector affect the steam jet inside the ejector, and how this, in turn, affects the optimum nozzle distance (L_{op}), as till now this point had not been tackled by any previous researcher.

2_ To find out a procedure for ejector design based on what is discovered by studying the first point and on what has been reported in the literature.

CHAPTER THREE

FLOW THROUGH THE NOZZLE

3.1. Introduction and Description of the Nozzle :

The nozzle is an important part of the ejector, as it introduces the motive steam into the suction chamber of the ejector. Moreover, its design, in the view of many researchers, has a major effect on the performance of the ejector. Thus, it was considered advisable to devote a separate chapter to it.

The nozzle, which is normally used in the ejector, is of the converging-diverging circular section type and it is refered to as a "De Laval" nozzle. The principal dimensions of the nozzle are shown in Figure 3.1. :

1. The diameter of the throat, (d_t).
2. The total angle of divergence, (ζ).
3. The outlet diameter, (d_o).
4. The length of the divergent part (l_c), (found by d_t, d_o, and ζ) .
5. Well rounded or conical inlet.

3.2. Compressible Flow Through the Nozzle :

3.2.1. One-Dimensional Theoretical Approach :

For isentropic flow of a perfect gas with constant specific heats in a nozzle, the ratio of the upstream stagnation pressure (P_o) to the local static pressure (P) at a given station along the nozzle can be related to the local Mach number (M) at the point where the pressure is (P) by the relation (Plapp (1968)) :

$$\frac{P_o}{P} = \left[1 + \left(\frac{\gamma - 1}{2}\right) M^2\right]^{\left(\frac{\gamma}{\gamma - 1}\right)} \qquad 3.1.$$

For an isentropic flow, it is also possible to relate the local cross-sectional area to the local Mach number (M) by using :

_ The general continuity equation for steady, one-dimensional flow,

$$\frac{\dot{m}}{A} = \rho U$$

_ The velocity of sound, defined as,

$$a = \sqrt{\gamma R T}$$

_ The temperature ratio in terms of the Mach number (M),

$$\frac{T_o}{T} = 1 + \left(\frac{\gamma - 1}{2}\right) M^2$$

_ The perfect-gas equation of state,

$$\frac{P}{\rho} = R T$$

_ The pressure ratio in terms of the Mach number (M),

$$\frac{P_o}{P} = \left[1 + \left(\frac{\gamma - 1}{2}\right) M^2\right]^{\left(\frac{\gamma}{\gamma - 1}\right)}$$

to derive Equation (3.2.) :

$$\frac{\dot{m}}{A} = \frac{P_o \; M \sqrt{\frac{\gamma}{R T_o}}}{\left[1 + \left(\frac{\gamma - 1}{2}\right) M^2\right]^{\left(\frac{\gamma + 1}{2(\gamma - 1)}\right)}} \qquad 3.2.$$

The subscript (o) refers to the stagnation state, and Appendix I shows the derivations for all the above equations.

By assuming that (T_o), (P_o), and (ρ_o) are constant along the flow, and since (m), (γ), and (R) are also assumed constant we have, from Equation (3.2.):

$$\frac{A_1}{A_2} = \frac{M_2}{M_1} \left[\frac{1 + \left(\frac{\gamma - 1}{2}\right) M_1^2}{1 + \left(\frac{\gamma - 1}{2}\right) M_2^2}\right]^{\left(\frac{\gamma + 1}{2(\gamma - 1)}\right)} \qquad 3.3.$$

By substituting (M_2 = 1), so that (A_2 = A_t) is the cross-sectional area of the nozzle where the flow is sonic, and setting (A_1= A) as the local cross-sectional area corresponding to the local Mach number (M_1 = M), Equation (3.3.) would be written as (Barrere (1960)) :

$$\frac{A}{A_t} = \frac{1}{M} \left[\frac{2+(\gamma-1)M^2}{\gamma+1} \right]^{\left(\frac{\gamma+1}{2(\gamma-1)}\right)} \qquad 3.4.$$

If a nozzle is to be designed to produce a supersonic jet of gas flowing at a prescribed exit Mach number, Equation (3.4.) can be employed to determine the ratio of the cross-sectional area (A_o) at the exit to the cross-sectional area (A_t) at the throat. The two Equations (3.1.) and (3.4.) can be combined to eliminate the Mach number (M). The area ratio may be expressed as a function of the pressure ratio according to the Equation below :

$$\frac{A}{A_t} = \frac{\left(\frac{2}{\gamma-1}\right)^{\left(\frac{\gamma+1}{2(\gamma-1)}\right)} \left(\frac{P_1}{P}\right)^{\left(\frac{\gamma+1}{2\gamma}\right)}}{\sqrt{\left(\frac{2}{\gamma-1}\right)\left[\left(\frac{P_1}{P}\right)^{\left(\frac{\gamma-1}{\gamma}\right)} - 1\right]}} \qquad 3.5.$$

3.2.2. Application of the One-Dimensional Approach :

Consider the flow of a perfect gas in convergent-divergent nozzle, as shown in figure (3.2.). In the case where the back pressure is below (P_m), gas is drawn through the nozzle, its static pressure decreases in the converging part. At the same time, if the flow reaches sonic velocity at the throat, a supersonic velocity prevails in the diverging part of the nozzle.

3.2.3. Two-dimensional Theoretical Approach : Method of Characteristics :

3.2.3.1. Introduction :

Analytical solutions of the equations describing fluid flow have been found only for simplified problems. Some methods are based on linearisation of the equations of motion for describing steady, irrotational flow for both subsonic and supersonic streams in terms of the velocity potential, so that the solution is only approximate. In the case of supersonic flow, a more accurate solution of the complete nonlinear equation for potential flow can be obtained by the use of numerical techniques. The procedure, called the method of characteristics, indicates the properties of a perfect gas in which continuous waves of small but finite amplitude are present as the gas flows supersonically, irrotationally, and shock-free at constant specific heats. It can be applied to one-dimensional unsteady flow, to two- and three-dimensional steady flows, and to axisymmetric steady flow. This section deals only with two-dimensional steady flows.

3.2.3.2. Establishment of Equations:

Consider the flow of a compressible fluid through a differential control volume of dimensions (dx), (dy), (dz) parallel to the x-, y-, z-axes, respectively as shown in Figure (3.3.). The components of velocity in the x-, y-, z-direction are (u), (v), and (w)

respectively. The mass flow rate through the control volume is related to the rate of change of mass within the control volume. So, referring to Figure (3.3.), which shows the mass flow rates entering and leaving the control volume, the mass fluxes are calculated as follows (Saad (1985)) :

_ At the left face of the control volume the mass flow rate is :

$$\rho\, u\, dy\, dz$$

while at the right face the mass flow rate is :

$$\rho\, u\, dy\, dz + \frac{\delta}{\delta x}\left(\rho\, u\, dy\, dz\right) dx$$

The net flow rate into the control volume in the x-direction only, is the difference between the mass flow rate across these two surfaces, and equal to :

$$-\frac{\delta}{\delta x}\left(\rho\, u\right) dx\, dy\, dz$$

Similarly, the net flow into the control volume in the y- and z-directions only are, respectively:

$$-\frac{\delta}{\delta y}\left(\rho\, v\right) dy\, dz\, dx$$

and

$$-\frac{\delta}{\delta z}\left(\rho\, w\right) dz\, dx\, dy$$

So that the total net flow into the control volume is:

$$-\left[\frac{\delta(\rho u)}{\delta x} + \frac{\delta(\rho v)}{\delta y} + \frac{\delta(\rho w)}{\delta z}\right] dx\, dy\, dz$$

But the rate of change of mass within the control volume can be expressed as :

$$\frac{\delta}{\delta t}(\rho\, dx\, dy\, dz) = \frac{\delta \rho}{\delta t}\, dx\, dy\, dz$$

By equating the two terms, the principle of conservation of mass takes the general form :

$$\frac{\delta \rho}{\delta t} + \frac{\delta(\rho u)}{\delta x} + \frac{\delta(\rho v)}{\delta y} + \frac{\delta(\rho w)}{\delta z} = 0$$

or

$$\frac{\delta u}{\delta x} + \frac{\delta v}{\delta y} + \frac{\delta w}{\delta z} + \frac{1}{\rho}\left(u\frac{\delta \rho}{\delta x} + v\frac{\delta \rho}{\delta y} + w\frac{\delta \rho}{\delta z} \right) = 0 \qquad 3.6.$$

For steady irrotational flow (dU=0), the Euler's momentum equation may be written as :

$$dP + \rho\frac{dU^2}{2} = 0$$

and as $U^2 = u^2 + v^2 + w^2$, hence

$$\frac{dP}{\rho} + \frac{1}{2}d\left(u^2 + v^2 + w^2\right) = 0$$

The velocity of sound is given by $a^2 = (\delta P/\delta \rho)_s$, but, for isentropic flow, it may be written as $a^2 = dP/d\rho$. By eliminating (dP) from these two Equations we get :

$$d\rho = -\frac{\rho}{2a^2}\, d\left(u^2 + v^2 + w^2\right) \qquad 3.7.$$

from which, by differentiation with respect to the three coordinate axes, we get :

$$\frac{\delta\rho}{\delta x} = -\frac{\rho}{a^2}\left(u\frac{\delta u}{\delta x} + v\frac{\delta v}{\delta x} + w\frac{\delta w}{\delta x}\right)$$

$$\frac{\delta\rho}{\delta y} = -\frac{\rho}{a^2}\left(u\frac{\delta u}{\delta y} + v\frac{\delta v}{\delta y} + w\frac{\delta w}{\delta y}\right)$$

$$\frac{\delta\rho}{\delta z} = -\frac{\rho}{a^2}\left(u\frac{\delta u}{\delta z} + v\frac{\delta v}{\delta z} + w\frac{\delta w}{\delta z}\right)$$

Substituting these three equations into Equation (3.6.), yields :

$$\left(1-\frac{u^2}{a^2}\right)\frac{\delta u}{\delta x} + \left(1-\frac{v^2}{a^2}\right)\frac{\delta v}{\delta y} + \left(1-\frac{w^2}{a^2}\right)\frac{\delta w}{\delta z}$$

$$-2\frac{u\,v}{a^2}\frac{\delta u}{\delta y} - 2\frac{v\,w}{a^2}\frac{\delta v}{\delta z} - 2\frac{w\,u}{a^2}\frac{\delta w}{\delta x} = 0 \qquad 3.8.$$

Now, if we consider the case of two-dimensional, steady, potential flow, Equation (3.8.) simplifies to give:

$$\left(1-\frac{u^2}{a^2}\right)\frac{\delta u}{\delta x} + \left(1-\frac{v^2}{a^2}\right)\frac{\delta v}{\delta y} - 2\frac{u\,v}{a^2}\frac{\delta u}{\delta y} = 0 \qquad 3.9.$$

or

$$A\frac{\delta u}{\delta x} + 2B\frac{\delta u}{\delta y} + C\frac{\delta v}{\delta y} = 0 \qquad 3.10.$$

where $A=1-u^2/a^2$, $B=-uv/a^2$, and $C=1-v^2/a^2$.

The coefficient (A), (B), and (C) are generally functions of the independent variables of (x) and (y), and the dependent variables (u) and (v). The speed of sound is not an additional independent variable, and for a perfect gas it may be expressed as :

$$a^2 = \frac{\gamma-1}{2}\left[U_{max}^2 - (u^2+v^2)\right]$$

Equation (3.10.) is related to the three types of equations : elliptical, parabolic, or hyperbolic, and depends on the sign of the expression B^2 -AC. But :

$$B^2 - A\,C = \left(\frac{u\,v}{a^2}\right)^2 - \left(1 - \frac{u^2}{a^2}\right)\left(1 - \frac{v^2}{a^2}\right) = \frac{u^2 + v^2}{a^2} - 1 = \frac{U^2}{a^2} - 1$$

Therefore in

_ Subsonic flow, $U < a \Rightarrow B^2 - AC < 0 \Rightarrow$ Eq. 3.10. is elliptical type.

_ Sonic flow, $U = a \Rightarrow B^2 - AC = 0 \Rightarrow$ Eq. 3.10. is parabolic type.

_ Supersonic flow, $U > a \Rightarrow B^2 - AC > 0 \Rightarrow$ Eq. 3.10. is hyperbolic type.

With the last case, only two real solutions are possible, associated with two families of characteristic curve on the x-y plane, which are known as physical characteristics, and with two sets of curves plotted on the u-v velocity plane, which are known as the hodograph characteristics. Curves which represent solutions to Equation (3.9.) and along with the velocity gradient, may be discontinuous while the velocity itself is continuous, are called "characteristics". Since the velocity components (u) and (v) are continuous, then changes in the velocity components are :

$$du = \frac{\delta u}{\delta x}\,dx + \frac{\delta u}{\delta y}\,dy \qquad 3.11.$$

and

$$dv = \frac{\delta v}{\delta x}\,dx + \frac{\delta v}{\delta y}\,dy \qquad 3.12.$$

But the condition of irrotationality implies that

$$\frac{\delta u}{\delta y} - \frac{\delta v}{\delta x} = 0$$

Therefore

$$dv = \frac{\delta u}{\delta y}\, dx + \frac{\delta v}{\delta y}\, dy \qquad 3.13.$$

Equations (3.10.), (3.11.), and (3.13.) may be considered as a system of three simultaneous linear equations for the three unknowns $\delta u/\delta x$, $\delta u/\delta y$, and $\delta v/\delta y$. These equations which completely define the problem, are now arranged as follows :

$$A\left(\frac{\delta u}{\delta x}\right) + 2B\left(\frac{\delta u}{\delta y}\right) + C\left(\frac{\delta v}{\delta y}\right) = 0$$

$$dx\left(\frac{\delta u}{\delta x}\right) + dy\left(\frac{\delta u}{\delta y}\right) + 0\left(\frac{\delta v}{\delta y}\right) = du$$

$$0\left(\frac{\delta u}{\delta x}\right) + dx\left(\frac{\delta u}{\delta y}\right) + dy\left(\frac{\delta v}{\delta y}\right) = dv$$

Using the method of elementary algebra, we may solve the three equations simultaneously for any one of the unknowns in terms of the coefficients. Solving for $\delta u/\delta x$, we get :

$$\frac{\delta u}{\delta x} = \frac{\begin{vmatrix} 0 & 2B & C \\ du & dy & 0 \\ dv & dx & dy \end{vmatrix}}{\begin{vmatrix} A & 2B & C \\ dx & dy & 0 \\ 0 & dx & dy \end{vmatrix}} = \frac{-du(2B\ dy - C\,dx) + dv(-C\,dy)}{A(dy\ dy) - dx\,(2B\ dy - C\,dx)} \qquad 3.14.$$

Because the velocity gradient may be discontinuous, the unknowns $\delta u/\delta x$, $\delta u/\delta y$, and $dv/\delta y$ must not be unique. This means that their values are indeterminate, however, the denominator of Equation (3.14.), must be zero. Setting the denominator equal to zero gives :

$$A\,(dy)^2 - 2\,B\,dx\,dy + C\,(dx)^2 = 0$$

or

$$A\left(\frac{dy}{dx}\right)^2 - 2\,B\left(\frac{dy}{dx}\right) + C = 0$$

After solving the quadratic,

$$\frac{dy}{dx} = \frac{B \pm \sqrt{B^2 - A\,C}}{A}$$

Expressing (dy/dx) in terms of (u) and (v), by substituting for (A), (B), and (C) :

$$\frac{dy}{dx} = \frac{-\frac{uv}{a^2} \pm \sqrt{\frac{u^2+v^2}{a^2} - 1}}{1 - \frac{u^2}{a^2}} \qquad 3.15.$$

This equation defines two families of curves corresponding to the plus and minus signs in the x-y space. Each point in the flow fields has two physical characteristics (C_I) and (C_{II}). The term (dy/dx) represents the slope of the physical characteristic at any point in the flow, so that for characteristic (C_I) :

$$\left(\frac{dy}{dx}\right)_{C_I} = \frac{-\frac{uv}{a^2} + \sqrt{\frac{u^2+v^2}{a^2} - 1}}{1 - \frac{u^2}{a^2}} \qquad 3.16.$$

and for characteristic C_{II} :

$$\left(\frac{dy}{dx}\right)_{C_{II}} = \frac{-\frac{uv}{a^2} - \sqrt{\frac{u^2+v^2}{a^2} - 1}}{1 - \frac{u^2}{a^2}} \qquad 3.17.$$

Since $(\delta u/\delta x)$ is, in general finite, it is necessary that the numerator as well as the denominator must be equal to zero. Therefore :

$$-2\,B\,du\,dy + C\,du\,dx - C\,dv\,dy = 0$$

or

$$\frac{dv}{du} = \frac{dx}{dy} - \frac{2B}{C}$$

Substituting for the values of (B) and (C) and for (dx/dy) from Equation (3.15.) gives :

$$\frac{dv}{du} = \frac{1 - \frac{u^2}{a^2}}{-\frac{uv}{a^2} \pm \sqrt{\frac{u^2+v^2}{a^2} - 1}} + \frac{2\frac{uv}{a^2}}{1 - \frac{v^2}{a^2}}$$

Rationalising this equation will gives :

$$\frac{dv}{du} = \frac{\frac{uv}{a^2} \mp \sqrt{\frac{u^2+v^2}{a^2} - 1}}{1 - \frac{v^2}{a^2}} \qquad 3.18.$$

This equation defines two families of alternate characteristics, which are the hodograph characteristics C_I and C_{II}. Thus, in the hodograph plane u-v the slope of the hodograph characteristic C_I is :

$$\left(\frac{dv}{du}\right)_{C_I} = \frac{\frac{uv}{a^2} - \sqrt{\frac{u^2+v^2}{a^2} - 1}}{1 - \frac{v^2}{a^2}} \qquad 3.19.$$

and the slope of the hodograph characteristic C_{II} is :

$$\left(\frac{dv}{du}\right)_{C_{II}} = \frac{\frac{uv}{a^2} + \sqrt{\frac{u^2+v^2}{a^2} - 1}}{1 - \frac{v^2}{a^2}} \qquad 3.20.$$

When the initial values of the velocity components (u) and (v) are known along a particular curve, then the characteristics of the entire flow field in the physical and hodograph planes can be calculated by using the integral forms of Equations (3.16.), (3.17.), (3.19.), and (3.20). It is evident from these equations that values of the characteristics are real only when the flow is supersonic i.e. $[(u^2+v^2)/a^2 > 1]$.

The solution to these equations may be considerably simplified when the slopes of the characteristics in the physical plane are expressed in polar coordinates. The velocity components (u) and (v) are :

$$u = U\cos\theta$$

$$v = U\sin\theta$$

$$\frac{v}{u} = \tan\theta$$

where (θ) is the angle that the velocity vector (U) makes with the u-axis, turning in the counterclockwise direction Figure (3.4.). (The angle (θ) is considered positive when turning in a counterclockwise direction, negative when turning clockwise). Substituting these expressions in Equation (3.15.), it can be shown that :

$$\frac{dy}{dx} = \frac{\tan\theta \mp \tan\alpha}{1 \pm \tan\theta \ \tan\alpha} = \tan(\theta \pm \alpha)$$

So that :

$$\left(\frac{dy}{dx}\right)_{C_I} = \tan(\theta - \alpha) \qquad 3.21a.$$

and

$$\left(\frac{dy}{dx}\right)_{C_{II}} = \tan(\theta + \alpha) \qquad 3.21b.$$

where (α) is the local Mach angle.

The characteristic (C_I) is inclined at an angle ($-\alpha$) with the velocity vector, whereas characteristic (C_{II}) is inclined at an angle ($+\alpha$) with the velocity vector. Since (α) is the Mach angle, this means that the characteristic lines are Mach lines. Hence, in supersonic flow, the slope of the physical characteristic is the same as the slope of the Mach lines. (C_I) is called a right-running characteristic, and (C_{II}) a left-running characteristic.

The physical characteristic (C_I) is perpendicular to the hodograph characteristic (C_{II}), this can be proved by multiplying Equations (3.16.) and (3.20.), therefore :

$$\left(\frac{dy}{dx}\right)_{C_I}\left(\frac{dv}{du}\right)_{C_{II}} = -1$$

In a similar way, it can be shown from Equations (3.17.) and (3.19.), that the physical characteristic (C_{II}) is perpendicular to the hodograph characteristic (C_I) :

$$\left(\frac{dy}{dx}\right)_{C_{II}}\left(\frac{dv}{du}\right)_{C_I} = -1$$

The relationship between the slopes of the characteristic curves in the physical and hodograph planes is shown in Figure (3.5.).

$$\text{Since } U^2 = u^2 + v^2 \Rightarrow U\,dU = u\,du + v\,dv \qquad 3.22.$$

$$\text{But } \tan\theta = \left(\frac{v}{u}\right) \text{ and } d\tan\theta = Sec^2\theta\,d\theta = \frac{u\,dv - v\,du}{u^2}, \text{ so that}$$

$$d\theta = \frac{u\,dv - v\,du}{U^2} \qquad 3.23.$$

Combining Equations (3.22.) and (3.23.) and using the expression of (dv/du) gives :

$$\frac{1}{U}\frac{dU}{d\theta} = \frac{\left[\dfrac{uv^2}{a^2} \mp v\sqrt{\dfrac{u^2+v^2}{a^2}-1} \;+\; u\right]}{1-\dfrac{v^2}{a^2}} = \mp\frac{1}{\sqrt{M^2-1}}$$

$$\left[\dfrac{\dfrac{u^2v}{a^2} \mp u\sqrt{\dfrac{u^2+v^2}{a^2}-1} \;-\; v}{1-\dfrac{v^2}{a^2}}\right] \qquad 3.24.$$

But $\tan\alpha = \dfrac{1}{\sqrt{M^2-1}}$, therefore : $\dfrac{1}{U}\dfrac{dU}{d\theta} = \mp \tan\alpha$

Hence, along characteristic (C_I) :

$$\frac{1}{U}\frac{dU}{d\theta} = -\frac{1}{\sqrt{M^2-1}} = -\tan\alpha \qquad 3.25.$$

and along characteristic (C_{II}) :

$$\frac{1}{U}\frac{dU}{d\theta} = +\frac{1}{\sqrt{M^2-1}} = +\tan\alpha \qquad 3.26.$$

Between any two points, along characteristic (C_I), the change in the angle is :

$$\int d\theta = -\int\left(\sqrt{M^2-1}\right)\frac{dU}{U}$$

But the expression, derived from the energy equation for an adiabatic process, for velocity change as a function of Mach number is :

$$\frac{dU}{U} = \frac{d(M^2)}{2\,M^2\left(1+\frac{\gamma-1}{2}M^2\right)} \qquad 3.27.$$

Hence:

$$\int d\theta = -\int \frac{\sqrt{M^2-1}}{2M^2\left(1+\frac{\gamma-1}{2}M^2\right)}\, d(M^2) \qquad 3.28.$$

Similarly, for (C_{II}) :

$$\int d\theta = +\int \frac{\sqrt{M^2-1}}{2M^2\left(1+\frac{\gamma-1}{2}M^2\right)}\, d(M^2) \qquad 3.29.$$

The integration of Equations (3.28.) and (3.29.) gives :

$$\theta = \mp \left\{ \sqrt{\frac{\gamma+1}{\gamma-1}}\ \arctan\sqrt{\frac{\gamma-1}{\gamma+1}(M^2-1)} - \arctan\sqrt{M^2-1} + c \right\} \qquad 3.30.$$

The right-hand side of the above expression, except the integration constant (c), is equal to the Prandtl-Meyer angle (ν) which is the angle through which sonic flow turns to attain a supersonic Mach number (M).

Hence the above expression becomes :

$$\nu+\theta = C_I \qquad \text{for characteristic } C_I \qquad 3.31.$$

$$\nu-\theta = C_{II} \qquad \text{for characteristic } C_{II} \qquad 3.32.$$

where C_I and C_{II} are constants of integration.

From Equations (3.31.) and (3.32.), flow direction and Mach number can each, in turn, be expressed in terms of the characteristic constants (C_I) and (C_{II}) :

$$\theta = \frac{C_I - C_{II}}{2} \qquad 3.33.$$

$$\nu = \frac{C_I + C_{II}}{2} \qquad 3.34.$$

3.2.4. Application of the Two-Dimensional Approach : Numerical Computation (Lattice Point Method):

Two procedures are available for calculating properties along two dimensions of flow at supersonic velocities. The first method, known as the "point-to-point method" or the "lattice point method", calculates properties at points by progressively proceeding downstream. Characteristic curves are propagated from known starting points and where these curves intersect each other, new points in the flow field are established. In the second method, the "region to region method", the field of flow is divided into regions of uniform flow which are separated by characteristic curves. The average values of flow properties in each region can then be calculated.

The lattice point method was chosen for its simplicity in calculations and drawing the characteristic net of the flow (Saad (1985)). Figure (3.6.) shows characteristic lines of a typical flow field. A number of initial points such as points (a) and (b), along a starting line, are selected with known geometric coordinates and

flow properties. From the values of (θ) and (ν)for these two points, numerical values of characteristic (C_I) and (C_{II}) passing through point (b) Equations (3.31.) and (3.32.).

As the characteristic (C_I) passing through point (a) intersects at point (d) with characteristic (C_{II}) passing through point (b); the values of (θ) and (ν) at point (d) may then be calculated by the simultaneous solution of Equations (3.33.) and (3.34.) as follows :

$$C_I = \nu_a + \theta_a = \nu_d + \theta_d$$

and

$$C_{II} = \nu_b - \theta_b = \nu_d - \theta_d$$

The resulting flow direction (θ) and the Prandtl-Meyer (ν) at point (d) are determined by these characteristic values, (C_I) and (C_I) :

$$\theta_d = \frac{(\nu_a + \theta_a) - (\nu_b - \theta_b)}{2} = \frac{C_I - C_{II}}{2}$$

and

$$\nu_d = \frac{(\nu_a + \theta_a) + (\nu_b - \theta_b)}{2} = \frac{C_I + C_{II}}{2}$$

The Mach number and Mach angle corresponding to (ν_d) may then be calculated. The procedure may then be continued to other points in the flow field, and the complete net of characteristic curves describing the flow pattern can be determined.

3.3. Steam Flow Through the Nozzle :

3.3.1. Physical Phenomena :

Condensation phenomena, in the case of rapid expansion in nozzles, have been investigated by many authors because this kind of flow is closely related to that of expanding flows in a steam turbine and in a liquid-metal type channel. To clarify these phenomena, let us take the case when steam is expanded rapidly through a De Laval nozzle. There is time (t) at which the vapour becomes saturated and as time increases it becomes supersaturated; then generation of numerous condensation nuclei take place. The generated nuclei grow quickly in this region of the nozzle (this region is usually called the condensation zone), then a condensation process progresses rapidly.

It follows that, the nozzle flow will be affected by the cooling vapour; corresponding to the work of expansion and the latent heat released by its condensation. In the case when this heat exceeds a certain critical quantity a condensation shock forms which becomes unstable and propagates upstream, causing a periodic flow oscillation in the nozzle.

3.3.1.1. Mechanism of Formation of Condensation Shock Waves :

The mechanism of formation of this condensation shock wave may be described as following. There are, basically, three types of

condensation shock waves as schematically shown in Figure (3.7.), where broken lines and solid lines, represent sonic line and the line of onset of condensation, respectively (Matsuo et al (1985)). When the supersaturation of the upstream of the nozzle increases gradually, at first, oblique compression waves are generated in the condensation zone by the release of latent heat. Increase in the supersaturation from this state the oblique compression waves come together to form an oblique shock wave, which is reflected at the nozzle centre line so that its shape becomes X-type. This wave is called a condensation shock wave. In this way, an oblique condensation shock is generated. In the case of a comparatively small supersaturation, the flow remains supersonic in the region downstream of the sonic line as shown in Figure (3.7a.).

As the supersaturation increases, a part of this oblique condensation shock wave near the centre line becomes normal to the flow. Hence, in this case, the oblique condensation shock wave becomes bifurcated, as shown in Figure (3.8b.). The flow just downstream of the normal part of the shock wave is subsonic (region abc in Figure 3.7b.). But, as this region is located in the condensation zone, the flow will again be supersonic due to the latent heat released by condensation.

When the supersaturation is higher than the previous case, the normal part of the bifurcated condensation shock wave becomes longer and finally a normal condensation shock wave is formed as shown in Figure (3.7c.). The flow just after this shock is

sonic (region de f g in Figure 3.7c.). But, it will again be supersonic due to the same reason as in the case of Figure (3.7b.). From examination of Figure (3.7.) one can summise, that with an increase in the supersaturation of the flow, the location where the condensation shock wave appears, shifts upstream and the slope of the condensation shock wave changes from an oblique shock, to a bifurcated shock, and to a normal shock wave, depending on the amount of the release of latent heat due to condensation of water vapour.

3.3.1.2. Mechanism of Flow with Condensation :

Matsuo et al (1985) examined the effect of the condensation shock wave on the flow of a nozzle. They found that the pressure distribution versus the distance from the nozzle throat is as shown schematically in Figure (3.8.). They found also that the static pressure of the flow decreases along with the curve of the dry flow. It begins to deviate from it at a point (a) and reaches a maximum at a point (b); thereafter, it keeps decreasing steadily. The point (a) is considered to be the point where the supersaturation reaches its maximum i.e., it is the point of onset of condensation. Then, the supersaturation decreases until it reaches its minimum value at point (b), which is the point where condensation nuclei are generated. From these results, it can be said that the region between (a) and (b) is the non equilibrium condensation region, and its length can be determined from the static pressure distributions. In brief, a condensation zone can be divided into a non equilibrium

and an equilibrium condensation region, and the static pressure distribution in the former becomes different from that of an isentropic one, with the pressure reaching a peak; thereafter, it decreases steadily in the latter. Hence, the greatest effect due to condensation appears in the non equilibrium condensation zone.

Based on what it has been said earlier, the flow behaviour accompanying condensation without and with a shock wave is shown schematically in Figure (3.7.) Although the static pressure increases and the flow decelerates because of the effect of released latent heat by condensation in Figure (3.7a.), the flow stays supersonic everywhere down stream of the nozzle throat. But, in the case of a normal condensation shock wave, the velocity just downstream of it is subsonic and it is accelerated to supersonic speed. This fact was confirmed by the mechanism of formation of condensation shock waves (see Figure 3.7c.).

3.3.2. Application of the One-Dimensional Approach : Use of the Thermodynamics Equations :

In one-dimensional flow it is assumed that the velocity, and the fluid properties, change only in the direction of the flow. This means that, the fluid velocity is assumed to remain constant at a mean value across the cross-section of the nozzle and a uniform distribution of pressure over the cross-section, i.e. only the pressure gradient in the direction of the flow is taken into account. Also, the fluid at any point is in a state of thermal equilibrium.

Applying the steady-flow energy equation (3.35.), between section one and any other section x-x (Figure 3.1.) where the pressure is (P), the enthalpy is (h), and the velocity is (U), we have (Eastop (1978)) :

$$h_1 + \frac{U_1^2}{2} = h + \frac{U^2}{2} \qquad 3.35.$$

i.e.

$$U^2 = 2\,(h_1 - h) + U_1^2$$

or

$$U = \sqrt{\{2(h_1 - h) + U_1^2\}} \qquad 3.36.$$

In most practical applications the velocity at the inlet to a nozzle is negligibly small in comparison with the exit velocity. It can be seen from the general continuity equation for steady, one-dimensional flow ($m=\rho AU$), that for a constant (m), a negligibly small velocity implies a very large area, and most nozzles (as in our case) are in fact shaped at *inlet in such a way that the nozzle* converges rapidly over the first fraction of its length; this is illustrated in the diagram of a nozzle shown in Figure (3.2.). Now Equation (3.36.), will be written after neglecting (U_1),

$$U = \sqrt{2(h_1 - h)} \qquad 3.37.$$

Since enthalpy is usually expressed in (kJ/kg), then an additional constant of (10^3) will appear within the root sign if (U) is to be expressed in (m/s), (where $1kJ=10^3$ Nm). Hence,

$$U = 44.72 \sqrt{h_1 - h} \qquad m/s \qquad 3.38.$$

Because the losses in nozzles are small i.e. short length giving negligible friction losses, the flow in the nozzle can be considered isentropic.

In the design of nozzles the entropy of the motive steam is found and equated to the entropy at the nozzle throat pressure (P_t) and nozzle exit pressure (P_e).

The nozzle throat pressure (P_t) in relation with the motive pressure (P_m) would be equal to :

$$P_t = P_m \left(\frac{2}{\gamma + 1}\right)^{\left(\frac{\gamma}{\gamma - 1}\right)} \qquad 3.39a.$$

which for wet steam ($\gamma = 1.135$) gives :

$$P_t = 0.577\, P_m \qquad 3.39b.$$

This gives the steam dryness fraction at the throat (x_t) and at the exit sections (x_e) since :

$$x_t = \frac{S_{gt} - S_{ft}}{S_{gm} - S_{ft}} \qquad 3.40a.$$

and

$$x_e = \frac{S_{ge} - S_{fe}}{S_{gm} - S_{fe}} \qquad 3.40b.$$

In actual fact, no condensation will occur at the nozzle throat, as the condensation appears after the throat where the normal condensation shock wave takes place. This means that the dryness fraction at the throat (x_t) is equal to unity.

Thus the enthalpy (h_t) at the throat section can be found from the steam tables at the throat pressure (P_t), and at the exit section it can be calculated at the nozzle exit pressure (P_e) using the dryness fraction as :

$$h_e = x_e\, h_{ge} + (1 - x_e)\, h_{fe} \qquad 3.41.$$

The throat and exit velocities can then be found using Equation (3.38.) :

$$U_t = 44.72 \sqrt{h_m - h_t} \qquad 3.42a.$$

and

$$U_e = 44.72 \sqrt{h_m - h_e} \qquad 3.42b.$$

These are ideal velocities not allowing for losses in the nozzle and can be corrected by the use of Martin's linear relation (Johannesen(1951)) between the nozzle efficiency and the enthalpy drop :

$$\eta_{t,e} = 102.7 - 0.4521\, \Delta h_{t,e}$$

where ($\Delta h_{t,e}$) is the isentropic heat change ($h_m - h_{t,e}$) in kJ/kg.

The corrected velocities can then be calculated as :

$$U_t = 44.72 \sqrt{\eta (h_m - h_t)} \qquad 3.43\,a.$$

and

$$U_e = 44.72 \sqrt{\eta (h_m - h_e)} \qquad 3.43b.$$

Finally the mass flow, applying the continuity of mass flow, using (m_t) for the throat and (m_e) for the exit, gives :

$$\dot{m}_t = \frac{U_t A_t}{v_t} \qquad 3.44\,a.$$

and

$$\dot{m}_e = \frac{U_e A_e}{x_e v_e} \qquad 3.44b.$$

and is used in estimating the throat and exit areas hence diameters.

Figure (3.2.) shows the three main important points in the nozzle, the inlet, throat, and exit point. The inlet motive steam pressure (P_m) is known and by using it with the steam tables we get (S_{gm}) and (h_{gm}) at the inlet. From the steam tables we can find (h_t), (S_{gt}), (S_{ft}), and (v_t) at the throat pressure (P_t) which could be found from Equation (3.39b.). Then, by using Equation (3.43a.), the velocity at throat (U_t) can be found, from which the mass flow rate (m_t) of the steam at the throat will be calculated by the use of Equation (3.44a.). Then, applying the trail-and-error method by setting an exit pressure (P_e) and using the steam tables, Equations (3.40b.), (3.41.), and (3.43b.), the outlet mass of steam (m_e) can be

calculated using Equation (3.44b.). When this mass is equal to (m_t), then the estimated exit pressure (P_e) is the exit pressure of the nozzle. A computer program was written to do the calculations, which is explained and illustrated in Appendix II.

3.3.3. Application of the Two-Dimensional Approach :

Based on what it has been noted in Section (3.2.3.), we are able to compute the average slopes (b_I) and (b_{II}) of the line (a-d), and the line (b-d) in Figure (3.6.) respectively. From Equations (3.21a.) and (3.21b.), we may write approximately (Shapiro (1953)):

$$b_I = \tan \frac{1}{2} \left[(\theta_d - \alpha_d) + (\theta_a - \alpha_a) \right] = \tan \overline{(\theta - \alpha)_{a\text{-}d}} \qquad 3.45a.$$

$$b_{II} = \tan \frac{1}{2} \left[(\theta_d + \alpha_d) + (\theta_b + \alpha_b) \right] = \tan \overline{(\theta + \alpha)_{b\text{-}d}} \qquad 3.45b.$$

and thus (b_I) and (b_{II}) are known.

Now, from the formulae of analytic geometry,

$$y_d - y_a = b_I (x_d - x_a)$$
$$y_d - y_b = b_{II} (x_d - x_b)$$

we may find (x_d) and (y_d) by solving the above two simultaneous equations,

$$x_d = \frac{(y_b - b_I x_b) - (y_a - b_I x_a)}{b_I - b_{II}} \qquad 3.46\,a.$$

$$y_d = \frac{(y_b - b_{II} x_b) - b_{II}(y_a - b_I x_a)}{b_I - b_{II}} \qquad 3.46b.$$

The procedure may then be continued to other points in the flow field, and the complete net of characteristic lines describing the flow pattern can be determined. The whole calculation process is done using a computer program taken from Saad (1985). This program was modified to give the required results and is described in Appendix III.

3.4. Conclusions :

Based on what it has been covered in this chapter, a comparison can be made between the use of the thermodynamic equations in the one-dimensional approach, and the use of the two-dimensional approach.

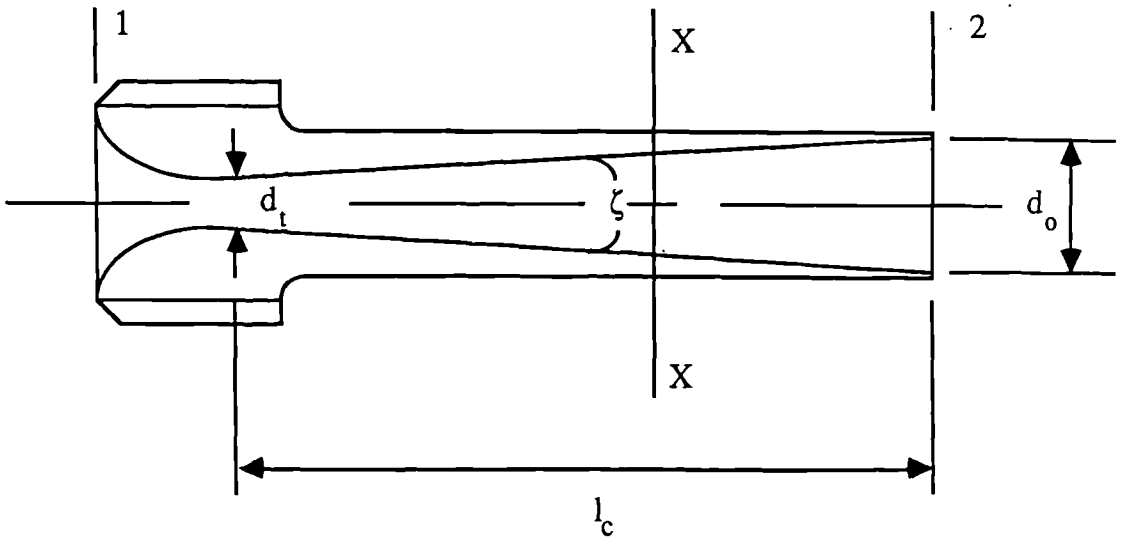

Figure 3.1. The Principal Dimensions of the Nozzle.

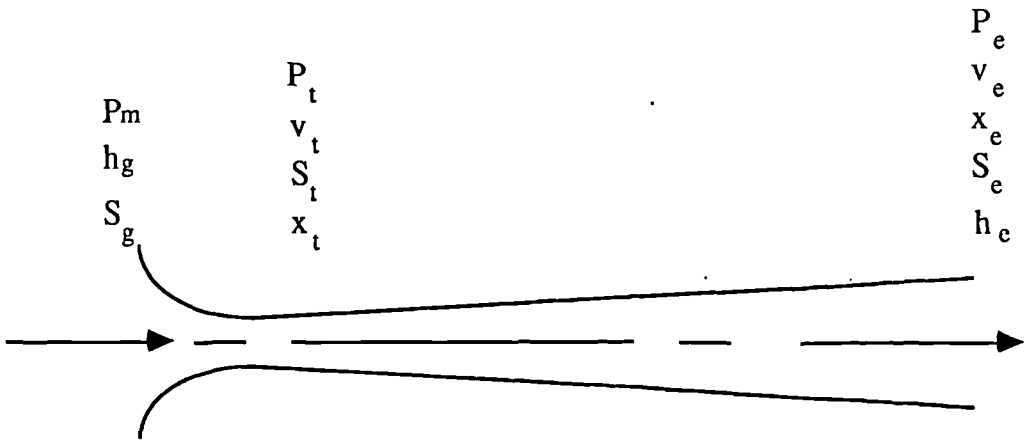

Figure 3.2. The Main three Points in the Nozzle : The Inlet, The Throat, and The Exit.

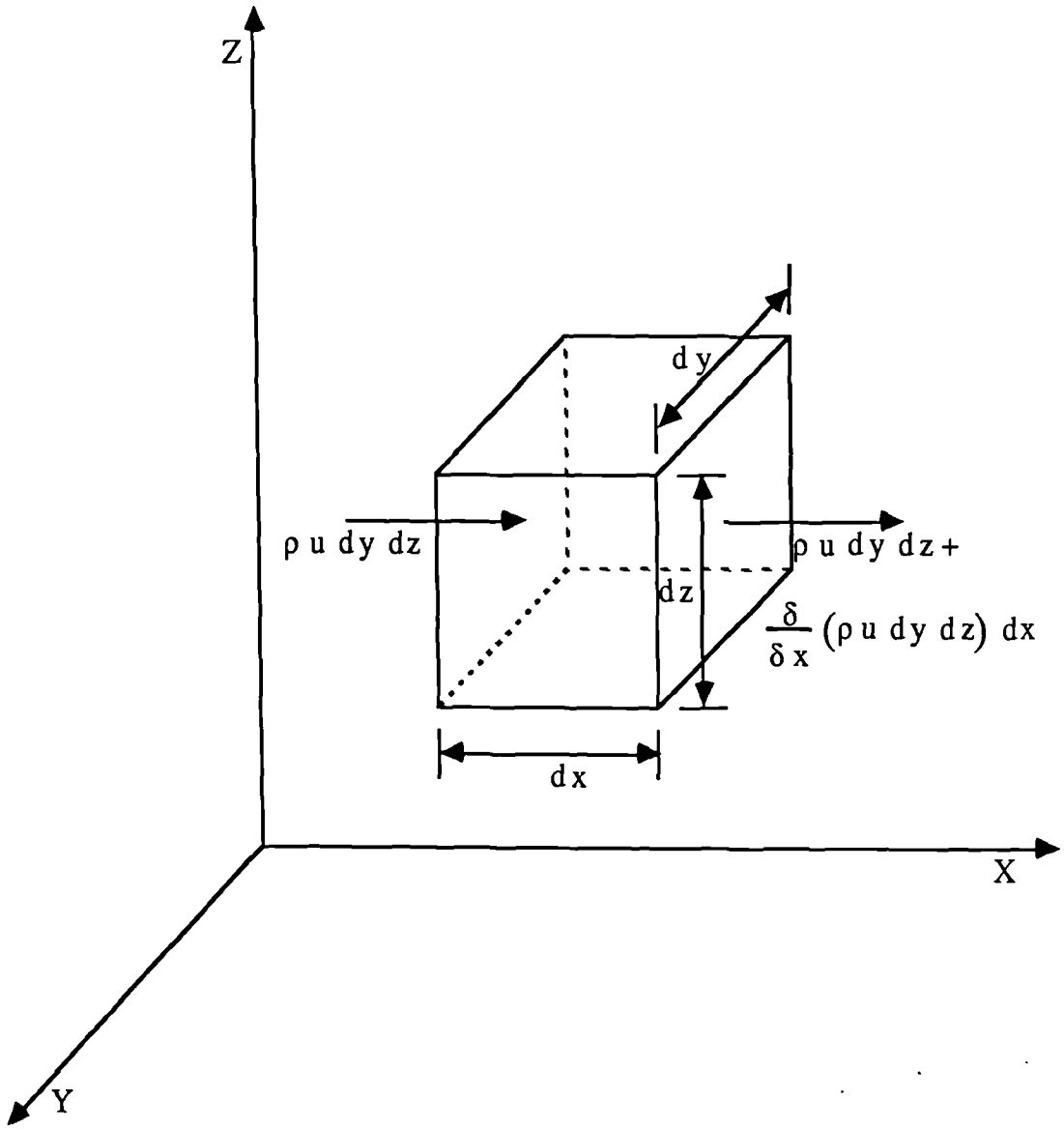

Figure 3.3. Mass Flow Through a Differential Control Volume.

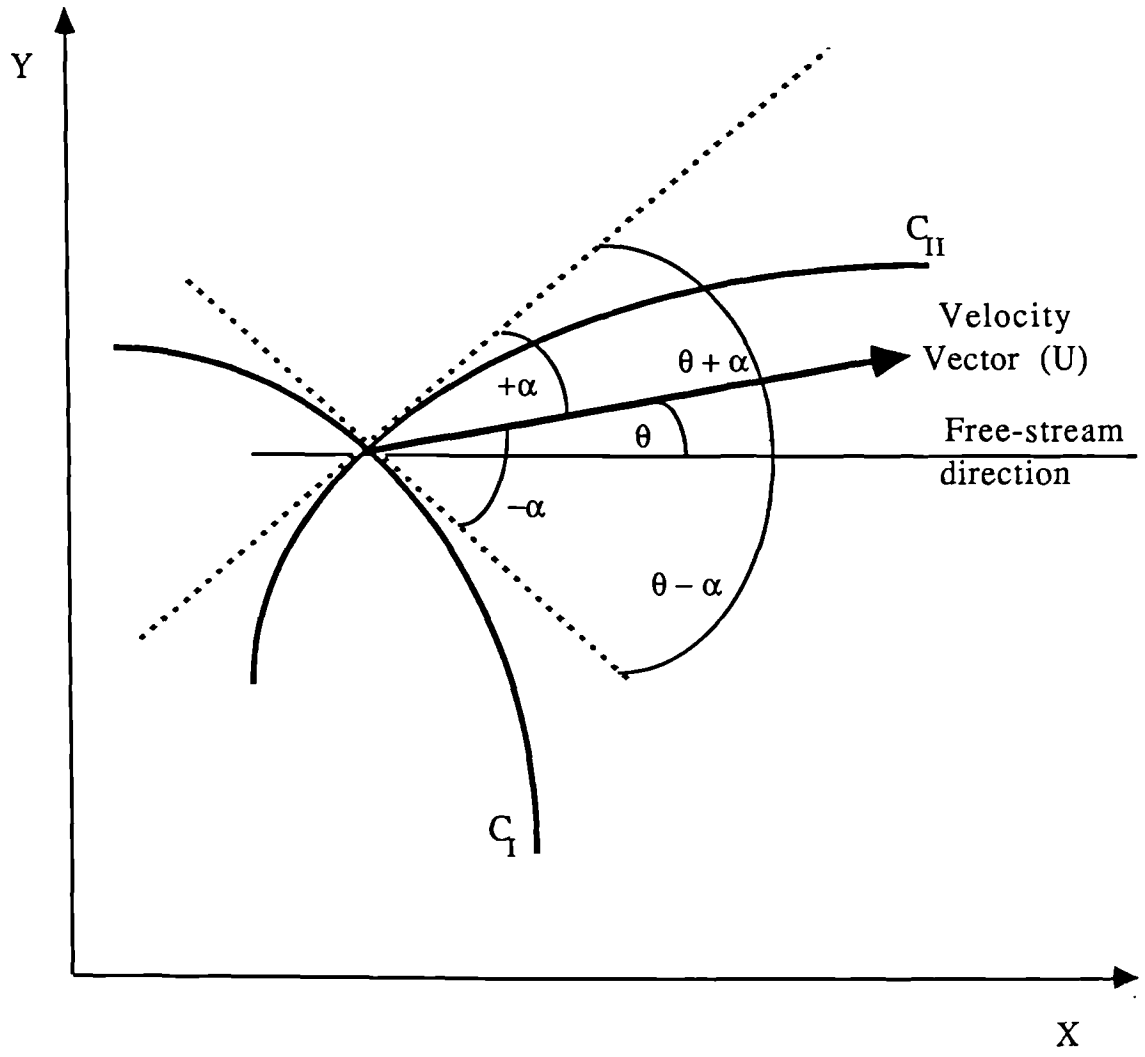

Figure 3.4. Inclination of the Characteristic Curves Relative to the Flow Direction.

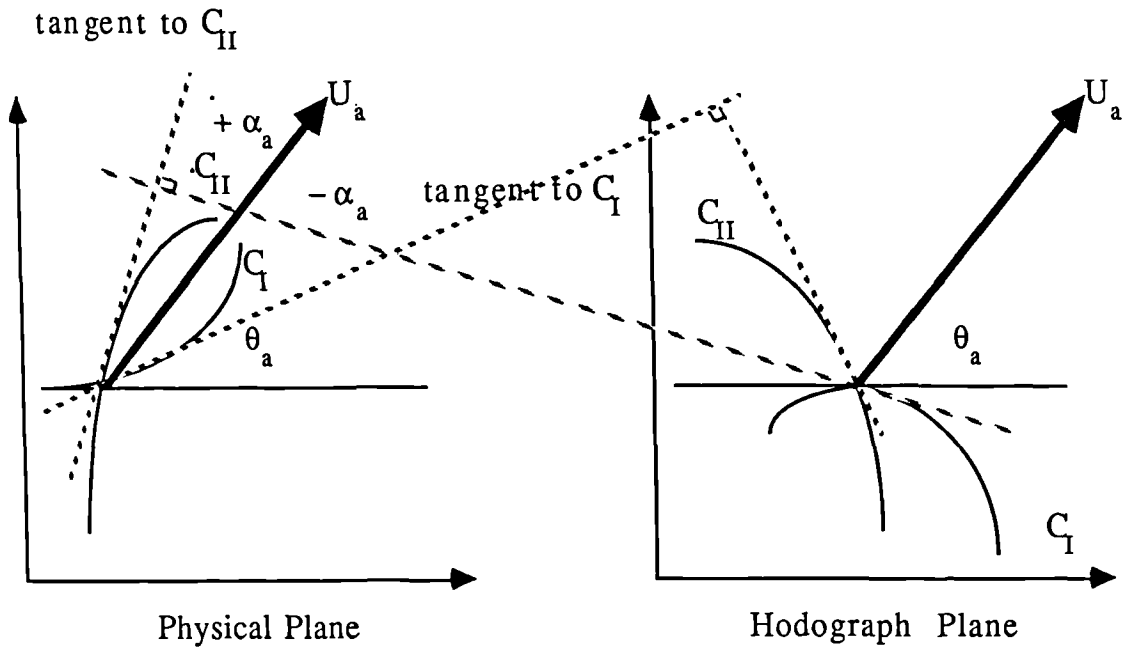

Figure 3.5. Relation between Slopes of Characteristic Curves in the Physical and Hodograph Planes.

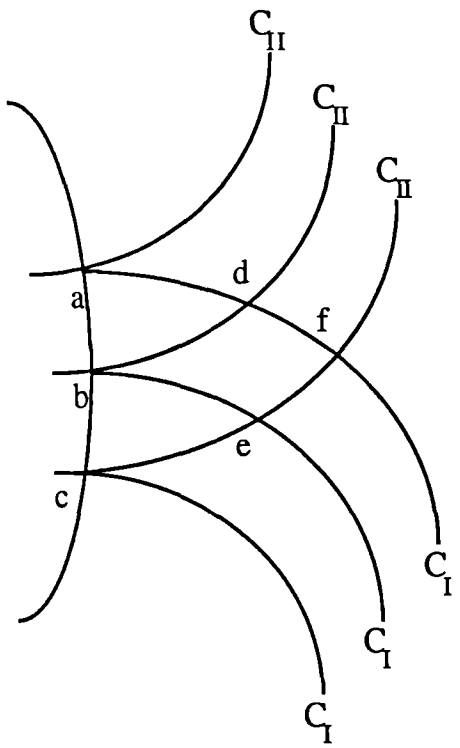

Figure 3.6. Construction of Characteristic Curves by the Lattice-Point Method.

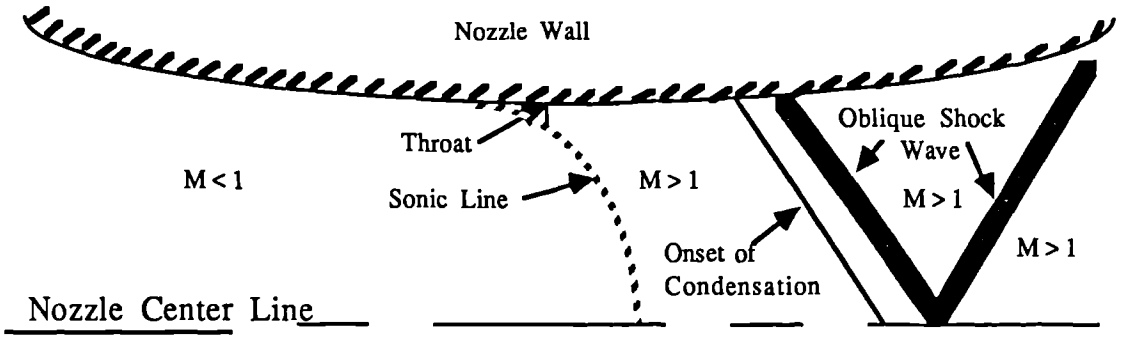

(a) Oblique Condensation Shock.

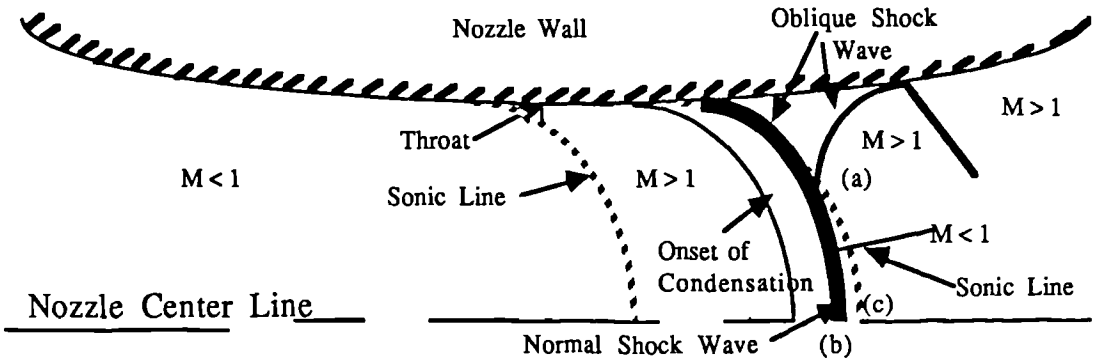

(b) Bifurcated Condensation Shock.

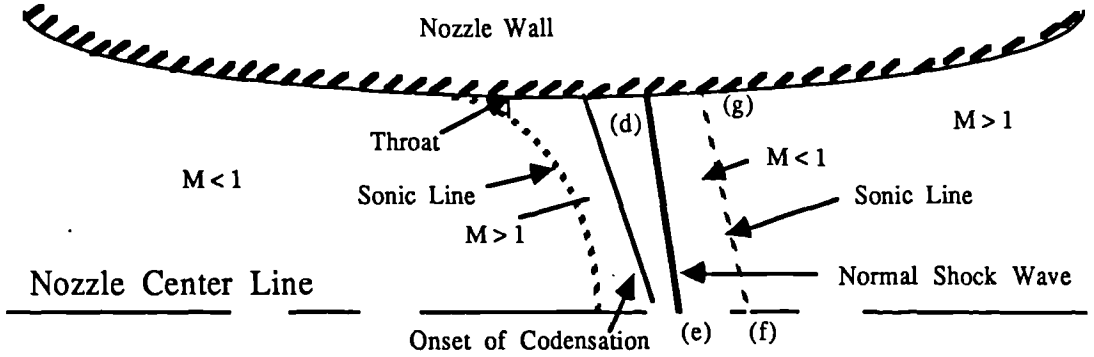

(c) Normal Condensation Shock.

Figure 3.7. Mechanism of Formation of Condensation Shock (after Matsuo et al (1985)).

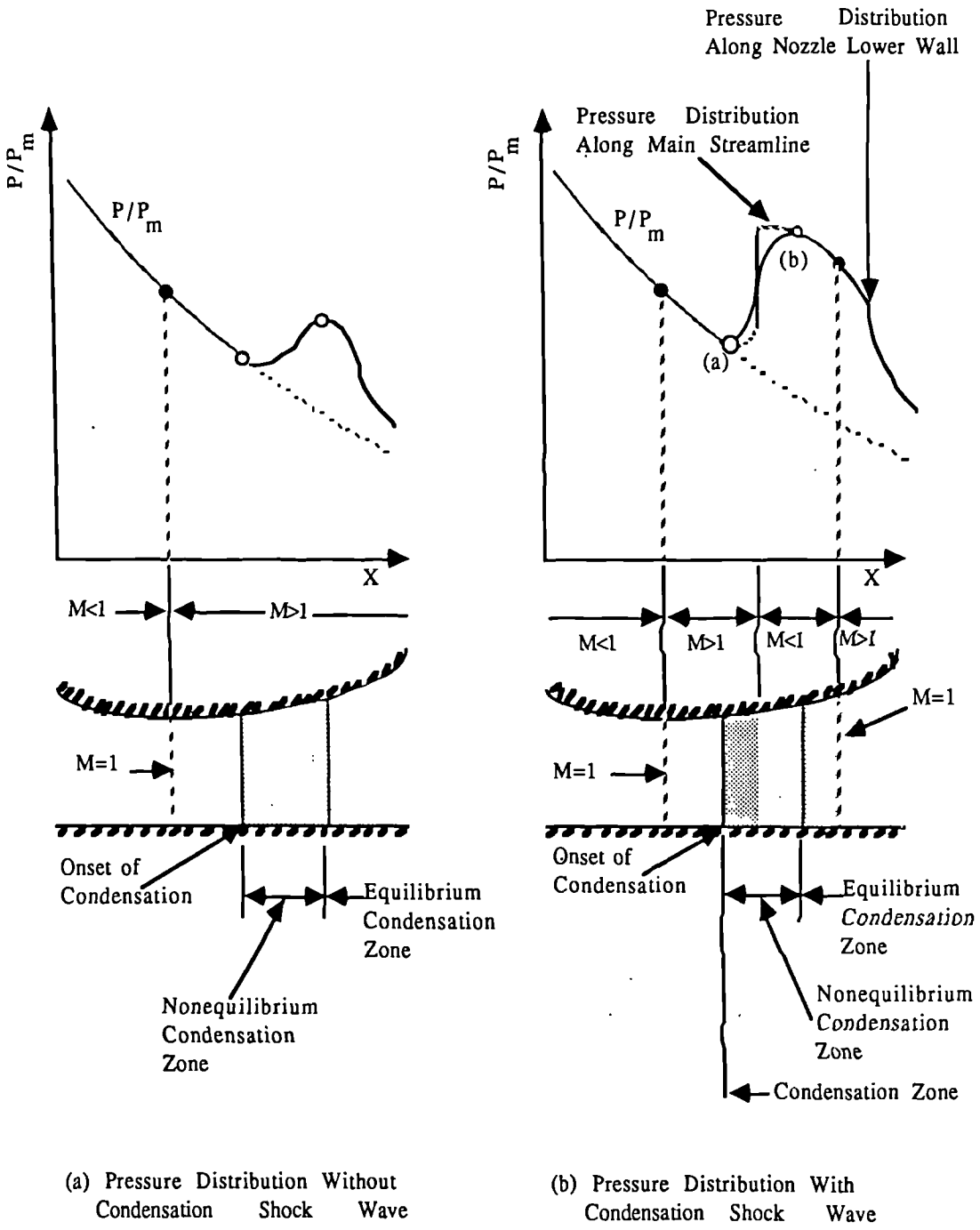

(a) Pressure Distribution Without Condensation Shock Wave

(b) Pressure Distribution With Condensation Shock Wave

Figure 3.8. Mechanism of Flow with Condensation (after Matsuo et al (1986)).

CHAPTER FOUR

SUPERSONIC JETS IN EJECTORS

4.1. INTRODUCTION :

In general, and according to the gas-dynamic parameters the flow field in a supersonic jet exhausting into a stationary medium or a uniform subsonic stream can be divided into three regions (Abramovich 1963) as shown in Figure (4.1a.) :

(a) The gas dynamic region,

(b) Transition region, and

(c) The basic region.

Moreover, three regimes of flow can be distinguished on the basis of (n) which is the ratio between the nozzle exit pressure (P_e) and the suction pressure (P_s), (Ramskill (1985)) :

(1) The overexpanded regime ($n < 1$)

(2) The nominal regime ($n = 1$)

(3) The underexpanded regime ($n > 1$)

The basic differences between the jets, corresponding to these three regimes, lie near the nozzle exit in the "initial gas-dynamic region", which is sometimes called the "first barrel". In this chapter our interest lies in jets of this type of underexpanded regime.

4.2. General Description of Underexpanded Jet Structure :

4.2.1. Structure of the Turbulent Axially Symmetric Underexpanded Jet :

The underexpanded jet can, in turn, be divided into two further regimes; depending on the value of (n), (Ramskill (1985)) :

(i) $1.1 < n < 2$ The jet is moderately underexpanded

(ii) $2 < n < \infty$ The jet is highly underexpanded

4.2.1.1. The Moderately Underexpanded Regime :

In this regime a periodic structure is formed due to the superposition of expansion and compression waves when they are reflected from the jet boundaries. This, in turn, creates a system of density discontinuities or *oblique shocks* which appear inside the jet. The behaviour of these oblique shocks is said to be regular shock reflection as they intersect on the jet axis to give a characteristic "shock diamond" or "cell" structure (Figure 4.1a.).

If we enlarge the dotted circle in Figure (4.1a.), we get a picture showing the pressure regions inside the first shock cell (Figure 4.1b.). This picture is for an ideal supersonic underexpanded jet. In region (1), the internal pressure inside the jet is higher than the external suction pressure (P_s). In region (2)

and (4) the pressure must be equal to (P_s) as there are no pressure discontinuities possible across the jet boundary.

Hence, the waves which separate region (1) from (2) are called expansion waves. In region (3) the pressure is relatively low, and as the pressure in region (4) is equal to the suction pressure, the waves between region (3) and region (4) are called compression waves. After the intersection of these waves a recovery of the pressure occurs to the original value of the pressure ratio, and the pressure in region (5) will be equivalent to the pressure in region (1). Ideally, this pattern is repeated in the absence of friction but in practice this periodic structure soon dies out.

4.2.1.2. The Highly Underexpanded Regime :

In this region irregular shock reflection occurs at the start of the jet causing a normal shock or Mach Disk instead of the oblique shocks crossing. It is thought that it will be repeated possibly twice (Ramskill (1985)) and then the shocks will be of an oblique structure as shown in Figure (4.2a.).

In this normal shock (Figure 4.2b.), an expansion fan forms, at the tip of the nozzle, and moves out until it reaches the suction pressure at the jet boundary. Then, to keep this constant pressure boundary; the expansion waves reflect as compression waves,

which in turn form the oblique intercepting shock. As these shocks are oblique to the upstream jet flow, they require the downstream flow to be supersonic and increasing in strength towards the axis. The cylindrical character of the barrel shock and the singularity as the axis is approached causes the barrel shock to degenerate into a Mach Disk and reflected shock.

When the reflected shock meets the constant pressure boundary the conditions may be similar to the original conditions at the tip of the nozzle and so the process may be repeated for a second time. The slip line separates the subsonic flow which passed through the Mach Disk and the supersonic region. This could be repeated twice (Ramskill (1985)) , as the flow decelerates forming a structure of oblique shocks until reaching the developed region of the jet.

4.2.2. Calculation of some Jet Dimensions :

In the supersonic jet, the gas-dynamic region can be characterised by the following geometric parameters (Figure 4.3.) :

$\bar{w}$: The length of the first barrel

$\bar{l}$: The position of the point at which the incident shock (Mach Disk) is reflected

$\bar{\lambda}$: The wave length of the periodic structure (i.e. the distance between shock-reflection points)

These three parameters are made dimensionless with respect to the outlet diameter of the nozzle (d_o).

4.2.2.1. Determination of the Length of the First Barrel ($\bar{w}$) :

Many references put forward methods of calculating the length of the first barrel. Love (1959) proposed an empirical formula for finding out this length for any values of (n) and the Mach exit number (M_e) :

when $n \leq 2$

$$\bar{w} = 1.55\sqrt{n M_e^2 - 1} - 0.55\sqrt{M_e^2 - 1} \qquad 4.1\,a.$$

when $n \geq 2$

$$\bar{w} = 1.52\, n^{0.437} + 1.55\sqrt{2M_e^2 - 1} - 0.55\sqrt{M_e^2 - 1} + 0.3226\sqrt{(n-2)(M_e^2 - 1)} - 2.05 \qquad 4.1\,b.$$

Che^-haing (1968) derived similar semi-empirical relation for ($\bar{w}$) :

when $n \leq 2$

$$\bar{w} = 1.55\sqrt[5]{M_e}\left[\sqrt{n M_e^2 - 1} - \sqrt{M_e^2 - 1}\right] + \sqrt{M_e^2 - 1} \qquad 4.2\,a.$$

when $n \geq 2$

$$\bar{w} = \left[1.55\sqrt[5]{M_e}\left[\sqrt{n M_e^2 - 1} - \sqrt{M_e^2 - 1}\right] + \sqrt{M_e^2 - 1}\right]\left(\frac{n}{2}\right)^t \qquad 4.2b.$$

where

$$t = \frac{0.523}{\sqrt{M_2}} \qquad \text{when } M_e \leq 1.5 \qquad 4.3a.$$

$$t = 0.451 - 0.016\, M_e \qquad \text{when } M_e \geq 1.5 \qquad 4..3b.$$

Antsupov (1974) correlates ($\bar{w}$), also, for supersonic jets :

$$\bar{w} = \frac{n}{0.80+0.25\, n} \sqrt{\gamma \left(M_e^2 - 1 \right)} \qquad 4.4.$$

for any value of (n).

4.2.2.2. Determination of the Distance to the Mach Disk ($\bar{l}$) :

Two of the mentioned references in the last paragraph have suggested empirical correlations for this distance ($\bar{l}$). Che^-haing (1968) linked it with ($\bar{w}$) in the formula :

$$\bar{l} = 0.8\ \bar{w} \qquad 4.5.$$

for any value of (n).

while Antsupov (1974) gave this correlation :

$$\bar{l} = \frac{n}{1.2+0.3\, n} \sqrt{\gamma \left(M_e^2 - 1 \right)} \qquad 4.6.$$

for any value of (n).

4.2.2.3. Determination of the Wave Length of the Periodic Jet Structure ($\bar{\lambda}$) :

The wave length of the periodic jet structure is the distance between two adjacent shock-reflection points. Prandtl (1952), has given an equation relating ($\bar{\lambda}$) to the mean jet diameter (d_m) and the exit Mach number (M_e) :

$$\bar{\lambda} = 2\, d_m \sqrt{M_e^2 - 1} \qquad 4.7.$$

for any value of (n).

while Antsupov (1974) described ($\bar{\lambda}$) by the following equation as a function of (n) and the exit Mach number (M_e) :

$$\bar{\lambda} = \left(1.05\sqrt{n} - 0.1\right)\sqrt{\gamma\left(M_e^2 - 1\right)} \qquad 4.8.$$

for any value of (n).

4.3. Jet Characteristic Net by the Use of Method of Characteristics :

4.3.1. Introduction :

To predict theoretically the shape of the steam jet inside the ejector the method of characteristics was applied. Chow and Addy (1964) have also applied the method of characteristics in their

model to predict the jet in the ejector. The analysis, which is presented here, was used to predict the jet in the steam ejector. The system will have these basic geometric features (Figure (4.4.)) :

(1) A convergent-divergent primary nozzle, assumed always to flow full, which produces a supersonic underexpanded jet at its exit.
(2) The jet flows into a diffuser mixing tube.

The flow model is shown in Figure (4.5.) and based on the following assumptions :

(1) The primary flow is solved by the method of characteristics for two-dimensional, steady, and irrotational supersonic flow.
(2) The secondary flow can be treated by the use of the one-dimensional gas dynamic equations.
(3) The two flows are treated uniformally at their entrance to the mixing tube, i.e. section (m).
(4) There is a pressure continuity across the boundary between the two flow, before mixing occurs between them.

4.3.2. Calculation of the Jet Characteristic Net :

The method of characteristics for two-dimensional, steady, irrotational flow, which is described thoroughly in chapter three, left us at the end with these two equations :

$$\theta + \nu = C_I \qquad \text{for characteristic } C_I \qquad 4.9.$$

$$\theta - \nu = C_{II} \qquad \text{for characteristic } C_{II} \qquad 4.10.$$

This means that the flow will consist of two sets of families, one of left-running waves (Mach waves of family II), and the other of right-running waves (Mach waves of family I). These two equations can be written (Shapiro (1953)) :

$$\theta + \nu = 2\,I - 1000 \qquad 4.11.$$

$$\theta - \nu = 2\,II - 1000 \qquad 4.12.$$

By adding and then subtracting these two equations we get :

$$\theta = I + II - 1000 \qquad 4.13.$$

$$\nu = I - II \qquad 4.14.$$

where (ν) is the turning angle of the flow i.e. the Prandtl-Meyer angle and equal to :

$$\nu = \sqrt{\frac{\gamma+1}{\gamma-1}}\ \arctan\sqrt{\frac{\gamma-1}{\gamma+1}\,(M^2-1)} - \arctan\sqrt{M^2-1} \qquad 4.15.$$

To get the calculations for the characteristic net started the ejector geometry (Figure 4.4.), and some experimental data should be given :

X_o, Y_o : The coordinates for the tip of the nozzle

A_{sm} : The secondary flow area at the inlet section (m)

h : The distance between the tip of the nozzle and the start of the diffuser throat section (i.e. the parallel mixing tube)

Y_t : The distance from the ejector centre line to the diffuser wall in the constant area diffuser section (i.e. the parallel mixing tube)

Y_s : The distance from the ejector centre line to the diffuser wall at the section (m)

Beta/2 : Half the convergent angle of the ejector entrance

P_{sm}/P_{os} : The ratio of the secondary flow static pressure at section (m) over the stagnation pressure of the secondary flow

P_{sm}/P_{op} : The ratio of the secondary flow static pressure at section (m) over the stagnation pressure of the primary flow

M_e : The Mach number at the exit of the nozzle.

As the steam flow reaches the tip of the nozzle, it undergoes a Prandtl-Meyer expansion fan centred at the nozzle corner. The calculation for the flow properties will be solved by using the "Lattice Point Method" which was explained in Section (3.2.4.). To make the calculation as clear as possible, the solution was divided into a number of sections.

4.3.2.1. Calculation of the First Left-Running Wave (1-(nw+1)) :

Figure (4.5.) shows the flow model for the jet going out of the nozzle. The first step in the calculation is to find out the Prandl-Meyer expansion fan angle $(v)_{nw}$ for the flow which is divided, in this calculation, to a number of Mach waves (nw), with

equal interval or step. On the last wave of this expansion fan, we have two points from the same family wave (I), i.e. point (o) on the nozzle corner and the point (nw). At these two points, the pressure must be equal to the secondary flow pressure, in order to satisfy the assumption made, i.e. the pressure continuity across the boundary.

Starting the calculation, by using the given value (P_{sm}/P_{op}), the inlet Mach number for the primary flow will be calculated using the one-dimensional isentropic relation :

$$M_{pm} = \sqrt{\left(\frac{2}{\gamma-1}\right)\left[\left(\frac{P_{sm}}{P_{op}}\right)^{-\left(\frac{\gamma-1}{\gamma}\right)} - 1\right]} \qquad 4.16.$$

Then substituting the calculated value of (M_{pm}) into Equation (4.15.), the value of $(\nu)_{nw}$ can be calculated.

Since we are working with a supersonic nozzle ; (M_{po}) will definitly have a value greater than one. So, using Equation (4.15.), the value of $(\nu)_1$ can be found. Also, as point (1) is on the centre line, $(\theta)_1$ will be equal to zero. Therefore, using Equations (4.13.) and (4.14.) leads to :

$$(I)_1 = \frac{1000 + (\nu)_1}{2} \qquad 4.17.$$

and

$$(II)_1 = \frac{1000 - (\nu)_1}{2} \qquad 4.18.$$

Now, knowing the information about the starting point (1). It is possible to get the values of (θ), (ν), (I), and (II) until the point (nw); as all of them are on the same wave of family (II), i.e. :

$$(II)_1 = (II)_2 = \cdots\cdots\cdots = (II)_{nw} = \frac{1000 - (\nu)_1}{2}$$

and (ν) is known by the equation below :

$$(\nu)_i = (\nu)_1 + (i - 1)\,\text{step} \quad ; \; (i = 2, nw)$$

where "step" is the interval into which the angle $(\nu)_{nw}$ is divided.

The Mach number (M_p) for the same points can be found iteratively for a known value of (ν) from Equation (4.15.). Then, the fluid properties for all these points can be found by using the equations :

$$\frac{P_p}{P_{op}} = \left[1 + \left(\frac{\gamma - 1}{2}\right) M_p^2\right]^{\left(\frac{-\gamma}{\gamma - 1}\right)} \qquad 4.19.$$

$$\frac{T_p}{T_{op}} = \left[1 + \left(\frac{\gamma - 1}{2}\right) M_p^2\right]^{-1} \qquad 4.20.$$

$$\frac{\rho}{\rho_{op}} = \left[1 + \left(\frac{\gamma-1}{2}\right) M_p^2\right]^{\left(\frac{-1}{\gamma-1}\right)} \qquad 4.21.$$

$$\alpha = \arcsin\left(\frac{1}{M_p}\right) \qquad 4.22.$$

In order to get the characteristics line drawn, it remains to calculate the physical coordinates of the point (1) to (nw). These can be determined by the use of Equations (3.45a.), (3.45b.), (3.46a.), and (3.46b.).

The only remaining point on this wave is the boundary point (nw+1). At the plane of this point, it is clear that the pressure is different from that at the inlet section (m). But, to get the fluid properties for this point it is estimated that the pressure at this boundary point is equal to the pressure at the inlet section (m), i.e. (P_{sm}). At this stage, we have three points with the same pressure : point (o), point (nw), and the boundary point (nw+1). Therefore, the two points (nw) and (nw+1) have the same fluid properties since both have the same pressure and are on the same family wave (II). Finally, the physical coordinates can be found from the same four previous mentioned equations.

4.3.2.2. Calculation of the Second Left-Running Wave ((nw+2)-2(nw+1)) :

The calculation for the points on this line wave are similar to

the previous calculation. Starting with the first point (nw+2) its (θ) will be equal to zero as it is on the centre line, and it lies on the wave of family (I) as point (2), therefore :

$$\theta_{(nw+2)} = 0.0 \qquad 4.23.$$

$$I_{(nw+2)} = I_{(2)} \qquad 4.24.$$

Then, by using the two Equations (4.13.) and (4.14.), the values of $II_{(nw+2)}$ and $\nu_{(nw+2)}$ can be found. After finding out $(M_p)_{(nw+2)}$ the remaining fluid properties can be found from Equations (4.19.) to (4.22.) and then the physical coordinates can be found. From Equation (4.31.), it can be said, for the points from (nw+3) to (2nw+1) that :

$$I_{(i)} = I_{(i-nw)}$$

Also, as all these points are on the same wave family (II), then :

$$II_{(i)} = II_{(i-1)}$$

Using the two Equations (4.13.) and (4.14.); the values for $\theta_{(i)}$ and $\nu_{(i)}$ can be found. After finding out $(M_p)_{(i)}$ iteratively from Equation (4.15.); the remaining fluid properties for the points from (nw+3) to (2nw+1) can be found using the Equations (4.19.) to (4.22.).

With the final point on this line wave, i.e. the boundary point (2(nw+1)) we have :

$$II_{(2(nw+1))} = II_{(2nw+1)}$$

Again, the same assumption for the first boundary point (nw+1) is applied here and the physical coordinates for the points of this wave are found in the same way as the previous wave.

In this way, the calculation may then be continued to other points in the flow field, and the complete net of characteristic lines describing the first barrel of the flow properties can be found until the shock wave takes place in the flow field.

4.4. Conclusions:

The whole calculation process is carried through using a computer program and it is presented in Appendix IV. Such a program was written for steam-air ejectors and was based on the method presented by Benson and Eustace (1973). Using this computer program, the net characteristic curves for any set of experimental data can be constructed.

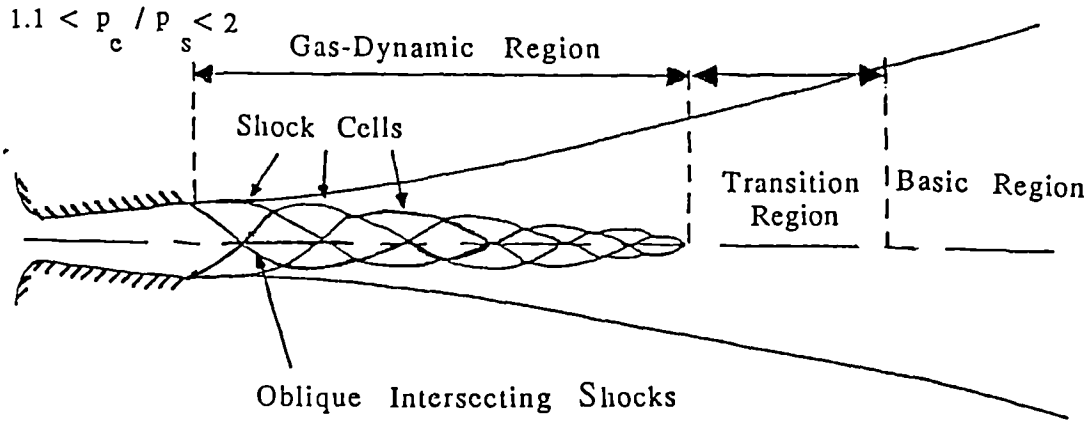

Figure 4.1a. Diagram of a Moderately Underexpanded Jet (after Ramskill).

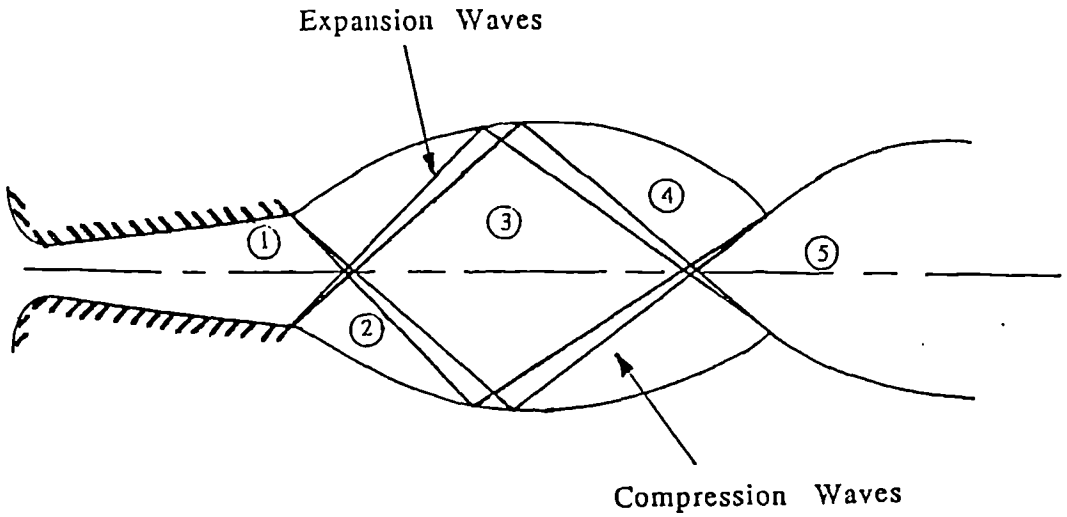

Figure 4.1b. Diagram Showing the Pressure Regions Inside an Underexpanded Jet (after Ramskill).

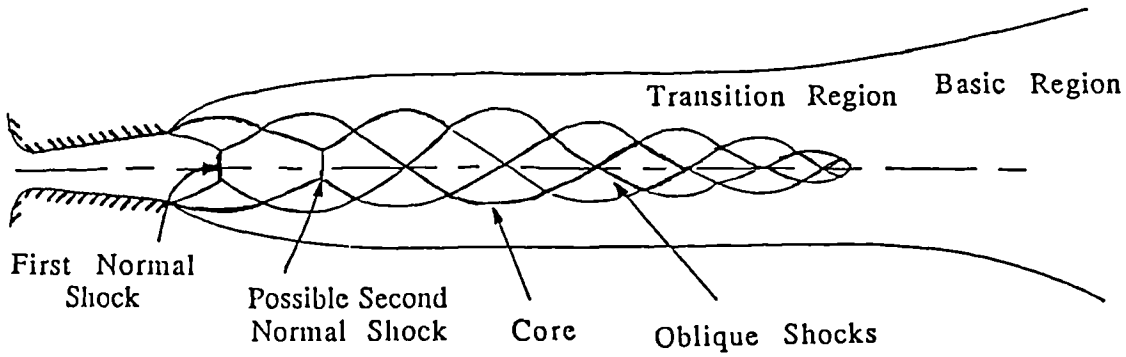

Figure 4.2a. Diagram of a Highly Underexpanded Jet (after Ramskill).

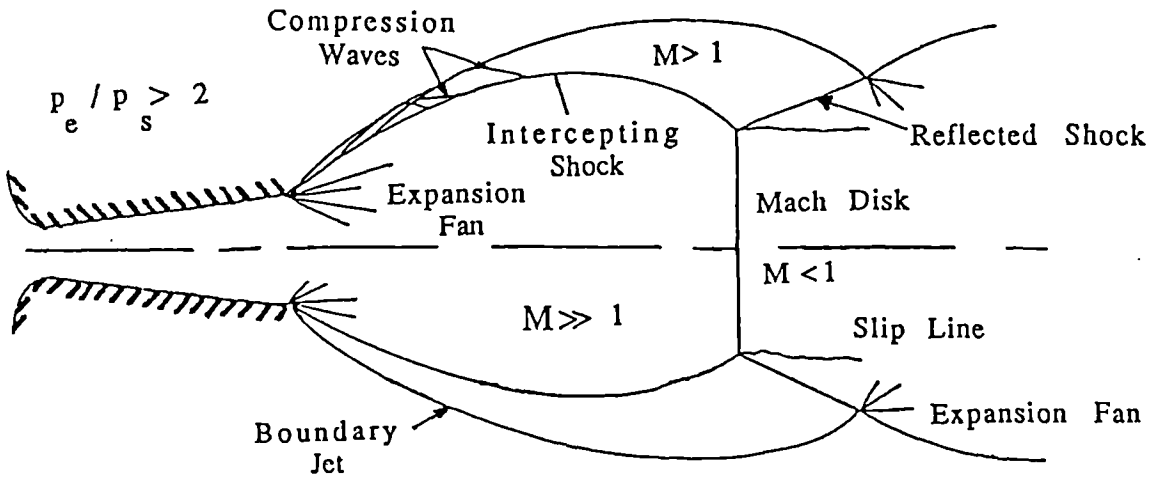

Figure 4.2b. Diagram Showing the Normal Shock in a Highly Underexpanded Jet (after Ramskill).

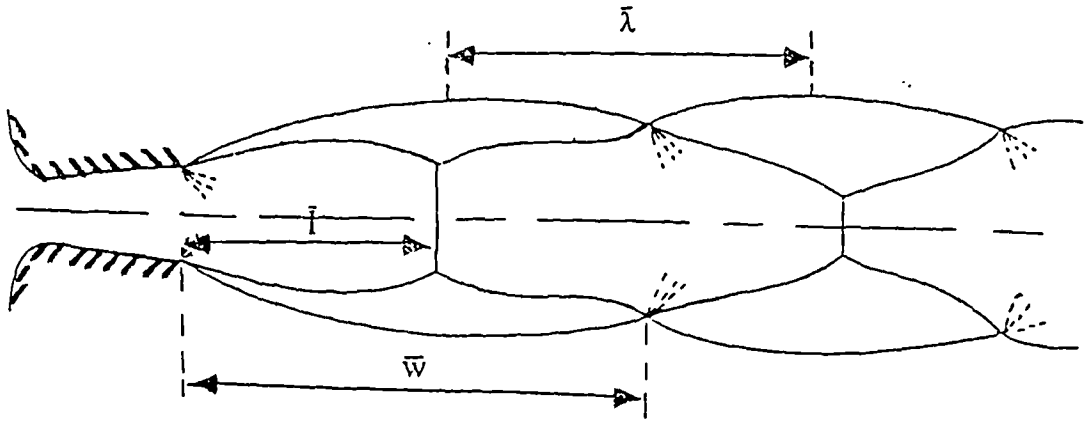

Figure 4.3. The Geometric Parameters of the Gas-Dynamic Region (after Adamson).

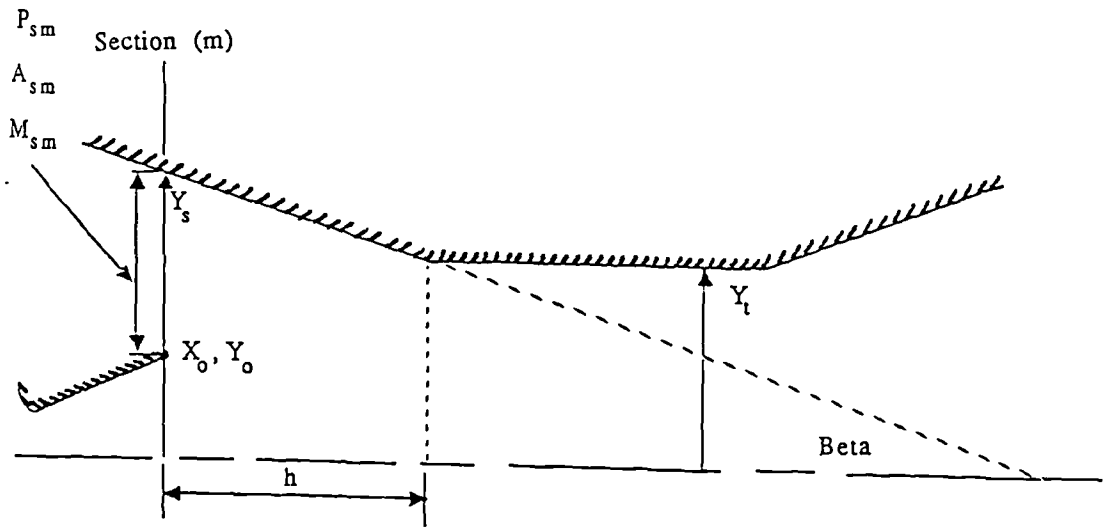

Figure 4.4. The Ejector Geometry.

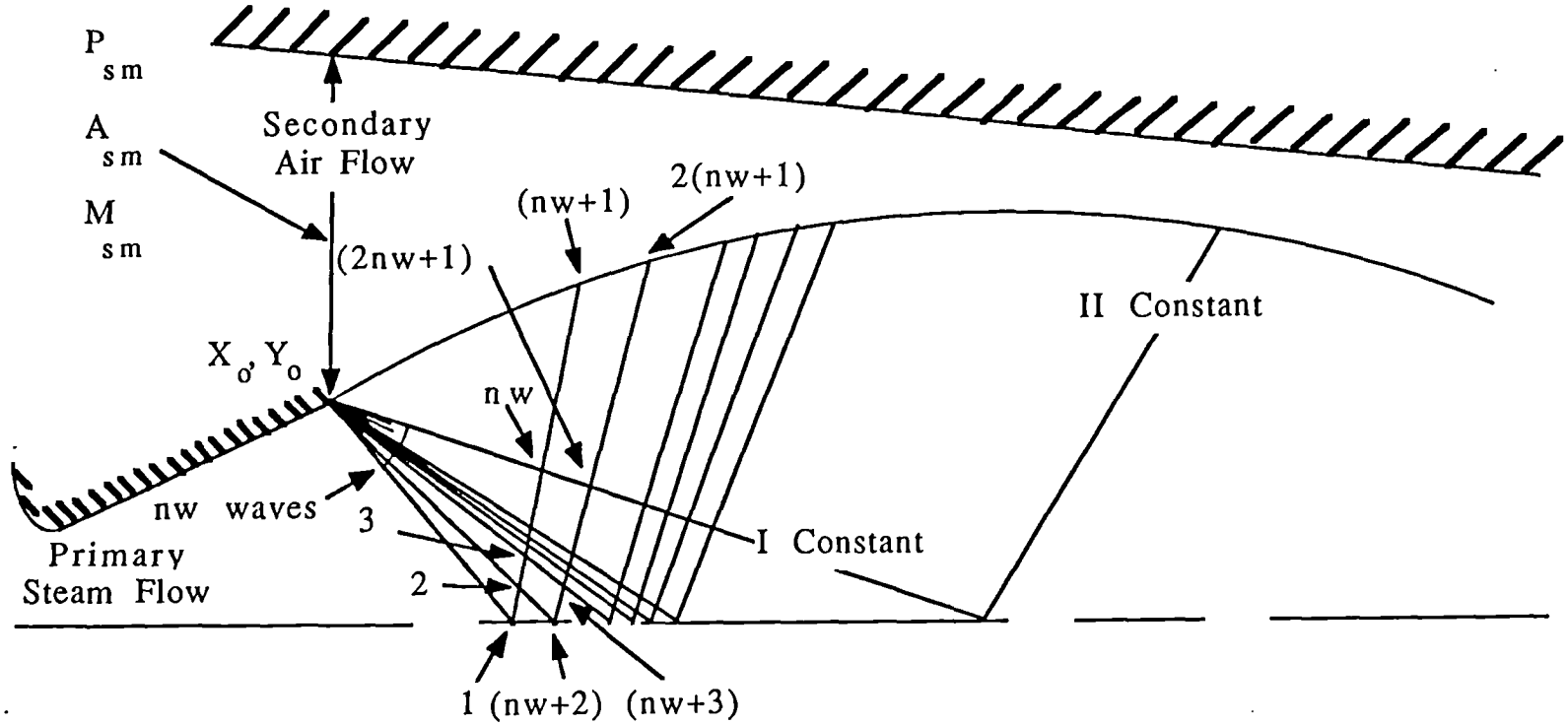

Figure 4.5. The Flow Model Analysed by the Method of Characteristics.

CHAPTER FIVE

TEST EQUIPMENT AND INSTRUMENTATION

5.1. Introduction :

As it was explained in chapter one; the steam ejector is comprised of an expanding steam nozzle producing high supersonic velocities, a suction branch to admit the air load, a combining chamber for mixing the motive steam with the entrained air, and a diffuser to compress the mixture to the discharge pressure. From experimental work done by previous investigators, for example Mellanby (1928), it has been shown that the shape of the air inlet has no effect on the characteristic performance of the ejector and on the nozzle optimum distance (L_{op}). It was decided, therefore, in presenting the results of the experimental work, to take into consideration only the dimensions of the nozzle and the diffuser.

5.2. Experimental Objectives :

The main experimental objective was to find, for the highest vacuum for a given load, the optimum distance (L_{op}) between the nozzle outlet and the diffuser throat. This could be found by physically varying the nozzle distance relative to the diffuser body, when testing the ejector, until the highest vacuum was obtained.

Rather than finding this distance for every ejector in this way, the need is to find some correlation or empirical equation relating this distance with the dimensional parameters of the ejector i.e. the dimensions of the nozzle and the diffuser; taking into consideration the motive steam pressure (P_m) and the air load i.e. the mass of air (m_a) that must be entrained, so that it can be "set" when the ejector is assembled.

The experimental work was carried out on two test facilities; one for a single and the other a two-stage ejector.

5.3. General Equipment :

Each test facility consisted of the ejector together with associated pipework, for admitting the steam, and control valves. Mounted on the suction branch of the ejector was a "blind" pipe into which was fitted five sonic nozzles for setting the air load. The discharge from the ejector passed into a direct water spray condenser. More detail of the equipment is given in the following paragraphs.

5.3.1. Boiler :

The motive steam was supplied by a boiler which produced steam at pressures of between 135 and 150 (psig.). As the rig, on which the experimental work was carried out, is away from the

boiler; the steam pressure reaches the rig after passing through a reducing valve at a maximum of 105 (psig.). Steam pressure was measured by the use of a "Bourden" gauge.

5.3.2. Condenser :

The outlet mixture of the motive steam and the induced air from the diffuser exit was passed into a direct contact spray condenser supplied, by a pump, with a flow rate of 700 gal/hr of water in order to condense the steam. The condensate and the water were then fed to the drain via gravity into a hotwell and any non-condensate steam was carried over with air through a vent in the top of the condenser.

The condenser itself was constructed of a 22 8.6 (mm)diameter QVF glass approximately fifty (cm) high. It was connected to the ejector through 7.5 (cm) diameter expansion bellows to isolate it from vibration and possible damage. The spray nozzle was situated centrally in the top of the condenser. The condensate and spray water were taken out through a 2.5 (cm) pipe diameter at the bottom of the condenser.

5.3.3. Airflow Measuring System :

The air intake system designed to HEI standards (HEI (1967)) is shown in Figure (5.1.). It consisted of a 35 (cm) length of a 5.08 (cm) dia. pipe which opened to a larger pipe, 30 (cm) long of a 10.16 (cm) dia.

pipe closed at its end. Mounted into this were five ASME long radius sonic nozzles each of a different diameter. Combination of these allowed the air load or the mass of air (m_a) entrained by the motive steam to be preset to a desired value. The diameters of these five nozzles had been measured accurately in order to calculate exactly the mass of air (m_a) that passed through them. The basic equations used in the calculation are presented in Appendix V and the diameters with the corresponding air mass flow rate for the nozzles are presented in Table (5.1.).

5.4. Description of the Single-Stage Ejector Rig :

The single-stage ejector rig is shown photographically in Figure (5.2.). The experimental work on this rig was carried out using sixteen ejectors, constructed from four diffusers and four nozzles. After manufacture, it was necessary to find a method of measurement to obtain their exact dimensions.

5.4.1. Measurement Steps for the Diffusers :

All the diffuser dimensions that must be found are shown in Figure (5.3.). The first and probably the easiest dimension to be determined was the diffuser throat diameter (D_{th}). This was done by the use of a ball micrometer. The ball micrometer was inserted into the diffuser throat and sighting it up until it had expanded to the diameter of the throat. Then, the ball micrometer was

withdrawn and the diffuser throat diameter (D_{th}) was found by measuring the set ball micrometer using a sliding vernier calliper.

The sliding vernier was used also to find the diffuser inlet diameter (D_i) and the outlet diameter (D_o). The only exact way to find out the length of the convergent and the divergent section (L_c) and (L_d) respectively inside the ejector was to construct a mould of these section by using Plaster of Paris. Firstly the diffuser was greased to ease the removal process of the mould, then a piece of "Bluetac" was inserted into the diffuser throat to act as a blockage for the plaster. The diffuser was then stood vertically and the plaster was poured into the convergent part.

After making sure that the plaster had hardened, it was removed by pushing the "Bluetac" from the other side of the diffuser. Once the mould was out, it was easy to mark the starting point of the convergence part and the length of this section of the diffuser (L_c) can easly be measured (Figure 5.4.). The same procedure was repeated to find out the length of the divergent section of the diffuser (L_d).

The overall length of the diffuser (L_T) was measured by using a tape measure, which from it after deducting the length of the convergent and the divergent parts (L_c) and (L_d), we found the length of the diffuser throat (L_{th}). The last two dimensions relevent

to the diffuser were the convergence and the divergence angles (Beta) and (Gamma) respectively. These can be found easily once we had the length of these sections (L_c) and (L_d), their outlet diameters (D_i) and (D_o) and the diffuser throat diameter (D_{th}). These measuring steps were repeated on the four diffusers and all the dimensions found are presented in Table (5.2.).

5.4.2. Measurement Steps for the Nozzles :

The principal dimensions of the nozzle were shown in Figure (3.1.). Finding the nozzle throat diameter (d_t) was more difficult than finding the throat diameter for the diffuser. It was impossible to use the ball micrometer because the nozzle throat was so small. The only way was to use a set of drill bits as shown in Figure (5.5a.) and find which was the best tight fit for the nozzle throat. The drill bit which fitted was then measured using a micrometer to get the size of the nozzle throat diameter (d_t).

The sliding vernier calliper was used to measure the outlet diameter (d_o). Measuring the length of the diverging section of the nozzle (l_c) was difficult when using the same approach used with the diffuser (i.e. the plastic mould) as it was impossible to push the mould out of the nozzle without destroying it. So, it was decided to insert a drill bit with a diameter slightly larger than the nozzle throat diameter (d_t) into the nozzle as shown in Figure (5.5b.), and

then mark it at the edge of the nozzle (point O) then the distance from that mark to the edge of the tip of this drill bit is measured which is nearly the length of the nozzle diverging section (l_c). At the end, the nozzle divergence angle (Zeta) could now be found by using the nozzle outlet diameter (d_o), the length of the diverging section (l_c) and the nozzle throat diameter (d_t). These measuring steps were repeated on the four nozzles and all the dimensions were found are presented in Table (5.3.).

5.4.3. The Spacers :

Seven spacers were made with different length (2, 3, 4, 5, 10, 15, and 20 mm). These spacers were used to alter the distance between the nozzle outlet and the diffuser throat, and a picture of them is shown in Figure (5.6.) together with the four nozzles and the four diffusers which formed the sixteen ejectors for this rig.

5.5. Description of the Two-Stage Ejector Rig :

This rig is shown in Figure (5.7.). Only the first (low pressure) stage was used for this investigation. This rig was manufactured by "Transvac Co. Ltd." as a "commercial" ejector. The design of the steam nozzle mounting allowed its position, relative to the diffuser, to be continuously varied by using an external adjustment screw. This permitted the nozzle optimum distance (L_{op}) to be obtained directly.

Three new nozzles were manufactured with divergence angle (Zeta) bigger than the original which was already in the ejector (Figure 5.8.) and their dimensions are presented in Table (5.4.) with the dimension of the original nozzle and the diffuser.

So, in total the experimental work on this rig was conducted by using four ejectors having the same diffuser and four different nozzles.

5.6. Ejectors Geometry :

Twenty ejectors were used on the two rigs for the experimental work. They are combinations of eight nozzles and five diffusers in total. As noted previously the dimensions for these nozzles and diffusers are presented in Tables (5.2. to 5.4.), and their combination is presented in Table (5.5.).

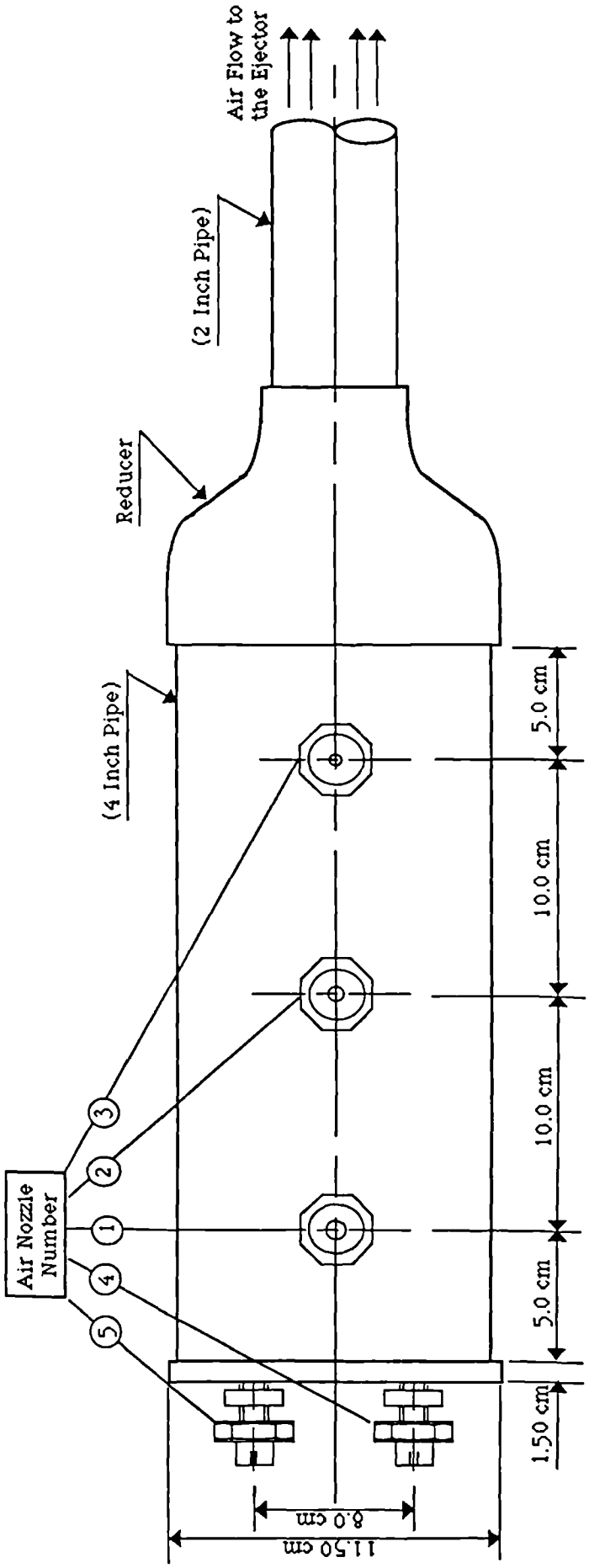

Figure 5.1. A Plan View for the Air Flow Measuring System

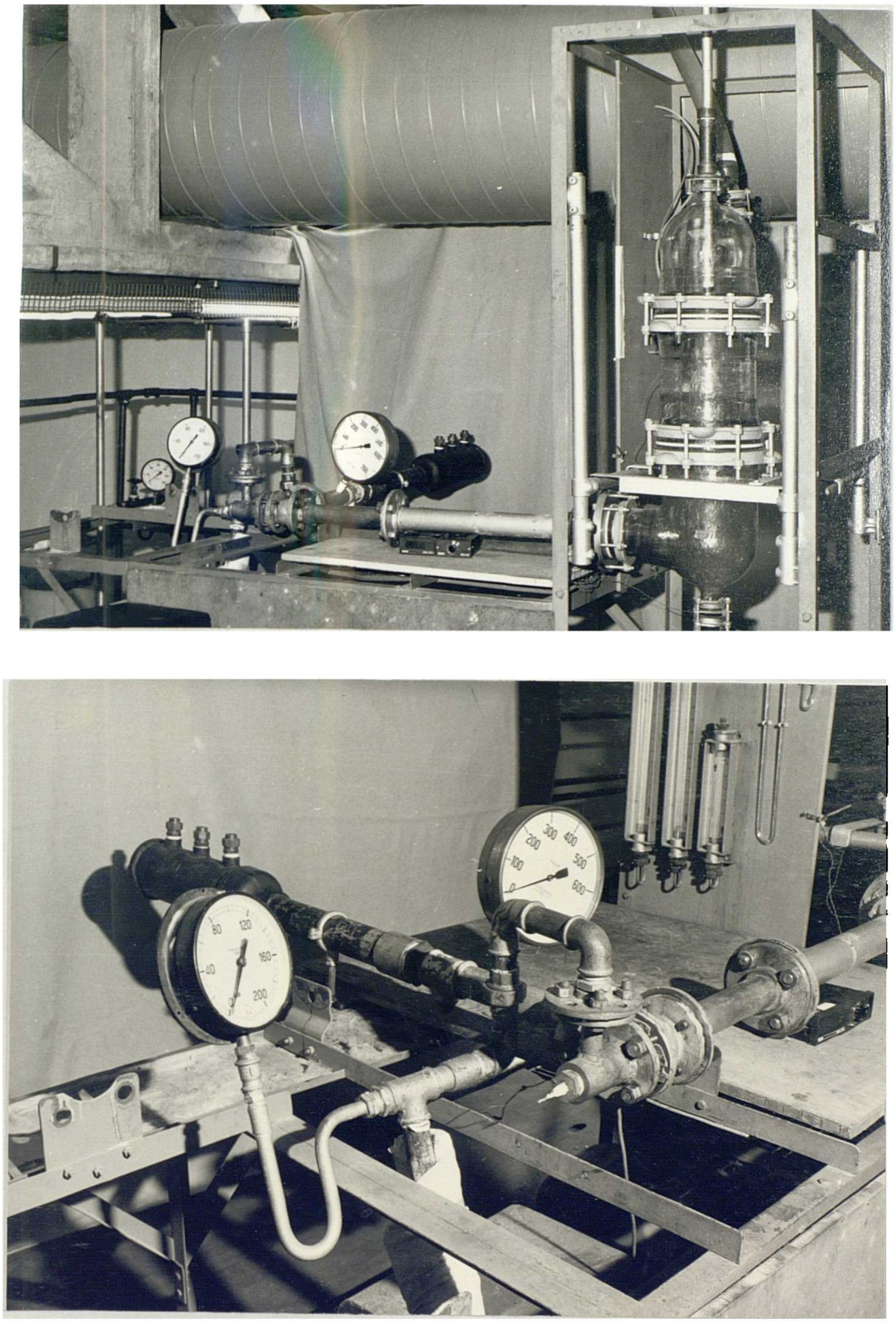

Figure 5.2. The General Arrangement of the Single-Stage Ejector Rig.

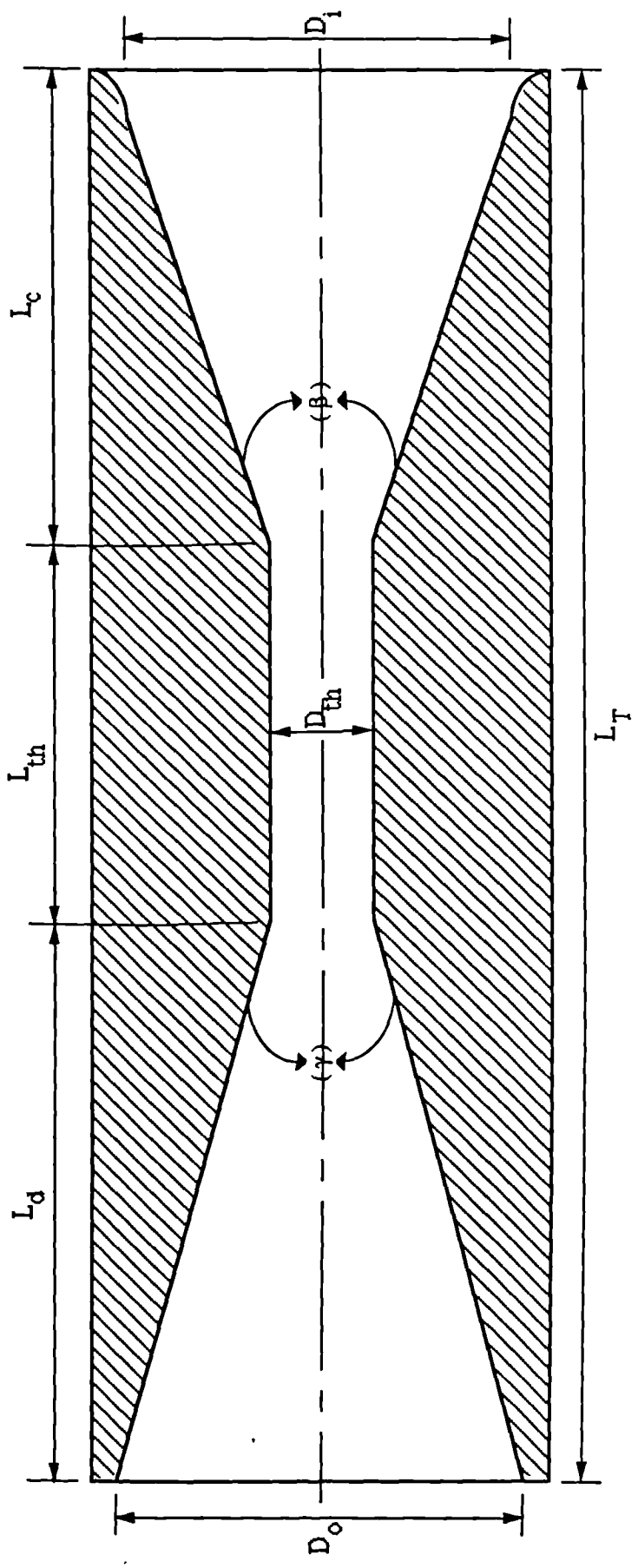

Figure 5.3. The Prinicipal Dimensions of the Diffuser.

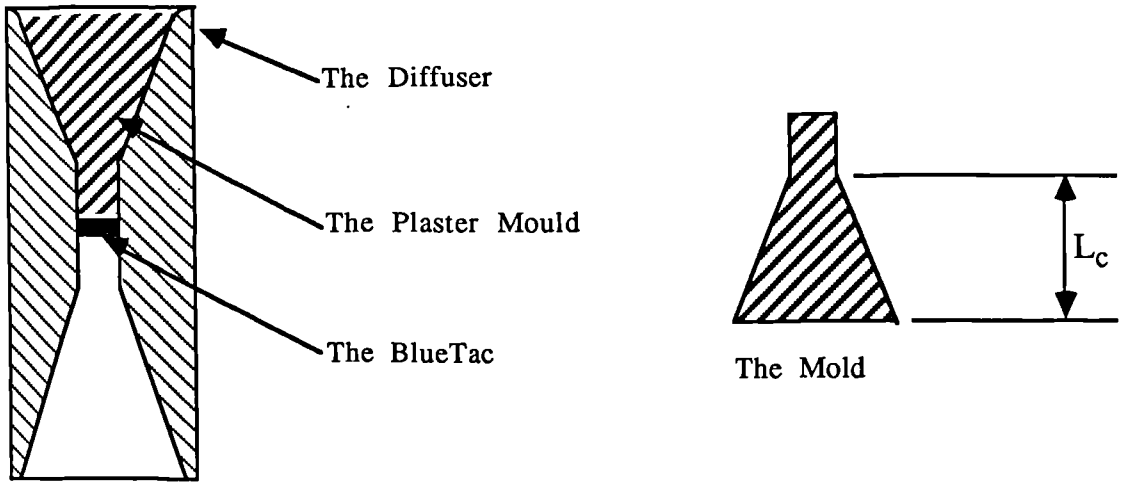

Figure 5.4. The Method by which the Convergent and the Divergent Section of the Diffusers were Measured.

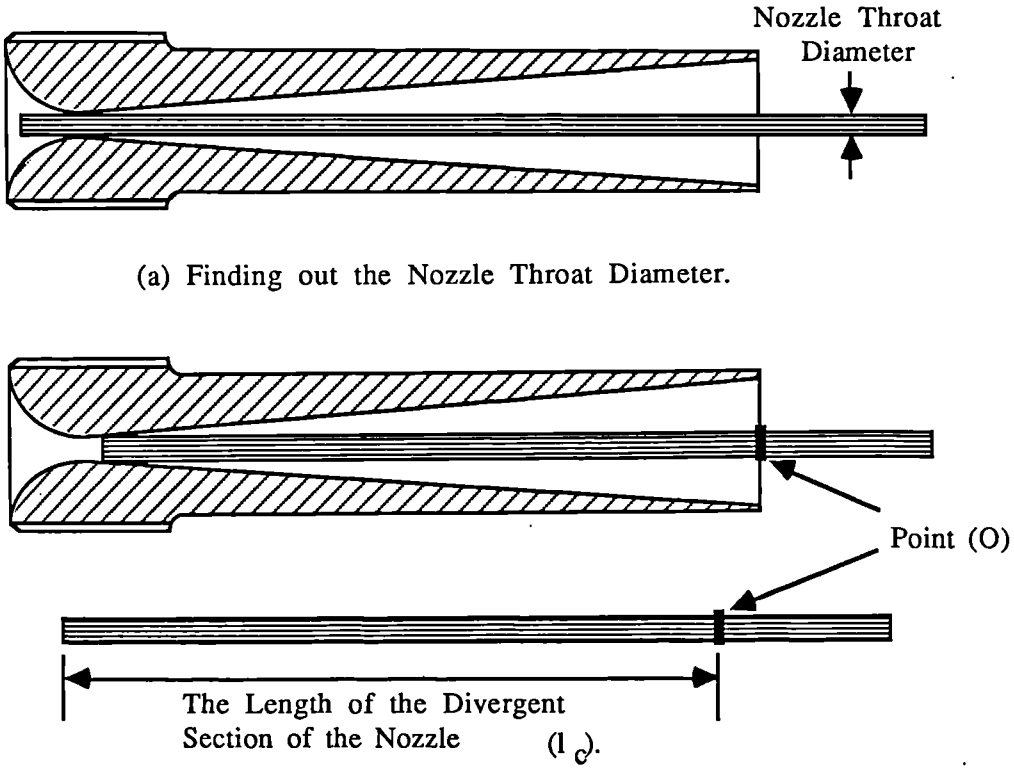

(a) Finding out the Nozzle Throat Diameter.

(b) Finding out the Length of the Divergent Section of the Nozzle.

Figure 5.5. The Method by which the Divergent Section of the Throat Diameters of the Nozzles were Measured.

Figure 5.6. The Spacers, the Nozzles, and the Diffusers that Were Used to Form the Sixteen Ejectors for the Single-Stage Rig.

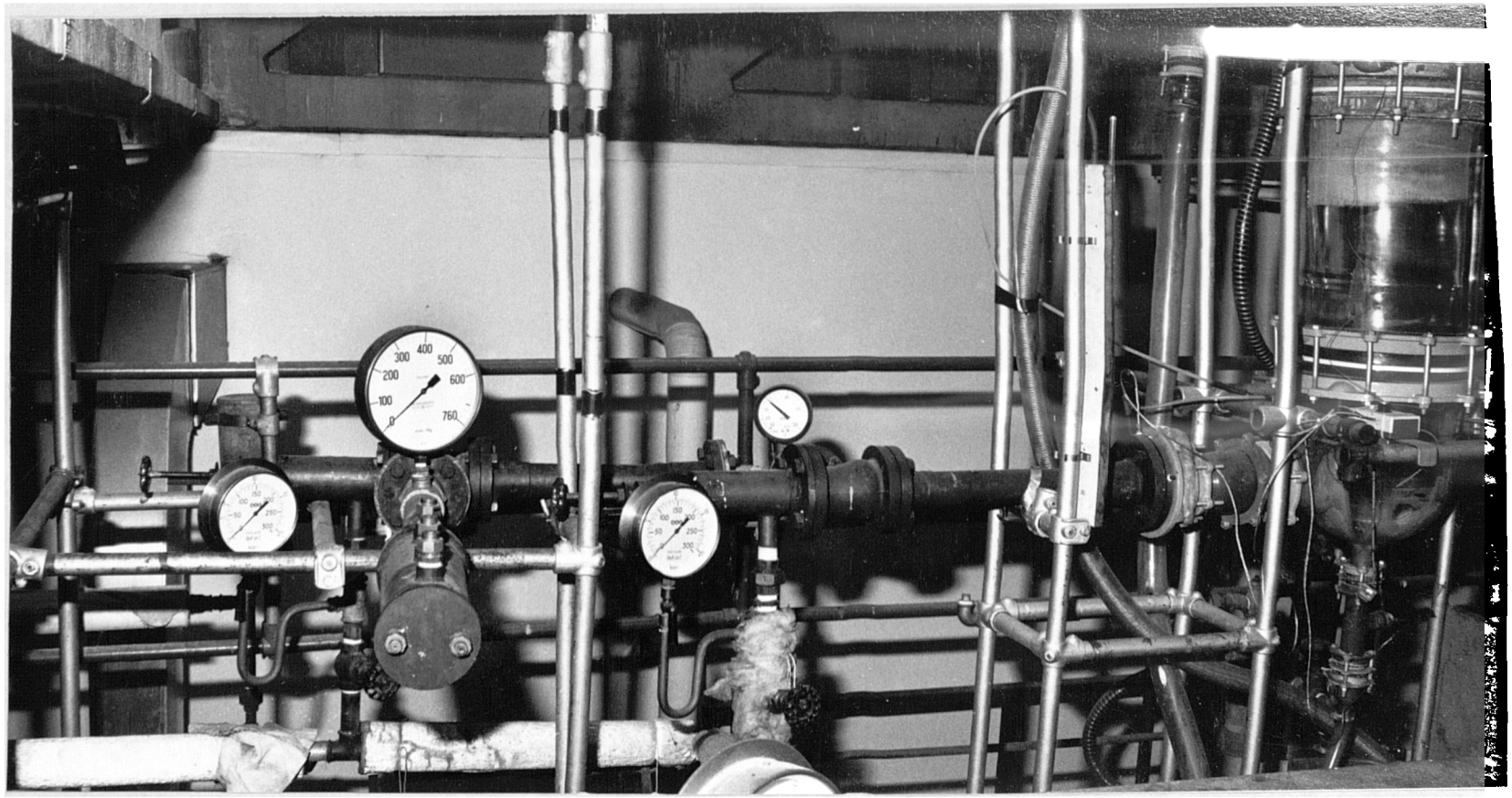

Figure 5.7. The General Arrangement of the Two-Stage Ejector Rig.

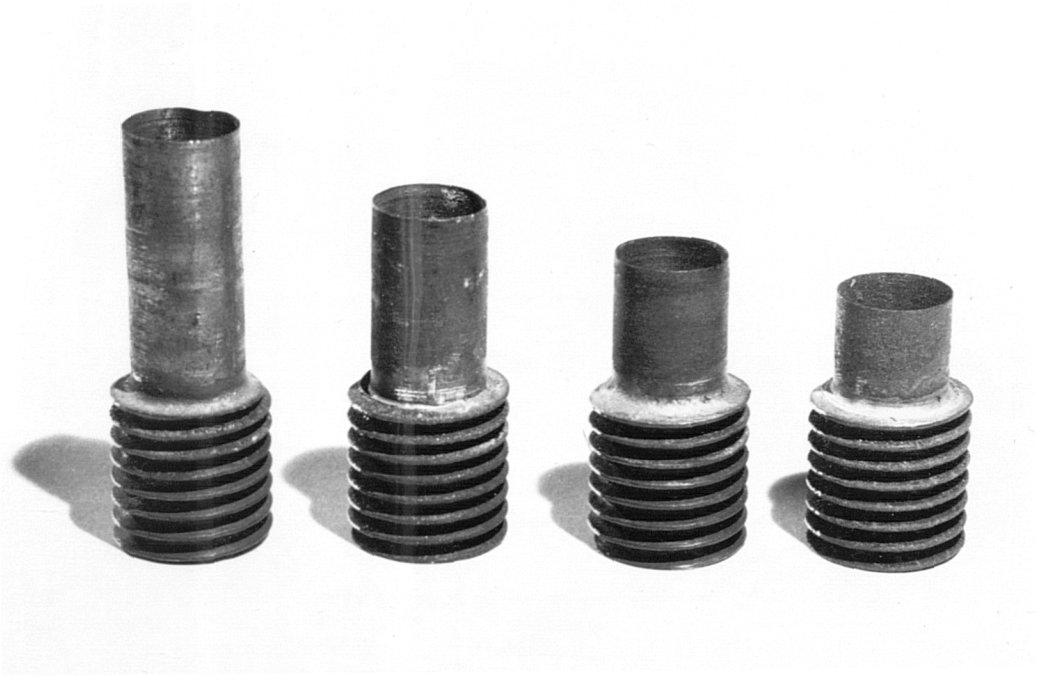

Figure 5.8. The four Nozzles that Were Used on the First-Stage of the Two-Stage Ejector Rig.

Air Nozzle Number	Nozzle Diameter (mm)	Nozzle Area (mm^2)	Nozzle Mass Flowrate (Kg/hr)
3	7.95	49.64	43.00
2	6.35	31.67	27.52
1	4.78	17.95	15.48
4	3.18	7.94	6.88
5	1.60	2.01	1.72

Table 5.1. The Flowrate of the Air Intake System Measuring Nozzles.

Diffuser Number	D1	D2	D3	D4
Diffuser Throat Diameter (mm)	15.80	15.20	16.90	13.70
Diffuser Inlet Diameter(mm)	27.70	27.10	30.50	23.70
Diffuser Outlet Diameter(mm)	35.70	35.30	37.80	31.70
Diffuser Total Length(mm)	265.00	255.00	282.00	234.00
Length of the Convergent Section (mm)	100.80	104.10	111.70	98.80
Length of the Divergent Section (mm)	96.10	97.70	98.00	82.90
Length of the Diffuser Throat (mm)	68.10	53.20	72.30	52.70
Diffuser Convergence Angle(Degree)	7.40	7.00	7.60	6.50
Diffuser Divergence Angle(Degree)	11.80	11.70	12.20	12.40

Table 5.2. The Geometrical Dimensions for the four Diffusers Used on the Single-Stage Ejector Rig.

Steam Nozzle Number	Nozzle Throat Diameter (mm)	Nozzle Outlet Diameter (mm)	Length of the Divergent Section (mm)	Nozzle Divergence Angle (Degree)
N1	5.50	15.50	43.50	13.10
N2	5.50	15.20	37.90	14.60
N3	6.00	10.70	24.10	11.10
N4	5.50	15.10	57.70	9.50

Table 5.3. The Geometrical Dimensions for the four Nozzles Used on the Single-Stage Rig.

Steam Nozzle Number	Nozzle Throat Diameter (mm)	Nozzle Outlet Diameter (mm)	Length of the Divergent Section (mm)	Nozzle Divergence Angle (Degree)
N5	2.90	13.13	58.45	10.00
N6	2.90	13.13	41.66	14.00
N7	2.90	13.13	32.30	18.00
N8	2.90	13.13	26.31	22.00

Diffuser Number = D5				
Diffuser Throat Diameter (mm)	Diffuser Inlet Diameter (mm)	Diffuser Outlet Diameter (mm)	Diffuser Total Length (mm)	Length of the Diffuser Throat (mm)
19.05	47.63	34.93	438.18	76.20

Length of the Convergent Section (mm)	Length of the Divergent Section (mm)	Diffuser Divergence Angle (Degree)	Diffuser Convergence Angle (Degree)
230.19	131.76	7.00	7.00

Table 5.4. The Geometrical Dimensions for the four Nozzles and the Diffuser Used on the Two-Stage Ejector Rig.

Ejector Number	Nozzle Number	Diffuser Number
E1	N4	D4
E2	N3	D4
E3	N1	D4
E4	N2	D4
E5	N4	D2
E6	N3	D2
E7	N1	D2
E8	N2	D2
E9	N4	D1
E10	N3	D1
E11	N1	D1
E12	N2	D1
E13	N4	D3
E14	N3	D3
E15	N1	D3
E16	N2	D3
E17	N5	D5
E18	N6	D5
E19	N7	D5
E20	N8	D5

Table 5.5. The Ejectors Combinations from the Nozzles and the Diffusers.

CHAPTER SIX

EXPERIMENTAL PROCEDURE AND RESULTS

6.1. Experimental Procedure :

The experimental work was carried out on two test rigs; a single-stage and the first stage of a two-stage steam-jet ejector rig. Some initial tests were performed on the two rigs to ensure that no leaks occurred and that repeatable results could be obtained.

The primary motive fluid was dry saturated steam with varying motive pressure (P_m) from 60 to 105 (psig.), in incremental step of 15 (psig.); i.e. P_m = 60, 75, 90, and 105 *(psig.)*. The secondary induced fluid was air introduced into the system through any combination of five sonic nozzles by which the mass of air (m_a) flowing into the system can be controlled and measured (see Section 5.3.3.). On the whole, the experiments were carried out in the order in which they are described herewith.

6.1.1. Two-Stage Steam Ejector :

At the beginning of every series of tests on this rig, Figure (6.1.), the distance from the nozzle outlet to the diffuser throat (L) was set as far apart as possible, in the first stage of the ejector, by

using the distance control valve (V_1). The valve (V_2) was opened to let the water flow into the condenser, and valve (V_3) was opened to let the motive steam through the second stage of the ejector, which was set to a constant motive pressure for all the tests.

The air was admitted into the system at a large but reasonable flow rate set by a selected combination of the air nozzles. Then, the valve (V_4) was opened to let the motive steam into the first stage of the ejector, and its pressure fixed to 60 (psig.), which was read from the pressure gauge (G_1). Each test consisted of a number of readings of the suction pressure (P_s) for varying (m_a), (P_m), and (L). The procedure was as follows :

1. Allow the suction pressure (P_s) to reach steady state by observing the pressure gauge (G_2). When steady it was noted down with its corresponding values of the mass of the induced air (m_a), the steam motive pressure (P_m), and the distance (L). This first step was repeated for different values of (m_a), until "dead-end", i.e. (m_a=zero) was reached.

2. By decreasing the distance (L), (the nozzle moving towards the diffuser), step one could be repeated again. This step was repeated for many values of (L) until it reached its lowest possible value.

3. Step one and two were repeated for the four different values of motive pressure (P_m).

6.1.2. Single-Stage Steam Ejector :

With this rig Figure (6.2.), the experimental steps are nearly the same as described in the previous paragraph, but with a few changes in the way in which the steps were taking place. As it is a single-stage ejector, there is only one steam inlet valve (V_5) and its pressure could be read from the pressure gauge (G_3).

The change in the distance (L) was accomplished by using spacers inserted between the two flanges of the diffuser and the nozzle assembly respectively (see Figure (6.3.)). The nozzle was set to its maximum distance into the diffuser, and then its position was changed by adding the spacers. There were only these two differences in the procedural steps for the two- and single-stage steam ejectors in the experimental results presented in the following paragraph.

6.2. Experimental Results :

The experimental work has been divided into five test series (A-E), each of which is given in one of the sections presented in this chapter. All of the data for all the test series are tabulated in Appendix VI.

6.2.1. The Optimum Nozzle Distance Relative to the Diffuser Throat (L_{op}) :

To find out the best and optimum distance (L_{op}) for any ejector ('best' in the sense of giving lowest value of the suction pressure at constant m_a), the test was carried out in the manner described in the previous section. Test series (A) is presented here as an example of how to find this optimum distance. This test was carried out using the four single-stage ejectors (E1, E2, E3, and E4). The data from this test are presented in (Table 6.1. to Table 6.4.). These data enabled us to draw a set of curves for each ejector on a graph, were the abscissa is the distance (L) and the ordinate is the suction pressure (P_s), for the four values of the motive pressure (P_m), and are presented in Figures (6.4. to 6.11.). The diagrams were used to find the best and optimum distance for these four ejector. In this way, the optimum distance was found for every ejector in all test series carried out in the experimental work, and are tabulated in Table (6.5.).

6.2.2. The Optimum Nozzle Distance (L_{op}) with Respect to Motive Steam Pressure (P_m) and Mass of Induced Air (m_a) :

Each ejector was tested with four different motive steam pressures, and the optimum distance (L_{op}) was found for each value of the suction air load (m_a). It was observed, as in Figures (6.4. to

6.11.), that this distance is unchanged for any value of suction air load (m_a) when the motive steam pressure is changed. This is true with all the test series which were carried out on the single-stage ejectors. However, with the two-stage ejector, a change appeared when the pressure was 60 and 75 (psig.), and for a very small interval of suction air load (m_a). This change only appeared with two ejectors (E18 and E19) having a nozzle divergence angle (Zeta) equal to 14 and 18 (degrees) of the twenty tested ejectors, and can be seen in Figure (6.12.).

6.2.3. The Optimum Nozzle Distance (L_{op}) with Respect to the Nozzle Divergence Angle (Zeta) :

Test series (B) was designed to discover how the optimum distance changed with the nozzle divergence angle (Zeta). This test series was a comparison between four ejectors (E17, E18, E19, and E20) having the same diffuser (D5), and using four nozzles (N5, N6, N7, and N8) identical in throat and outlet diameters but with four different divergence angle (Zeta), (Table 5.4.).

The conclusions of each set of test for each ejector was as follows :

- For ejector (E17, Zeta=10°) : The optimum distance (L_{op}) was the same for any value of motive steam pressure (P_m) and any suction air load (m_a), and was equal to 163.76 (mm).

- For ejector (E18, Zeta=14°) : The optimum distance (L_{op}) had different values with respect to the motive steam pressure (P_m) and the suction air load (m_a) :

  (a) At P_m=60 (psig.), two values for (L_{op}) were found for two intervals of (m_a) :

  Interval I : $0.0 \leq m_a \leq 1.72$ L_{op} was equal to 135.76 (mm)

  Interval II : $1.72 \leq m_a \leq 58.48$ L_{op} was equal to 100.76 (mm)

  (b) At P_m=75, 90, 105 (psig.), the two values for the optimum distance (L_{op}) for the two air intervals I and II, were unchanged and equal to :

  Interval I : $0.0 \leq m_a \leq 1.72$ L_{op} was equal to 156.76 (mm)

  Interval II : $1.72 \leq m_a \leq 58.48$ L_{op} was equal to 100.76 (mm)

- For ejector (E19, Zeta=18°) : With this ejector three intervals were found for suction air load with respect to the value of the optimum distance (L_{op}) :

  (a) At P_m=60 (psig.), the values for (L_{op}) with respect to (m_a) were found to be :

  Interval I : $0.0 \leq m_a \leq 1.72$ L_{op} was equal to 114.76 (mm)

  Interval II : $1.72 \leq m_a \leq 34.40$ L_{op} was equal to 100.76 (mm)

  Interval III : $34.4 \leq m_a \leq 58.48$ L_{op} was equal to 135.76 (mm)

  (b) At P_m=75 (psig.), the values for the optimum distance (L_{op}) with respect to (m_a) were changed to :

Interval I : $0.0 \leq m_a \leq 1.72$ L_{op} was equal to 156.76 (mm)

Interval II : $1.72 \leq m_a \leq 34.40$ L_{op} was equal to 100.76 (mm)

Interval III : $34.4 \leq m_a \leq 58.48$ L_{op} was equal to 114.76 (mm)

(c) At P_m=90, and 105 (psig.), the three air intervals were reduced to two with respect to the (L_{op}) :

Interval I : $0.0 \leq m_a \leq 1.72$ L_{op} was equal to 156.76 (mm)

Interval II : $1.72 \leq m_a \leq 58.48$ L_{op} was equal to 100.76 (mm)

- For ejector (E20, Zeta=22°) : The optimum distance (L_{op}) was found to be the same for any value of steam motive pressure (P_m) and any mass of air (m_a), and was equal to 170.76 (mm).

These results are shown graphically on diagrams of (L_{op}) versus (Zeta) for different intervals of suction air load and different steam motive pressure (Figures 6.12. and 6.13.).

6.2.4. The Optimum Nozzle Distance (L_{op}) with Respect to the Nozzle Outlet Diameter (d_o) :

Test series (C) was carried out to find the relation between the (L_{op}) and the nozzle outlet diameter (d_o). Three nozzles (N1, N2, and N4) were used with three diffusers (D1, D2, and D3) forming nine different ejectors (E5, E7, E8, E9, E11, E12, E13, E15, and E16). The optimum nozzle position was found to change with the nozzle outlet diameter as shown graphically in Figure (6.14.).

6.2.5. The Optimum Nozzle Distance (L_{op}) with Respect to the Diffuser Throat Diameter (D_{th}) :

Test series (D) was carried out to find the relation between the (L_{op}) and the diffuser throat diameter (D_{th}). Three nozzles (N1, N2, and N3) were used with four diffusers (D1, D2, D3, D4) forming twelve different ejectors (E2, E3, E4, E6, E7, E8, E10, E11, E12, E14, E15, and E16). After finding the optimum nozzle distance (L_{op}); a graph can be drawn between (L_{op}) and the diffuser throat diameter (D_{th}). This graph is shown in Figure (6.15.), three separate curves are formed from the value of (L_{op}) for the nozzles (N1, N2, and N3) with all of the four diffusers.

6.2.6. The Optimum Distance (L_{op}) with Respect to the Diffuser Convergence Angle (Beta) :

Test series (E) was carried out to find the relation (L_{op}) and the diffuser convergence angle (Beta). The three nozzles that were used with the four diffusers (D1, D2, D3, and D4) are (N1,N2, and N3); forming twelve different ejectors (E2, E3, E4, E6, E7, E8, E10, E11, E12, E14, E15, and E16). Finding the optimum nozzle distance (L_{op}) for these ejectors enabled us to draw a graph between (L_{op}) and the diffuser convergence angle (Beta). Three separate curves are shown in Figure (6.16.), for the three nozzles (N1, N2, and N3), showing the relation between (L_{op}) and (Beta).

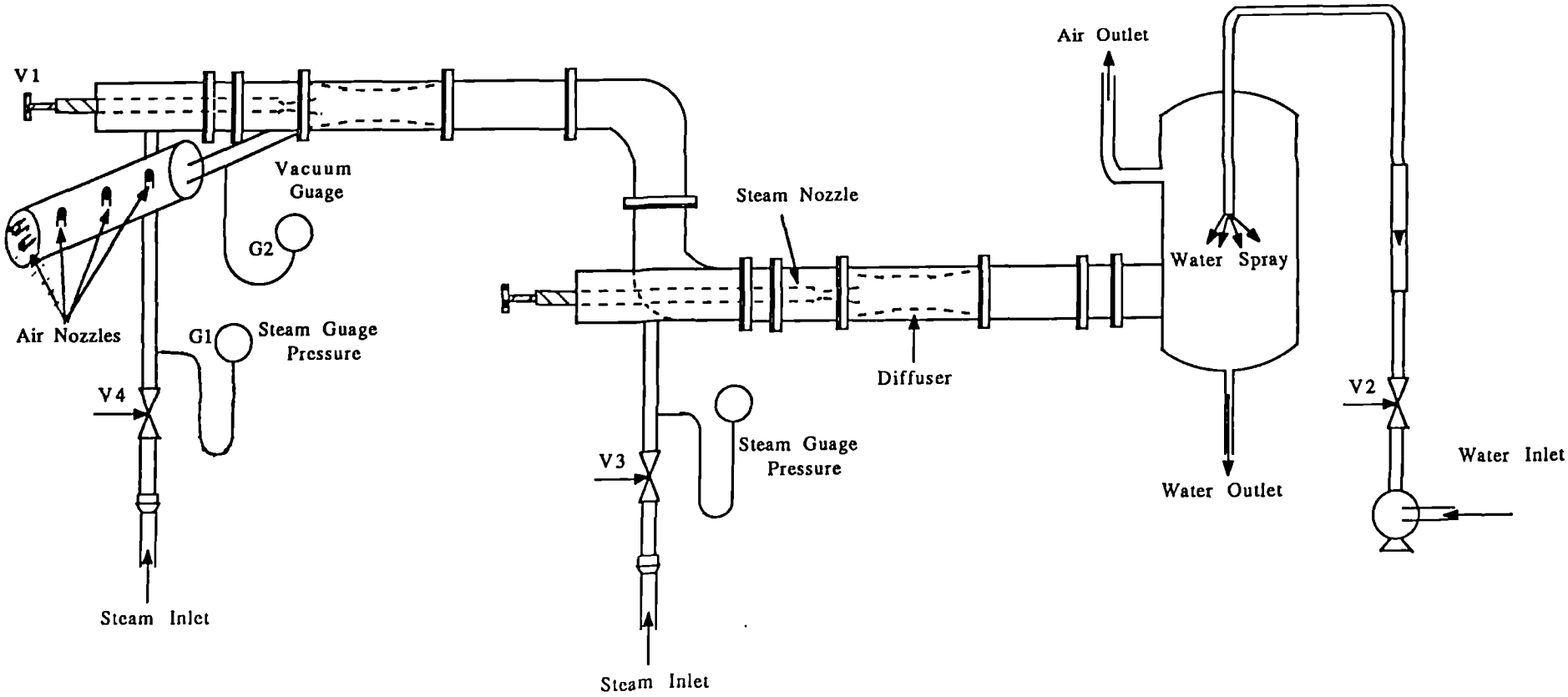

Figure 6.1. Genereal Arrengement of the Two-Stage Ejector Rig.

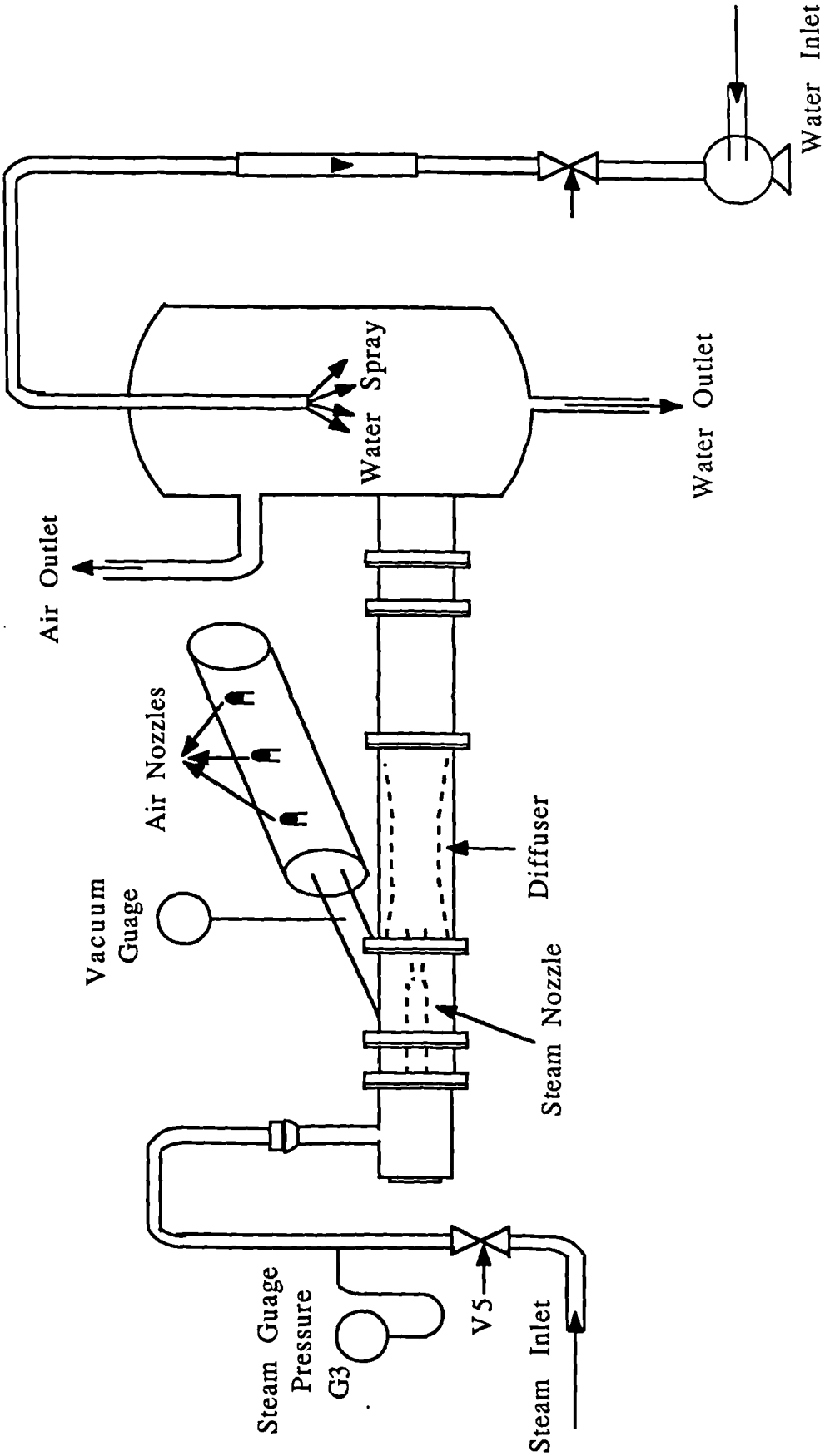

Figure 6.2. General Arrengement of the Single-Stage Ejector Rig.

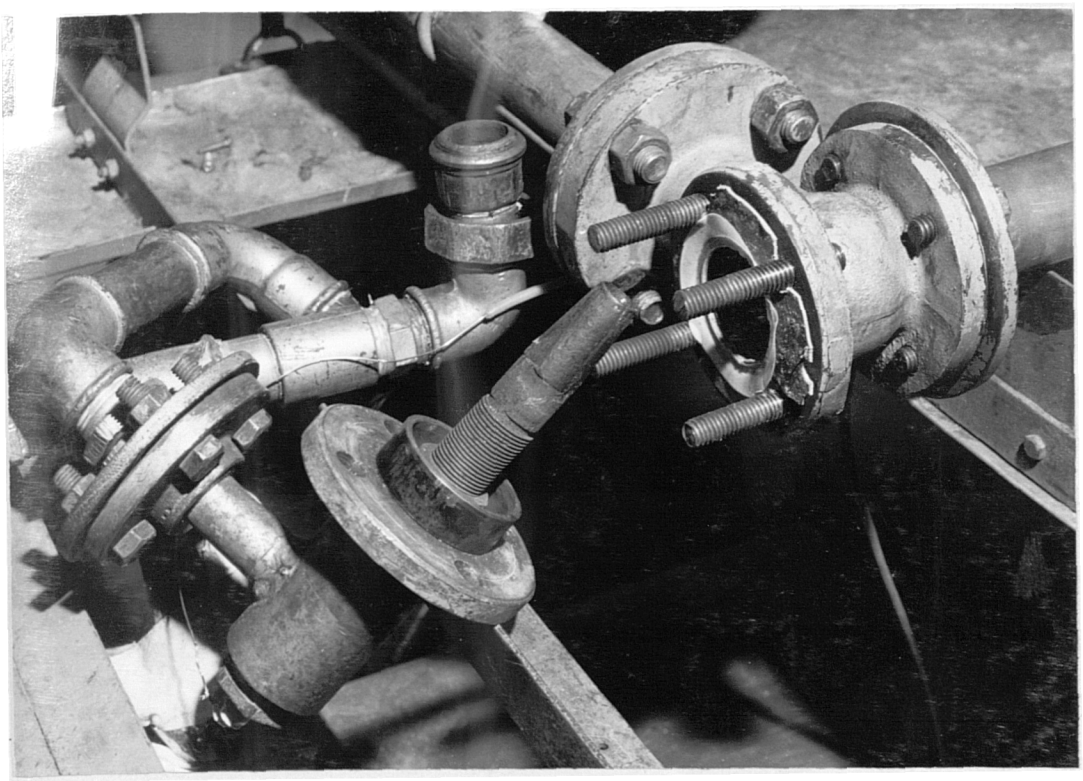

Figure 6.3. The Adjustment of the Distance between the Nozzle and the Diffuser by the Use of the Spacers in the Single-Stage Ejector Rig.

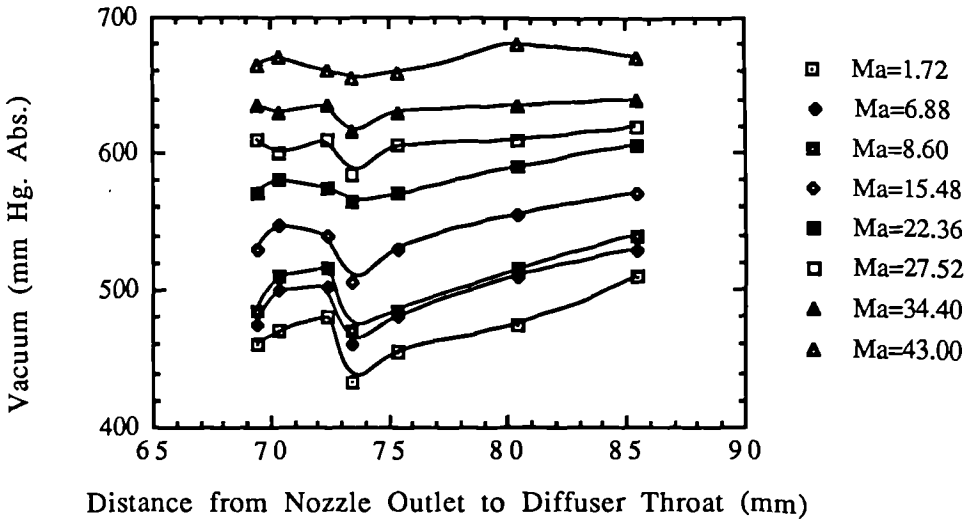

(a) Ejector Number, E1

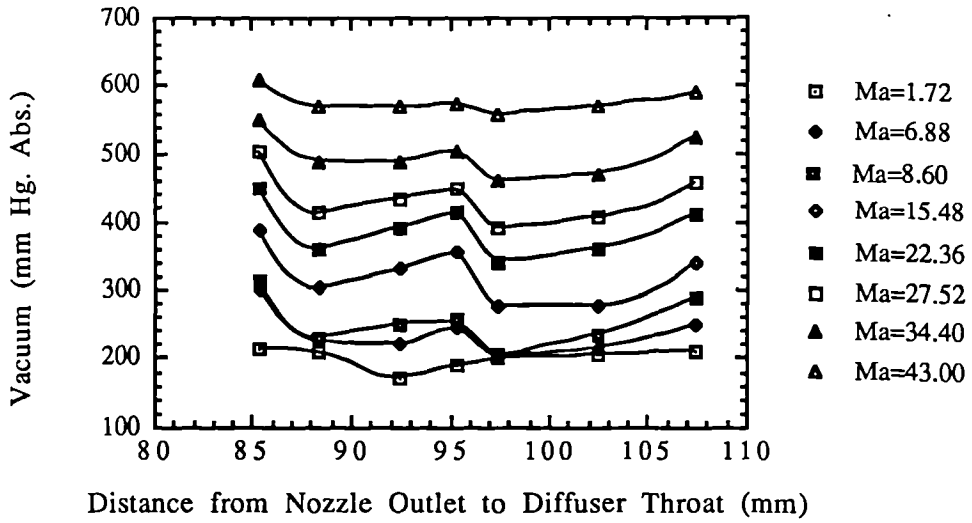

(b) Ejector Number, E2

Figure 6.4. The Suction Pressure (P_s) at Different Nozzle Setting with Respect to the Diffuser Throat, Steam Motive Pressure, P_m = 60 (psig.).

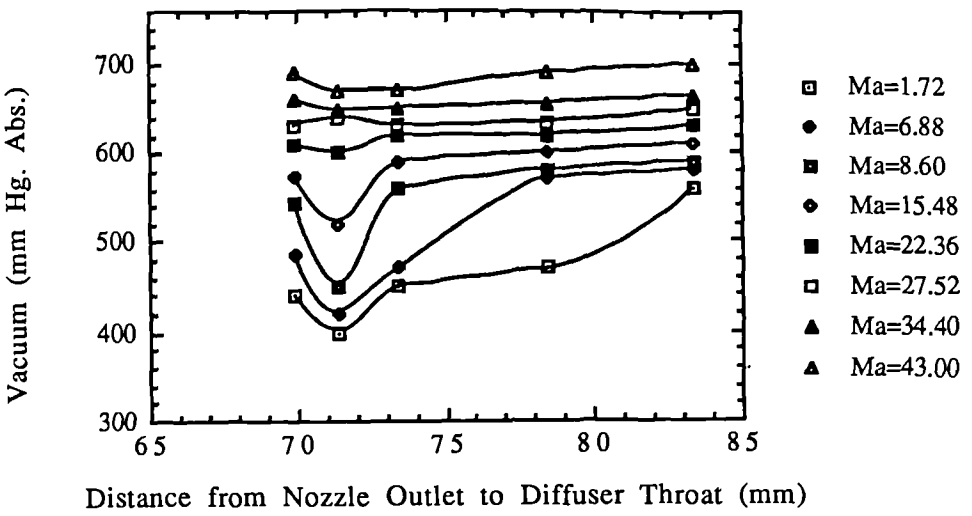

(a) Ejector Number, E3

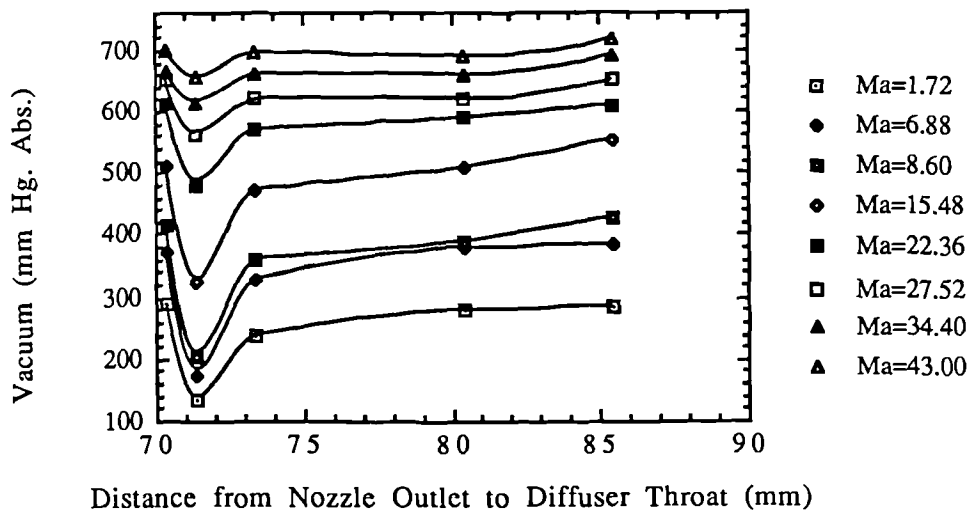

(b) Ejector Number, E4

Figure 6.5. The Suction Pressure (P_s) at Different Nozzle Setting with Respect to the Diffuser Throat, Steam Motive Pressure, P_m = 60 (psig.).

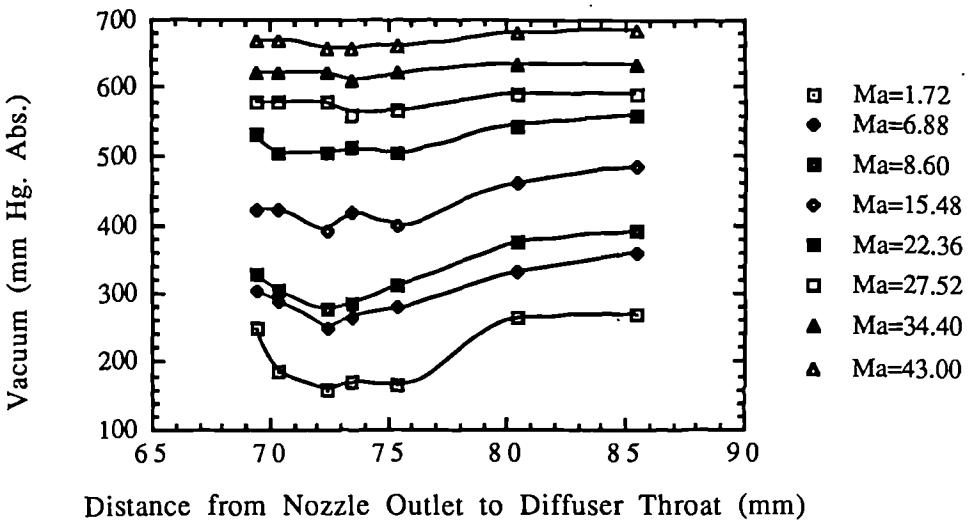

(a) Ejector Number, E1

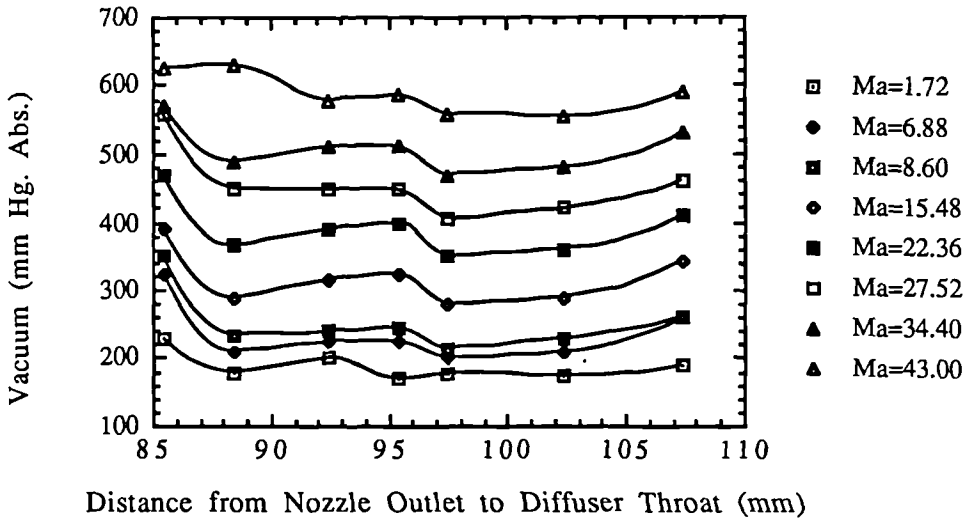

(b) Ejector Number, E2

Figure 6.6. The Suction Pressure (P_s) at Different Nozzle Setting with Respect to the Diffuser Throat, Steam Motive Pressure, P_m = 75 (psig.).

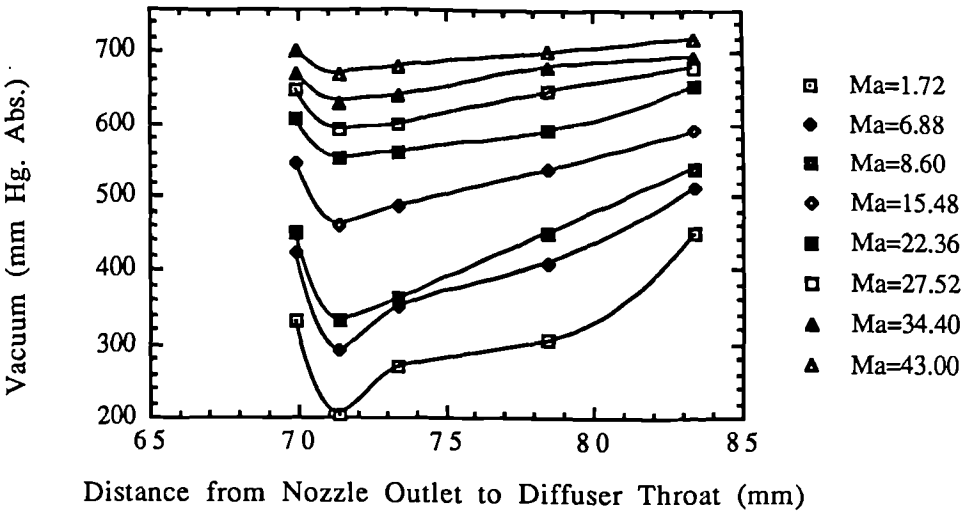

(a) Ejector Number, E3

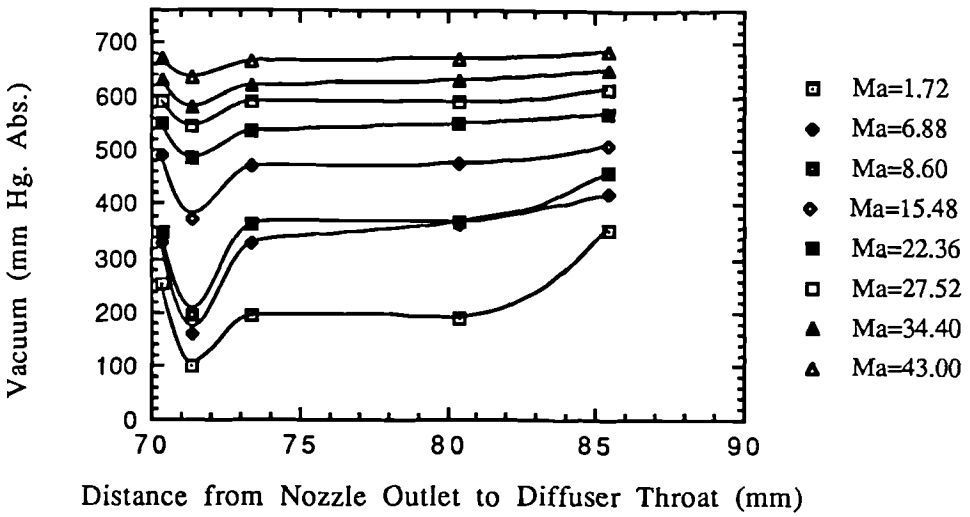

(b) Ejector Number, E4

Figure 6.7. The Suction Pressure (P_s) at Different Nozzle Setting with Respect to the Diffuser Throat, Steam Motive Pressure, P_m = 75 (psig.).

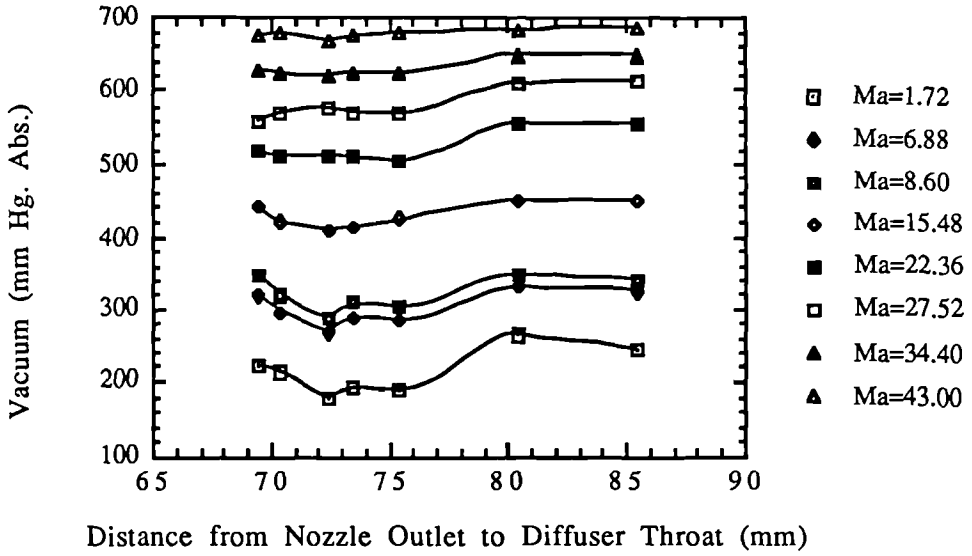

(a) Ejector Number, E1

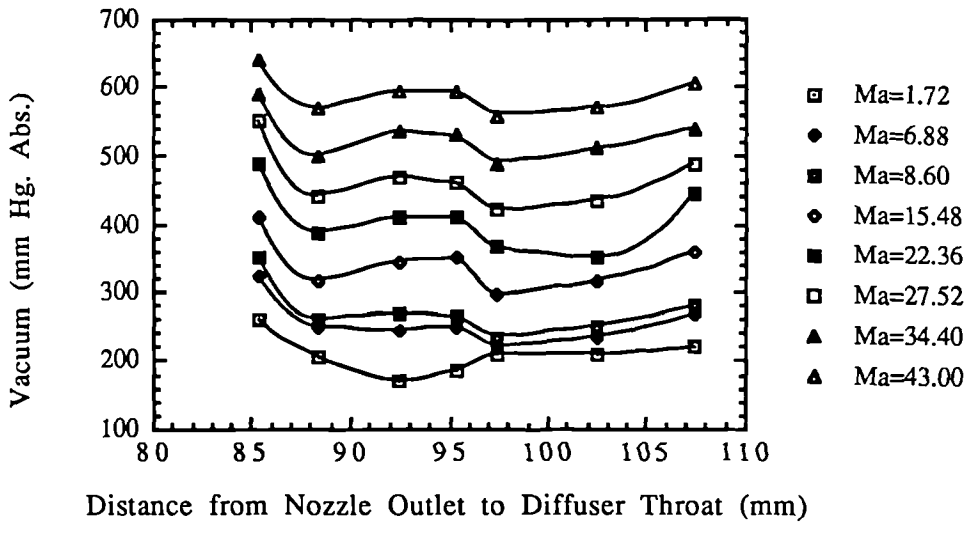

(b) Ejector Number, E2

Figure 6.8. The Suction Pressure (P_s) at Different Nozzle Setting with Respect to the Diffuser Throat, Steam Motive Pressure, P_m = 90 (psig.).

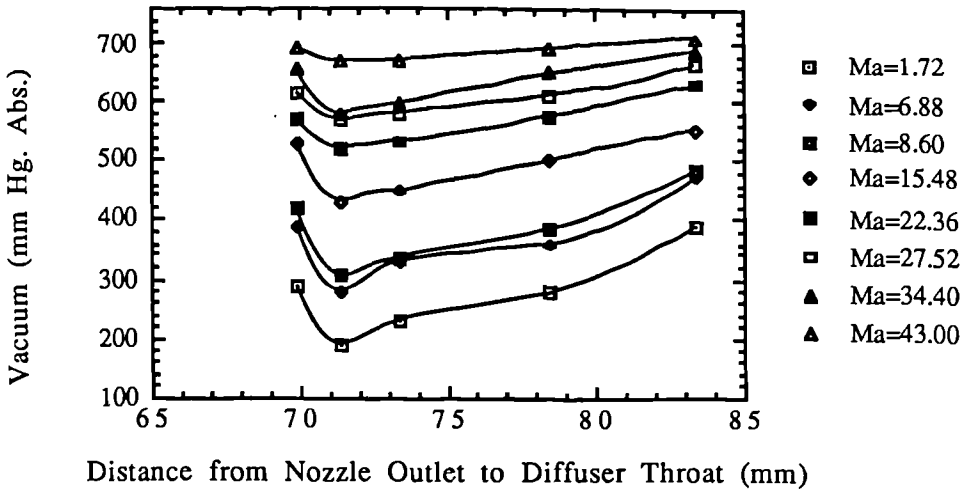

(a) Ejector Number, E3

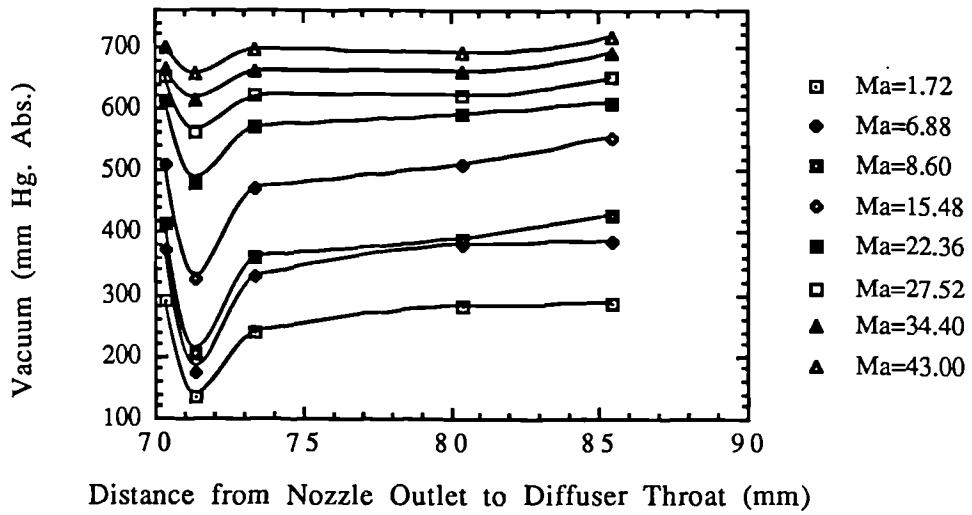

(b) Ejector Number, E4

Figure 6.9. The Suction Pressure (P_s) at Different Nozzle Setting with Respect to the Diffuser Throat, Steam Motive Pressure, P_m = 90 (psig.).

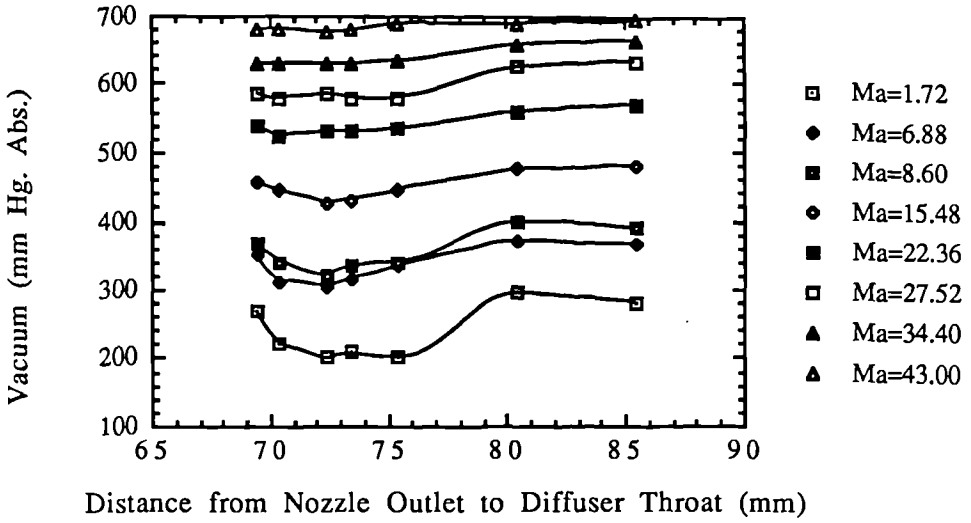

(a) Ejector Number, E1

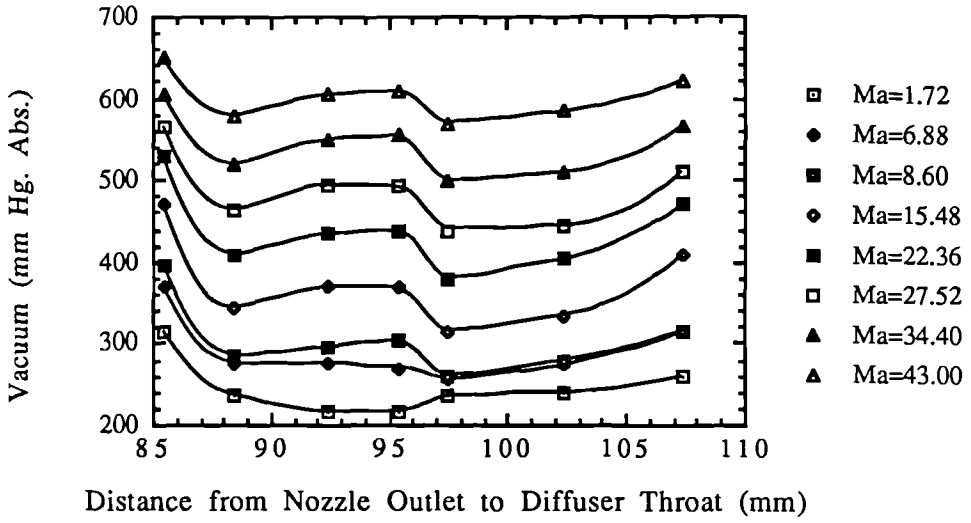

(b) Ejector Number, E2

Figure 6.10. The Suction Pressure (P_s) at Different Nozzle Setting with Respect to the Diffuser Throat, Steam Motive Pressure, P_m = 105 (psig.).

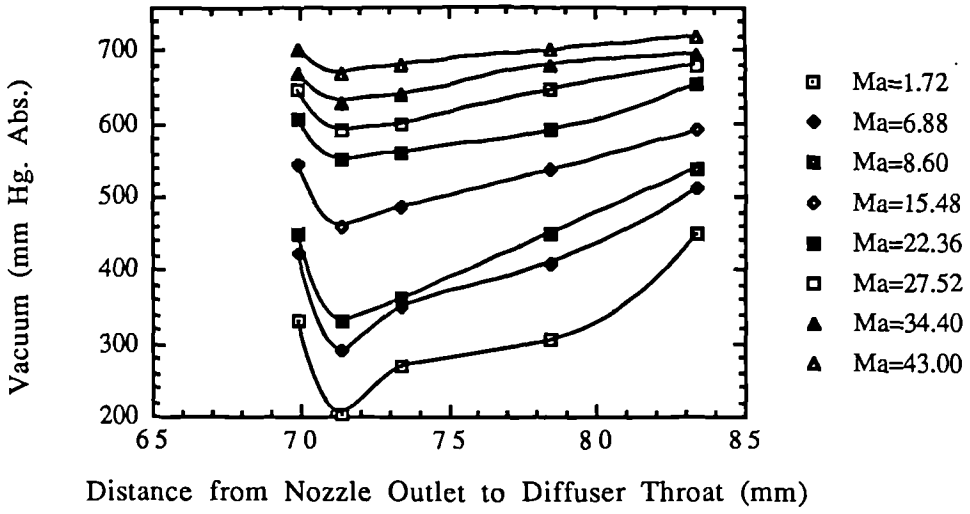

(a) Ejector Number, E3

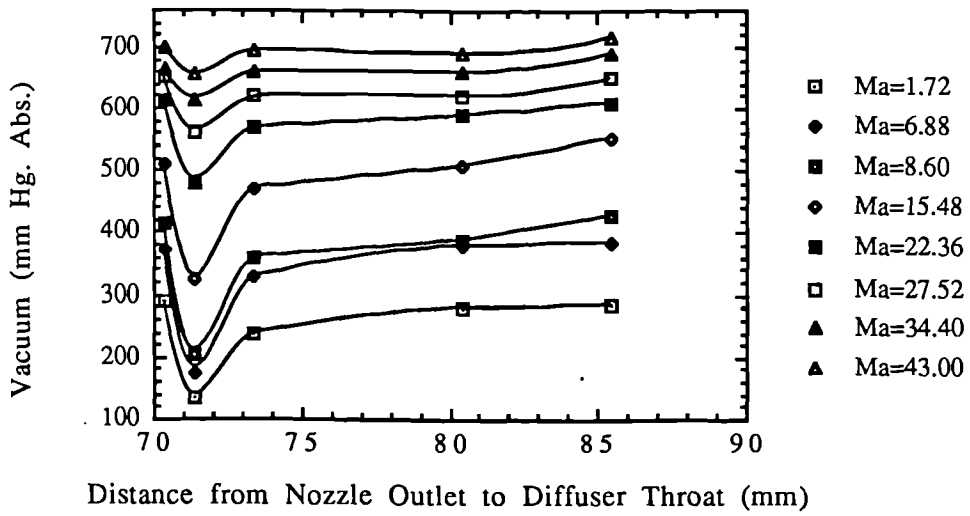

(b) Ejector Number, E4

Figure 6.11. The Suction Pressure (P_s) at Different Nozzle Setting with Respect to the Diffuser Throat, Steam Motive Pressure, P_m = 105 (psig.).

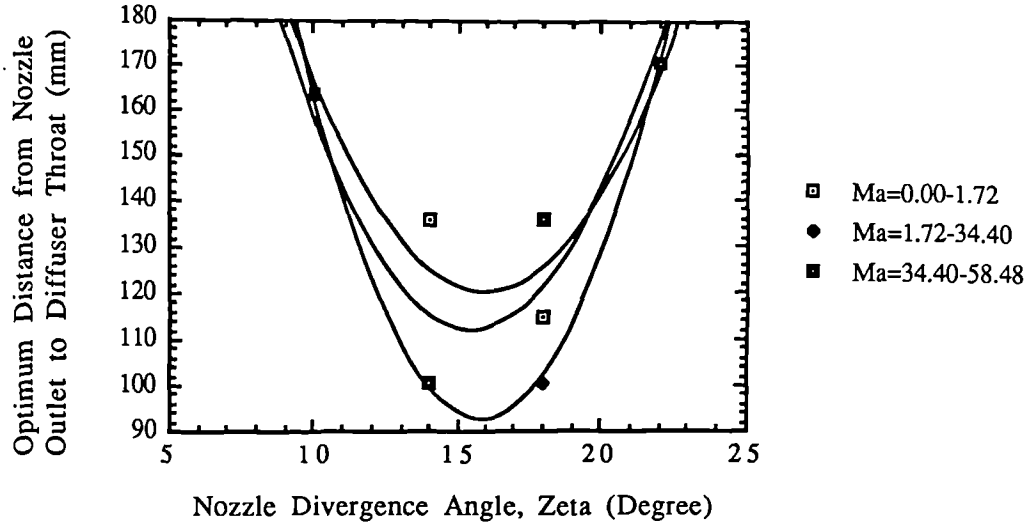

(a) Motive Steam Pressure, Pm = 60 (psig.).

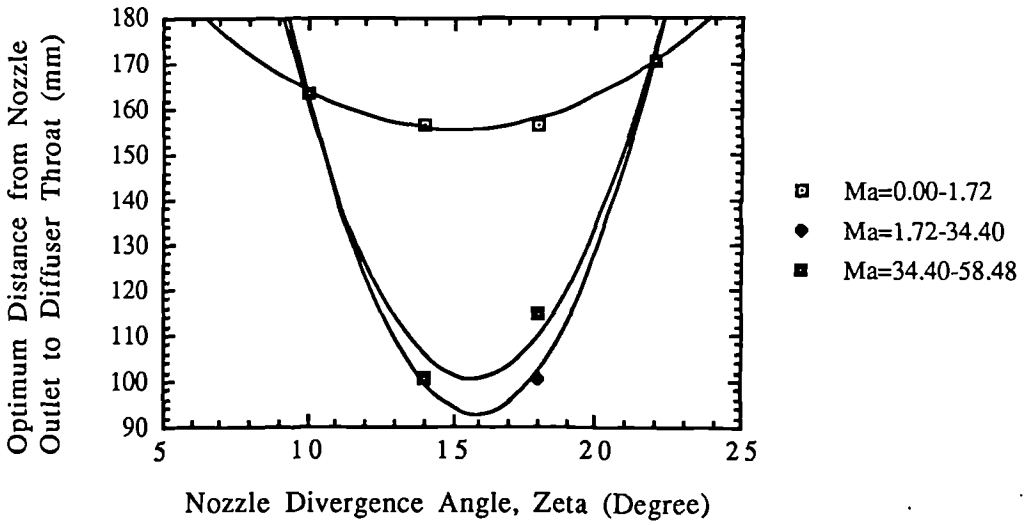

(b) Motive Steam Pressure, Pm = 75 (psig.).

Figure 6.12. Optimum Nozzle Distance (L_{op}) at Different Nozzle Divergence Angle, with a Diffuser of Convergence Angle, Beta = 7.0°.

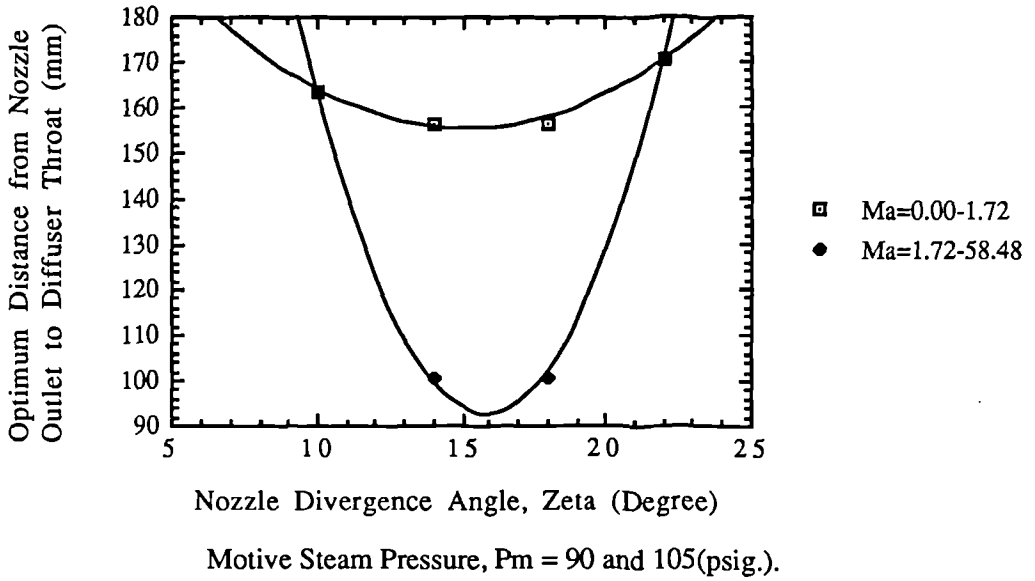

Figure 6.13. Optimum Nozzle Distance (L_{op}) at Different Nozzle Divergence Angle, with a Diffuser of Convergence Angle, Beta = 7.0°.

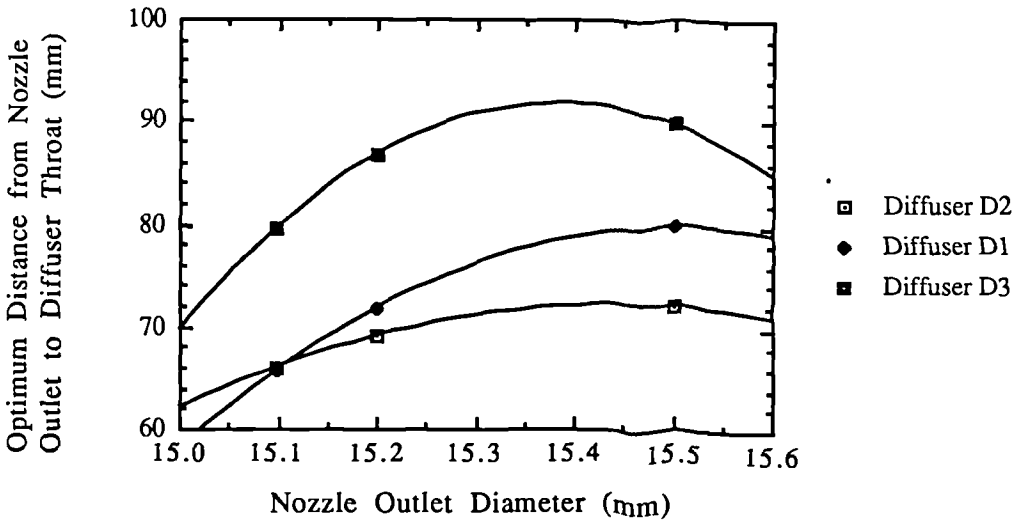

Figure 6.14. Optimum Nozzle Distance (L_{op}) at Different Nozzle Outlet Diameter (d_o).

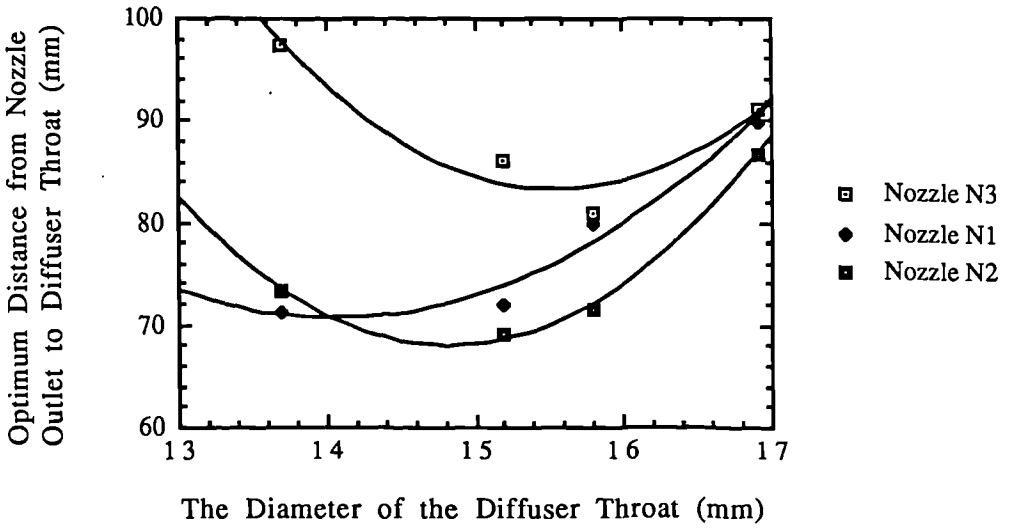

Figure 6.15. Optimum Nozzle Distance (L_{op}) at Different Diffuser Throat Diameter (D_{th}).

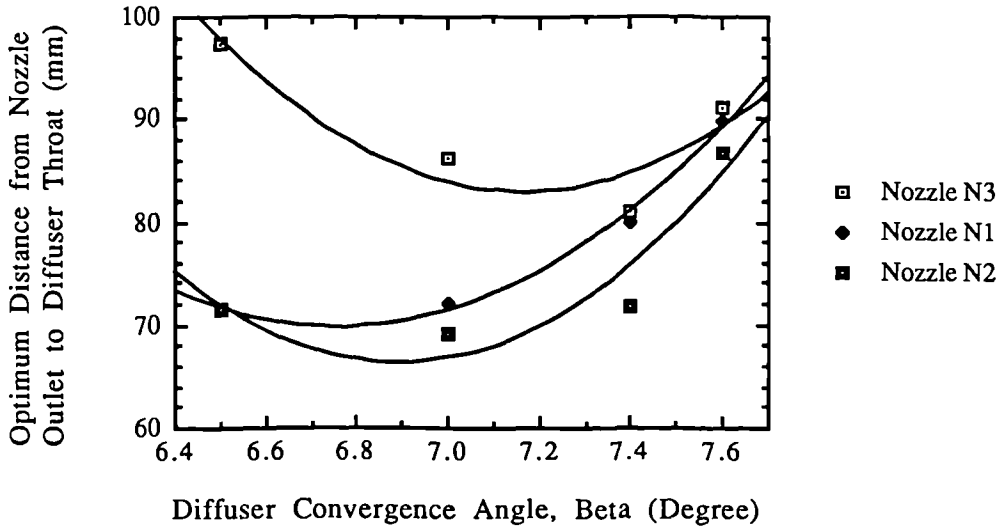

Figure 6.16. Optimum Nozzle Distance (L_{op}) at Different Diffuser Convergence Angle, Beta.

The Distance from the Nozzle Outlet to Diffuser Throat L (mm)	The Mass of Air Entrained by The Motive Steam m_a (kg/hr.)								Motive Steam Pressure P_m (psig.)
	1.72	6.88	8.60	15.48	22.36	27.52	34.40	43.00	
	The Suction Pressure P_s (mm Hg. Abs.)								
85.4	280	365	390	480	570	635	665	695	
80.4	295	370	400	475	560	625	658	690	
75.4	200	335	340	445	535	580	633	690	
73.4	208	315	335	430	530	580	630	680	105
72.4	200	305	320	425	530	585	630	675	
70.4	220	313	340	445	525	580	630	680	
69.4	270	350	365	455	540	585	630	680	
85.4	245	325	340	450	555	615	650	690	
80.4	265	330	347	450	555	610	650	685	
75.4	190	285	303	425	505	570	625	680	
73.4	193	290	310	413	510	570	627	675	90
72.4	180	270	290	410	513	580	620	670	
70.4	213	298	320	420	510	570	625	680	
69.4	223	320	347	440	520	560	630	675	
85.4	270	360	390	485	560	590	635	685	
80.4	265	330	375	460	545	590	635	680	
75.4	165	279	310	398	505	567	620	660	
73.4	170	265	285	418	510	560	610	658	75
72.4	160	250	275	390	505	580	620	655	
70.4	186	288	302	420	505	580	620	670	
69.4	250	305	328	420	530	580	620	670	
85.4	510	530	540	570	605	620	640	670	
80.4	475	510	515	555	590	610	635	680	
75.4	455	480	485	530	570	605	630	659	
73.4	433	460	470	505	565	585	615	655	60
72.4	480	502	515	540	575	610	635	660	
70.4	470	500	510	547	580	600	630	670	
69.4	460	475	485	530	570	610	635	665	

Table 6.1. The Suction Pressure (P_s) at Different Nozzle Setting with Respect to the Diffuser Throat for Ejector (E1).

The Distance from the Nozzle Outlet to Diffuser Throat L (mm)	The Mass of Air Entrained by The Motive Steam m_a (kg/hr.)								Motive Steam Pressure P_m (psig.)
	1.72	6.88	8.60	15.48	22.36	27.52	34.40	43.00	
	The Suction Pressure P_s (mm Hg. Abs.)								
107.4	260	315	315	410	470	510	565	620	105
102.4	240	275	280	335	405	445	510	585	
97.4	235	255	260	315	380	440	500	570	
95.4	215	270	305	370	440	495	555	610	
92.4	215	275	295	370	435	495	550	605	
88.4	235	275	285	344	410	465	520	580	
85.4	315	370	396	470	530	565	605	650	
107.4	220	270	280	360	445	490	540	605	90
102.4	210	235	250	315	350	435	510	570	
97.4	210	221	235	295	365	420	490	560	
95.4	185	250	265	350	410	460	530	595	
92.4	170	245	270	345	410	470	535	595	
88.4	205	250	260	315	386	440	500	570	
85.4	260	325	350	410	490	550	590	640	
107.4	190	260	260	345	410	460	530	590	75
102.4	175	210	230	290	360	420	480	555	
97.4	180	200	215	280	350	405	470	560	
95.4	170	225	245	325	400	450	510	585	
92.4	201	225	240	315	390	450.	510	580	
88.4	180	210	235	290	365	450	489	630	
85.4	230	325	350	390	470	560	570	625	
107.4	210	250	290	340	410	455	525	590	60
102.4	205	215	235	275	360	405	470	570	
97.4	200	202	205	275	340	390	460	560	
95.4	190	245	255	355	415	450	505	575	
92.4	170	220	250	330	390	435	490	570	
88.4	210	225	230	302	360	412	490	570	
85.4	215	300	310	385	450	505	550	610	

Table 6.2. The Suction Pressure (P_s) at Different Nozzle Setting with Respect to the Diffuser Throat for Ejector (E2).

The Distance from the Nozzle Outlet to Diffuser Throat L (mm)	The Mass of Air Entrained by The Motive Steam m_a (kg/hr.)								Motive Steam Pressure P_m (psig.)
	1.72	6.88	8.60	15.48	22.36	27.52	34.40	43.00	
	The Suction Pressure P_s (mm Hg. Abs.)								
83.4	450	510	538	590	655	680	695	720	
78.4	305	410	450	535	590	645	680	700	
73.4	270	350	360	485	560	600	640	680	105
71.4	205	290	330	460	550	590	630	670	
69.9	330	425	450	545	605	645	670	700	
83.4	390	475	485	555	630	665	687	710	
78.4	280	360	385	500	575	610	650	690	
73.4	230	330	335	450	530	580	595	670	90
71.4	190	280	305	430	520	570	580	670	
69.9	290	390	418	528	570	613	655	690	
83.4	385	435	450	520	600	640	670	700	
78.4	310	385	410	480	540	630	660	690	
73.4	245	330	370	435	520	560	620	680	75
71.4	180	305	325	430	500	550	600	660	
69.9	305	390	425	505	565	600	650	695	
83.4	560	580	590	610	630	650	665	700	
78.4	470	570	580	600	620	635	656	690	
73.4	450	470	560	590	620	630	650	670	60
71.4	400	420	450	520	600	640	650	670	
69.9	440	485	545	573	610	630	660	690	

Table 6.3. The Suction Pressure (P_s) at Different Nozzle Setting with Respect to the Diffuser Throat for Ejector (E3).

The Distance from the Nozzle Outlet to Diffuser Throat L (mm)	The Mass of Air Entrained by The Motive Steam m_a (kg/hr.)								Motive Steam Pressure P_m (psig.)
	1.72	6.88	8.60	15.48	22.36	27.52	34.40	43.00	
	The Suction Pressure P_s (mm Hg. Abs.)								
85.4	285	385	430	555	610	650	690	715	
80.4	280	380	390	510	590	620	660	690	
73.4	240	330	360	470	570	620	660	695	105
71.4	135	173	202	325	480	560	615	655	
70.4	290	370	415	510	615	650	665	700	
85.4	275	350	420	520	585	635	665	695	
80.4	220	340	350	460	570	620	645	680	
73.4	195	290	340	445	550	610	650	672	90
71.4	120	167	190	320	485	530	590	655	
70.4	245	350	375	465	570	610	650	690	
85.4	355	420	460	510	570	615	650	685	
80.4	190	365	370	475	550	590	630	670	
73.4	195	330	365	470	535	590	620	665	75
71.4	100	160	195	375	485	545	580	635	
70.4	255	330	350	490	550	590	630	670	
85.4	505	545	550	570	600	630	655	680	
80.4	480	530	535	555	590	630	650	675	
73.4	470	490	495	555	590	610	635	670	60
71.4	445	460	465	498	550	575	605	640	
70.4	450	470	475	530	575	610	635	675	

Table 6.4. The Suction Pressure (P_s) at Different Nozzle Setting with Respect to the Diffuser Throat for Ejector (E4).

Ejector Number	Optimum Nozzle Distance L_{op} (mm)
E1	73.40
E2	97.40
E3	71.40
E4	71.40
E5	66.10
E6	86.10
E7	72.10
E8	69.10
E9	66.10
E10	80.80
E11	79.80
E12	71.80
E13	79.70
E14	91.20
E15	89.70
E16	86.70
E17	163.76
E18	100.76
E19	100.76
E20	170.76

Table 6.5. The Optimum Nozzle Distance (L_{op}) for every Ejector Used in the Experimental Work.

CHAPTER SEVEN

THEORETICAL RESULTS

7.1. Introduction :

Two previous chapters, three and four, were devoted to the theory of the fluid flow inside the ejector. Chapter three dealt with the flow inside the nozzle. The value of the Mach number and the static pressure along the centre line of the nozzle were found using the perfect gas dynamic equations. The first law of thermodynamics was used also to find the exit Mach number (M_e) of the nozzle.

The derivation of the Method of Characteristics was presented, also, in this chapter and was used with the "Lattice Point Method" to construct the characteristic net for the flow inside the nozzle, from which the Mach number along the centre line of the nozzle was also found.

Chapter four was divided into two sections. The first dealt with the jets of the type with underexpanded regime (i.e. n>1) and empirical formulas on how to find some of the principal dimensions of the jet were presented. The second part dealt with, in some detail, the derivation of the Method of Characteristic. How to use it

to predict the shape i.e. the characteristic net, of the steam jet leaving the nozzle and entering the diffuser, inside the ejector was presented.

7.2. The Results of the One-Dimensional Approach :

7.2.1. The Use of the Perfect Gas dynamics Equations :

The two equations which were derived by using the perfect gas one-dimensional theoretical approach in Section (3.2.1.) are :

$$\frac{A}{A_t} = \frac{1}{M} \left[\frac{2 + (\gamma - 1) M^2}{\gamma + 1} \right]^{\left(\frac{\gamma+1}{2(\gamma-1)}\right)} \qquad 7.1.$$

and

$$\frac{A}{A_t} = \frac{\left(\frac{2}{\gamma-1}\right)^{\left(\frac{\gamma+1}{2(\gamma-1)}\right)} \left(\frac{P_1}{P}\right)^{\left(\frac{\gamma+1}{2\gamma}\right)}}{\sqrt{\left(\frac{2}{\gamma-1}\right) \left[\left(\frac{P_1}{P}\right)^{\left(\frac{\gamma-1}{\gamma}\right)} - 1\right]}} \qquad 7.2.$$

Applying these two equations to any nozzle, the change in Mach number (M) and the static pressure along the centre line for the nozzle can be found. Four nozzles were taken for comparison (N5, N6, N7, and N8) and the results are presented graphically in Figures (7.1. to 7.3.), and are tabulated in Tables (7.1. to 7.4.).

7.2.2. The Use of the First Law of Thermodynamics :

The basic equations for this approach are described in Section (3.3.2.). All these equations together with the thermodynamics property equations for saturated steam (Irvine, 1984) were combined in the computer programme illustrated in Appendix II.

Using this computer programme, the exit pressure (P_e) for any nozzle can be found for any motive steam pressure. The exit pressures (P_e) for four nozzles (N5, N6, N7, and N8) were found for the four different values of the motive steam pressure (P_m). The exit pressure (P_e) was found to be only one value (P_e = 0.472 psia.). The reason for this, firstly because of the change in the motive pressure (P_m) was not large enough in our experiments (limited by the capacity of the boiler) to make a significant change in the enthalpy which has a great effect on the calculations in the program, and secondly that the area ratio (A_o/A_t) is the same for the four nozzles. The exit Mach number (M_e) for the four nozzles can be found using the equation :

$$M_e = \sqrt{\left(\frac{2}{\gamma-1}\right)\left[\left(\frac{P_m}{P_e}\right)^{\left(\frac{\gamma-1}{\gamma}\right)} - 1\right]} \qquad 7.3.$$

and is tabulated in Table (7.5.).

7.3. The Results of the Two-Dimensional Approach :

7.3.1. Steam Flow in Nozzles :

The application of the two-dimensional approach (Method of Characteristics) was described in Section (3.3.3.) and the characteristic net for the flow inside the nozzle can be constructed using the computer programme presented in Appendix III. The characteristic net for the same four nozzles (N5, N6, N7, and N8) were drawn to show the output results that can be obtained from the computer program. These nets are shown in Figures (7.4. to 7.7.) where the abscissa is the distance along the centre line from the throat to the outlet of the nozzle and the ordinate is the distance from the centre line to the wall of the nozzle. The change in the Mach number (M) along the centre line of the nozzle can be found from part of the output data of the computer results and is shown in Figure (7.8.) and tabulated in Table (7.6.).

After finding the exit Mach number (M_e) for the four nozzles by the use of these two methods, the Percentage Error Method was used to find out the lowest and the highest value of error. The lowest value was found to be (-1.99%) and the highest value was found to be (5.28%). A representative graph (Figure 7.9.) was presented where the abscissa is the motive steam pressure (P_m) and the ordinate is the Mach exit number (M_e).

7.3.2. Steam Flow in Ejectors :

The theoretical shape i.e. the Characteristic Net of a steam jet leaving the nozzle and entering a diffuser was explained in Section (4.3.) and shown in Figure (4.5.). When applying the theory to the experimental data, the point was found where the nozzle steam jet meets the diffuser wall. Although the theoretical approach will stay the same, theoretical shapes will be slightly different from the one in Figure (4.5.). Ejector (E1), was chosen to show the shape of the steam nozzle jet entering the diffuser. The maximum suction pressure (P_s) for any ejector will be at its "Dead-End" point, m_a=0.0. This point can be found by experiments or by the extension, of the performance characteristic curve of the ejector, towards the zero mass point on the mass of air scale. Typical example of the performance characteristic curves is presented in Figure (7.10.) for two different ejectors (E2, and E10). At this point and at the optimum nozzle distance (L_{op}) for this ejector the shape and the constant density lines within the steam nozzle jet were found and are presented in Figures (7.11. to 7.12.). From these figures we found the steam nozzle jet diameter at the point when it hits the diffuser wall. This diameter we have called the optimum diameter (D_{op}) as the steam nozzle jet shape was found when the nozzle outlet is at a distance (L_{op}) from the diffuser throat. The optimum jet diameter (D_{op}) was found for every single-stage ejector in the same way and all these diameters are presented in Table (7.7.).

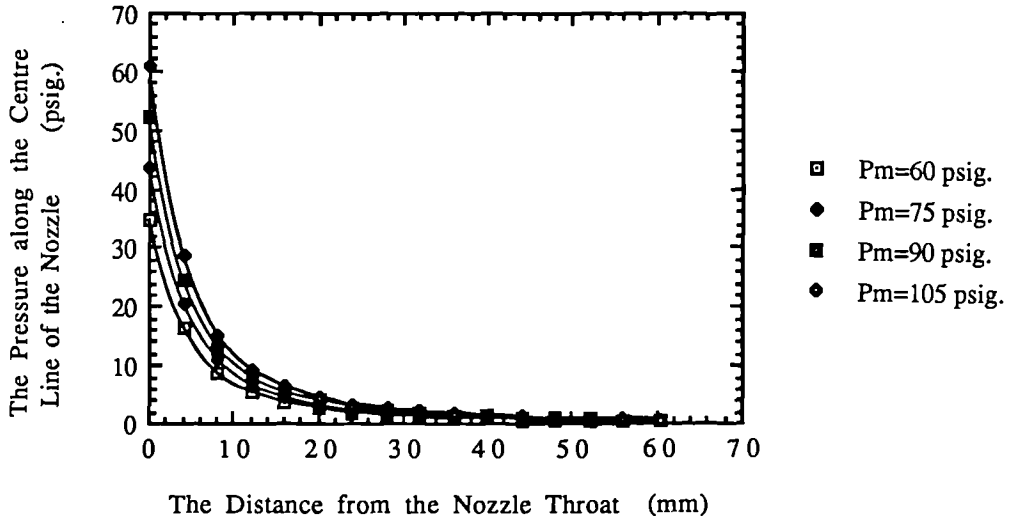

(a) Nozzle Divergence Angle, Zeta = 10^{o}.

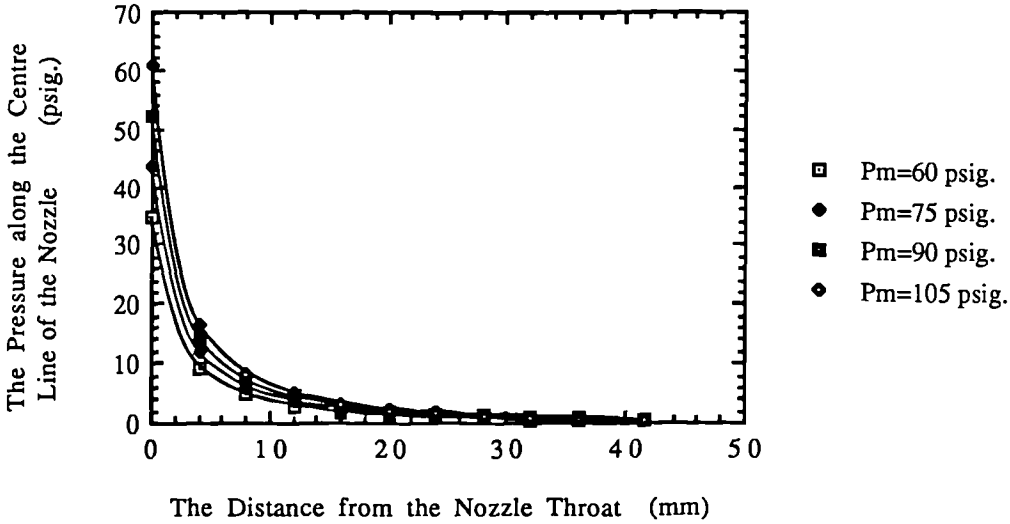

(b) Nozzle Divergence Angle, Zeta = 14^{o}.

Figure 7.1. The Change of the Pressure along the Centre Line of the Nozzle.

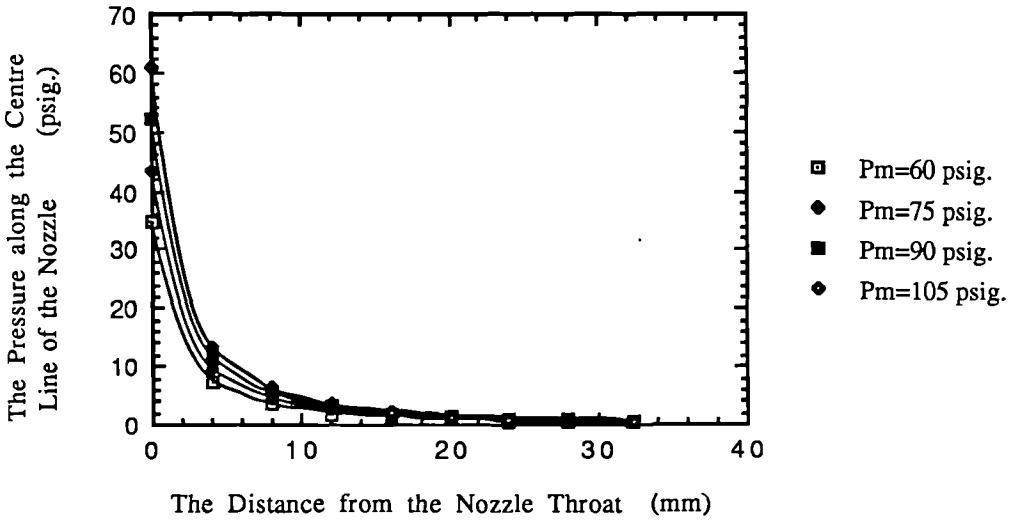

(a) Nozzle Divergence Angle, Zeta = 18°.

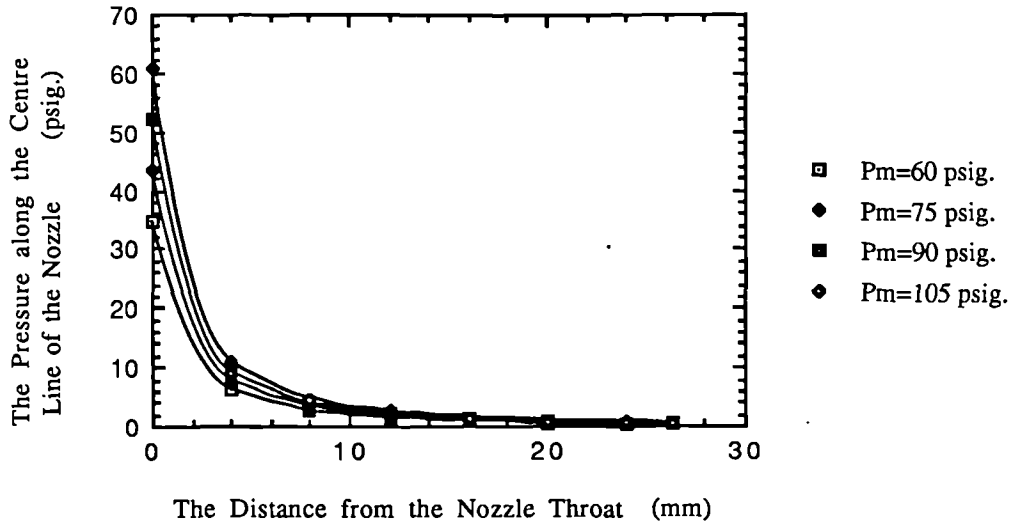

(b) Nozzle Divergence Angle, Zeta = 22°.

Figure 7.2. The Change of the Pressure along the Centre Line of the Nozzle.

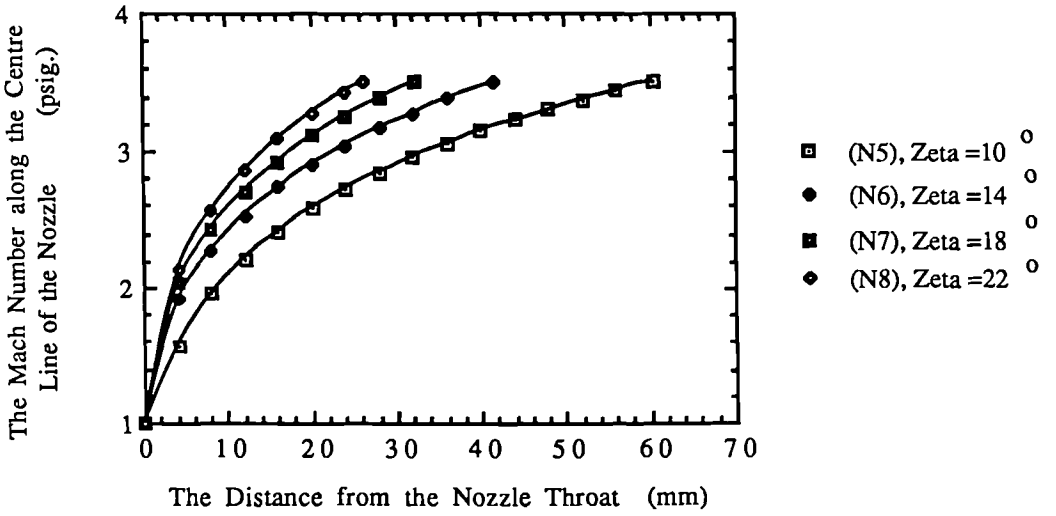

Figure 7.3. The Change of the Mach Number (M) along the Centre Line of the Nozzle.

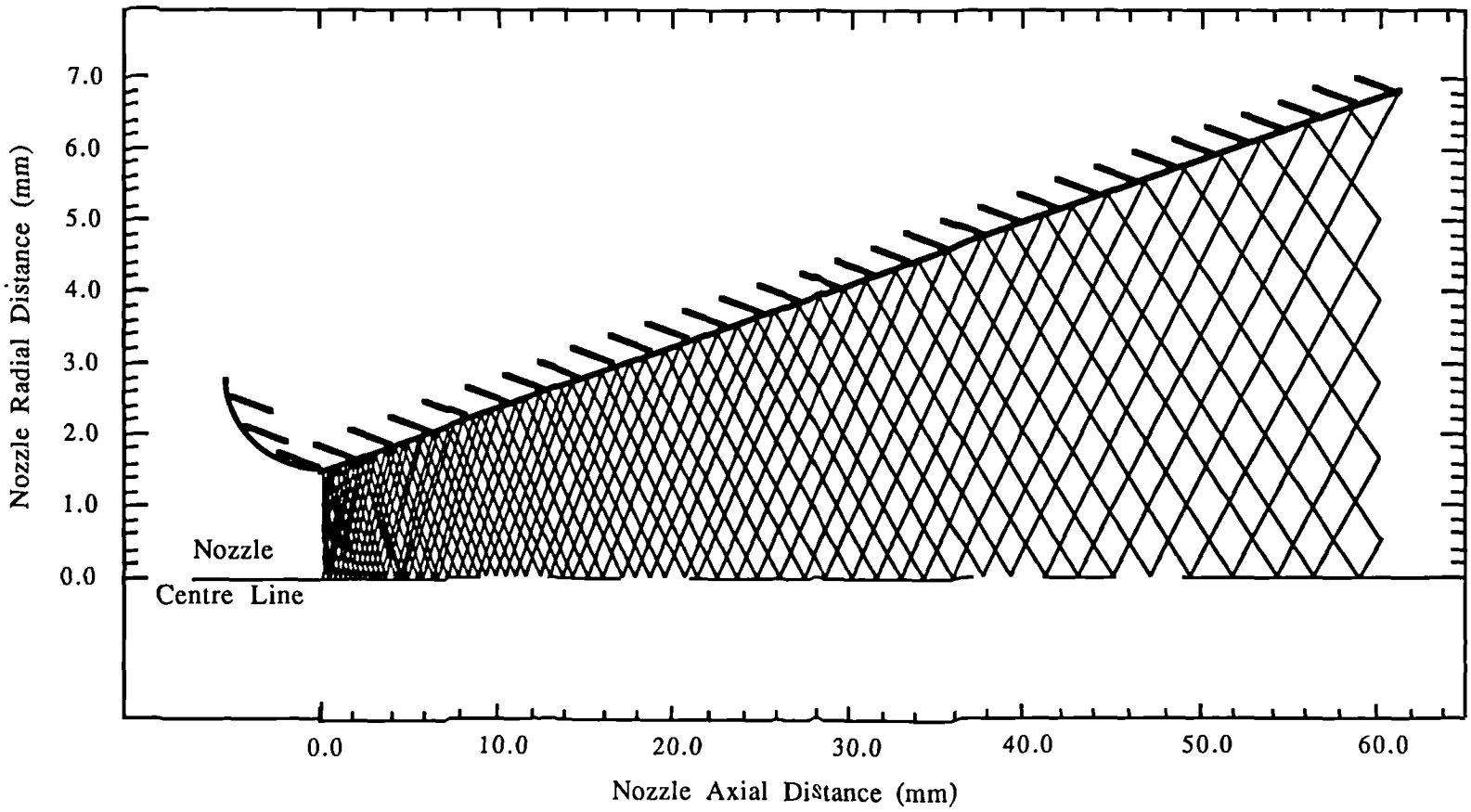

Figure 7.4. The Characteristic Net for Steam Flow in Nozzle Number N5 (Zeta =10^{o}).

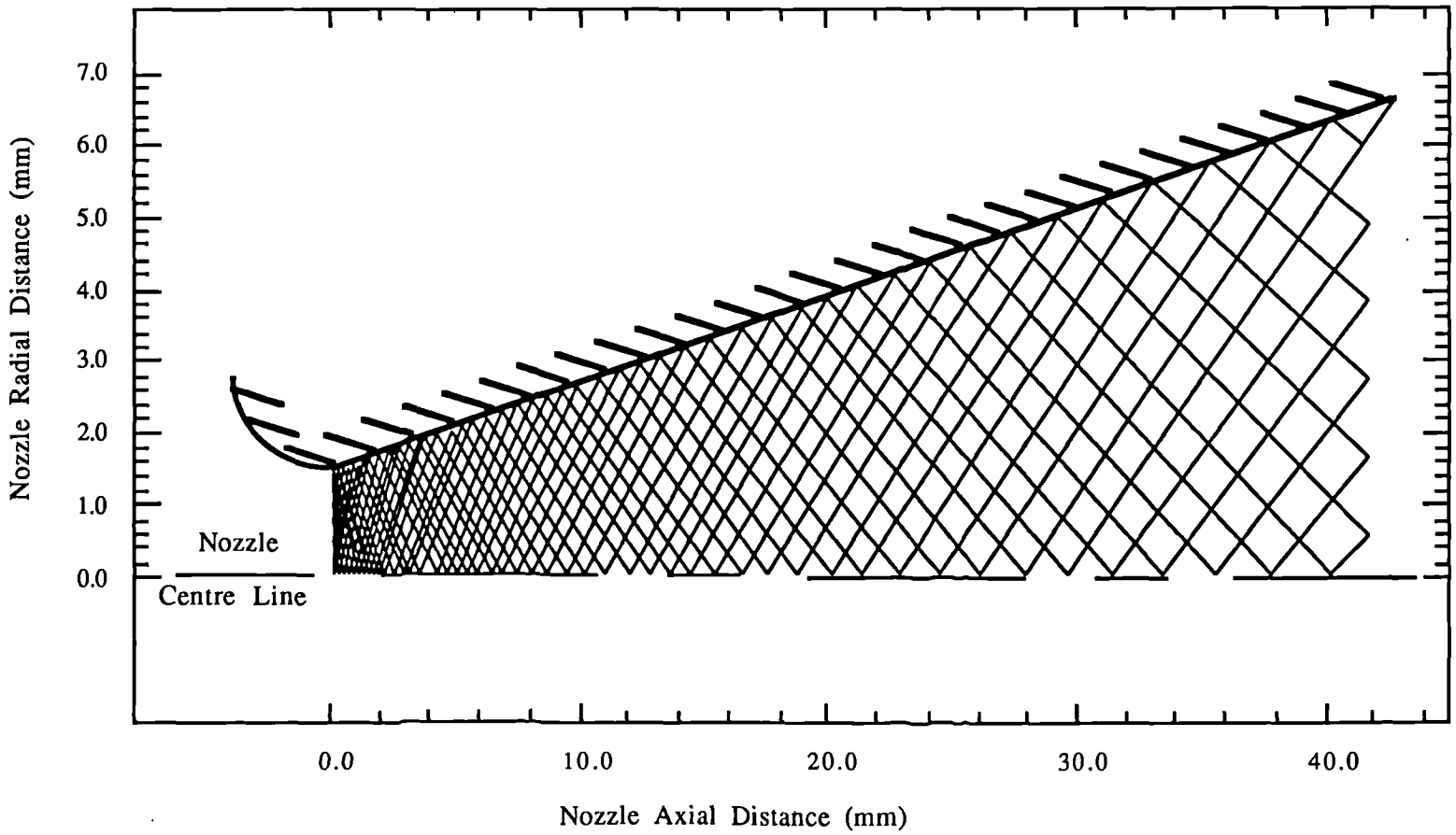

Figure 7.5. The Characteristic Net for Steam Flow in Nozzle Number N6 (Zeta =14^{o}).

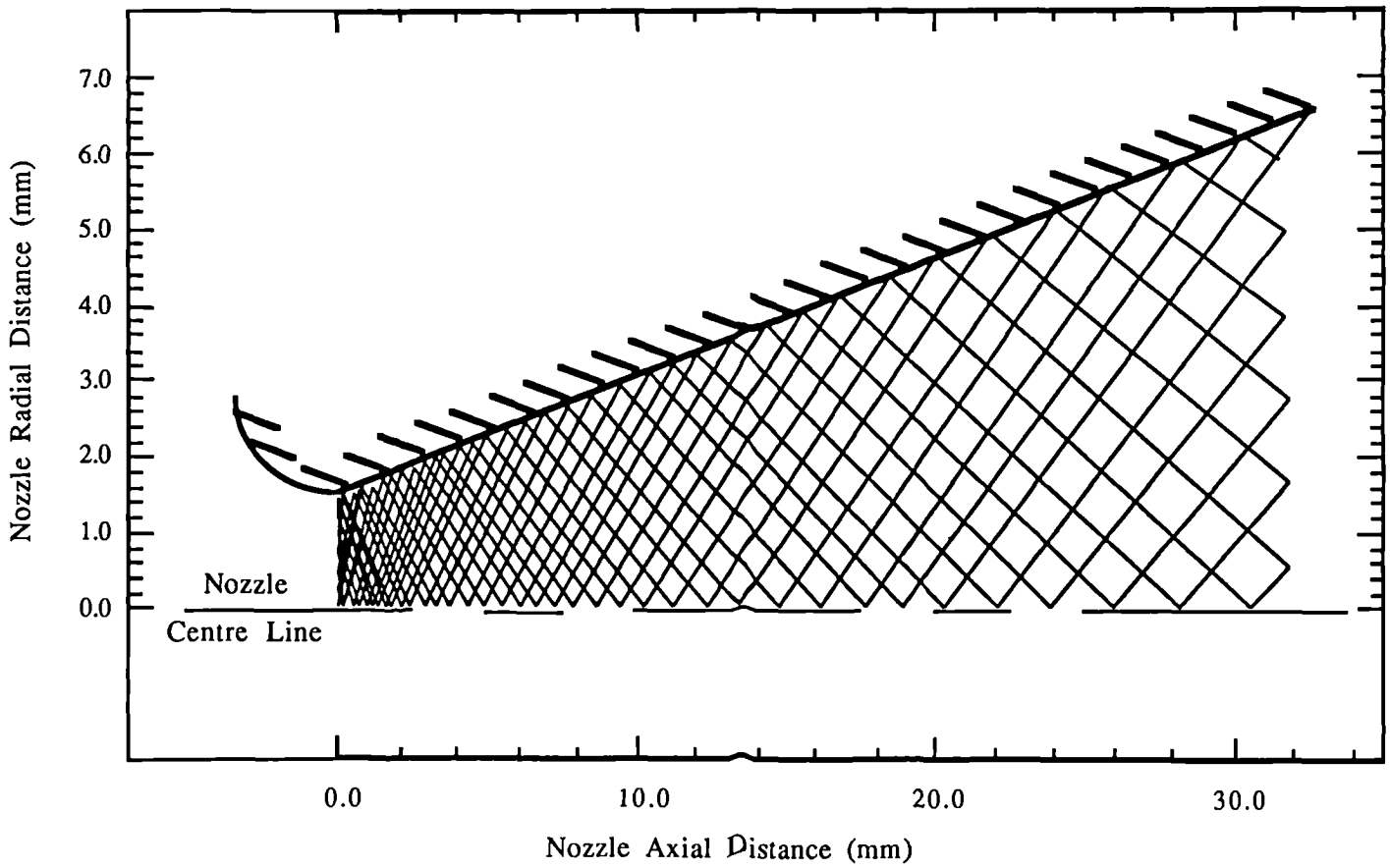

Figure 7.6. The Characteristic Net for Steam Flow in Nozzle Number N7 (Zeta=18^{o}).

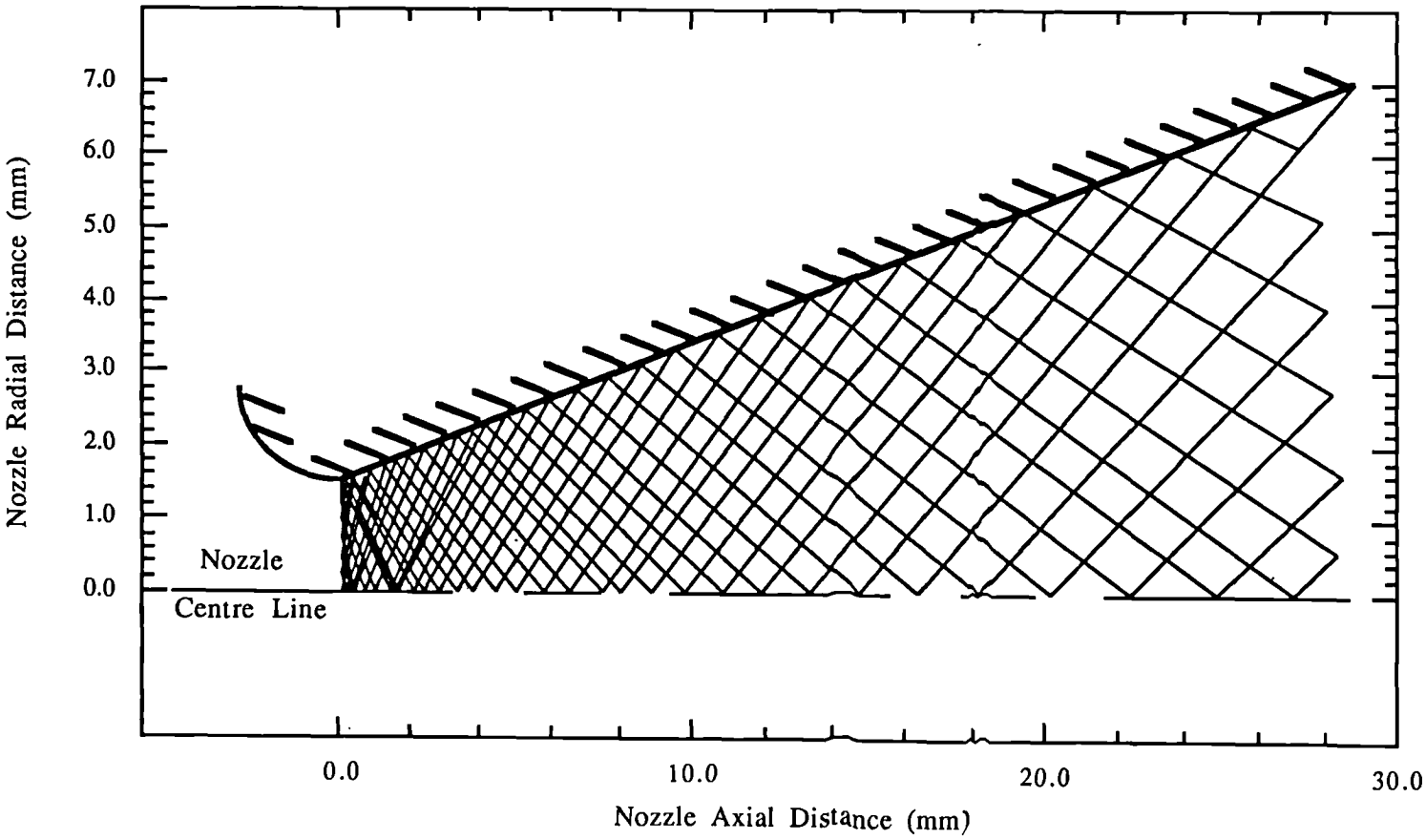

Figure 7.7. The Characteristic Net for Steam Flow in Nozzle Number N8 (Zeta =22^{o}).

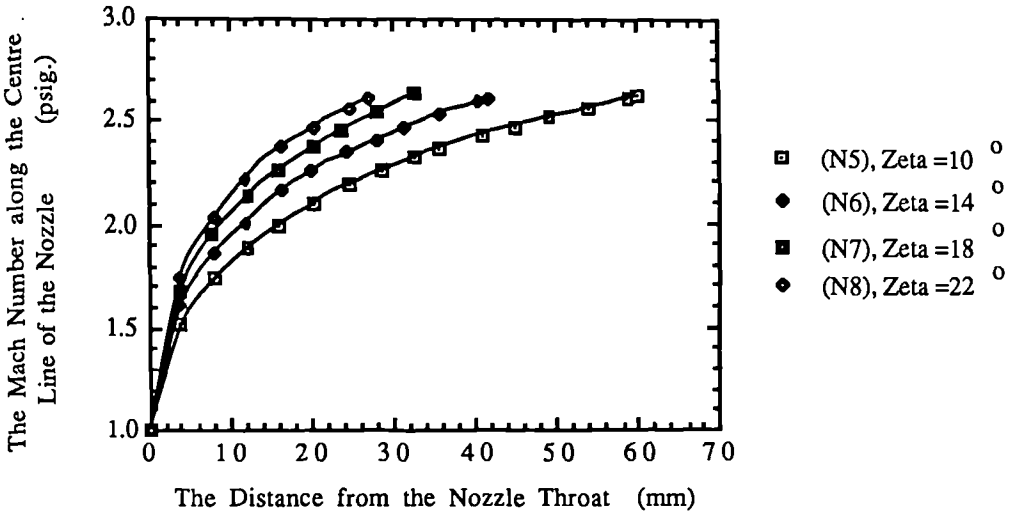

Figure 7.8. The Change of the Mach Number (M) along the Centre Line of the Nozzle.

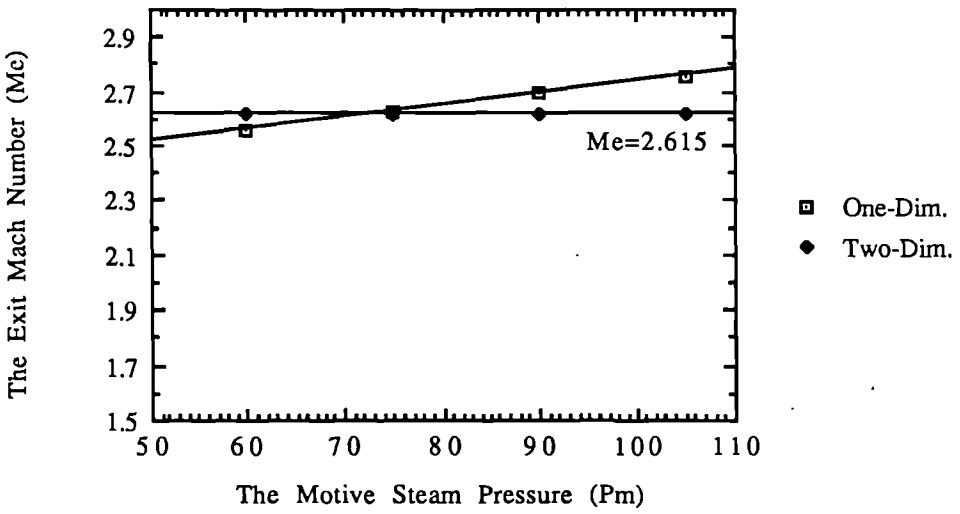

Figure 7.9. Comparison between the One-Dimensional and the Two-Dimensional Methods in Determining the Exit Mach Number (M_e).

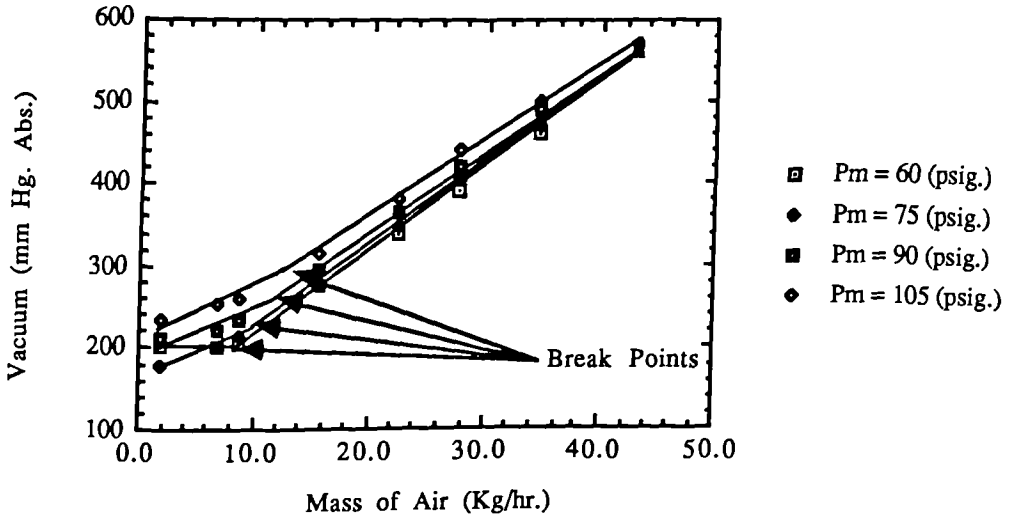

(a) Performance Characteristic Curve for Ejector Number, E2

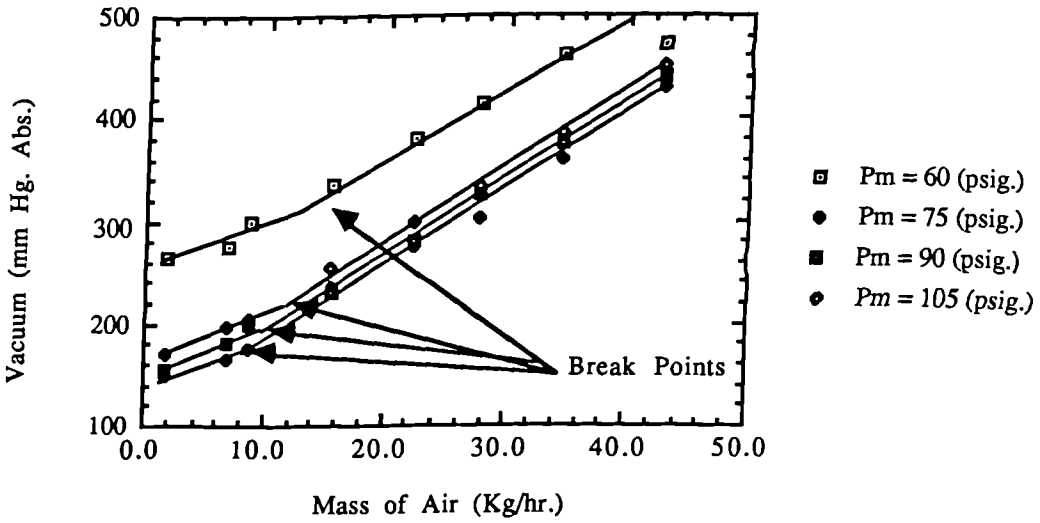

(b) Performance Characteristic Curve for Ejector Number, E10

Figure 7.10. *Typical Examples of the Performance Characteristic Curves of an Ejector.*

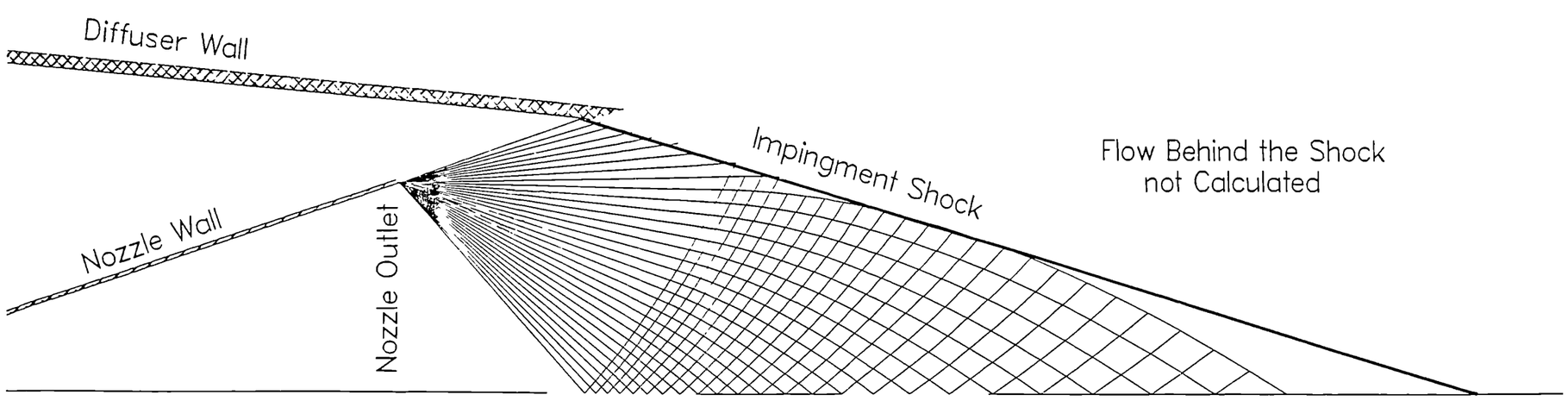

Figure 7.11. The Characteristic Net for the Steam Jet Inside the Ejector Number E1.

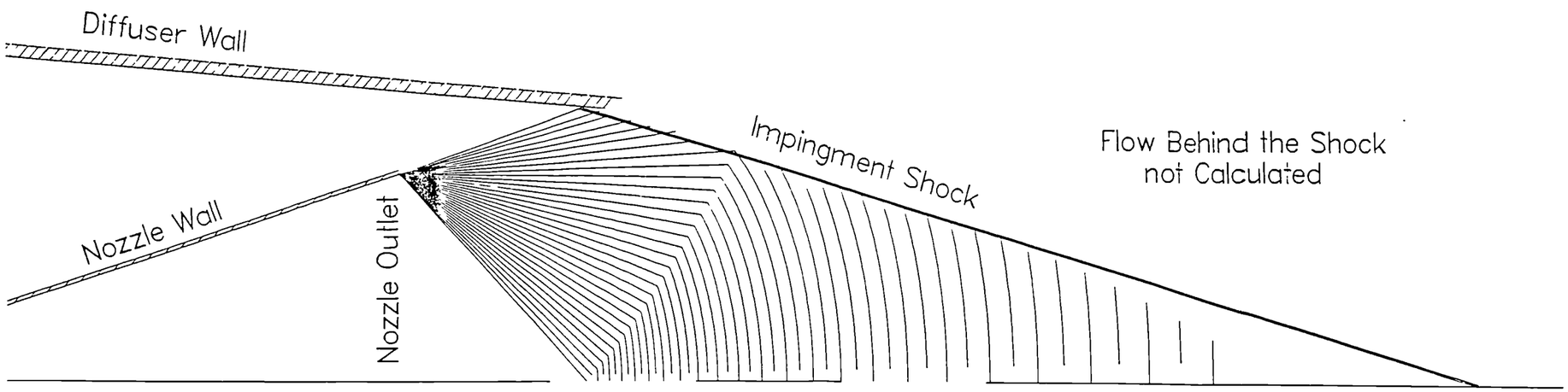

Figure 7.12 The Constant Density Lines for the Steam Jet Inside the Ejector Number E1.

Distance from the Throat =X (mm)	The Area at X (mm^2)	The Mach Number M	The Motive Pressure P_m (psig.)			
			60	75	90	105
			The Pressure Along the C_L(psia.)			
0.0	6.6	1.00	34.65	43.31	51.97	60.63
4.0	8.48	1.57	16.52	20.65	24.78	28.91
8.0	12.44	1.96	8.63	10.79	12.95	15.11
12.0	17.2	2.22	5.36	6.69	8.03	9.37
16.0	22.73	2.42	3.63	4.54	5.45	6.36
20.0	29.03	2.59	2.61	3.26	3.92	4.57
24.0	36.1	2.73	1.96	2.45	2.94	3.34
28.0	43.94	2.85	1.52	1.89	2.27	2.65
32.0	52.55	2.96	1.2	1.5	1.8	2.1
36.0	61.925	3.06	0.975	1.22	1.465	1.71
40.0	72.07	3.15	0.805	1.01	1.21	1.41
44.0	83.0	3.23	0.675	0.84	1.01	1.18
48.0	94.68	3.31	0.57	0.715	0.86	1.0
52.0	107.14	3.38	0.49	0.61	0.73	0.855
56.0	120.36	3.45	0.42	0.53	0.635	0.74
60.325	135.4	3.515	0.365	0.458	0.55	0.64

Table 7.1. The Change of the Mach Number (M) and the Pressure along the Nozzle Centre Line with, Zeta =10°.

Distance from the Throat =X (mm)	The Area at X 2 (mm)	The Mach Number M	The Motive Pressure P_m (psig.)			
			60	75	90	105
			The Pressure Along the C_L(psia)			
0.0	6.6	1.0	34.65	43.31	51.97	60.63
4.0	11.824	1.91535	9.34	11.67	14.01	16.34
8.0	18.56	2.27735	4.81	6.01	7.21	8.42
12.0	26.8	2.5343	2.9	3.63	4.36	5.08
16.0	36.52	2.7359	1.94	2.41	2.89	3.37
20.0	47.8	2.9037	1.36	1.7	2.04	2.38
24.0	60.56	3.04695	1.003	1.255	1.455	1.757
28.0	75.12	3.17465	0.764	0.955	1.146	1.337
32.0	89.6	3.27759	0.613	0.766	0.919	1.072
36.0	108.25	3.3867	0.484	0.605	0.726	0.847
41.66	135.4	3.5144	0.366	0.485	0.55	0.642

Table 7.2. The Change of the Mach Number (M) and the Pressure along the Nozzle Centre Line with, Zeta =14°.

Distance From The Throat =X (mm)	The Area at X (mm^2)	The Mach Number M	The Motive Pressure P_m (psig.)			
			60	75	90	105
			The Pressure Along the C_L(psia.)			
0.0	6.6	1.0	34.65	43.31	51.97	60.63
4.0	13.63	1.04	7.515	9.395	11.28	13.15
8.0	23.184	2.44	3.535	4.42	5.3	6.19
12.0	35.26	2.71	2.02	2.52	3.03	3.53
16.0	49.86	2.93	1.29	1.61	1.93	2.25
20.0	66.98	3.11	0.885	1.105	1.325	1.545
24.0	86.622	3.26	0.64	0.8	0.96	1.12
28.0	108.79	3.39	0.48	0.6	0.72	0.84
32.3	135.4	3.515	0.365	0.458	0.55	0.64

Table 7.3. The Change of the Mach Number (M) and the Pressure along the Nozzle Centre Line with, Zeta =18°.

Distance From The Throat =X (mm)	The Area at X (mm^2)	The Mach Number M	The Motive Pressure P_m (psig.)			
			60	75	90	105
			The Pressure Along the C_L(psia.)			
0.0	6.6	1.0	34.65	43.31	51.97	60.63
4.0	15.53	2.14	6.2	7.76	9.135	10.86
8.0	28.28	2.57	2.7	3.38	4.05	4.73
12.0	44.82	2.86	1.48	1.85	2.22	2.58
16.0	65.15	3.09	0.91	1.14	1.37	1.60
20.0	89.27	3.275	0.615	0.77	0.92	1.08
24.0	117.19	3.435	0.44	0.55	0.66	0.70
26.32	135.4	3.515	0.365	0.458	0.55	0.64

Table 7.4. The Change of the Mach Number (M) and the Pressure along the Nozzle Centre Line with, Zeta =22°.

The Exit Pressure P_e = 0.472 (psia.)			
The Motive Pressure P_m (psig.)			
60.0	75.0	90.0	105.0
The Exit Mach Number M_e			
2.56	2.63	2.70	2.75

Table 7.5. The Exit Mach Number (M_e) Depending on (P_e) and (P_m).

Total Divergent Angle of the Nozzle = ζ							
10^o		14^o		18^o		22^o	
X	M	X	M	X	M	X	M
0.0	1.0	0.0	1.0	0.0	1.0	0.0	1.0
4.0	1.52	4.01	1.62	3.73	1.68	3.76	1.75
8.15	1.74	8.00	1.86	7.81	1.95	7.97	2.03
12.16	1.89	11.83	2.01	12.31	2.14	11.93	2.22
15.96	1.99	16.43	2.16	16.10	2.26	16.30	2.37
20.38	2.1	20.05	2.25	20.37	2.37	20.08	2.46
24.68	2.19	24.49	2.34	23.86	2.45	24.74	2.56
28.52	2.25	27.98	2.40	28.07	2.54	26.94	2.61
32.73	2.32	31.44	2.46	32.90	2.62		
35.76	2.36	35.57	2.53				
40.95	2.43	40.34	2.59				
44.87	2.47	41.64	2.61				
49.20	2.52						
53.97	2.56						
58.78	2.61						
60.10	2.62						

Table 7.6. The Change of the Mach Number (M) Against the Distance from the Throat (X) along the Nozzle Centre Line.

Ejector Number	The Optimum Jet Diameter D_{op} (mm)
E1	19.50
E2	19.50
E3	19.60
E4	20.00
E5	21.80
E6	20.80
E7	22.20
E8	22.00
E9	22.40
E10	21.80
E11	23.20
E12	22.28
E13	24.20
E14	23.10
E15	24.80
E16	25.20

Table 7.7. The Optimum Jet Diameter (D_{op}) for every Single-Stage Ejector Used in the Experimental Work.

CHAPTER EIGHT

INTERPRETATION AND DISCUSSIONS OF THE RESULTS

8.1. Introduction :

The shape of the steam jet inside the ejector, and the point where it meets the diffuser wall is a result of some of the dimensional parameters of the ejector which affect the ejector performance.

The steam jet can be divided, for practical purposes, into two parts (Hickman (1972)). The first is before the point at which it meets the diffuser wall, and the second is after this point. The first part begins at the nozzle exit plane and continues downstream to the section where the potential core in the jet ends, i.e. it is the gas dynamic region in the theory of free jets. In this region, and at the nozzle exit plane, the static pressure in the supersonic steam motive flow is different from the static pressure in the surrounding air flow.

So, before any mixing of the two flows begins, the primary jet expands isentropically until its static pressure matches that of the secondary flow. At this point where this accommodation is completed, the mixing of the primary and the secondary flows begins.

But with the steam jet, the flow expands very quickly and meets the diffuser wall before the potential core in the jet ends. At this point the stream lines are deflected by the angle (δ) through an oblique shockwave forming the angle (ϕ) with the incoming velocity (Figure 8.1.) (Johannesen (1951)).

The second part i.e. downstream of the point at which the jet attaches to the wall, an adverse pressure gradient is generally established but the relatively high shearing forces near the wall tend to accelerate the fluid against the pressure gradient.

This pressure gradient was shown in many figures of previous researchers without mentioning or knowing why at this point the pressure starts to rise. The earliest researcher was Mellanby (1928) and the latest is Watanabe (1972) who showed this effect. One of the pressure gradient curves found by Watanabe is shown in Figure (8.2.).

8.2. The Effect of the Ejector Dimensional Parameters on its Performance :

8.2.1. The Effect of the Nozzle Divergence Angle :

The results from test series (B) was used to find the effect of the nozzle divergence angle on the performance of its ejector. The performance of the ejector is represented here in the form of

motive steam pressure (P_m) over the suction pressure (P_s) i.e. the steam expansion ratio. As mentioned earlier in Section (6.2.3.), this test was constructed from four ejectors (E17, E18, E19, E20) having identical dimensions but their nozzle divergence angle is different. (As a result of this difference, the length of the diverging section will change as the nozzle outlet diameter (d_o) is unchanged). Figure (8.3.) shows how the ejector performance is affected by the increase in the nozzle divergence angle for four different motive steam pressures (P_m). It is clear that the nozzle with divergence angle equal to (14°) has given the best vacuum for the four different motive steam pressure (P_m) and for any mass flow of air (m_a). We note that ESDU (1986) recommend that this angle should be about 10°. Figure (8.4.) presents the relation between the steam expansion ratio (P_m/P_s) and (P_{at}/P_s) the ratio of the atmospheric pressure (P_{at}) over the suction pressure (P_s) . This figure shows that the relation is a straight line as it was demonstrated by Dutton (1988), (he showed this relation on a log scale). It shows also that this line is only affected (i.e. it is moved up or down) by the motive steam pressure (P_m), as the performance of the four ejectors lie on the same line for this particular motive steam pressure which is (60 psig.) for this graph.

8.2.2. The Effect of the Diffuser Convergence Angle :

Results from the test results (A, C, and D) were combined

together to get an idea of how the diffuser convergence angle will affect the ejector performance. three diffusers (D4, D1, and D3) were used respectively with three nozzles (N4, N3, and N1) forming these three combinations :

- Combination one (C1) : is formed from the three ejectors (E1, E9, and E13), when nozzle (N4) was used on the three diffusers.
- Combination two (C2) : is formed from the three ejectors (E2, E10, and E14), when nozzle (N3) was put together respectively with the three diffusers.
- Combination three (C3) : is formed from the three ejectors (E3, E11, and E15), by combining nozzle (N1) with the same three diffusers.

Figure (8.5.) shows the performance curves for the three combinations (C1, C2, and C3), where the abscissa is the diffuser convergence angle and the ordinate is the steam expansion ratio (P_m/P_s). It is clear from this figure that the best diffuser convergence angle (Beta) is between (7.1°) and (7.3°).

This diffuser convergence angle lies in the interval 5° to 10° recommended by Kastner and Spooner (1950) and ESDU (1986) who recommended the interval 2° to 10°.

8.2.3. The Effect of the Area Ratio (A_o/A_{th}) :

The same combinations that were used in Section (8.2.2.) are

used in this section as well. The area ratios of the nozzle outlet to the diffuser throat were found for each ejector of these three combinations. The relation between this area ratio (A_o/A_{th}) and the performance of each combination are shown in Figure (8.6.). It is clear from this figure that for each nozzle there is an optimum area ratio (i.e. an optimum diffuser throat diameter) that gives the best performance for an ejector having this nozzle and area ratio.

8.2.4. The Effect of the Length of the Diffuser Converging Section (L_c) :

The length of the converging section of the diffuser (L_c) was found to affect the performance of the ejector. Figure (8.7.) shows how the performance was affected by this length. The length is presented non-dimensionalized with respect to the diffuser throat *diameter* (D_{th}) *i.e.* (L_c/D_{th}).

The relationship was found for the same three combinations (C1, C2, and C3), and it showed that the ejector which has the lowest value of this ratio (L_c/D_{th}) was performing better than the other ejectors which have diffusers with bigger values of that ratio. This converging section is a main part of the mixing chamber for the ejector. Its function is to introduce and mix the steam and the air flow so that there is a momentum and energy transfer between these two flows.

If this section is excessively long, increase in the friction losses will offset any performance gains from the improved mixing between the steam and the air flow. And, if it is too short, the exchange of the momentum and the energy will continue after this section and through the diffuser section, resulting in an off-design performance for the ejector. Therefore, the recommended length for this section from the experimental work and other sources is to be between 5 to 6 times the diffuser throat diameter, (D_{th}).

8.3. The Relation between the Optimum Jet Diameter (D_{op}) and the Area Ratio (A_o/A_{th}) :

The two dimensional approach, which was mainly illustrated in Section (4.3.), and its computer program, which is presented in Appendix IV, were used to find out the optimum jet diameter, (D_{op}), for every ejector. These were presented in Table (7.1.). The area ratio, (A_o/A_{th}), for the first sixteen ejectors (E1, ..., E16) were found. These sixteen ejectors were divided into four combinations :

- Combination four (C4) : is formed from (E1, E5, E9, E13).
- Combination five (C5) : is formed from (E2, E6, E10, E14).
- Combination six (C6) : is formed from (E3, E7, E11, E15).
- Combination seven (C7) : is formed from (E4, E8, E12, E16).

Figure (8.8.) shows the relationship between the area ratio, (A_o/A_{th}), and the optimum jet diameter, (D_{op}), for each combination.

With the aid of the mathematical curve fitting technique, the relationship between the area ratio (A_o/A_{th}) and the optimum jet diameter (D_{op}) was found to be in the general form of :

$$(D_{op})_e = A + B \, Log\left[\frac{A_o}{A_{th}}\right] \qquad 8.1.$$

where the suffix (e) was added to show that this (D_{op}) was found by the use of the equation.

The nozzle outlet diameter (d_o) was the major parameter which determines the dimension of the optimum jet diameter (D_{op}) in the computer program. So, it was decided to normalise (A) and (B) with respect to it, i.e. to the nozzle outlet diameter (d_o). The general equation was found then to be in the form given below :

$$(D_{op})_e = (-1.4121 + 1.5428\, d_o) + (-2.1212 - 1.6309\, d_o)\, Log\left[\frac{A_o}{A_{th}}\right] \qquad 8.2.$$

This equation was then used to find out the $(D_{op})_e$ for the sixteen ejectors and the results are compared with the ones found from the computer program together with the area ratio (A_o/A_{th}) in Table (8.1.).

Using the computer program, the optimum nozzle distance $(L_{op})_e$ can be measured when the jet diameter is equal to the calculated one $(D_{op})_e$ as shown in Figure (8.9.). The Percentage Error Method was used to find the error between (L_{op}) and $(L_{op})_e$ for each ejector. The average percentage error for this theoretical approach compared with the experimental results was found to be 1.23%. The percentage error, the optimum nozzle distance $(L_{op})_e$, and the optimum nozzle distance (L_{op}) found from the experimental results for the sixteen ejector were presented in Table (8.2.).

8.4. Design Procedure for a Single Stage Steam Ejector :

8.4.1. Determine the Constraints on the Design :

The constraints may be related to the required performance of the ejector or may be dimensional, restricting the size of the ejector. For most applications, the main design constraint falls into the following categories :

a) the motive steam pressure (P_m), is specified,

b) the suction pressure (P_s), is specified,

c) the secondary mass flow rate i.e. the mass of air (m_a), is specified.

8.4.2. Calculate the Unknown Design Parameters :

a) Finding the degree of expansion, $E = P_m/P_s$.

b) Finding the degree of compression, $K = P_d/P_s$.

c) Finding the injection coefficient, $U = m_a/m_s$. This can be found by using the Equation (8.3.). This equation was derived by using data extracted from a graph presented in Vild'er (1963) using a standard NAG library routine E04 FDF (see Appendix VII).

$$U = 1.9539 \sqrt{\frac{0.9825 - E^{-0.3154}}{0.9694 - K^{-0.57}}} - 1.914 \qquad 8.3.$$

d) Finding the mass flow rate of the inlet steam, $m_s = m_a/E$.

8.4.3. Calculate the Optimum Geometry for the Nozzle :

a) Using Equation (2.9.) the nozzle throat diameter (d_t) can be found :

$$d_t = 1.6 \sqrt{\frac{m_s \ (kg/hr)}{P_m \ (kgf/cm^2 \ Abs.)}} \qquad 8.4.$$

b) the nozzle outlet diameter (d_o) can be found using the two Equations (2.10.) and (2.11.) :

$$d_o = I\, d_t \qquad 8.5.$$

where,

$$I = 0.54\ (2.64)^{\mathrm{Log}\,(E)} \qquad 8.6.$$

c) The recommended nozzle divergence angle (Zeta), is set equal to 14° as found from the experimental results. It is the optimum within the motive steam pressure (P_m) range from 60 to 105 (psig.).

8.4.4. Calculate the Optimum Geometry for the Diffuser :

Six main dimensions for the diffuser can be recommended :

a) The diffuser throat diameter (D_{th}) which can be found by using Equation (2.8.) :

$$D_{th} = 1.6 \sqrt{\frac{\frac{18}{29}\,(m_a) + m_s \quad (kg/hr)}{P_d \quad (kgf/cm^2)}} \qquad 8.7.$$

b) The diffuser throat length (L_{th}) : It was found from the literature survey that most of the researchers recommended this length to be 4 times the throat diameter (D_{th}).

c) The diffuser entrance and outlet :

(i) The recommended entrance shape for the diffuser is to be the constant pressure mixing entrance i.e. the conical shape with full converging angle, (Beta) equal to 7.2°. This was

found from the experimental results presented in Section (8.2.2.). So, from the experimental results the ejector with the length for this converging section (L_c) over its diffuser throat diameter (D_{th}) near to 6 performed better than the others with bigger ratio (L_c/D_{th}). It is recommended that this length should be 6 times the diffuser throat diameter (D_{th}).

(ii) The recommended outlet diffuser section should have a diverging angle (Gamma) between 10^o to 12^o, and its length (L_d) equal to 6 times the diffuser throat diameter (D_{th}).

8.4.5. Calculate the Optimum Nozzle Distance (L_{op}) :

After finding the nozzle outlet diameter (d_o) and the diffuser throat diameter (D_{th}); the area ratio (A_o/A_{th}) can be used with Equation (8.2.), to find out the optimum jet diameter $(D_{op})_e$. Finally the optimum nozzle distance $(L_{op})_e$ can be found as it was explained in Section (8.3.).

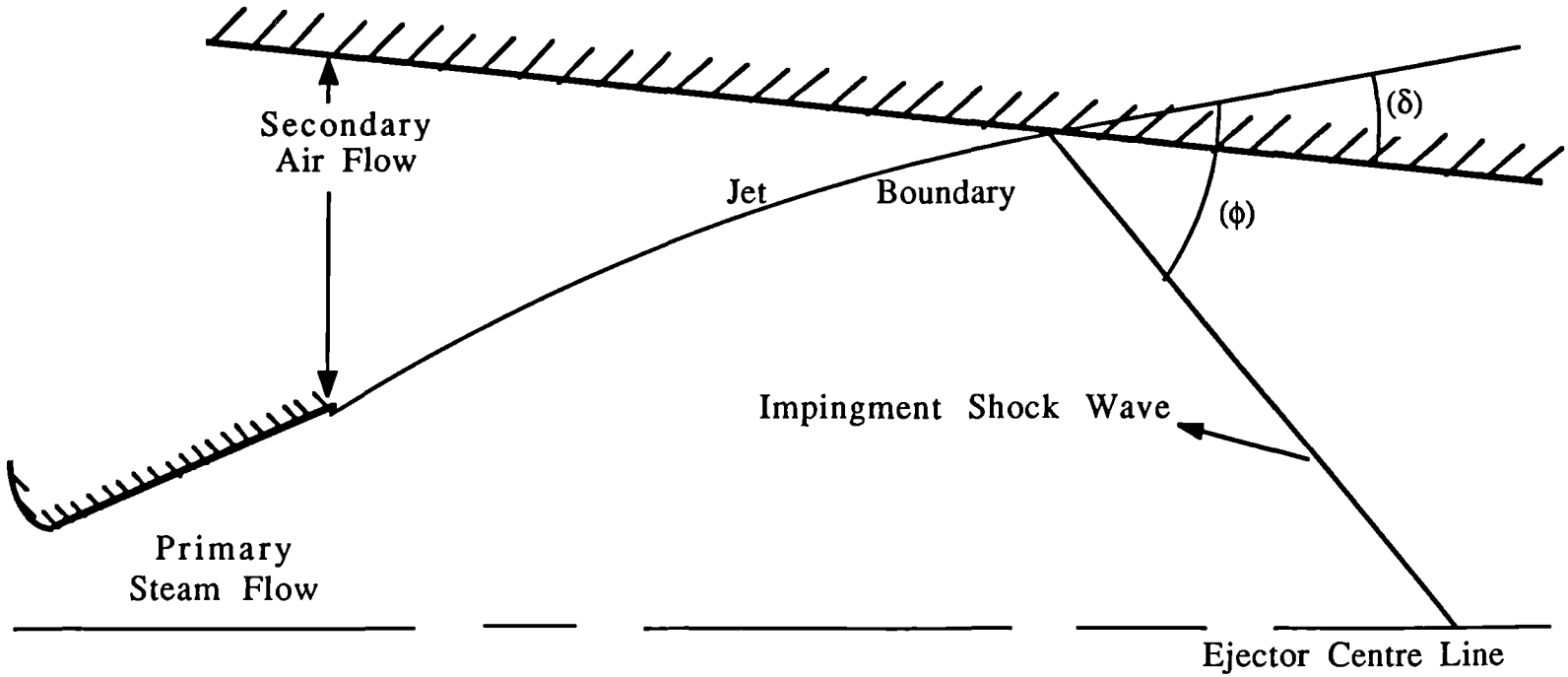

Figure 8.1. Deflection of the Boundary Streamlines at the Diffuser Wall.

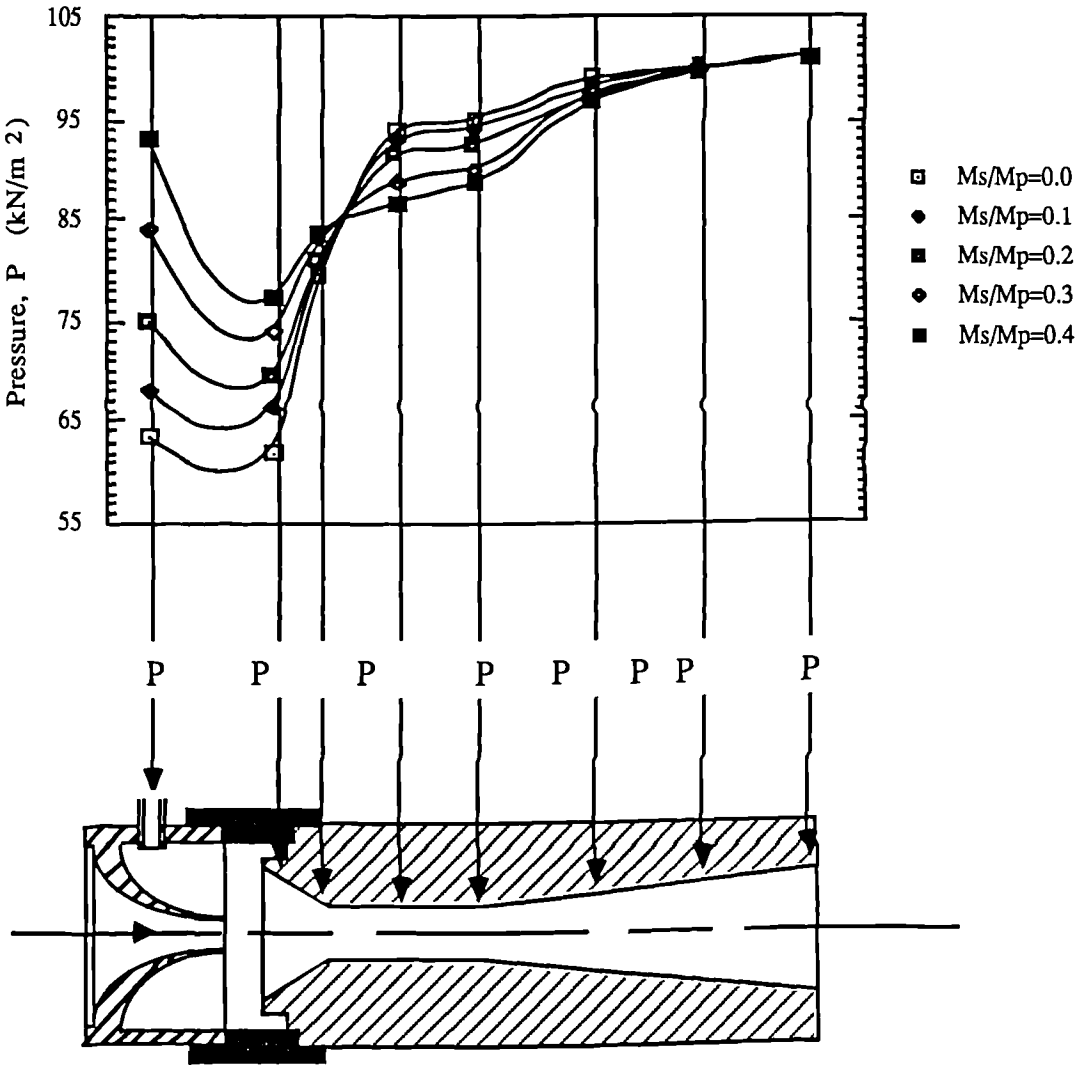

Figure 8.2. Pressure Gradiant Distributions Curves along the Ejector, (after Watanabe).

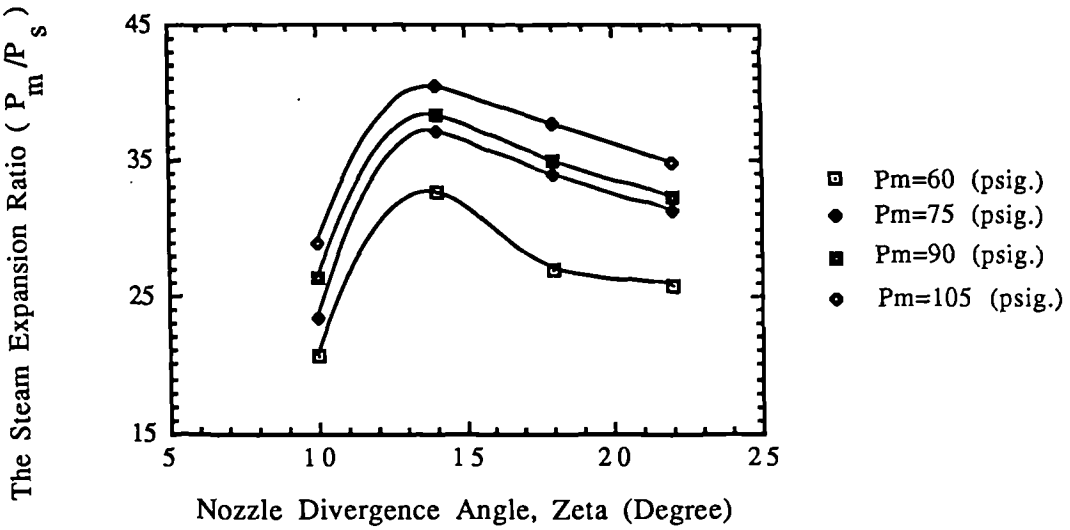

Figure 8.3. The Relation between the Steam Expansion Ratio (P_m/P_s) and its Nozzle Divergence Angle (Zeta).

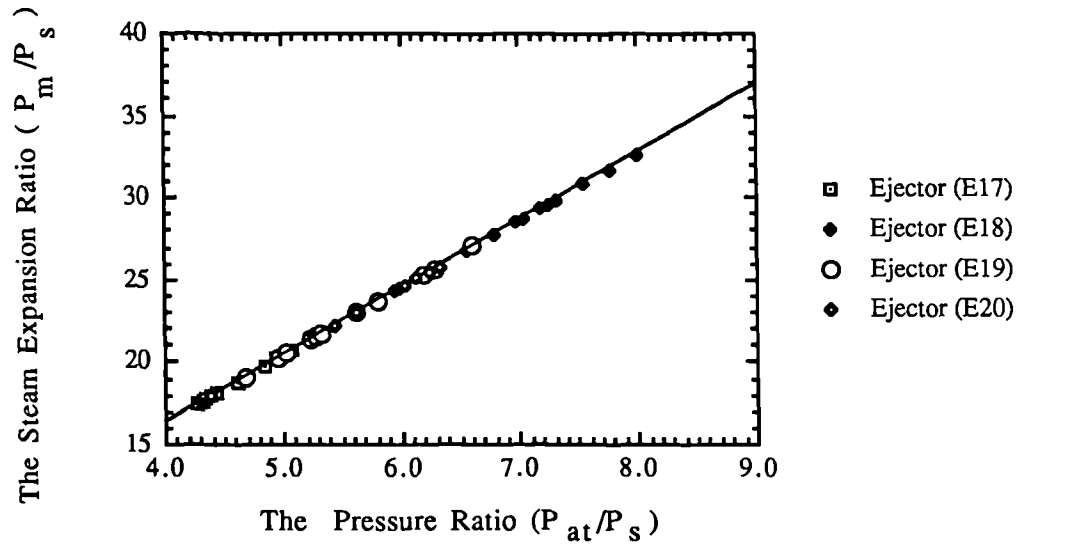

Figure 8.4. The Relation between the Steam Expansion Ratio (P_m/P_s) and the Pressure ratio (P_{at}/P_s) at the Motive steam pressure P_m = 60 (psig.).

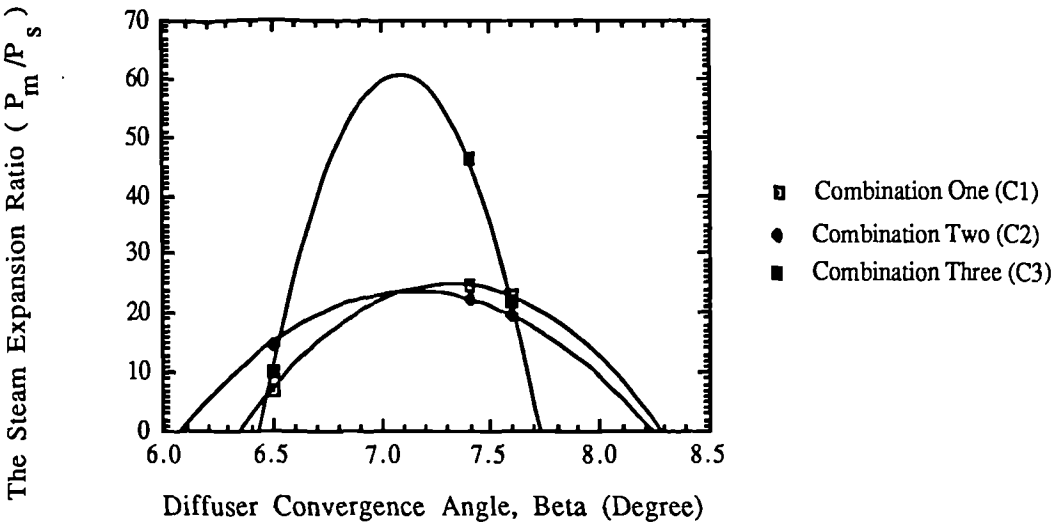

Figure 8.5. The Relation between the Steam Expansion Ratio (P_m/P_s) and its Diffuser Convergence Angle (Beta).

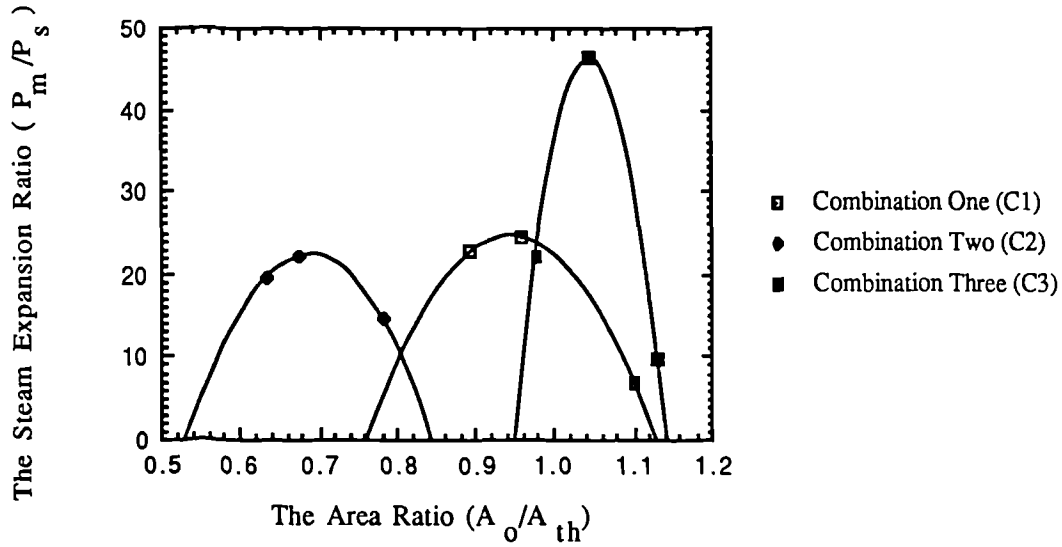

Figure 8.6. The Relation between the Steam Expansion Ratio (P_m/P_s) and the Area Ratio (A_o/A_{th}).

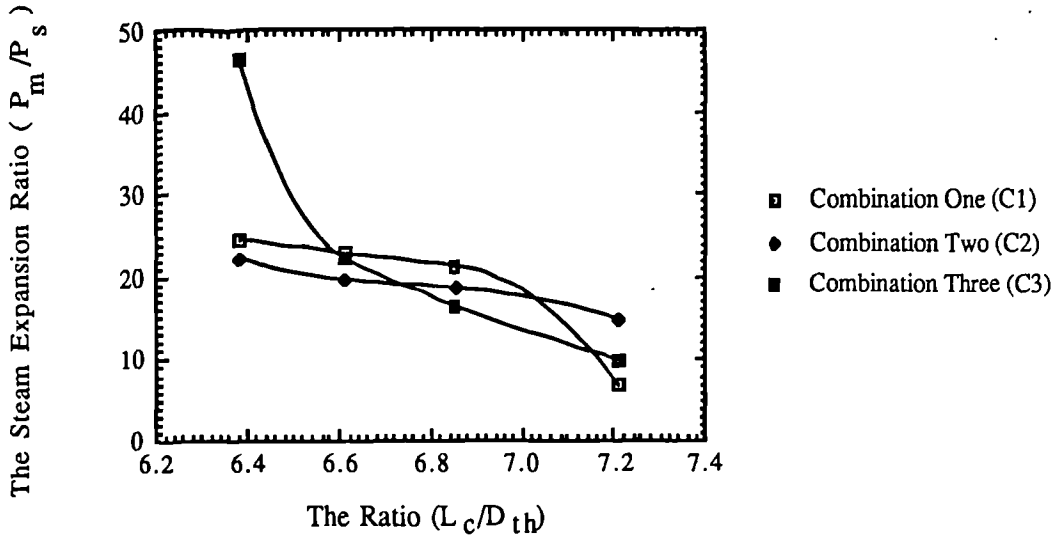

Figure 8.7. The Relation between the Steam Expansion Ratio (P_m/P_s) and the Ratio (L_c/D_{th}).

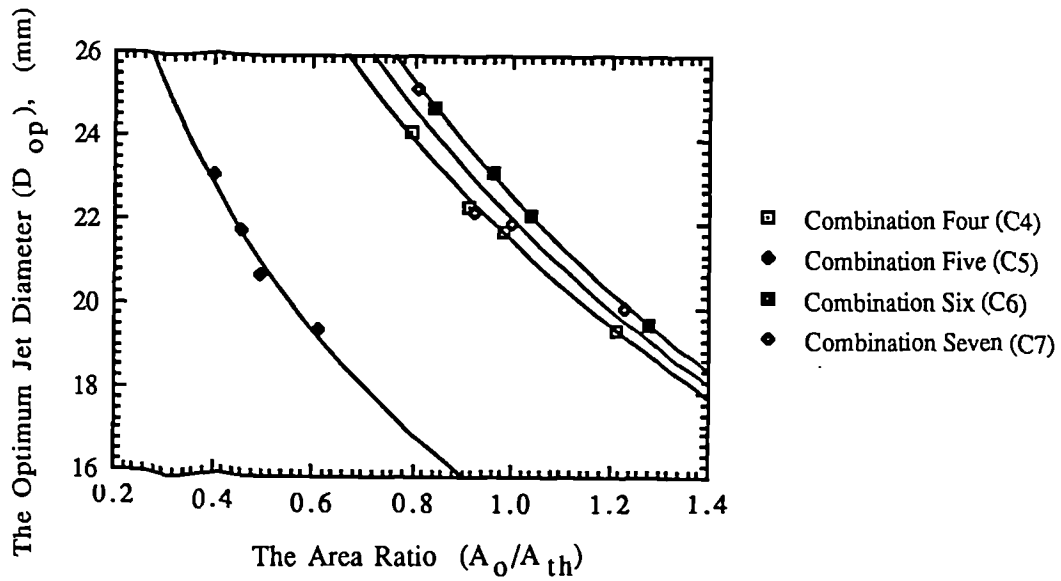

Figure 8.8. The Relation between the Optimum Jet Diameter (D_{op}) and the Area Ratio (A_o/A_{th}).

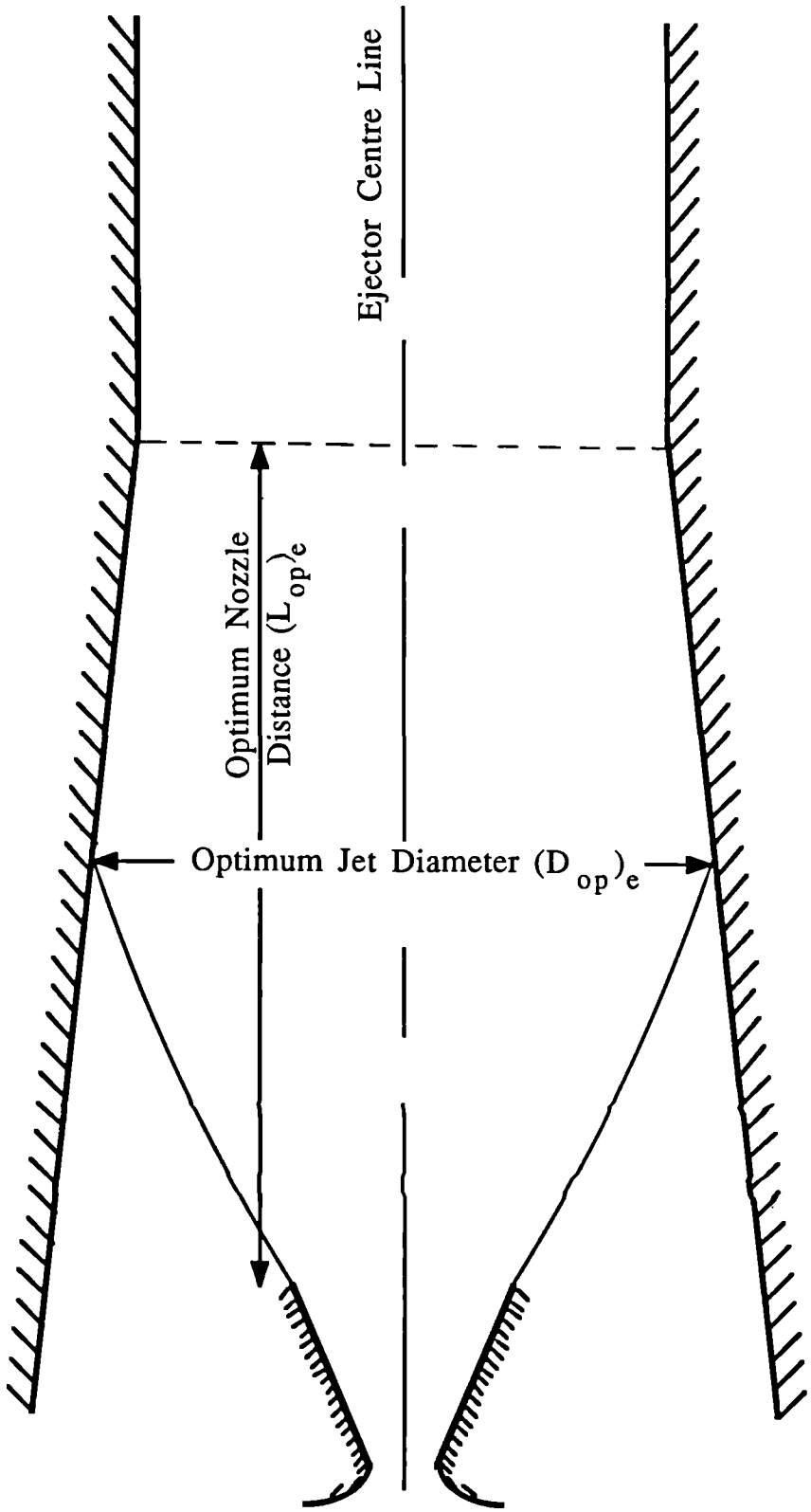

Figure 8.9. Finding the Optimum Nozzle Distance $(L_{op})_e$.

Ejector Number	The Area Ratio A_o/A_{th}	The Optimum Jet Diameter D_{op} (mm)	The Optimum Jet Diameter (D_{op})$_e$ (mm)
E1	1.215	19.50	19.62
E2	0.610	19.50	19.30
E3	1.280	19.60	19.56
E4	1.231	20.00	19.61
E5	0.986	21.80	22.05
E6	0.495	20.80	21.09
E7	1.039	22.20	22.05
E8	1.000	22.00	22.04
E9	0.913	22.40	22.94
E10	0.458	21.80	21.73
E11	0.962	23.20	22.96
E12	0.925	22.28	22.95
E13	0.798	24.20	24.50
E14	0.400	23.10	22.88
E15	0.841	24.80	24.56
E16	0.809	25.20	24.52

Table 8.1. The Sixteen Ejector with their Area Ratio (A_o/A_{th}), their Optimum Jet Diameter Found from the Computer Program (D_{op}), and their Optimum Jet Diameter $(D_{op})_e$ Found from Equation (8.2.).

Ejector Number	Optimum Nozzle Distance L_{op} (mm)	Optimum Nozzle Distance $(L_{op})_e$ (mm)	The Percentage Error between L_{op} and $(L_{op})_e$
E1	73.40	75.07	-2.27
E2	97.40	94.62	+2.85
E3	71.40	70.85	+0.77
E4	71.40	66.80	+6.44
E5	66.10	68.70	+3.93
E6	86.10	89.74	+4.23
E7	72.10	70.66	-1.99
E8	69.10	69.52	+0.60
E9	65.80	71.40	+8.51
E10	80.80	80.16	-0.79
E11	79.80	77.25	-3.19
E12	71.80	79.13	+10.2
E13	79.70	82.77	+3.85
E14	91.20	88.74	-2.69
E15	89.70	87.09	-2.91
E16	86.70	79.94	-7.79

Table 8.2. The Sixteen Ejector with their Optimum Nozzle Distance Found from the Experimental Work (L_{op}), their Optimum Nozzle Distance Found from the Computer Program $(L_{op})_e$, and the Percentage Error between them.

CHAPTER NINE

CONCLUSIONS AND SUGGESTIONS FOR FURTHER WORK

9.1. Conclusions :

The results of the research reported in this thesis has advanced the knowledge in the following aspects of the steam ejector :

9.1.1. The Optimum Nozzle Distance (L_{op}) :

(i) The air mass flow rate (m_a) and the motive steam pressure (P_m) was found not to affect this distance within the range of the experimental work.

(ii) The nozzle divergence angle (ζ) was found to affect this distance also the performance of the steam ejector. The best angle (i.e. vacuum wise) was found to be 14^o within the tested range which is 10^o-22^o.

(iii) The computer program written to predict the shape of the steam jet within the ejector was a new tool in the way of finding the optimum nozzle distance (L_{op}). As the point where the steam jet meets the diffuser wall is affected by the

nozzle outlet area (A_o), the diffuser throat area (A_{th}), and the suction pressure (P_s); the jet diameter at this point will be directly affected by these parameters as well. Equation (8.2.)

$$(D_{op})_e = (-1.4121 + 1.5428\, d_o) + (-2.1212 - 1.6309\, d_o) \log\left[\frac{A_o}{A_{th}}\right] \qquad 8.2.$$

relating the optimum jet diameter (D_{op}) with the area ratio (A_o/A_{th}) and the nozzle outlet diameter (d_o) was found and by using this program the optimum nozzle distance (L_{op}) could be found within an average error of 1.23%.

9.1.2. Design Procedure for the Ejector :

This procedure was written based on the experimental and the theoretical results from the work presented in this thesis together with some of the related published work in this field. It presents the design of the steam ejector in five steps resulting in the determination of all the dimensional parameters for the nozzle, the diffuser and the most important setting which is the optimum nozzle distance (L_{op}).

9.2. Suggestions for Further Work :

(i) A wider range of the motive steam pressure (P_m) should be investigated to ensure that the optimum nozzle distance (L_{op}) is independent of this pressure under any range.

(ii) The effect of the air mass flow rate (m_a) on a bigger steam ejector scale should be investigated to ensure that the size of the ejector will not affect the results drawn from the experimental work.

(iii) The present computer program for the flow model inside the ejector could be improved by taking into consideration the density change within the jet itself. This will probably reduce this 1.23% error in the presented design method. The temperature difference between the two flows could also be studied, although it was reported by some investigators that it has no effect on the optimum nozzle distance (L_{op}).

APPENDIX I

COMPRESSIBLE FLOW IN A CONVERGING-DIVERGING NOZZLE

The general continuity equation for steady, one-dimensional flow through a closed conduit is :

$$\dot{m} = \rho U A \qquad \text{I.1.}$$

where:

m : the mass flow of fluid passing in unit time through a cross-section where the density is (ρ) and the velocity is (U).

A : the cross-sectional area.

The differential form of this relation may be written as:

$$\frac{d\rho}{\rho} + \frac{dU}{U} + \frac{dA}{A} = 0 \qquad \text{I.2.}$$

The differentials ($d\rho$), (dU), and (dA) here may be viewed as the changes in (ρ), (U), and (A) corresponding to a change (dx) in distance along the control volume of the flow.

The relation between the sonic velocity (a) and the isentropic derivative of pressure with respect to density for a fluid is :

$$\left(\frac{\delta P}{\delta \rho}\right)_s = a^2 \qquad \text{I.3.}$$

Thus, for an isentropic process the relation between a differential change ($d\rho$) in density and the corresponding differential pressure change (dP), Equation (I.3.) is expressed as :

$$d\rho = \frac{1}{a^2}\, dP \qquad \text{I.4.}$$

Also, for a differential, reversible, thermodynamic process the first and second laws of thermodynamics can be combined to give the relation :

$$T\,ds = dh - \frac{1}{\rho}\, dp \qquad \text{I.5.}$$

As the system is assumed to undergo an isentropic process, Equation (I.5.) reduces to :

$$dh = \frac{1}{\rho}\, dP \qquad \text{I.6.}$$

The simple form of the differential equation of an adiabatic flow energy equation is :

$$dh + U\,dU = 0 \qquad \text{I.7.}$$

substitute (dh) from Equation (I.6.) into (I.7.) we get :

$$dP = -\rho\, U\, dU \qquad \text{I.8.}$$

The maximum fluid velocity obtainable in the isentropic expansion of a gas through a converging nozzle is the velocity corresponding to a Mach number of unity at the nozzle exit. If by

use of a different type of nozzle the velocity is increased beyond the sonic value, the local Mach number must become greater than unity because in an adiabatic flow the temperature and, hence, the sonic velocity, must decrease when the velocity increases (See Equations (I.12.) and (I.15.)).

So, by combining Equations (I.4.), (I.8.), the differential continuity Equation (I.2.), and replacing the ratio (U/a) by the local Mach number (M) it enables one to obtain the final equation :

$$\frac{dU}{U} = \left(\frac{1}{M^2 - 1}\right) \frac{dA}{A} \qquad \text{I.9.}$$

which applies to one-dimensional, steady, isentropic flow of a general compressible fluid. This equation indicates that when the local Mach number is greater than unity a positive increment dU in the fluid velocity must be accompanied by a positive increment dA in the cross-sectional area of the flow. It also indicates that when the local Mach number is less than unity a positive increment in velocity requires a negative increment in cross-sectional area. Therefore a nozzle designed to accelerate a gas to a supersonic velocity from a state of rest or from motion at a subsonic velocity must consist of a converging section followed by a diverging section. In the converging section the fluid is accelerated to a locally sonic velocity, and it is further accelerated from sonic to supersonic velocity in the diverging section. The junction between the converging and diverging sections where the cross-sectional area of the nozzle is minimum is called the throat.

The ordinary flow energy equation of thermodynamics after many simplifications can be written as:

$$h + \frac{U^2}{2} = h_o \qquad \text{I.10.}$$

where the subscript (o) refers to the stagnation station.

If the fluid is a perfect gas, the enthalpy will depend only on the temperature, and if in addition the specific heat (C_p) of the gas is essentially constant. Equation (I.10.) would be written in the form :

$$C_pT + \frac{U^2}{2} = C_pT_o \qquad \text{I.11.}$$

where (T_o) is called the stagnation temperature.

Applying the general formulas of perfect gas:

$$M = \frac{U}{a} \qquad \text{I.12.}$$

$$C_p - C_v = R \qquad \text{I.13.}$$

$$\gamma = \frac{C_p}{C_v} \qquad \text{I.14.}$$

$$a = \sqrt{\gamma R T} \qquad \text{I.15.}$$

Equations (I.13.) and (I.14.) give:

$$C_p = \frac{\gamma R}{\gamma - 1} \qquad \text{I.16.}$$

and Equation (I.15.) gives:

$$\gamma = \frac{a^2}{RT} \qquad \text{I.17.}$$

By combining Equations (I.11.), (I.12.), (I.16.), and (I.17.) one can derive the basic formula for the ratio of the stagnation temperature (T_o) to the static temperature (T) :

$$\frac{T_o}{T} = 1 + \left(\frac{\gamma - 1}{2}\right) M^2 \qquad \text{I.18.}$$

The gas densities are ordinarily determined by use of the perfect-gas equations of state :

$$\frac{P}{\rho} = RT \qquad \text{I.19.}$$

and

$$\frac{P}{\rho^\gamma} = \frac{P_o}{\rho_o^\gamma} = \text{Const.} \qquad \text{I.20.}$$

The relation, for an isentropic process between a static state where the pressure, density and temperature are (P), (ρ) and (T), and a stagnation state where these quantities are (P_o), (ρ_o) and (T_o), can be found by combining the two Equations (I.19.) and (I.20.) :

$$\frac{P_o}{P} = \left(\frac{T_o}{T}\right)^{\left(\frac{\gamma - 1}{\gamma}\right)} \qquad \text{I.21.}$$

Applying this relation to Equation (I.18.), the pressure ratio will be in terms of Mach number (M) :

$$\frac{P_o}{P} = \left[1 + \left(\frac{\gamma - 1}{2}\right) M^2\right]^{\left(\frac{\gamma}{\gamma - 1}\right)} \qquad \text{I.22.}$$

For isentropic flow, of a perfect gas with constant specific heats in a nozzle, the ratio of the upstream stagnation pressure (P_1) to the local static pressure (P) at a given station along the nozzle can be related to the local Mach number (M) at the point where the pressure is (P) by substituting (P_1) for (P_o) in Equation (I.22.) to obtain the relation:

$$\frac{P_1}{P} = \left[1 + \left(\frac{\gamma - 1}{2}\right) M^2\right]^{\left(\frac{\gamma}{\gamma - 1}\right)} \qquad \text{I.23.}$$

For an isentropic flow, it is also possible to relate the local cross-sectional area to the local Mach number (M) by using the Equations (I.1.), (I.15.), (I.15.), (I.18.), (I.19.), and (I.22.) to derive the following Equation :

$$\frac{\dot{m}}{A} = \frac{P_o M \sqrt{\frac{\gamma}{R T_o}}}{\left[1 + \left(\frac{\gamma - 1}{2}\right) M^2\right]^{\left(\frac{\gamma + 1}{2(\gamma - 1)}\right)}} \qquad \text{I.24.}$$

APPENDIX II

This appendix presents the computer program for the use of the thermodynamic equations to find out the exit nozzle pressure (P_e). This program was written in Basic Computer language. The main one-dimensional equations used in this program were presented in Section (3.3.2.) and the thermodynamic property equations for the steam saturated and superheated are taken from Irvine (1983). Although the steam used in the experimental work was saturated steam; the program was written in such a way that it can deal with saturated and superheated steam as well. The meaning of the symbols used here are listed at the end of this appendix.

Saturation Properties :

To overcome the difficulty of fitting the property of the steam to the desired accuracy with a single expression from the triple point to the critical point, the entire temperature region was divided into ranges with separate equations, as follows :

Range I : 273.16 ≤ T(S) < 300 K
Range II : 300 ≤ T(S) < 600 K
Range III : 600 ≤ T(S) ≤ 647.3 K
Range IV : 273.16 ≤ T(S) < 600 K
Range V : 273.16 ≤ T(S ≤ 647.3 K

Using the above considerations, it was possible to represent the various thermodynamics properties with three types of equations from the triple point to the critical point. These properties are :

1. Saturation temperature
2. Saturation pressure
3. Liquid saturation specific volume
4. Vapour saturation specific volume
5. Liquid saturation enthalpy
6. Vapour saturation enthalpy
7. Latent heat of vaporisation
8. Liquid saturation entropy
9. Vapour saturation entropy

The basic equations which cover the nine properties are of the form :

_ For the Saturation Temperature T(S),

$$T(S) = A + \frac{B}{[LOG\ P(S)] + C} \qquad \text{II.1.}$$

Range IV	Range III
0.000611 ≤ P(S) < 12.33 MPA	12.33≤ P(S) ≤ 22.1 MPA
273.16 ≤ T(S) < 600 K	600 ≤ T(S) ≤ 647.3 K
A = 0.426776E2	A = -0.387592E3
B = -0.389270E4	B = -0.125875E2
C = -0.948654E1	C = -0.152578E2

_ For the Saturation Pressure P(S),

$$LOG\ P(S) = \sum_{N=0}^{9} A(N)\ T(S)^N + \frac{A(10)}{T(S) - A(11)} \qquad II.2.$$

Range V

$273.16 \leq T(S) \leq 647.3\ K$

A(0) = 0.104592E2

A(1) = -0.404897E-2

A(2) = -0.417520E-4

A(3) = 0.368510E-6

A(4) = -0.101520E-8

A(5) = 0.865310E-12

A(6) = 0.903668E-15

A(7) = -0.199690E-17

A(8) = 0.779287E-21

A(9) = 0.191482E-24

A(10) = -0.396806E4

A(11) = 0.395735E2

_ For constants for Saturation Properties : Specific Volume, Enthalpy, and Entropy,

$$Y(S) = A + BT(C)^{1/3} + CT(C)^{5/6} + DT(C)^{7/8} + \sum_{N=1}^{7} E(N)\ T(C)^N \qquad II.3.$$

and

$$T(C) = \frac{[\ T(CR) - T(S)\ ]}{T(CR)} \quad ; \quad T(CR) = 647.3\ K$$

Range V

V(F) = Y(S) V(FCR)

$273.16 \leq T(S) \leq 647.3\ K$

A = 1.0

B = -1.9153882

C = 1.2015186E1

D = -7.8464025

E(1) = -3.888614

Range V

V(G) = Y(S)P(CR)V(GCR)/P(S)

$273.16 \leq T(S) \leq 647.3\ K$

A = 1.0

B = 1.6351057

C = 5.2584599E1

D = -4.4694653E1

E(1) = -8.9751114

E(2) = 2.0582238

E(3) = -2.0829991

E(4) = 8.2180004E-1

E(5) = 4.7549742E-1

E(6) = 0.0

E(7) = 0.0

V(FCR) = 3.155E-3

E(2) = -4.3845530E-1

E(3) = -1.9179576E1

E(4) = 3.6765319E1

E(5) = -1.9462437E1

E(6) = 0.0

E(7) = 0.0

V(GCR) = 3.155E-3

P(CR) = 2.2089E1

Range I

H(F) = Y(S) H(FCR)

273.16 ≤ T(S) < 300 K

A = 0.0

B = 0.0

C = 0.0

D = 0.0

E(1) = 6.24698837E2

E(2) = -2.34385369E3

E(3) = -9.50812101E3

E(4) = 7.16287928E4

E(5) = -1.6353522E5

E(6) = 1.66531093E5

E(7) = -6.47854585E4

H(FCR) =2.0993E3

Range II

H(F) = Y(S) H(FCR)

300 ≤ T(S) < 600 K

A =8.839230108E-1

B = 0.0

C = 0.0

D = 0.0

E(1) = -2.67172935

E(2) = 6.22640035

E(3) = -1.31789573E1

E(4) = -1.91322436

E(5) = 6.87937653E1

E(6) = -1.24819906E2

E(7) = 7.21435404E1

H(FCR) = 2.0993E3

Range III

H(F) = Y(S) H(FCR)

Range V

H(FG) = Y(S) H(FGTP)

600 ≤ T(S) ≤ 647.3 K

A = 1.0

B = -4.41057805E-1

C = -5.52255517

D = 6.43994847

E(1) = -1.64578795

E(2) = -1.30574143

E(3) = 0.0

E(4) = 0.0

E(5) = 0.0

E(6) = 0.0

E(7) = 0.0

H(FCR) =2.0993E3

273.16 ≤ T(S) ≤ 647.3 K

A = 0.0

B = 7.79221E-1

C = 4.62668

D = -1.07931

E(1) = -3.87446

E(2) = 2.94553

E(3) = -8.06395

E(4) = 1.15633E1

E(5) = -6.02884

E(6) = 0.0

E(7) = 0.0

H(FGTP) = 2.5009E3

Range V

H(G) = Y(S) H(GCR)

273.16 ≤ T(S) ≤ 647.3 K

A = 1.0

B = 4.57874342E-1

C = 5.08441288

D = -1.48513244

E(1) = -4.81351884

E(2) = 2.69411792

E(3) = -7.39064542

E(4) = 1.04961689E1

E(5) = -5.46840036

E(6) = 0.0

Range I

S(F) = Y(S) S(FCR)

273.16 ≤ T(S) ≤ 300 K

A = 0.0

B = 0.0

C = 0.0

D = 0.0

E(1) = -1.83692956E3

E(2) = 1.47066352E4

E(3) = -4.31466046E4

E(4) = 4.86066733E4

E(5) = 7.9975096E3

E(6) = -5.83339887E4

E(7) = 0.0

H(GCR) =2.0993E3

Range II

S(F) = Y(S) S(FCR)

300 ≤ T(S) ≤ 600 K

A = 9.1276291E-1

B = 0.0

C = 0.0

D = 0.0

E(1) = -1.75702956

E(2) = 1.68754095

E(3) = 5.82215341

E(4) = -6.33354786E1

E(5) = 1.88076546E2

E(6) = -2.52344531E2

E(7) = 1.28058531E2

S(FCR) = 4.4289

Range V

S(G) = Y(S) S(GCR)

273.16 ≤ T(S) ≤ 647.3 K

A = 1.0

B = 3.77391E-1

C = -2.78368

D = 6.93135

E(1) = -4.34839

E(7) = 3.31400718E4

H(FC R) = 4.4289

Range III

S(F) = Y(S) S(FCR)

600 ≤ T(S) ≤ 647.3 K

A = 1.0

B = -3.24817650E-1

C = -2.990556709

D = 3.2341900

E(1) = -6.78067859E-1

E(2) = -1.91910364

E(3) = 0.0

E(4) = 0.0

E(5) = 0.0

E(6) = 0.0

E(7) = 0.0

S(FCR) = 4.4289

E(2) = 1.34672

E(3) = 1.75261

E(4) = -6.22295

E(5) = 9.99004

E(6) = 0.0

E(7) = 0.0

S(GCR) = 4.4289

Superheated Properties

The equations in the superheated region are much more complex since they must represent the changing nature of the intermolecular forces all the way from the saturation line to the perfect gas region :

_ For Specific Volume V(PT),

$$V(P,T) = \frac{RT}{P} - B(1)\,EXP[-B(2)\,T] + \frac{1}{10\,P}\left[B(3) - EXP\left(\sum_{N=0}^{2} A(N)\,T(S)^{N}\right)\right] EXP\left[\frac{T(S) - T}{M}\right] \quad \text{II.4.}$$

R = 4.61631E-4

M = 4.0E1

B(1) = 5.27993E-2

B(2) = 3.75928E-3

B(3) = 2.2E-2

A(0) = -3.741378

A(1) = -4.7838281E-3

A(2) = 1.5923434E-5

_ For Enthalpy H(PT),

$$H(PT) = \sum_{N=0}^{2} A(N)\, T^N - A(3)\, EXP\left[\frac{T(S) - T}{M}\right] \qquad \text{II.5.}$$

$A(0) = B(11) + B(12)\, P + B(13)\, P^2$

$A(1) = B(21) + B(22)\, P + B(23)\, P^2$

$A(2) = B(31) + B(32)\, P + B(33)\, P^2$

$A(3) = B(41) + B(42)\, T(S) + B(43)\, T(S)^2 + B(44)\, T(S)^3 + B(45)\, T(S)^4$

B(11)	= 2.04121E3	B(21)	= 1.610693
B(12)	= -4.040021E1	B(22)	= 5.472051E-2
B(13)	= -4.8095E-1	B(23)	= 7.517537E-4
B(31)	= 3.383117E-4	B(42)	= -1.699419E1
B(32)	= -1.975736E-5	B(43)	= 6.2746295E-2
B(33)	= -2.87409E-7	B(44)	= -1.0284259E-4
B(41)	= 1.70782E3	B(450	= 6.4561298E-8
M	= 4.5E1		

_ For Entropy S(PT),

$$S(PT) = \sum_{N=0}^{4} A(N)\, T^N + B(1)\, LOG[P+B(2)] - \left[\sum_{N=0}^{4} C(N)\, T(S)^N\right] EXP\left[\frac{T(S) - T}{M}\right] \qquad \text{II.6.}$$

A(0)	= 4.6162961	B(2)	= 1.0E-3

A(1)	= 1.039008E-2	C(0)	= 1.777804
A(2)	= -9.873085E-6	C(1)	= -1.802468E-2
A(3)	= 5.43411E-9	C(2)	= 6.854459E-5
A(4)	= -1.170465E-12	C(3)	= -1.184424E-7
B(1)	= -4.650306E-1	C(4)	= 8.142201E-11
M	= 8.5E1		

SYMBOLS USED

E(T)	Entropy function
H(F)	Saturated liquid enthalpy
H(FCR)	Saturated liquid enthalpy at critical point
H(FG)	Latent heat of vaporization
H(FGTP)	Latent heat of vaporization at triple point
H(G)	Saturated vapor enthalpy
H(GCR)	Saturated enthalpy at critical point
H(PT)	Superheat enthalpy
H(T)	Enthalpy
LOG	Natural logarithm
P	Pessure
P(S)	Saturation pessure
R	Gas constant
S(F)	Saturated liquid entropy
S(FCR)	Saturated liquid entropy at critical point
S(G)	Saturated vapor entropy
S(FG)	S(G) - S(F)
S(GCR)	Saturated vapor entropy at critical point
S(PT)	Superheat entropy
T(S)	Saturation temperature
T	Temperature
T(C)	[T(CR) - T(S)]/T(CR)
T(CR)	Critical temperature
V	Specific volume
V(F)	Saturated liquid specific volume
V(G)	Saturated vapor specific volume
V(PT)	Superheat specific volume

```
 10 REM SAVE"REM"
 20 @%=&20707
 30 BB=0:PROCSTEAM
 40 BB=1:At=6.6E-6:Ae=135.4E-6
 50 Sgm=Sg:Hgm=Hg
 60 Ps=0.577*Ps:GOTO 420
 70 Sft=Sf:Sgt=Sg:Hgt=Hg:Vgt=Vg
 80 m=102.7-0.4521*(Hgm-Hgt)
 90 VEt=(2000*m*(Hgm-Hgt))^(1/2):PRINT"VEt=";VEt
100 Mt=At*(VEt/Vgt):BB=2:PRINT"Mt=";Mt
110 FOR Ps=0.003548 TO 0.4 STEP 0.0000001
120 PRINT"Ps=";Ps
130 GOTO 420
140 Sfe=Sf:Sge=Sg:Hfe=Hf:Hge=Hg:Vg=Vg
150 X=(Sgm-Sfe)/(Sge-Sfe)
160 Vge=X*Vg
170 He=(1-X)*Hfe+Hge*X
180 m=102.7-0.4521*(Hgm-He)
190 VEe=(2000*m*(Hgm-He))^(1/2)
200 Me=Ae*(VEe/Vge):PRINT"Me=";Me
210 IF Me>=Mt AND Me<=Mt+0.0002 THEN GOTO 230
220 NEXT Ps
230 PRINT ."Me=";Me
240 PRINT "Pe=";Ps
250 END
260:
270 DEF PROCSTEAM
280 DIM A(12), E(7),B(14), C(4)
290 PRINT "ARE YOU IN THE SUPERHEATED OR THE SATURATION REGION ?"
300 INPUT "PLEASE ANSWER WITH SUPER OR SAT ONLY";F$
310 IF F$="SAT" THEN GOTO 330 ELSE IF F$="SUPER" THEN PROCSUPER ELSE GOTO 290
320 IF F$="SUPER" GOTO 350
330 INPUT "WHICH VALUE DO YOU HAVE Ps OR Ts";A$
340 IF A$="Ps" THEN PROCPS ELSE IF A$="Ts" THEN PROCTS ELSE GOTO 330
350 ENDPROC
360:
370 DEF FNof=A+B*(TC^(1/3))+C*(TC^(5/6))+D*(TC^(7/3))+POL/1
380:
390 DEF PROCPS
400 INPUT"ENTER VALUE OF Ps(IF YOU ARE IN THE SUPER ENTER THE VALUE OF P)";Ps
410 DEF FNofPs=A+B/(LN(Ps)+C)
420 IF Ps<0.000611 THEN PRINT "ERROR"
430 IF Ps>=0.000611ANDPs<12.33THEN PROCTEMP1:IF BB=1GOTO70 ELSEIF BB=2GOTO150
440 IF Ps>=12.33ANDPs<=22.1THEN PROCTEMP2:IF BB=1 GOTO70 ELSEIF BB=2GOTO150
450 ENDPROC
460:
470 DEF PROCTEMP1
480 A=0.426776E2:B=-0.389270E4:C=-0.948654E1
490 Ts=FNofPs
500 REM PRINT"Ts=";Ts
510 IF F$="SAT" THEN PROCALL ELSE PROCALLSUPER
520 ENDPROC
530:
540 DEF PROCTEMP2
550 A=-0.387592E3:B=-0.12587SE5:C=-0.152578E2
560 Ts=FNofPs
570 REM PRINT"Ts=";Ts
580 IF F$="SAT" THEN PROCALL ELSE PROCALLSUPER
590 ENDPROC
600:
610 DEF PROCTS
620 INPUT "ENTER VALUE OF Ts";Ts
630 DEF FNofTs=POLY(A(10)/(Ts-A(11))
640 IF Ts<273.16 THEN PRINT "ERROR":GOTO 620
650 IF Ts>=273.16 AND Ts<=647.3 THEN PROCPRESS ELSE PRINT "SUPER"
660 PROCALL
670 ENDPROC
680:
```

```
690 DEF PROCPRESS
700 A(0)=0.104592E2:A(1)=-0.404897E-2:A(2)=-0.417520E-4:A(3)=0.368510E-6
710 A(4)=-0.101520E-8:A(5)=0.865310E-12:A(6)=0.903668E-15:A(7)=-0.199690E-17
720 A(8)=0.779287E-21:A(9)=0.191482E-24:A(10)=-0.396806E4:A(11)=0.395735E2
730 POLY=0
740 FOR X=0 TO 9
750 POLY=A(X)*(Ts^X)+POLY
760 POLY=POLY
770 NEXT X
780 Y=FNofTs
790 Ps=2.7182818^Y
800 REM PRINT"Ps=";Ps
810 ENDPROC
820:
830 DEF PROCVF
840 A=1.0:B=-1.9153882:C=1.2015186E1:D=-7.9464025:E(1)=-3.888614
850 E(2)=2.0582238:E(3)=-2.0829991:E(4)=8.2180004E-1:E(5)=4.754974E-1
860 E(6)=0.0:E(7)=0.0:Vfcr=3.155E-3:TCR=647.3
870 TC=(TCR-Ts)/TCR
880 PROCPOLY1
890 Ys=FNof
900 Vf=Ys*Vfcr
910 REM PRINT"Vf=";Vf
920 ENDPROC
930:
940 DEF PROCVG
950 A=1.0:B=1.6351057:C=5.2584599E1:D=-4.4694653E1:E(1)=-8.9751114
960 E(2)=-4.3845530E-1:E(3)=-1.9179576E1:E(4)=3.6765319E1:E(5)=-1.9462437E1
970 E(6)=0.0:E(7)=0.0:Vgcr=3.155E-3:PCR=2.2089E1
980 PROCPOLY1
990 Ys=FNof
1000 Vg=Ys*PCR*Vgcr/Ps
1010 REM PRINT"Vg=";Vg
1020 ENDPROC
1030:
1040 DEF PROCHF1
1050 A=0.0:B=0.0:C=0.0:D=0.0:E(1)=6.2469837E2:E(2)=-2.3438536E3
1060 E(3)=-9.50812101E3:E(4)=7.1628792E4:E(5)=-1.63535221E5:E(6)=1.66531093E5
1070 E(7)=-6.47854585E4:HFCR=2.0993E3
1080 PROCPOLY1
1090 Ys=FNof
1100 Hf=Ys*HFCR
1110 REM PRINT"Hf=":Hf
1120 ENDPROC
1130:
1140 DEF PROCHF2
1150 A=8.839230108E-1:B=0.0:C=0.0:D=0.0:E(1)=-2.67172935:E(2)=6.22640035
1160 E(3)=-1.31789573E1:E(4)=-1.91322436:E(5)=6.87937653E1:E(6)=-1.24819906E2
1170 E(7)=7.21435404E1:HFCR=2.0993E3
1180 PROCPOLY1
1190 Ys=FNof
1200 Hf=Ys*HFCR
1210 REM PRINT"Hf=";Hf
1220 ENDPROC
1230:
1240 DEF PROCHF3
1250 A=1.0:B=-4.41057805E-1:C=-5.52255517:D=6.43994847:E(1)=-1.64578795
1260 E(2)=-1.30574143:E(3)=0.:E(4)=0.:E(5)=0.0:E(6)=0.0:E(7)=0.0:HFCR=2.0993E3
1270 PROCPOLY1
1280 Ys=FNof
1290 Hf=Ys*HFCR
1300 REM PRINT"Hf=";Hf
1310 ENDPROC
1320:
1330 DEF PROCHFG
1340 A=0.0:B=7.79221E-1:C=4.62668:D=-1.07931:E(1)=-3.87446:E(2)=2.94553
1350 E(3)=-8.06395:E(4)=1.15633E1:E(5)=-6.02884:E(6)=0.:E(7)=0.:HFGTP=2.5009E3
1360 PROCPOLY1
```

```
1370 Ys=FNof
1380 Hfg=Ys*HFGTP
1390 REM PRINT"Hfg=";Hfg
1400 ENDPROC
1410:
1420 DEF PROCHG
1430 A=1.0:B=4.57874342E-1:C=5.08441288:D=-1.48513244:E(1)=-4.81351884
1440 E(2)=2.69411792:E(3)=-7.39064542:E(4)=1.0496168?E1:E(5)=-5.46840036
1450 E(6)=0.0:E(7)=0.0:HGCR=2.0993E3
1460 PROCPOLY1
1470 Ys=FNof
1480 Hg=Ys*HGCR
1490 REM PRINT"Hg=";Hg
1500 ENDPROC
1510:
1520 DEF PROCSF1
1530 A=0.:B=0.:C=0.:E(1)=-1.83692956E3:E(2)=1.47066352E4:E(3)=-4.31466046E
1540 E(4)=4.86066733E4:E(5)=7.9975096E3:E(6)=5.83339987E4:E(7)=3.31400718E4
1550 SFCR=4.4289:D=0.0
1560 PROCPOLY1
1570 Ys=FNof
1580 Sf=Ys*SFCR
1590 REM PRINT "Sf=";Sf
1600 ENDPROC
1610:
1620 DEF PROCSF2
1630 A=9.12762917E-1:B=0.0:C=0.0:D=0.0:E(1)=-1.75702956
1640 E(2)=1.66754095:E(3)=5.82215341
1650 E(4)=-6.3335478?E1:E(5)=1.88076546E2:E(6)=-2.52344531E2:E(7)=1.28058531E2
1660 SFCR=4.4289
1670 PROCPOLY1
1680 Ys=FNof
1690 Sf=Ys*SFCR
1700 REM PRINT "Sf=";Sf
1710 ENDPROC
1720:
1730 DEF PROCSF3
1740 A=1.0:B=-3.24817650E-1:C=-2.990556709:D=3.2341900:E(1)=-6.78067859E-1
1750 E(2)=-1.91910364:E(3)=0.:E(4)=0.:E(5)=0.:E(6)=0.:E(7)=0.0:SFCR=4.4289
1760 PROCPOLY1
1770 Ys=FNof
1780 Sf=Ys*SFCR
1790 REM PRINT "Sf=";Sf
1800 ENDPROC
1810:
1820 DEF PROCSG
1830 A=1.0:B=3.77391E-1:C=-2.78368:D=6.93135:E(1)=-4.34939:E(2)=1.34672
1840 E(3)=1.75261:E(4)=-6.22295:E(5)=9.99004:E(6)=E(7)=0.0:SGCR=4.4289
1850 PROCPOLY1
1860 Ys=FNof
1870 Sg=Ys*SGCR
1880 REM PRINT "Sg=";Sg
1890 ENDPROC
1900:
1910 DEF PROCPOLY1
1920 POLY1=0
1930 FOR X=1 TO 7
1940 POLY1=E(X)*(TC^X)+POLY1
1950 POLY1=POLY1
1960 NEXT X
1970 ENDPROC
1980:
1990 DEF PROCALL
2000 PROCVF
2010 PROCVG
2020 IF Ts>=273.16 AND Ts<300 THEN PROCHF1:PROCSF1
2030 IF Ts>=300 AND Ts<600 THEN PROCHF2:PROCSF2
2040 IF Ts>=600 AND Ts<647.3 THEN PROCHF3:PROCSF3
2050 PROCHFG
```

```
2060 PROCHG
2070 PROCSG
2080 Sfg=Hfg/Ts
2090 REM PRINT"Sfg=";Sfg
2100 ENDPROC
2110:
2120 DEF PROCSUPER
2130 INPUT "ENTER VALUE OF P";P
2140 INPUT "ENTER VALUE OF T";T
2150 PROCPS
2160 ENDPROC
2170:
2180 DEF PROCALLSUPER
2190 PROCVPT
2200 PROCHPT
2210 PROCSPT
2220 ENDPROC
2230:
2240 DEF PROCVPT
2250 R=4.61631E-4:B(1)=5.27993E-2:B(2)=3.75928E-3:B(3)=2.2E-2:A(0)=-3.741378
2260 A(1)=-4.7838281E-3:A(2)=1.5923434E-5:M=4.0E1
2270 PROCPOLY2
2280 VPT=(R*T/P)-B(1)*EXP(-B(2)*T)+(1/10*P)*(B(3)-EXP(POLY2))*EXP((Ts-T)/M)
2290 REM PRINT VPT
2300 ENDPROC
2310:
2320 DEF PROCPOLY2
2330 POLY2=0
2340 FOR X=1 TO 2
2350 POLY2=A(X)*(Ts^X)+POLY2
2360 POLY2=POLY2
2370 NEXT X
2380 ENDPROC
2390:
2400 DEF PROCHPT
2410 B(1)=2.04121E3:B(2)=-4.040021E1:B(3)=-4.8095E-1:B(4)=1.610693
2420 B(5)=5.472051E-2:B(6)=7.517537E-4:B(7)=3.383117E-4:B(8)=-1.975736E-5
2430 B(9)=2.87409E-7:B(10)=1.70782E3:B(11)=-1.699417E1:B(12)=6.2746295E-2
2440 B(13)=-1.0284259E-4:B(14)=6.4561298E-8:M=4.5E1
2450 A(0)=B(1)+B(2)*P+B(3)*(P^2):A(1)=B(4)+B(5)*P+B(6)*(P^2)
2460 A(2)=B(7)+B(8)*P+B(9)*(P^2)
2470 A(3)=B(10)+B(11)*Ts+B(12)*(Ts^2)+B(13)*(Ts^3)+B(14)*(Ts^4)
2480 PROCPOLY3
2490 HPT=POLY3-A(3)*EXP((Ts-T)/M)
2500 REM PRINT HPT
2510 ENDPROC
2520:
2530 DEF PROCPOLY3
2540 POLY3=0
2550 FOR X=0 TO 2
2560 POLY3=A(X)*(T^X)+POLY3
2570 POLY3=POLY3
2580 NEXT X
2590 ENDPROC
2600:
2610 DEF PROCSPT
2620 A(0)=4.6162961:A(1)=1.039008E-2:A(2)=-9.873005E-6:A(3)=5.43411E-9
2630 A(4)=-1.170465E-12:B(1)=-4.650306E-1:B(2)=1.0E 3:M=8.5E1:C(0)=1.777804
2640 C(1)=-1.854459E-5:C(2)=6.854459E-5:C(3)=-1.154424E-7:C(4)=8.142201E-11
2650 PROCPOLY4
2660 SPT=POLY4+B(1)*LN(P+B(2))-POLY5*EXP((Ts-T)/M)
2670 REM PRINT SPT
2680 ENDPROC
2690:
2700 DEF PROCPOLY4
2710 POLY4=0:POLY5=0
2720 FOR X=0 TO 4
2730 POLY4=A(X)*(T^X)+POLY4
2740 POLY5=C(X)*(Ts^X)+POLY5
2750 POLY4=POLY4:POLY5=POLY5
2760 NEXT X
2770 ENDPROC
2780:
```

APPENDIX III

Two programs are presented in this Appendix, both were written using the Fortran77 computer language, and run on the Honeywell "Multics" computer system.

The first program designated "NEW.FORTRAN" is based on the two-dimensional theoretical approach (Method of Characteristics) described in Section (3.2.3.), and its main core was taken from Saad (1985). Three subroutines were written, and the four equations presented in Section (3.3.3.), were used to modify and rewrite the computer program in order to enable us to find the coordinates of each point for the characteristic mesh of the flow field inside the nozzle.

The second program designated "PLO.FORTRAN" was written in order to sort out the results created by the first program (i.e. the X's and Y's for the mesh points). The main task of this program was to pick up the data and rewrite them in the sequence that it should be drawn with on the multics computer "TELEGRAPH" drawing system or any other computer drawing system as shown in chapter three in this thesis.

A print out for the two programs are given in this Appendix and their flow charts are shown as well.

THE "NEW.FORTRAN" PROGRAM AND ITS FLOW CHART

```
C       "NEW.FORTRAN"
        integer b1,b2,divsns,e,f,h1,h2,i,j,k,l,m,n,points
        integer pos,t1,v1,x2,x3,x4
        real alpha(2000),ci(2000),cii(2000),mach(2000),prnang(2000)
        real tminus(2000),tplus(2000),th(2000)
        real XX(2000),YY(2000)
        real angle,divang,gamma,g2,g3,h1fang,m1,m6,newang,pi,u2,x,y
        real BB,BI,BII,YT,x9
        real sd1,sd2,sd3
        common /vars/ ci,cii,th,h1fang,b1,b2,divsns,e,h1,h2,j,k,f,pos,v1
        common /vars1/ tplus,tminus,XX,YY,YT
        data pi/3.14159/
        write(*,1)
1       format(1h ,'the radius of the nozzle throat',$)
        read(*,*) YT
        write(*,100)
        open(unit=8,file='ssss')
        open(unit=9,file='s000')
100     format(1h ,'number to multiply number of divisions ',
     +          'to get lattice points? ',$)
        read(*,*)points
190     write(*,200)
200     format(1h ,'number of divisiion pionts? ',$)
        read(*,*)divsns
        if (divsns .gt. 2) goto 290
        write (*,250)
250     format(1h ,'there must be more than 2 divisions. please reenter')
        goto 190
290     write(*,300)
300     format(1h ,'divergent angle of straight walled channel? ',$)
        read(*,*)angle
        write(*,400)
400     format(1h ,'mach number at start? ',$)
        read(*,*)m1
        write(*,500)
500     format(1h ,'gamma? ',$)
        read(*,*)gamma
        x2=(divsns+1)/2
        t1=(points*divsns)+1
        write(9,3303) points,divsns,x2,t1
3303    format(2x,4i5)
        v1=(points*divsns)+2+x2*2
        do 53 i=1,x2
           x9=x2
             if(mod(divsns,2).eq.0) then
```

```
                go to 13
                else
                go to 11
              end if
13          YY(i)= YT*((x9-i+1)/(x9+i-1))
            go to 17
11          YY(i)= YT*((x9-i)/(x9-1))
17          XX(i)=0.0
53        continue
          if (v1 .le. 2000 .and. v1+divsns .le. 2000 .and.
         +    t1 .le. 2000) goto 1000
          write(*,600)
600       format(1h ,'there is not enough array space allocated for'/
         +          h ,'calculation.  increase the size of arrays',
         +          'c1,c2,u,th,m,al,t1,t2.'/,
         +          1h ,'and then rerun the program.'//)
          goto 9000
1000      h1fang=angle/2.0
          divang=h1fang/float(divsns-1)
          x2=(divsns+1)/2
          x3=divsns-x2
          do 10 i=1,t1,divsns
            newang=h1fang+(divang*2.0)
            pos=i
              do 20 j=1,x2
                newang=abs(newang-(divang*2.0))
                if (newang .lt. 9.999999e-06) newang=0.0
                th(pos)=newang
                pos=pos+1
20            continue
10        continue
          x4=x2+1
          do 30 k=x4,t1,divsns
            newang=h1fang-divsns
            pos=k
              do 40 l=1,x3
                if (l .ne. 1) goto 1100
                newang=h1fang-divang
                goto 1200
1100            newang=abs(newang-(2.0*divang))
                if (newang .lt. 9.999999e-06) newang=0.0
1200            th(pos)=newang
                pos=pos+1
40            continue
30        continue
          do 50 m=1,x2
            mach(m)=m1
            if (mach(m) .ne. 1.0) goto 1300
            alpha(m)=90.0
```

```
                goto 1400
1300            y=1.0/mach(m)
                alpha(m)=(atan(y/(-y*y+1)**0.5))*180.0/pi
1400            tplus(m)=th(m)+alpha(m)
                tminus(m)=th(M)-alpha(m)
50          continue
            g2=(gamma+1)/(gamma-1)
            g3=(gamma-1)/(gamma+1)
            do 60 i=1,x2
                prnang(i)=g2**0.5*atan((g3*(mach(i)**2.0-1.0))**0.5)
                prnang(i)=prnang(i)-atan((mach(i)**2.0-1.0)**0.5)
                prnang(i)=prnang(i)*180.0/pi
                ci(i)=prnang(i)+th(i)
                cii(i)=prnang(i)-th(i)
60          continue
            b1=(divsns-1)/2
            b2=(divsns+1)/2
            h1=b1
            h2=divsns/2
            do 70 n=1,t1,divsns
                do 80 j=n,n+x2-1
                   e=0
                   pos=j
                   if (mod(divsns,2) .eq. 0.0) call c2even
                   if (mod(divsns,2) .ne. 0.0) call c2odd
80              continue
                do 90 k=n,n+x2-1
                   f=0
                   pos=k
                   if (mod(divsns,2) .eq. 0.0) call c1even
                   if (mod(divsns,2) .ne. 0.0) call c1odd
90              continue
70          continue
            do 110 i=x2+1,t1
                prnang(i)=(ci(i)+cii(i))/2.0
                u2=prnang(i)
                if (prnang(i) .ne. 0.0) goto 1500
                alpha(i)=90.0
                mach(i)=1.0
                goto 1600
1500            call prdmey(m1,m6,u2,g2,g3,pi)
                mach(i)=m6
                x=1.0/m6
                alpha(i)=atan(x/(-x*x+1)**0.5)*180.0/pi
1600            tplus(i)=th(i)+alpha(i)
                tminus(i)=th(i)-alpha(i)
                   do 95  k=1,t1
                      tem=divsns
                      sd1=(i-1)/tem
```

```
                if (sd1.eq.k) then
                      call upper(i,pi)
                      goto 110
                      else
                      go to 33
                end if
33              tem1=k
                if (i.eq.(((2*tem1-3)/2)*tem-0.5))  goto  34
                sd2=(i+(((3*tem)+1)/2-1))/tem
                if(sd2.eq.k) then
                      call lowerodd(i,pi)
                      goto 110
                      else
                      go to 34
                end if
34              if(mod(divsns,2).eq.0)  then
                      go to 47
                      else
                      go to  39
                end if
39              if (i.eq.(k*tem-tem))  goto  95
47              sd3=(i+tem)/tem
                if(sd3.eq.k) then
                      call lowereven(i,pi)
                      goto 110
                      else
                      go to 95
                end if
 95           continue
             if(mod(divsns,2).eq.0) then
                go to 21
                else
                go  to 23
             end if
21           do 99  ll=(2-x2),0
                do  101  m=0,(t1-(divsns-x2-1))/divsns
                   if (i.eq.(x2+1+(m*divsns)))  then
                      z=(i+(divsns-x2-1))/divsns
                      go to  102
                      else
                      go to 101
                   end if
101             continue
102             if (i.eq.(z*divsns-1+ll))  then
                   go to 23
                   else
                   go to 99
                end if
99           continue
```

```
22          a1=i-x2-1
            b1= i-x2
            go to 67
23          a1=i-x2
            b1=i-x2+1
67          BI=tan(0.5*pi/180*((th(i)-alpha(i))+(th(a1)-alpha(a1))))
            BII=tan(0.5*pi/180*((th(i)+alpha(i))+(th(b1)+alpha(b1))))
            BB=BI-BII
            XX(i)=((YY(b1)-BII*XX(b1))-(YY(a1)-BI*XX(a1)))/BB
            YY(i)=(BI*(YY(b1)-BII*XX(b1))-BII*(YY(a1)-BI*XX(a1)))/BB
110       continue
          write(*,3000)
3000      format(1h ,70('_')///,
     +          1h ,7x,54('=')/,
     +          1h,7x,'supersonic flow in a diverging straight walled nozzle'/,
     +          1h ,7x,54('=')//,
     +          1h ,22x,'(lattice point method)'//)
          write(*,3100)m1,angle,divsns,gamma
3100      format(1h ,18x,'mach at entrance=',f6.4,' (mach).'/,
     +           1h ,18x,'angle of divergence=',f5.2,' (degrees).'/,
     +           1h ,18x,'number of divisions=',i2,/,
     +           1h ,18x,'gamma='f4.2//,
     +           1h ,'lattice'/,
     +           1h ,' points',4x,'c-1',4x,'c-2',5x,'u',5x,'th',
     +          6x,'m',5x,'al',3x,'th+al',2x,'th-al'/)
          do 120 j=1,t1
             write(8,3200) j,ci(j),cii(j),prnang(j),th(j),mach(j),alpha(j),XX(j),YY(j)
             write(9,3201) XX(j),YY(j)
3200         format(2x,i3,3x,8f7.2)
3201         format(2x,2f7.2)
120       continue
          write(*,3300)
3300      format(/,1h ,4x,'u=pran-mey angle,',6x,'th=theta,',
     +          6x,'m=mac,',6x,'al=alpha'//,70('_'))
          close(unit=8)
          close(unit=9)
9000      stop
          end
c
          subroutine prdmey(m1,m6,u2,g2,g3,pi)
             real m1,m3,m6,u,u2,g2,g3,pi,m2
             m2=m1
             m3=10.0
             if ((m1 .le. m3) goto 1000
             write(*,100)
100          format(//, 1h ,'starting mac to high, recommend changing upper'/,
     +           1h ,'limit'(m3) to something higher for trial and'/,
     +           1h ,'error produce.'/)
             stop
```

```
1000        m6=(m2+m3)/2.0
            u=g2**0.5*atan((g3*(m6**2.0-1.0))**0.5)
            u=u-atan((m6**2.0-1.0)**0.5)
            u=u*180.0/pi
            if (u/u2 .lt. 0.9999001) goto 2000
            if (u/u2 .lt. 1.0001) return
2000        if (u .ge. u2) goto 3000
            m2=m6
            goto 1000
3000        if (u .le. u2) return
            m3=m6
            goto 1000
        end
c
        subroutine c2odd
            real ci(2000),cii(2000),th(2000),hf1ang
            integer b1,b2,divsns,e,h1,h2,j,k,f,pos,v1
            common /vars/ ci,cii,th,h1fang,b1,b2,divsns,e,h1,h2,j,k,f,pos,v1
            if (pos .eq. 1.0) return
1000        if (th(pos) .ne. h1fang) goto 1100
            return
1100        pos=pos+b1
            if (pos .ge. v1) return
            cii(pos)=cii(j)
            goto 1000
        end
c
        subroutine c1odd
            real ci(2000),cii(2000),th(2000),hf1ang
            integer b1,b2,divsns,e,h1,h2,j,k,f,pos,v1
            common /vars/ ci,cii,th,h1fang,b1,b2,divsns,e,h1,h2,j,k,f,pos,v1
            if (pos+th(pos) .eq. 1.0) return
1000        if (th(pos) .ne. 0.0) goto 1100
            ci(pos)=ci(k)
            cii(pos)=ci(pos)-2.0*th(pos)
            return
1100        pos=pos+b2
            if (pos .ge. v1) return
            ci(pos)=ci(k)
            goto 1000
        end
c

        subroutine c2even
            real ci(2000),cii(2000),th(2000),hf1ang
            integer b1,b2,divsns,e,h1,h2,j,k,f,pos,v1
            common /vars/ ci,cii,th,h1fang,b1,b2,divsns,e,h1,h2,j,k,f,pos,v1
            if (pos .eq. 1.0) return
2000        if (th(pos) .ne. h1fang) goto 1000
```

```
            ci(pos)=2.0*th(pos)+cii(pos-b1)
            return
1000        e=e+1
            if (mod(e,2) .eq. 0) b1=h1+1
            if (mod(e,2) .ne. 0) b1=h1
            pos=pos+b1
            if (pos .ge. v1) return
            cii(pos)=cii(j)
            goto 2000
        end
c
        subroutine c1even
            real ci(2000),cii(2000),th(2000),hf1ang
            integer b1,b2,divsns,e,h1,h2,j,k,f,pos,v1
            common /vars/ ci,cii,th,h1fang,b1,b2,divsns,e,h1,h2,j,k,f,pos,v1
2000        if (th(pos) .ne. 0) goto 1000
            cii(pos)=ci(k)-2.0*th(pos)
            return
1000        f=f+1
            if (mod(f,2) .eq. 0) b2=h2+1
            if (mod(f,2) .ne. 0) b2=h2
            pos=pos+b2
            if (pos .ge. v1) return
            ci(pos)=ci(k)
            if (mod(pos,divsns) .eq. 0) cii(pos+b2)=ci(pos)
            goto 2000
        end
c
        subroutine upper(i,pi)
            integer b1,b2,divsns,e,f,h1,h2,i,j,k,l,m,n,points
            integer pos,t1,v1,x2,x3,x4
            real alpha(2000),ci(2000),cii(2000),mach(2000),prnang(2000)
            real tminus(2000),tplus(2000),th(2000), XX(2000),YY(2000)
            real angle,divang,gamma,g2,g3,h1fang,m1,m6,newang,pi,u2,x,y
            real BB,BI,BII,YT,x9
            common /vars/ ci,cii,th,h1fang,b1,b2,divsns,e,h1,h2,j,k,f,pos,v1
            common /vars1/ tplus,tminus,XX,YY,YT
            jj=(2*i-divsns+1)/2
            AA=tan(pi*th(i)/180.0)
            a=tan((0.5*pi/180.0)*(tplus(i)+tplus(jj)))
            bb=YY(jj)-a*XX(jj)
            YY(i)=(bb*AA-a*YT)/(AA-a)
            XX(i)=(YY(i)-bb)/a
            return
        end
c
        subroutine lowerodd(i,pi)
            integer b1,b2,divsns,e,f,h1,h2,i,j,k,l,m,n,points
```

```
      integer pos,t1,v1,x2,x3,x4
      real alpha(2000),ci(2000),cii(2000),mach(2000),prnang(2000)
      real tminus(2000),tplus(2000),th(2000), XX(2000),YY(2000)
      real angle,divang,gamma,g2,g3,h1fang,m1,m6,newang,pi,u2,x,y
      real BB,BI,BII,YT,x9
      common /vars/ ci,cii,th,h1fang,b1,b2,divsns,e,h1,h2,j,k,f,pos,v1
      common /vars1/ tplus,tminus,XX,YY,YT
       jj=(2*i-divsns-1)/2
      a=tan((0.5*pi/180.0)*(tminus(i)+tminus(jj)))
      bb=YY(jj)-a*XX(jj)
      YY(i)=0.0
      XX(i)=-bb/a
      return
    end

c

    subroutine lowereven(i,pi)
      integer b1,b2,divsns,e,f,h1,h2,i,j,k,l,m,n,points
      integer pos,t1,v1,x2,x3,x4
      real alpha(2000),ci(2000),cii(2000),mach(2000),prnang(2000)
      real tminus(2000),tplus(2000),th(2000)
      real XX(2000),YY(2000)
      real angle,divang,gamma,g2,g3,h1fang,m1,m6,newang,pi,u2,x,y
      real BB,BI,BII,YT,x9
      common /vars/ ci,cii,th,h1fang,b1,b2,divsns,e,h1,h2,j,k,f,pos,v1
      common /vars1/ tplus,tminus,XX,YY,YT
      jj=(2*i-divsns)/2
      a=tan((0.5*pi/180.0)*(tminus(i)+tminus(jj)))
      bb=YY(jj)-a*XX(jj)
      YY(i)=0.0
      XX(i)=-bb/a
      return
    end
```

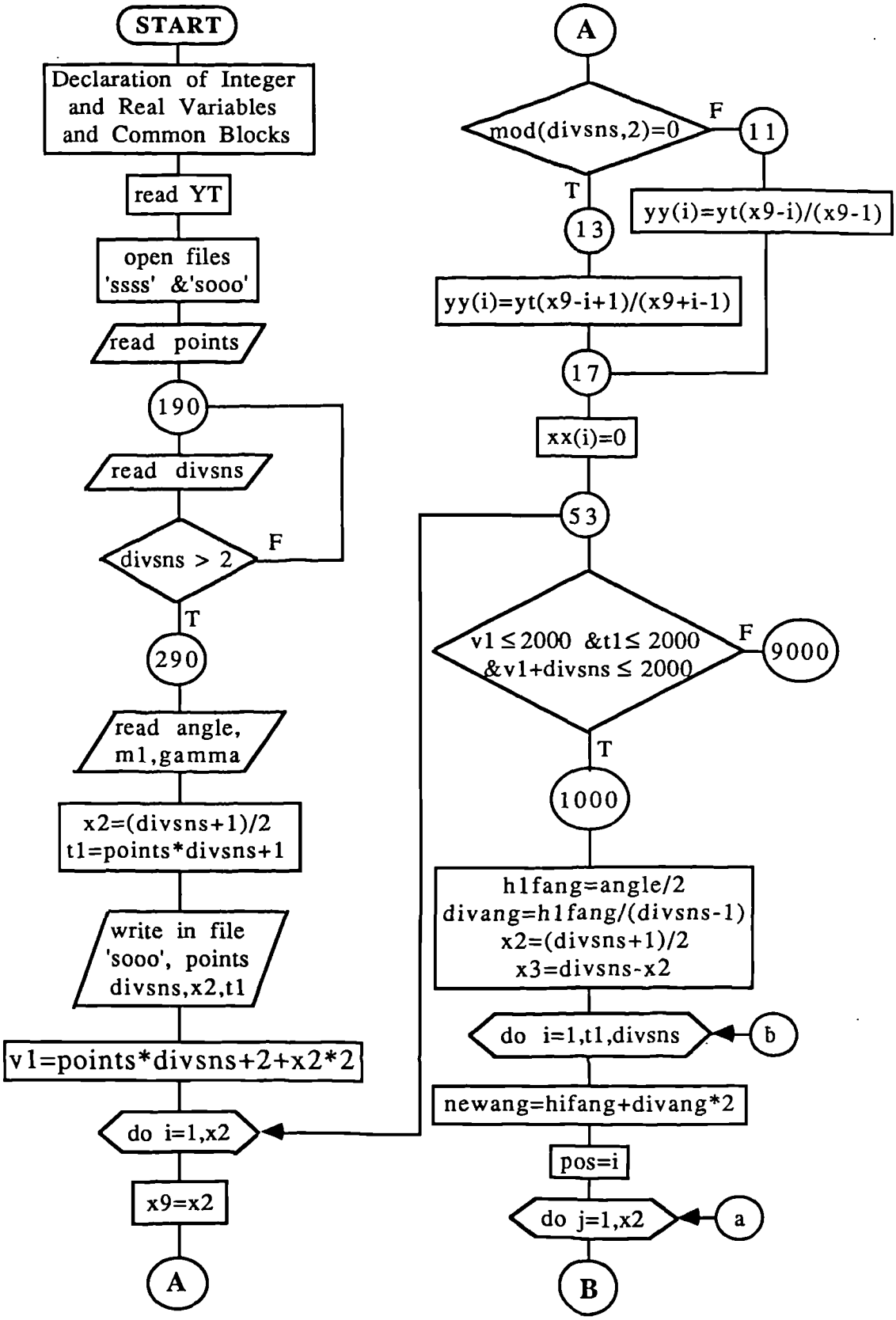
START
Declaration of Integer and Real Variables and Common Blocks
read YT
open files 'ssss' &'sooo'
read points
190
read divsns
divsns > 2
F
T
290
read angle, m1,gamma
x2=(divsns+1)/2
t1=points*divsns+1
write in file 'sooo', points divsns,x2,t1
v1=points*divsns+2+x2*2
do i=1,x2
x9=x2
A
A
mod(divsns,2)=0
F
11
T
13
yy(i)=yt(x9-i)/(x9-1)
yy(i)=yt(x9-i+1)/(x9+i-1)
17
xx(i)=0
53
v1 ≤ 2000 &t1≤ 2000 &v1+divsns ≤ 2000
F
9000
T
1000
h1fang=angle/2
divang=h1fang/(divsns-1)
x2=(divsns+1)/2
x3=divsns-x2
do i=1,t1,divsns
b
newang=hifang+divang*2
pos=i
do j=1,x2
a
B

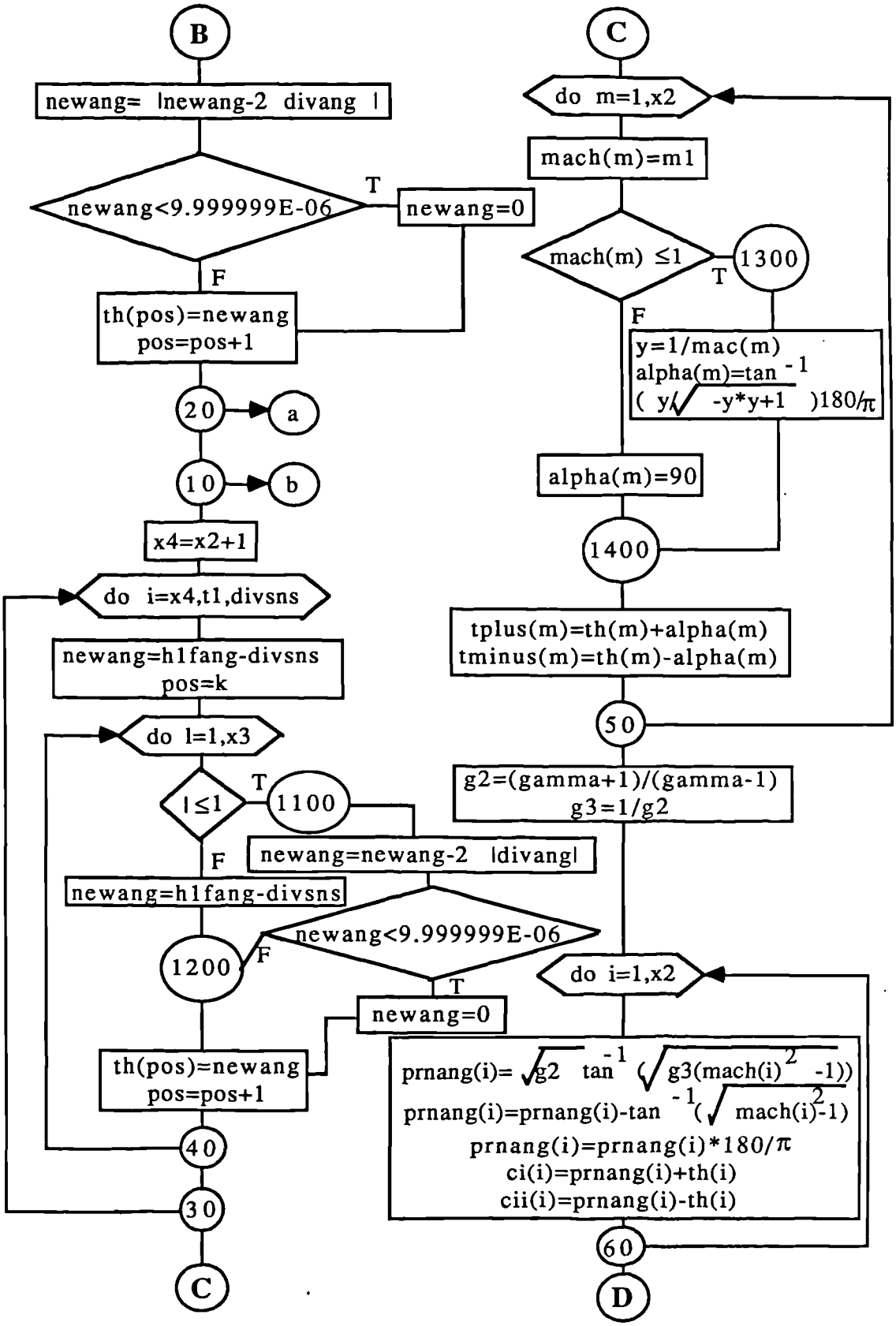
B
newang= |newang-2 divang |
newang<9.999999E-06
T
newang=0
F
th(pos)=newang
pos=pos+1
20
a
10
b
x4=x2+1
do i=x4,t1,divsns
newang=h1fang-divsns
pos=k
do l=1,x3
l≤1
T
1100
F
newang=newang-2 |divang|
newang=h1fang-divsns
newang<9.999999E-06
1200
F
T
newang=0
th(pos)=newang
pos=pos+1
40
30
C
C
do m=1,x2
mach(m)=m1
mach(m) ≤1
T
1300
F
y=1/mac(m)
alpha(m)=tan -1
(y√ -y*y+1)180/π
alpha(m)=90
1400
tplus(m)=th(m)+alpha(m)
tminus(m)=th(m)-alpha(m)
50
g2=(gamma+1)/(gamma-1)
g3=1/g2
do i=1,x2
prnang(i)= √g2 tan -1 (√g3(mach(i) 2 -1))
prnang(i)=prnang(i)-tan -1(√ mach(i) 2-1)
prnang(i)=prnang(i)*180/π
ci(i)=prnang(i)+th(i)
cii(i)=prnang(i)-th(i)
60
D

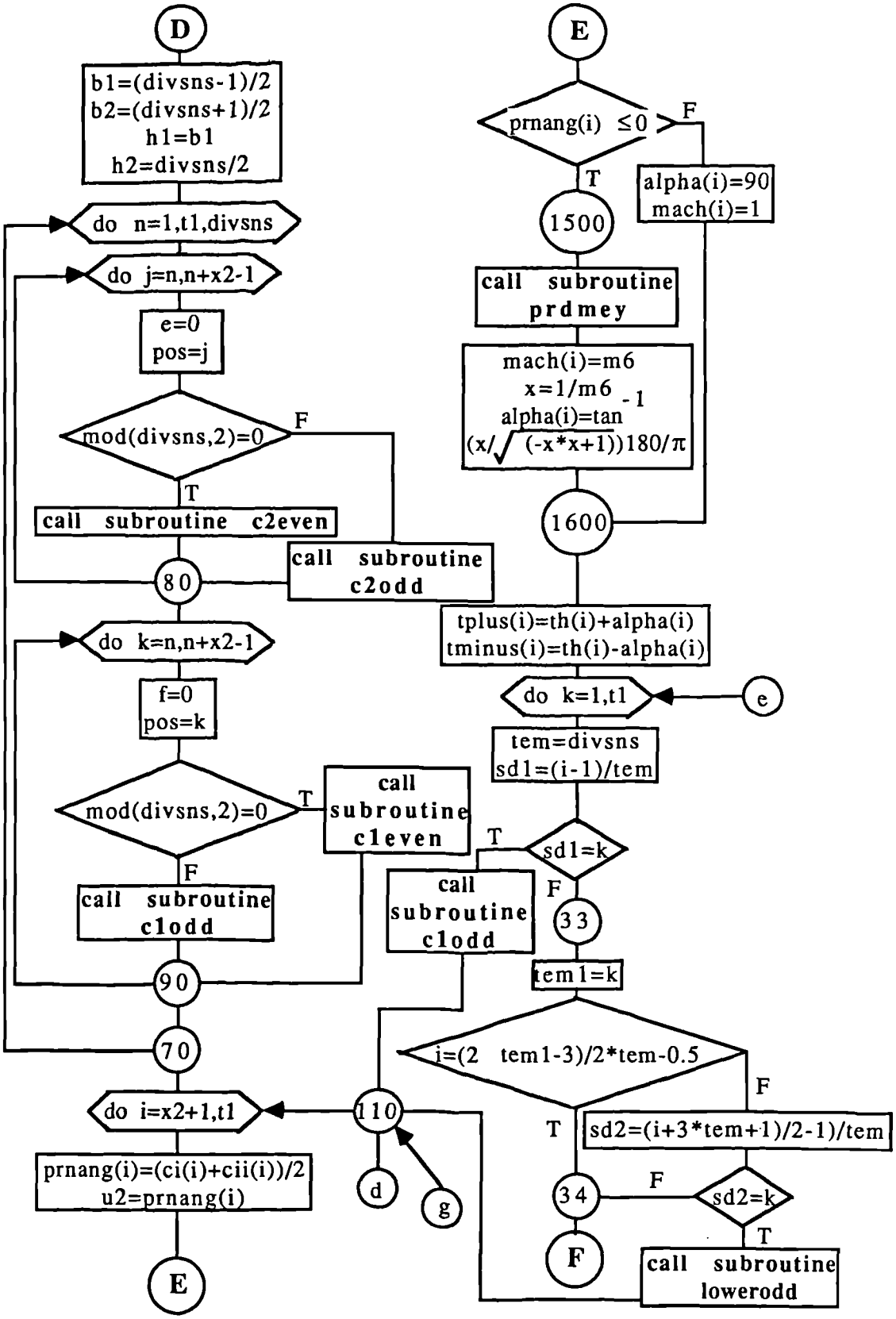
D
b1=(divsns-1)/2
b2=(divsns+1)/2
h1=b1
h2=divsns/2
do n=1,t1,divsns
do j=n,n+x2-1
e=0
pos=j
mod(divsns,2)=0
F
T
call subroutine c2even
call subroutine c2odd
80
do k=n,n+x2-1
f=0
pos=k
mod(divsns,2)=0
T
call subroutine c1even
F
call subroutine c1odd
90
70
do i=x2+1,t1
prnang(i)=(ci(i)+cii(i))/2
u2=prnang(i)
E
d
g
110
E
prnang(i) ≤0
F
T
alpha(i)=90
mach(i)=1
1500
call subroutine prdmey
mach(i)=m6
x=1/m6
alpha(i)=tan
(x/√(-x*x+1))180/π
1600
tplus(i)=th(i)+alpha(i)
tminus(i)=th(i)-alpha(i)
do k=1,t1
e
tem=divsns
sd1=(i-1)/tem
sd1=k
T
F
call subroutine c1odd
33
tem1=k
i=(2 tem1-3)/2*tem-0.5
F
T
sd2=(i+3*tem+1)/2-1)/tem
34
F
sd2=k
T
F
call subroutine lowerodd

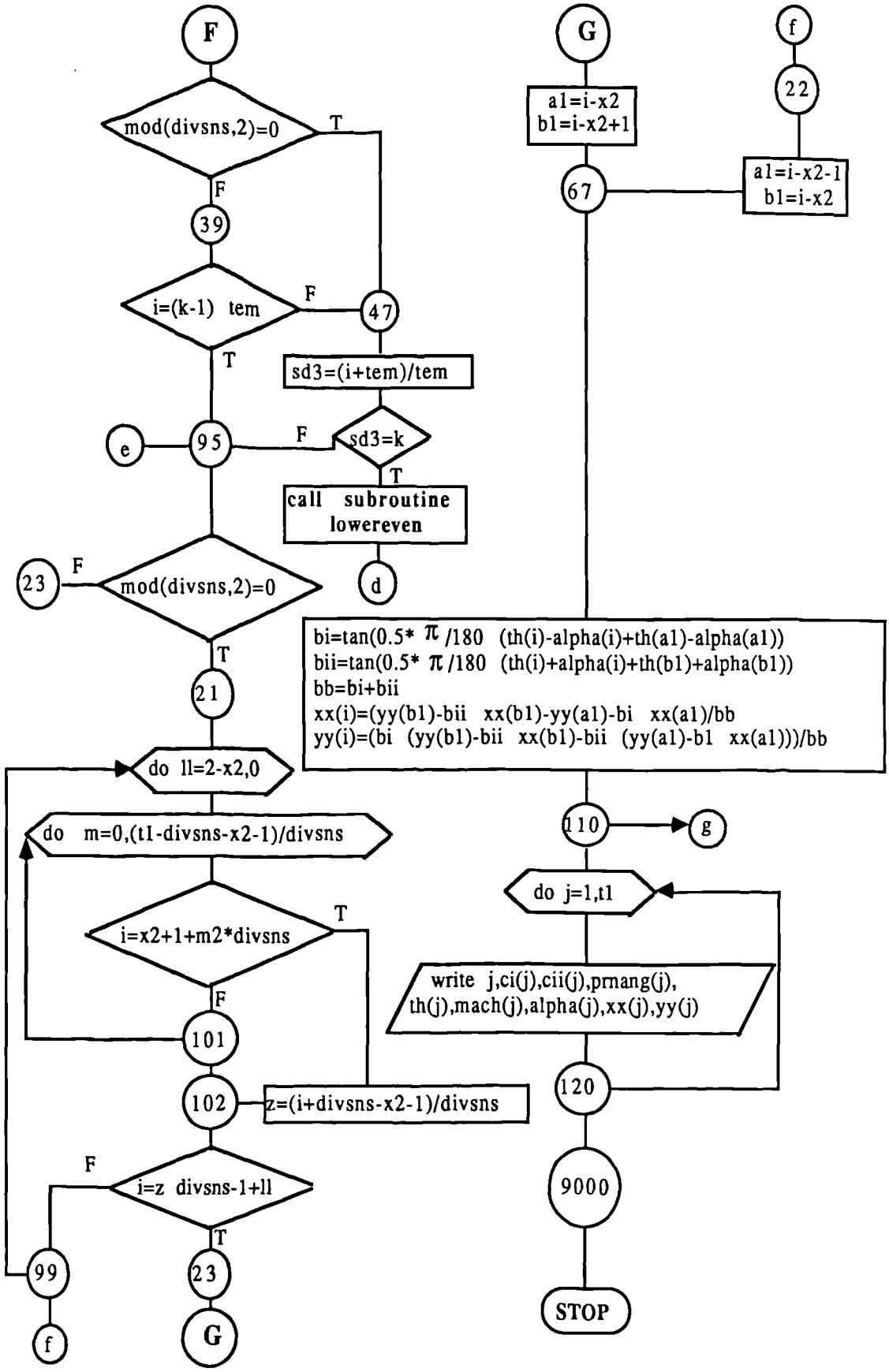
F
mod(divsns,2)=0
T
F
39
i=(k-1) tem
F
47
T
sd3=(i+tem)/tem
e
95
F
sd3=k
T
call subroutine lowereven
d
23
F
mod(divsns,2)=0
T
21
do ll=2-x2,0
do m=0,(t1-divsns-x2-1)/divsns
i=x2+1+m2*divsns
T
F
101
102
z=(i+divsns-x2-1)/divsns
F
i=z divsns-1+ll
T
99
23
f
G
G
a1=i-x2
b1=i-x2+1
67
f
22
a1=i-x2-1
b1=i-x2
bi=tan(0.5* π /180 (th(i)-alpha(i)+th(a1)-alpha(a1))
bii=tan(0.5* π /180 (th(i)+alpha(i)+th(b1)+alpha(b1))
bb=bi+bii
xx(i)=(yy(b1)-bii xx(b1)-yy(a1)-bi xx(a1)/bb
yy(i)=(bi (yy(b1)-bii xx(b1)-bii (yy(a1)-b1 xx(a1)))/bb
110
g
do j=1,t1
write j,ci(j),cii(j),prnang(j),
th(j),mach(j),alpha(j),xx(j),yy(j)
120
9000
STOP

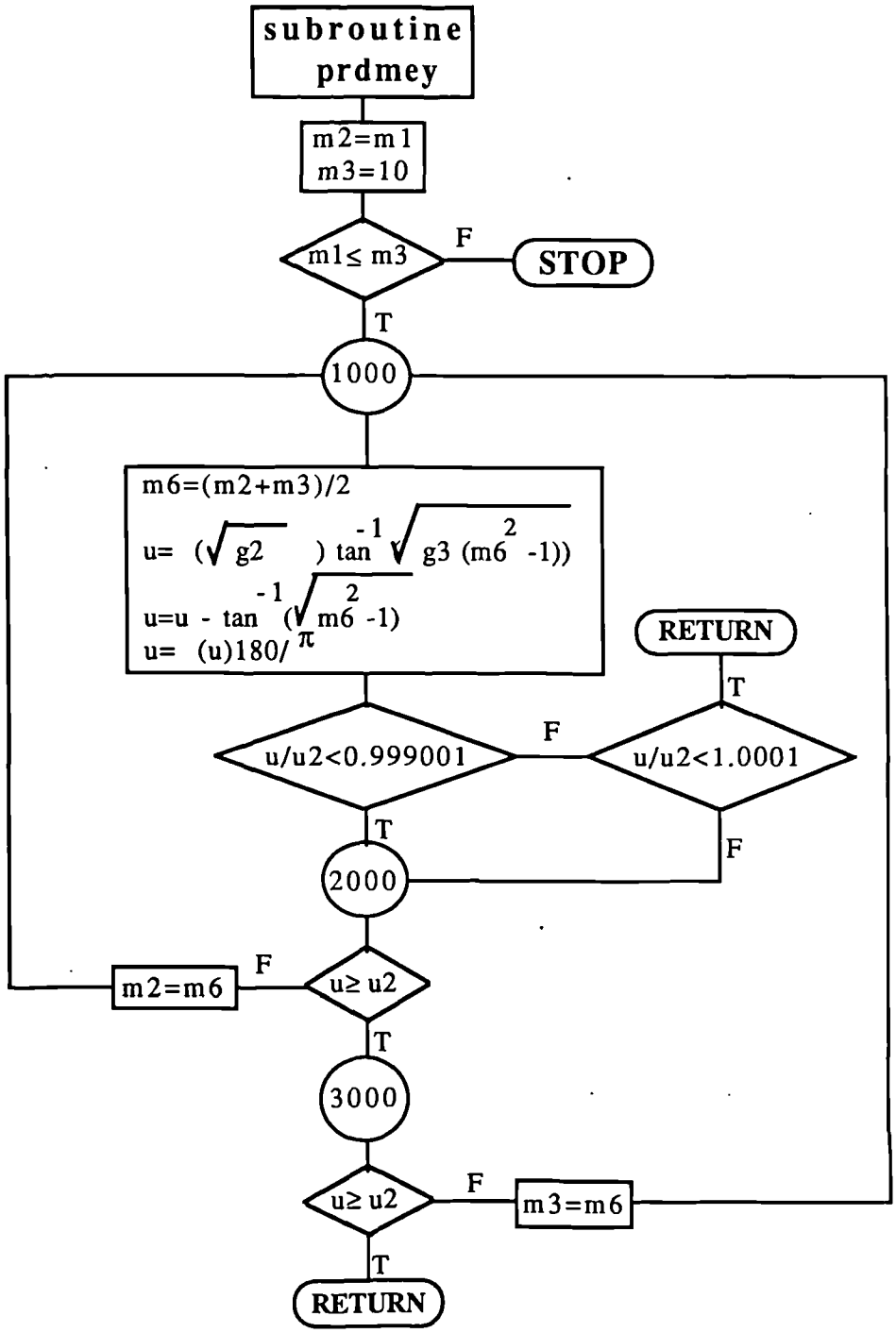
subroutine
prdmey
m2=m1
m3=10
m1≤ m3
F
STOP
T
1000
m6=(m2+m3)/2
u= (√g2) tan^-1 √g3 (m6^2 -1))
u=u - tan^-1 (√m6^2 -1)
u= (u)180/π
RETURN
T
u/u2<0.999001
F
u/u2<1.0001
T
F
2000
m2=m6
F
u≥ u2
T
3000
u≥ u2
F
m3=m6
T
RETURN

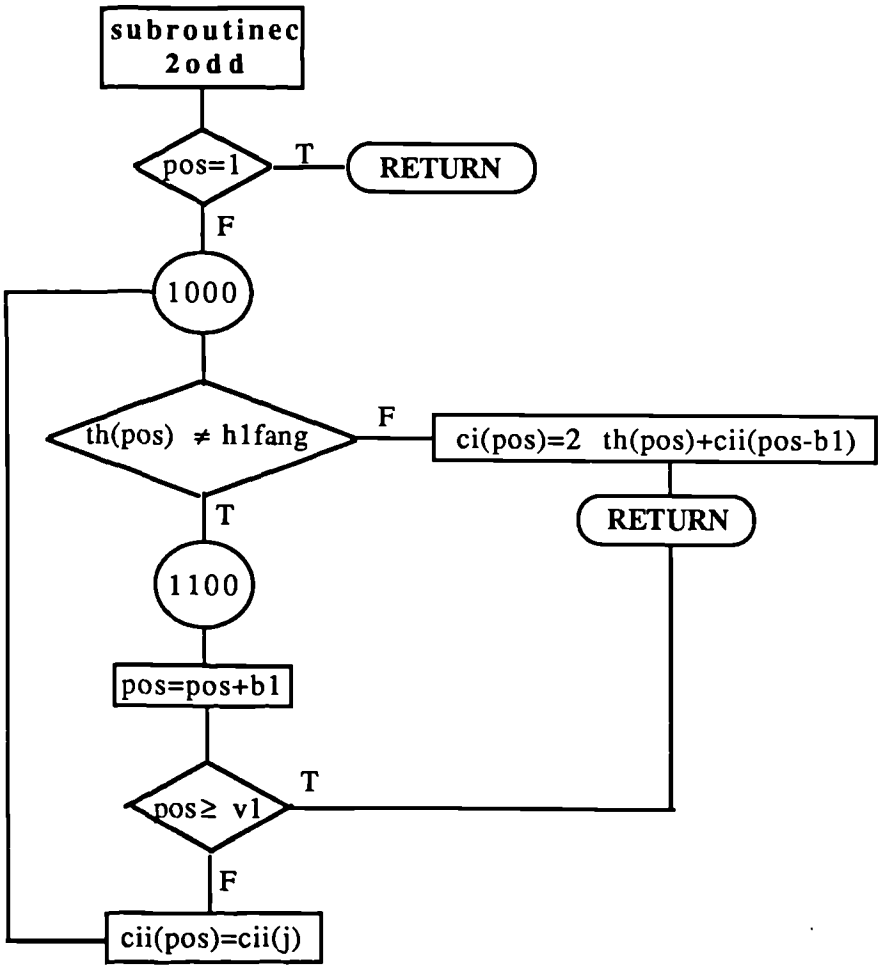
subroutinec
2odd
pos=1
T
RETURN
F
1000
th(pos) ≠ h1fang
F
ci(pos)=2 th(pos)+cii(pos-b1)
RETURN
T
1100
pos=pos+b1
T
pos≥ v1
F
cii(pos)=cii(j)

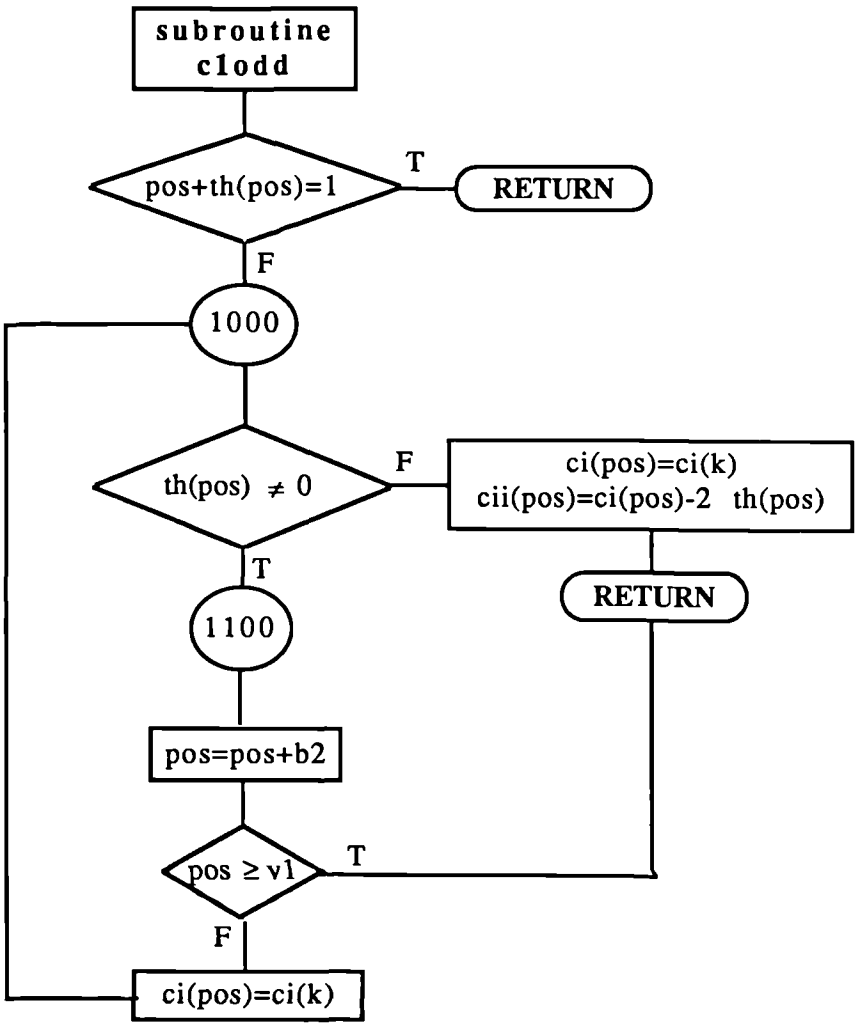
subroutine
clodd
pos+th(pos)=1
T
RETURN
F
1000
th(pos) ≠ 0
F
ci(pos)=ci(k)
cii(pos)=ci(pos)-2 th(pos)
T
RETURN
1100
pos=pos+b2
pos ≥ v1
T
F
ci(pos)=ci(k)

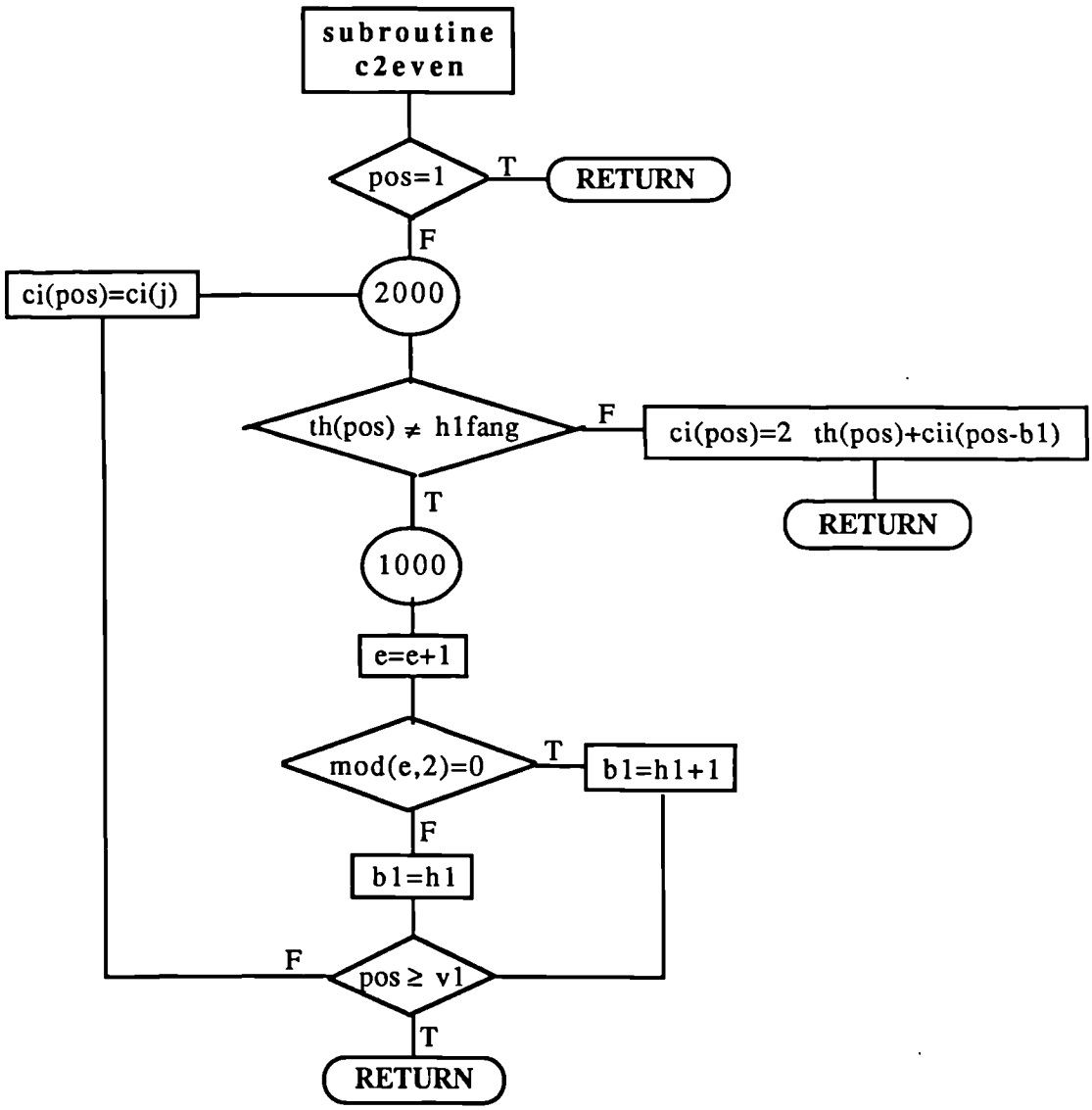
subroutine
c2even
pos=1
T
RETURN
F
ci(pos)=ci(j)
2000
th(pos) ≠ h1fang
F
ci(pos)=2 th(pos)+cii(pos-b1)
RETURN
T
1000
e=e+1
mod(e,2)=0
T
b1=h1+1
F
b1=h1
F
pos ≥ v1
T
RETURN

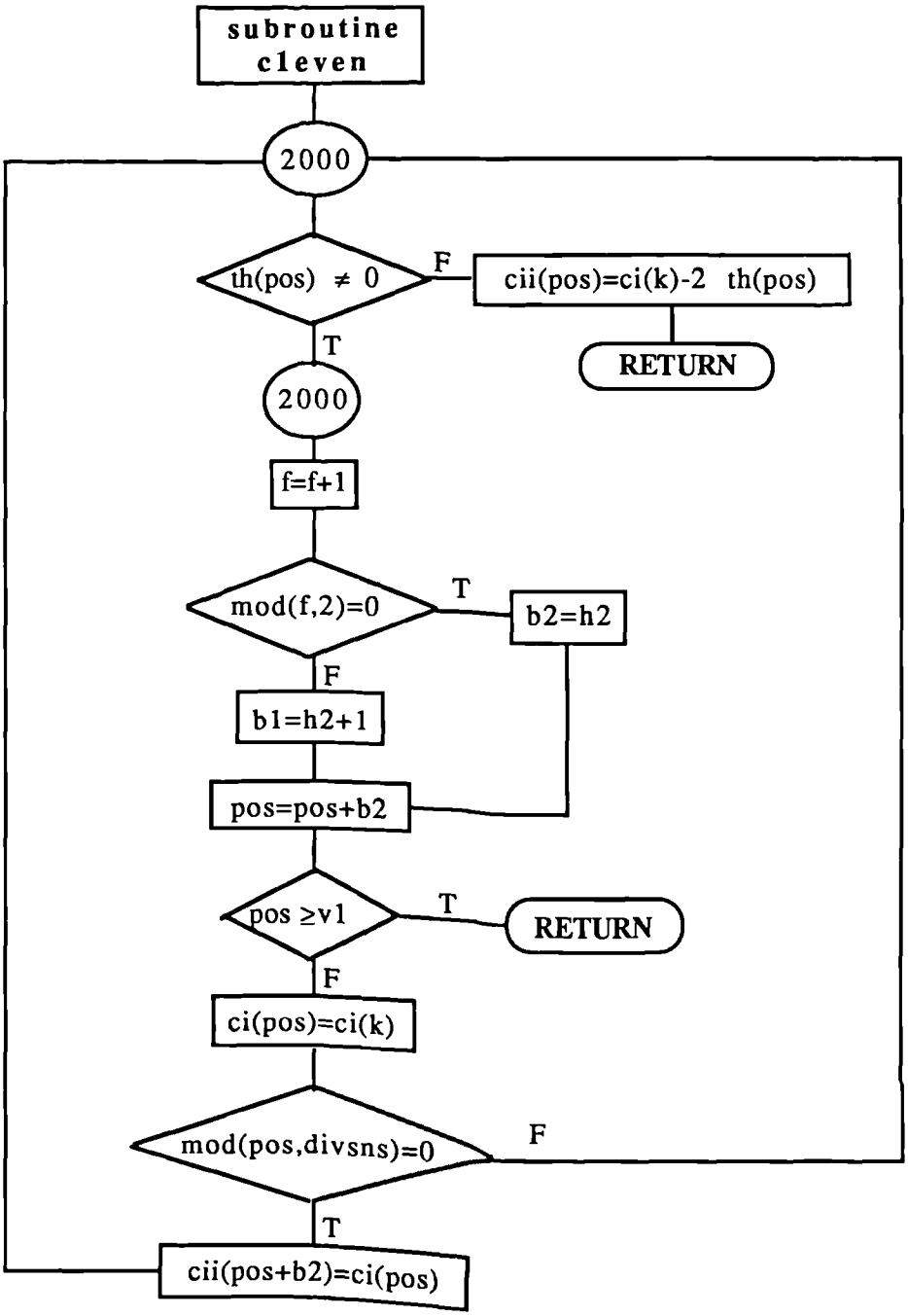
subroutine
c1even
2000
th(pos) ≠ 0
F
cii(pos)=ci(k)-2 th(pos)
RETURN
T
2000
f=f+1
mod(f,2)=0
T
b2=h2
F
b1=h2+1
pos=pos+b2
pos ≥v1
T
RETURN
F
ci(pos)=ci(k)
mod(pos,divsns)=0
F
T
cii(pos+b2)=ci(pos)

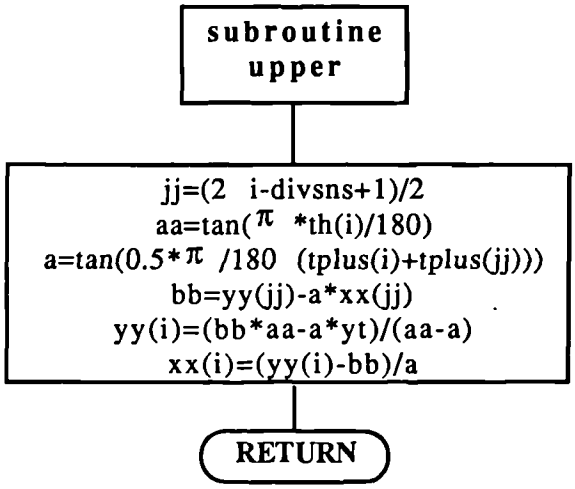
subroutine
upper
jj=(2 i-divsns+1)/2
aa=tan(π *th(i)/180)
a=tan(0.5*π /180 (tplus(i)+tplus(jj)))
bb=yy(jj)-a*xx(jj)
yy(i)=(bb*aa-a*yt)/(aa-a)
xx(i)=(yy(i)-bb)/a
RETURN

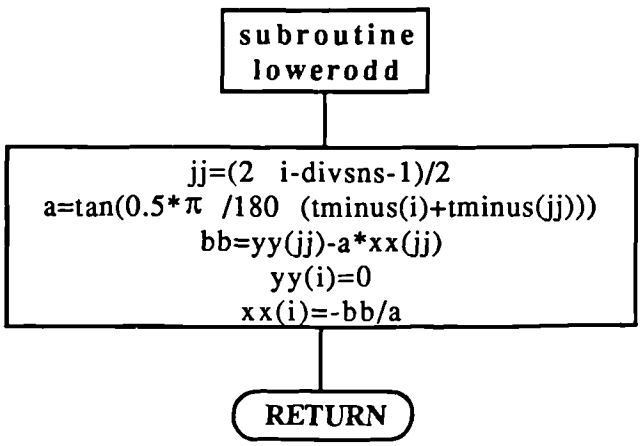
subroutine
lowerodd
jj=(2 i-divsns-1)/2
a=tan(0.5*π /180 (tminus(i)+tminus(jj)))
bb=yy(jj)-a*xx(jj)
yy(i)=0
xx(i)=-bb/a
RETURN

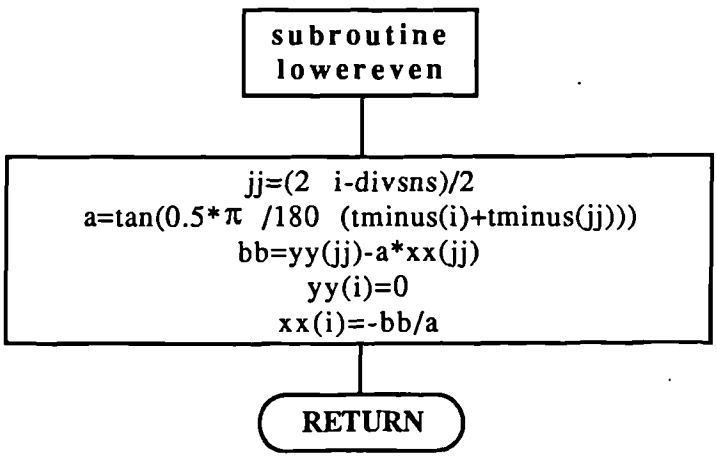
subroutine
lowereven
jj=(2 i-divsns)/2
a=tan(0.5*π /180 (tminus(i)+tminus(jj)))
bb=yy(jj)-a*xx(jj)
yy(i)=0
xx(i)=-bb/a
RETURN

THE "PLO.FORTRAN" PROGRAM AND ITS FLOW CHART

```
C       "PLO.FORTRAN"
        integer i,t1,divsns,x2,points,A,B,D,E
        real x(1000),y(1000)
        open (unit=5, file='s000')
        open (unit=6, file='outs')
        read(5,*)points,divsns,x2,t1
        do 7 i=1,t1
           read(5,*) x(i),y(i)
7       continue
        write (6,*) "input data."
        if (points.eq.x2-1.or.points.gt.x2-1) then
           A=x2-1
           else
           A=points
        end if
        do 10 i=1,A
           write (6,*) " 'l' "
           write (6,*) x(t1-i*divsns),y(t1-i*divsns)
           write (6,*) x(t1-divsns+x2+i-1),y(t1-divsns+x2+i-1)
10      continue
        if (points.eq.x2-1.or.points.gt.x2-1) then
           goto 1000
        end if
        do 20 i=1,(abs(x2-points-1))
           write (6,*) " 'l' "
           write (6,*) x(t1-points*divsns+i),y(t1-points*divsns+i)
           write (6,*) x(t1-divsns+x2+points+i-1), y(t1-divsns+x2+points+i-1)
20      continue
1000    do 30 i=1,points-1
           write (6,*) " 'l' "
              if (points.eq.x2.or.points.gt.x2) then
                 D=(points-x2)*divsns+1-(i-1)*divsns
                 else D=x2-points+i
              end if
              if (i.eq.points-x2+1.or.i.gt.points-x2+1) then
                 D=i-(points-x2)
              end if
           write(6,*) x(D),y(D)
           write (6,*) x(t1-x2-(i-1)*divsns), y(t1-x2-(i-1)*divsns)
30      continue
        if (points.eq.x2-1.or.points.gt.x2-1) then
           B=x2-2
           else
           B=points-1
        end if
        do 40 i=1,B
           write (6,*) " 'l' "
           write(6,*) x(t1-i*divsns+x2-1),y(t1-i*divsns+x2-1)
           write(6,*) x(t1-i*divsns+x2-1+(2*i-1)*(x2-1)),
```

```
     +                    y(t1-i*divsns+x2-1+(2*i-1)*(x2-1))
40        continue
          if (points.eq.x2-1.or.points.gt.x2-1) then
             goto 2000
          end if
          do 50 i=1,(x2-points-1)
             write (6,*) " 'l' "
             write(6,*) x(x2-i+1), y(x2-i+1)
             write (6,*) x(t1-points-i+1), y(t1-points-i+1)
50        continue
2000      do 60 i=1,points
             write (6,*) " 'l' "
                if (points.eq.x2.or.points.gt.x2) then
                   E=(x2+(points-x2-i+2)*divsns)
                   else E=points+2-i
                end if
                if (i.eq.points-x2+2.or.i.gt.points-x2+2) then
                   E=points+2-i
                end if
             write (6,) x(E), y(E)
             write (6,*) x(t1-(i-1)*divsns), y(t1-(i-1)*divsns)
60        continue
          write (6,*) " 'l' "
          write (6,*) x(1), y(1)
          write (6,*) x(t1), y(t1)
          write (6,*) "eod."
          write (6,*) "page border off."
          write (6,*) "every curve symbol type is 17."
          write (6,*) "every line texture is 1."
          write (6,*) "x axis label is 'X AXIS  ------>+'."
          write (6,*) "legend off."
          write (6,*) "y axis label is 'Y AXIS  ------>+'."
          write (6,*) "rotation is movie."
          close (unit=5)
          close (unit=6)
          end
```

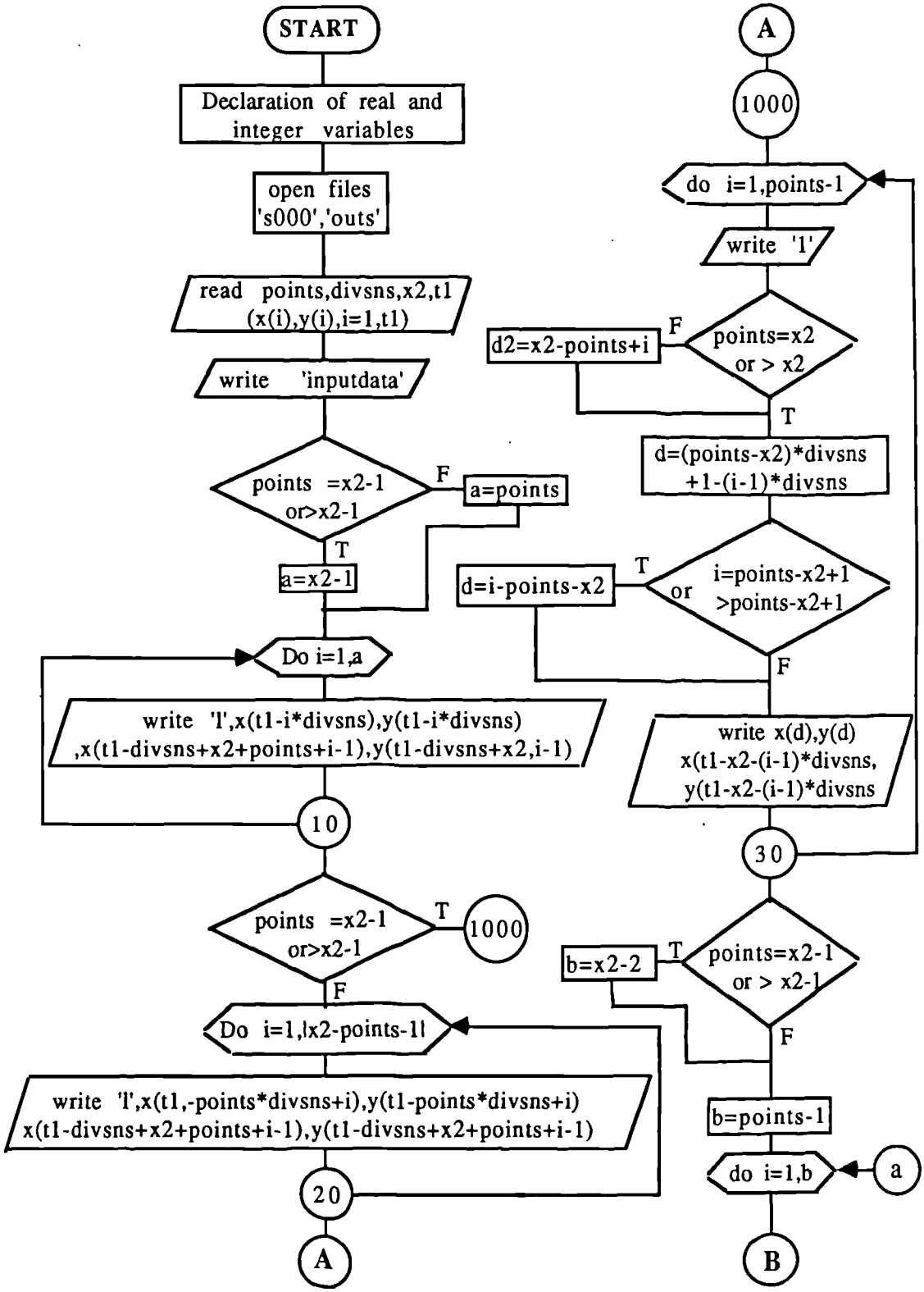
START
Declaration of real and integer variables
open files 's000','outs'
read points,divsns,x2,t1 (x(i),y(i),i=1,t1)
write 'inputdata'
points =x2-1 or>x2-1
F
a=points
T
a=x2-1
Do i=1,a
write 'l',x(t1-i*divsns),y(t1-i*divsns) ,x(t1-divsns+x2+points+i-1),y(t1-divsns+x2,i-1)
10
points =x2-1 or>x2-1
T
1000
F
Do i=1,|x2-points-1|
write 'l',x(t1,-points*divsns+i),y(t1-points*divsns+i) x(t1-divsns+x2+points+i-1),y(t1-divsns+x2+points+i-1)
20
A
A
1000
do i=1,points-1
write '1'
d2=x2-points+i
F
points=x2 or > x2
T
d=(points-x2)*divsns +1-(i-1)*divsns
d=i-points-x2
T
or
i=points-x2+1 >points-x2+1
F
write x(d),y(d) x(t1-x2-(i-1)*divsns, y(t1-x2-(i-1)*divsns
30
b=x2-2
T
points=x2-1 or > x2-1
F
b=points-1
do i=1,b
a
B

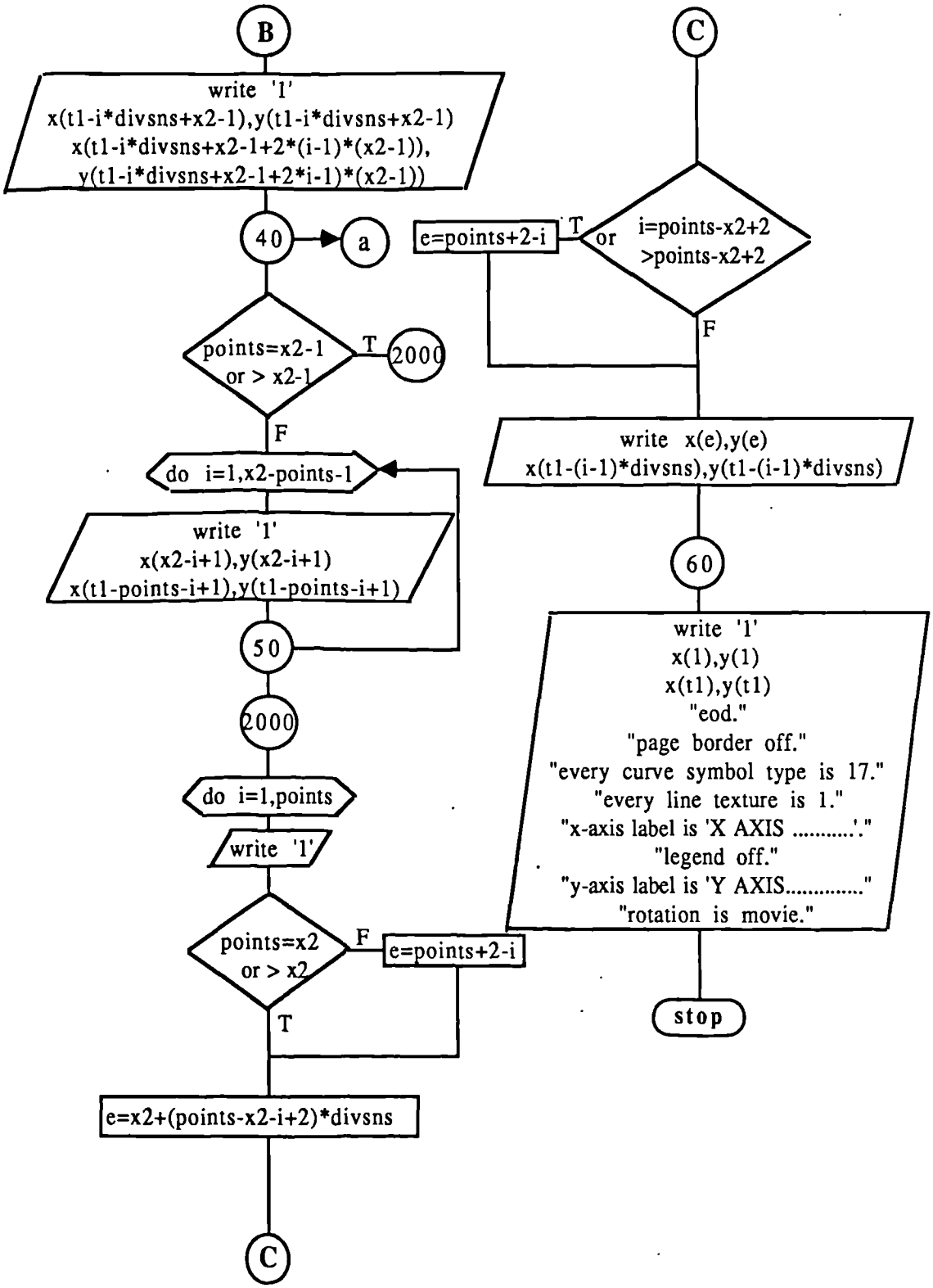
B
write '1'
x(t1-i*divsns+x2-1),y(t1-i*divsns+x2-1)
x(t1-i*divsns+x2-1+2*(i-1)*(x2-1)),
y(t1-i*divsns+x2-1+2*i-1)*(x2-1))
40
a
points=x2-1
or > x2-1
T
2000
F
do i=1,x2-points-1
write '1'
x(x2-i+1),y(x2-i+1)
x(t1-points-i+1),y(t1-points-i+1)
50
2000
do i=1,points
write '1'
points=x2
or > x2
F
e=points+2-i
T
e=x2+(points-x2-i+2)*divsns
C
C
e=points+2-i
T
or
i=points-x2+2
>points-x2+2
F
write x(e),y(e)
x(t1-(i-1)*divsns),y(t1-(i-1)*divsns)
60
write '1'
x(1),y(1)
x(t1),y(t1)
"eod."
"page border off."
"every curve symbol type is 17."
"every line texture is 1."
"x-axis label is 'X AXIS .....'."
"legend off."
"y-axis label is 'Y AXIS....."
"rotation is movie."
stop

APPENDIX IV

Two programs are presented in this Appendix, both were written using the Fortran77 computer language, and run on the Honeywell "Multics" computer system.

The first program designated "STAIR.FORTRAN" is based on the two-dimensional theoretical approach (Method of Characteristics) described in Section (3.2.3.), and the theoretical steps of the program were presented in Section (4.3.). The four equations presented in Section (3.3.3.) were used in this program as well.

The second program designated "CHARA.FORTRAN" was written in order to sort out the results created by the first program (i.e. the X's and Y's for the mesh points). The main task of this program was to pick up the data and rewrite them in the sequence that it should be drawn with on the multics computer "TELEGRAPH" drawing system or any other computer drawing system as shown in chapter seven in this thesis. A print out for the two programs are given in this Appendix.

THE "STAIR.FORTRAN" PROGRAM

```
C       "STAIR.FORTRAN"
*       begin
        implicit double precision (A-H, O-Z, a-h, o-z)
        double precision Ms,Psratiopos,Rhosratiorhoos, Psnratiopos, Psnratiopop, bI,
     +                   bII,ks,kks,Msn,xo,yo,ys,w, omegan,Mpn,fac,step,beta,ka,kka,
     +                   Lop, machnop
        integer i,m,q,p,line,mo,lo,nw,AMn,no,cases,break,n,z,block,add
        common/block1/ Ms,Psratiopos,Rhosratiorhoos,Psnratiopos, Psnratiopop, bI,
     +                 bII,ks,kks,Msn,xo,yo,ys,w,omegan,Mpn,fac,step, beta, ka, kka,
     +                 Lop,machnop
        common/block2/ i,m,q,p,line,mo,lo,nw,AMn,no,cases,break,n,jo,z,block,add
        double precision pi
        common/block3/ pi
        integer maxMmome
        parameter (maxMmome=2000)
        double precision Mm(1:maxMmome), ome(1:maxMmome)
        common/block10/ Mm, ome
        integer maxAMn
        parameter ( maxAMn=550)
        double precision M(1:maxAMn), A(1:maxAMn)
        common/block7/ M,A
        integer nin, nout1, nout2
        common/block5/ nin, nout1, nout2
        pi=acos(-1.0d0)
        nin=10
        nout1=11
        nout2=12
        call inpfil(nin)
        call outfil(nout1)
        call outfill(nout2)
        numset=0
        break=0
        read(nin, *) AMn
        do 100, i=1,AMn,1
           read(nin, *) M(i), A(i)
100     continue
        read (nin, *) Mmome
        do 102, i=1,Mmome,1
           read(nin, *) Mm(i), ome(i)
102     continue
        read(nin, *) cases
13      continue
        read(nin, *) xo,yo,yt,Psnratiopos,Psnratiopop
        read(nin, *) fac,beta,Mpnn,Lop
        ys=yt+(Lop*(dtan(beta*pi/180)))
        ka=1.4
        kka=sqrt((ka+1)/(ka-1))
        ks=1.135
        kks=sqrt((ks+1)/(ks-1))
        line=0
        Msn=sqrt((Psnratiopos**(-(ka-1)/ka)-1)*2/(ka-1))
```

```
      Mpn=sqrt((Psnratiopop**(-(ks-1)/ks)-1)*2/(ks-1))
      omegan=180*kks*arctan(kks,sqrt(Mpn**2-1))/pi-180*arctan(1.0d0,sqrt(
     +            Mpn**2-1))/pi
      z=int(omegan*fac)
      step=(omegan-0.5)/z
      integer maxnw
      parameter (maxnw=101)
      nw=2+z
      print *,nw
      double precision I,II,omega,theta,thetar,Mp,Ppratiopop,Tpratiotop,
     +                  Rhopratiorhoop,alpha,alphar,u,v,ur,vr,x,y
       common/block6/ I(1:2*(maxnw+1)),II(1:2*(maxnw+1)),
     +                  omega(1:2*(maxnw+1)),theta(1:2*(maxnw+1)),
     +                  thetar(1:2*(maxnw+1)),Mp(1:2*(maxnw+1)),
     +                  Ppratiopop(1:2*(maxnw+1)),Tpratiotop(1:2*(maxnw+1)),
     +                  Rhopratiorhoop(1:2*(maxnw+1)),alpha(1:2*(maxnw+1)),
     +                  alphar(1:2*(maxnw+1)),u(1:2*(maxnw+1)),
     +                  v(1:2*(maxnw+1)),ur(1:2*(maxnw+1)),vr(1:2*(maxnw+1)),
     +                  x(1:2*(maxnw+1)),y(1:2*(maxnw+1))
      omega(1)=180*kks*arctan(kks,sqrt(Mpn**2-1))/pi-180*arctan(1.0d0,
     +            sqrt(Mpn**2-1))/pi
      do 120, i=2,nw,1
         omega(i)=omega(1)+(i-1)*step
120   continue
      omega(nw+1)=omega(nw)
      do 160 i=1,(nw+1),1
         II(i)=500-(omega(1)/2)
         I(i)=omega(i)+II(i)
         theta(i)=I(i)+II(i)-1000
         thetar(i)=pi*theta(i)/180
         call fluid properties (omega(i),theta(i),thetar(i),Mp(i), Ppratiopop(i),
     +                        Tpratiotop(i),Rhopratiorhoop(i), alpha(i), alphar(i),
     +                        u(i),v(i),ur(i),vr(i))
160   continue
      numset=numset+1
      write (nout1, 1000) numset
1000  format (//, 1x, '**** Results for problem set number ', i3, //)
      p=1
      y(1)=0
      x(1)=-yo/tan(ur(1))
      i=1
      call print results(i,p)
      do 170, i=2,nw,1
          p=p+1
        bI=tan(ur(i))
        bII=tan((vr(i-1)+vr(i))/2)
        y(i)=(bI*(y(i-1)-bII*x(i-1))-bII*(yo-bI*xo))/(bI-bII)
        x(i)=((y(i-1)-bII*x(i-1))-(yo-bI*xo))/(bI-bII)
        call print results(i,p)
170   continue
      p=p+1
```

```
1       bI=tan((thetar(nw)+thetar(nw+1))/2)
        bII=tan((vr(nw)+vr(nw+1))/2)
        y(nw+1)=(bI*(y(nw)-bII*x(nw))-bII*(yo-bI*xo))/(bI-bII)
        x(nw+1)=((y(nw)-bII*x(nw))-(yo-bI*xo))/(bI-bII)
9       Psratiopos=(1+(ka-1)*Ms**2/2)**(-ka/(ka-1))
        call print results(nw+1,p)
4       continue
        p=p+1
        theta(nw+2)=0
        thetar(nw+2)=0
        I(nw+2)=I(2)
        II(nw+2)=1000-I(nw+2)
        omega(nw+2)=I(nw+2)-II(nw+2)
        call fluid properties (omega(nw+2),theta(nw+2),thetar(nw+2),Mp(nw+2),
     +                         Ppratiopop(nw+2),Tpratiotop(nw+2),
     +                         Rhopratiorhoop(nw+2),alpha(nw+2),alphar(nw+2),
     +                         u(nw+2), v(nw+2),ur(nw+2),vr(nw+2))
        bI=tan((ur(nw+2)+ur(2))/2)
        y(nw+2)=0
        x(nw+2)=-(y(2)-bI*x(2))/bI
        call print results(nw+2,p)
        do 180, i=(nw+3),(2*nw+1),1
          p=p+1
         I(i)=I(i-nw)
         II(i)=II(i-1)
         omega(i)=I(i)-II(i)
         theta(i)=I(i)+II(i)-1000
         thetar(i)=pi*theta(i)/180
         call fluid properties(omega(i),theta(i),thetar(i),Mp(i),Ppratiopop(i),
     +                         Tpratiotop(i),Rhopratiorhoop(i),alpha(i),alphar(i),
     +                         u(i),v(i),ur(i),vr(i))
         bI=tan((ur(i-nw)+ur(i))/2)
         bII=tan((vr(i-1)+vr(i))/2)
         y(i)=(bI*(y(i-1)-bII*x(i-1))-bII*(y(i-nw)-bI*x(i-nw)))/(bI-bII)
         x(i)=((y(i-1)-bII*x(i-1))-(y(i-nw)-bI*x(i-nw)))/(bI-bII)
         call print results(i,p)
            if (x(i).lt.x(i-1).or.x(i).lt.x(i-nw)) then
              else
              goto 12
            end if
         cases=cases-1
         print *,'case number=',cases
            if (cases.gt.0) then
              goto 13
              else
              close (nin)
              close (nout1)
              close (nout2)
              stop
            endif
12       continue
```

```
180     continue
        II(2*(nw+1))=II(2*(nw+1)-1)
        omega(2*(nw+1))=omega(nw+1)
        I(2*(nw+1))=II(2*(nw+1))+omega(2*(nw+1))
        theta(2*(nw+1))=I(2*(nw+1))+II(2*(nw+1))-1000
        thetar(2*(nw+1))=pi*theta(2*(nw+1))/180
        call fluid properties(omega(2*(nw+1)),theta(2*(nw+1)),thetar(2*(nw+1)),
     +                        Mp(2*(nw+1)),Ppratiopop(2*(nw+1)),
     +                        Tpratiotop(2*(nw+1)), Rhopratiorhoop(2*(nw+1)),
     +                        alpha(2*(nw+1)),alphar(2*(nw+1)),u(2*(nw+1)),
     +                        v(2*(nw+1)),ur(2*(nw+1)),vr(2*(nw+1)))
        p=p+1
8       bI=tan((thetar(nw+1)+thetar(2*(nw+1)))/2)
        bII=tan((vr(2*(nw+1))+vr(2*nw+1))/2)
        y(2*(nw+1))=(bI*(y(2*nw+1)-bII*x(2*nw+1))-bII*(y(nw+1)-bI*x(nw+1)))/
     +                  (bI-bII)
 x(2*(nw+1))=((y(2*nw+1)-bII*x(2*nw+1))-(y(nw+1)-bI*x(nw+1)))/(bI-bII)
6       Psratiopos=(1+(ka-1)*Ms**2/2)**(-ka/(ka-1))
        call print results(2*(nw+1),p)
        do 190, i=1, (nw+1),1
           I(i)=I(i+nw+1)
           II(i)=II(i+nw+1)
           omega(i)=omega(i+nw+1)
           theta(i)=theta(i+nw+1)
           thetar(i)=thetar(i+nw+1)
           Mp(i)=Mp(i+nw+1)
           Ppratiopop(i)=Ppratiopop(i+nw+1)
           Tpratiotop(i)=Tpratiotop(i+nw+1)
           Rhopratiorhoop(i)=Rhopratiorhoop(i+nw+1)
           alpha(i)=alpha(i+nw+1)
           alphar(i)=alpha(i+nw+1)
           u(i)=u(i+nw+1)
           v(i)=v(i+nw+1)
           ur(i)=ur(i+nw+1)
           vr(i)=vr(i+nw+1)
           x(i)=x(i+nw+1)
           y(i)=y(i+nw+1)
190     continue
        goto 4
191     cases=cases-1
        if (cases.gt.0) then
           goto 13
           else
           close(nin)
           close(nout1)
           close(nout2)
           stop
        end if
        end
*
*
```

```
      subroutine fluid properties(omega00,theta00,thetar00,Mp,Ppratiopop,
     +                            Tpratiotop,Rhopratiorhoop,alpha,alphar,u,v,ur,vr)
      implicit double precision (A-H, O-Z, a-h, o-z)
      double precision Ms,Psratiopos,Rhosratiorhoos,Psnratiopos, Psnratiopop, bI,
     +                 bII,ks,kks,Msn,xo,yo,ys,w,omegan,Mpn,fac,step,beta,ka, kka,
     +                 Lop,machnop
      integer i,m,q,p,line,mo,lo,nw,AMn,no,cases,break,n,jo,z,block,add
      common/block1/ Ms,Psratiopos,Rhosratiorhoos,Psnratiopos, Psnratiopop, bI,
     +                 bII,ks,kks,Msn,xo,yo,,ys,w,omegan,Mpn,fac,step,beta,ka,kka,
     +                 Lop,machnop
      common/block2/ i,m,q,p,line,mo,lo,nw,AMn,no,cases,break,n,jo,z,block,add
      double precision pi
      common/block3/ pi
      double precision Mp
      double precision machnop
      external machnop
      omega=omega00
      theta=theta00
      thetar=thetar00
      Mp=machnop(omega)
      Ppratiopop=(1+(ks-1)*Mp**2/2)**(-ks/(ks-1))
      Tpratiotop=Ppratiopop**((ks-1)/ks)
      Rhopratiorhoop=Ppratiopop**(1/ks)
      alpha=180*asin(1/Mp)/pi
      alphar=pi*alpha/180
      u=theta-alpha
      ur=thetar-alphar
      v=theta+alpha
      vr=thetar+alphar
       return
          end
*
      subroutine print results( i00,p00)
      implicit double precision (A-H, O-Z, a-h, o-z)
      integer i00, p00, p
      integer maxnw
      parameter(maxnw=101)
      double precision I,II,omega,theta,thetar,Mp,Ppratiopop,Tpratiotop,
     +                 Rhopratiorhoop,alpha,alphar,u,v,ur,vr,x,y
      common/block6/ I(1:2*(maxnw+1)),II(1:2*(maxnw+1)),
     +                 omega(1:2*(maxnw+1)),theta(1:2*(maxnw+1)),
     +                 thetar(1:2*(maxnw+1)),Mp(1:2*(maxnw+1)),
     +                 Ppratiopop(1:2*(maxnw+1)),Tpratiotop(1:2*(maxnw+1)),
     +                 Rhopratiorhoop(1:2*(maxnw+1)),alpha(1:2*(maxnw+1)),
     +                 alphar(1:2*(maxnw+1)),u(1:2*(maxnw+1)),
     +                 v(1:2*(maxnw+1)),ur(1:2*(maxnw+1)),vr(1:2*(maxnw+1)),
     +                 x(1:2*(maxnw+1)),y(1:2*(maxnw+1))
      integer nin, nout1, nout2
      common/block5/ nin, nout1, nout2
      i=i00
```

```
      p=p00
      write( nout1, 100) p, I(i),II(i),omega(i),theta(i),alpha(i),Ppratiopop(i)Mp(i),
     +                        Tpratiotop(i),Rhopratiorhoop(i),x(i),y(i)
100   format(1x,i4,2x,2f9.2,2f7.2,f8.2,4f8.4,2f8.3)
      write( nout2, 200)  x(i),y(i)
200   format (10x,f8.3,5x,f8.3)
      return
      end
*
      double precision function machnop( omega00)
      implicit double precision (A-H, O-Z, a-h, o-z)
      double precision Ms,Psratiopos,Rhosratiorhoos,Psnratiopos,Psnratiopop, bI,
     +                 bII,ks,kks,Msn,xo,yo,ys,w,omegan,Mpn,fac,step,beta,ka, kka,
     +                 Lop,machnop
      integer i,m,q,p,nw,AMn,no,cases,break,n,jo,z,block,add
      common/block1/ Ms,Psratiopos,Rhosratiorhoos,Psnratiopos,Psnratiopop,bI,
     +                 bII,ks,kks,Msn,xo,yo,ys,w,omegan,Mpn,fac,step,beta, ka,kka,
     +                 Lop,machnop
      common/block2/ i,m,q,p,line,mo,lo,nw,AMn,no,cases,break,n,jo,z,block,add
      double precision pi
      common/block3/pi
      integer maxMmome
      parameter (maxMmome=2000)
      double precision Mm(1:maxMmome), ome(1:maxMmome)
      common /block10/ Mm, ome
      double precision mx,dmx,fm1,fm2,omegar
      double precision funcm
      omega = omega00
      if (omega.gt.5) goto 4
      omegar=( pi*omega)/180
      mx=0.00001d0
      dmx=1.0d0
      mx=mx+dmx
1     continue
      fm1=funcm(mx,omegar)
2     continue
      mx=mx+dmx
      fm2=funcm(mx,omegar)
      if(fm1*fm2.gt.0) fm1=fm2
      if( fm1*fm2.gt.0) goto 2
      if(fm1*fm2.eq.0)goto 3
      if(dmx.lt.0.0001d0) goto 3
      mx=mx-dmx
      dmx=0.01d0*dmx
      goto 1
3     continue
      machnop = mx
      return
4     continue
      j=1
101   continue
```

```
      j=j+1
      if (omega.gt.ome(j)) goto 101
      machnop=Mm(j-1)+(Mm(j)-Mm(j-1))*(omega-ome(j-1))/(ome(j)-ome(j-1))
      return
      end
*
      double precision function funcm( m00,omegar00)
      implicit double precision (A-H, O-Z, a-h, o-z)
      double precision Ms,Psratiopos,Rhosratiorhoos,Psnratiopos, Psnratiopop, bI,
     +                 bII,ks,kks,Msn,xo,yo,,ys,w,omegan,Mpn,fac,step,beta,ka,kka,
     +                 Lop,machnop
      integer i,m,q,p,nw,AMn,no,cases,break,n,jo,z,block,add
      common/block1/ Ms,Psratiopos,Rhosratiorhoos,Psnratiopos,Psnratiopop,bI,
     +                 bII,ks,kks,Msn,xo,yo,ys,w,omegan,Mpn,fac,step,beta, ka,kka,
     +                 Lop,machnop
      common/block2/ i,m,q,p,nw,AMn,no,cases,break,n,jo,z,block,add
      double precision pi
      common/block3/ pi
      double precision r
      double precision m00, omegar00
      double precision mx, omegar
      double precision arctan
      external arctan
      mx = m00
      omegar = omegar00
      r=kks*arctan(sqrt(ks+1),sqrt((ks-1)*(mx**2 -1)))-arctan(1.0d0,sqrt(mx**2
     +          -1))-omegar
      funcm = r
      end
*
      double precision function arctan(a, b)
      implicit double precision (A-H, O-Z, a-h, o-z)
      double precision a, b
      arctan = atan(b/a)
      return
      end
*
      subroutine inpfil(nin)
*     subroutine  inpfil requests the user for an input file name
*     and opens the file on fortran unit  nin
      integer nin
      character infil*70
      integer ios
10    continue
      print20
20    format (1x, 'Please enter the input file name', /)
      read(*, '(a)') infil
      open(nin, file = infil,  status = 'old', iostat = ios)
      if(ios.ne.0) then
         print30, infil
30       format(/,1x,'****error**** on attempting to open the input file',
```

```
     +              /, 1x, "", a, "",
     +              /, 1x, 'possibly because it does not exist or is in use',
     +              /, 1x, 'Please try again', /)
            goto 10
          endif
          end
*
          subroutine outfil(nout1)
*         subroutine  outfil  requests the user for an output file name
*         (which must not exist) and opens the file on fortran unit nout1
          integer nout1
          character outpfl*70
          integer ios
10        continue
          print20
20        format(/, 1x, 'Please enter the first output file name ', /)
          read(*, '(a)') outpfl
          open(nout1, file = outpfl, status = 'new', iostat = ios)
          if(ios.ne.0) then
            print30, outpfl
30          format(/, 1x, '****error**** on attempting to open output file ',
     +              /, 1x, "", a, "",
     +              /, 1x, 'probably because it already exists  ',
     +              /, 1x, 'Please try again',/)
            goto 10
          end if
          end
*
          subroutine outfill(nout2)
*         subroutine  outfil  requests the user for an output file name
*         (which must not exist) and opens the file on fortran unit nout2
          integer nout2
          character outpfl*70
          integer ios
10        continue
          print20
20        format(/, 1x, 'Please enter the second output file name ', /)
          read(*, '(a)') outpfl
          open(nout2, file = outpfl, status = 'new', iostat = ios)
          if(ios.ne.0) then
            print30, outpfl
30          format(/, 1x, '****error**** on attempting to open output file ',
     +              /, 1x, "", a, "",
     +              /, 1x, 'probably because it already exists  ',
     +              /, 1x, 'Please try again',/)
            goto 10
          end if
          end
```

THE "CHARA.FORTRAN" PROGRAM

```
C       "CHARA.FORTRAN"
        integer i,j,nw
        real x(5000),y(5000)
        open (unit=5,file='2')
        open (unit=6,file='rcha2')
        write (*,100)
100     format(1h, 'nw',$)
        read (*,*) nw
        x(4999)=0.0
        y(4999)=0.0
        x(5000)=0.005
        y(5000)=6.565
        do 10  i=1,nw*(nw-39)+2
           read (5,*) x(i),y(i)
10      continue
        write (6,*) "rotation is movie."
        write (6,*) "input data."
        do 20 i=0,(nw-1)
           write (6,*) "'l'"
           write (6,*) x(5000),'     ',y(5000)
           do 21 j=0,i
              write (6,*) x(j*(nw+1)+1+i-j),'     ', y(j*(nw+1)+1+i-j)
21         continue
20      continue
        do 30 i=1,nw
           j=i-1
           write (6,*) "'l'"
           do 31 k=1,nw-j
              write (6,*) x(j*nw+k+j),'     ', y(j*nw+k+j)
31         continue
30      continue
        write (6,*) "'l'"
        write (6,*) x(5000),'     ', y(5000)
        write (6,*) x(1*(nw+1)),'     ', y(1*(nw+1))
        write (6,*) "eod."
        write (6,*) "page border off."
        write (6,*) "every curve symbol count is 0."
        write (6,*) "every line texture is 1."
        write (6,*) "x axis label is 'X AXIS  ------>+'."
        write (6,*) "legend off."
        write (6,*) "y axis label is 'Y AXIS  ------>+'."
        write (6,*) "x axis length is 9.5."
        write (6,*) "y axis tick marks is 10."
        write (6,*) "x axis maximum is 100."
        write (6,*) "x axix minimum is -30."
        write (6,*) "y axis maximum is 20."
        write (6,*) "y axis scale step is 1."
        write (6,*) "cross off."
        close (unit=5)
        close (unit=6)
        end
```

APPENDIX V

THE AIR MASS FLOW RATE THROUGH THE SONIC NOZZLES

The analysis is based on the one-dimensional fluid flow theory, where the necessary equations of state, for conveniance are summurized as below :

1. Equation of state for a perfect gas, Equation (V.1.) :

$$\frac{P}{\rho} = RT \qquad \text{V.1.}$$

2. Continuity equation, Equation (V.2.) and (V.3.) :

$$\dot{m} = \rho A U \qquad \text{V.2.}$$

or

$$\frac{d\rho}{\rho} + \frac{dU}{U} + \frac{dA}{A} = 0 \qquad \text{V.3.}$$

3. Momentum equation, a convinient form of the momentum equation for one-dimensional flow is obtained by integrating the compressible Navier-Stokes equation for frictionless flows along a streamline, and neglect the gravitational effects, the equation would be :

$$\int \frac{d\rho}{\rho} = \frac{U^2}{2} \qquad \text{V.4.}$$

Integrating this equation between the upstream section (o) and the exit section (e) of the nozzle would give :

$$\int_{P_o}^{P_e} \frac{d\rho}{\rho} = \frac{U_e^2}{2} \qquad \text{V.5.}$$

By substituting the isentropic pressure-density relation, Equation (V.6.) :

$$\frac{P}{\rho^{\gamma}} = \text{const.} \qquad \text{V.6.}$$

The integration could be solved in the form below :

$$U_e^2 = 2\,\frac{P_o}{\rho_o}\,\frac{\gamma}{\gamma-1}\left[1-\left(\frac{P_e}{P_o}\right)^{\left(\frac{\gamma-1}{\gamma}\right)}\right] \qquad \text{V.7.}$$

Substituting Equation (V.7.) into the continuity Equation (V.2.) gives :

$$\frac{\dot{m}}{A} = \sqrt{2\,\frac{P_o}{\rho_o}\,\rho_e^2\,\frac{\gamma}{\gamma-1}\left[1-\left(\frac{P_e}{P_o}\right)^{\left(\frac{\gamma-1}{\gamma}\right)}\right]} \qquad \text{V.8.}$$

Using Equation (V.5.) and the pressure ratio Equation (V.9.),

$$\frac{P_e}{P_o} = \left(\frac{2}{\gamma+1}\right)^{\left(\frac{\gamma}{\gamma-1}\right)} \qquad \text{V.9.}$$

Equation (V.8.) would be written in the form :

$$\frac{\dot{m}}{A} = \sqrt{\gamma\,P_i\,\rho_i\left(\frac{2}{\gamma+1}\right)^{\left(\frac{\gamma+1}{\gamma-1}\right)}} \qquad \text{V.10.}$$

The final air mass flow rate (m_a) equation would be equal to :

$$\dot{m}_a = 241.39\ A \qquad \text{V.11.}$$

where,

P_o =	Upstream air pressure	=	$1.013\ 10^5$	N/m^2
ρ_o =	Upstream air density	=	1.2269	kg/m^3
γ =	Ratio of specific heats for air	=	1.4	

APPENDIX VI

This appendix contains all the results for the experimental work carried out by the author of this thesis in the department of Chemical Engineering at Loughborough University of Technology.

Note that, the calculated mass of air (m_a) is only applicable with suction pressures (P_s) which are under the air nozzle critical pressure which is rounded to 440 mmHg. Abs.

The Distance from the Nozzle Outlet to Diffuser Throat L (mm)	The Mass of Air Entrained by The Motive Steam m_a (kg/hr.)								Motive Steam Pressure P_m (psig.)
	1.72	6.88	8.60	15.48	22.36	27.52	34.40	43.00	
	The Suction Pressure P_s (mm Hg. Abs.)								
85.4	280	365	390	480	570	635	665	695	
80.4	295	370	400	475	560	625	658	690	
75.4	200	335	340	445	535	580	633	690	
73.4	208	315	335	430	530	580	630	680	105
72.4	200	305	320	425	530	585	630	675	
70.4	220	313	340	445	525	580	630	680	
69.4	270	350	365	455	540	585	630	680	
85.4	245	325	340	450	555	615	650	690	
80.4	265	330	347	450	555	610	650	685	
75.4	190	285	303	425	505	570	625	680	
73.4	193	290	310	413	510	570	627	675	90
72.4	180	270	290	410	513	580	620	670	
70.4	213	298	320	420	510	570	625	680	
69.4	223	320	347	440	520	560	630	675	
85.4	270	360	390	485	560	590	635	685	
80.4	265	330	375	460	545	590	635	680	
75.4	165	279	310	398	505	567	620	660	
73.4	170	265	285	418	510	560	610	658	75
72.4	160	250	275	390	505	580	620	655	
70.4	186	288	302	420	505	580	620	670	
69.4	250	305	328	420	530	580	620	670	
85.4	510	530	540	570	605	620	640	670	
80.4	475	510	515	555	590	610	635	680	
75.4	455	480	485	530	570	605	630	659	
73.4	433	460	470	505	565	585	615	655	60
72.4	480	502	515	540	575	610	635	660	
70.4	470	500	510	547	580	600	630	670	
69.4	460	475	485	530	570	610	635	665	

Table VI.1. The Suction Pressure (P_s) at Different Nozzle Setting with Respect to the Diffuser Throat for Ejector (E1).

The Distance from the Nozzle Outlet to Diffuser Throat L (mm)	The Mass of Air Entrained by The Motive Steam m_a (kg/hr.)								Motive Steam Pressure P_m (psig.)
	1.72	6.88	8.60	15.48	22.36	27.52	34.40	43.00	
	The Suction Pressure P_s (mm Hg. Abs.)								
107.4	260	315	315	410	470	510	565	620	105
102.4	240	275	280	335	405	445	510	585	
97.4	235	255	260	315	380	440	500	570	
95.4	215	270	305	370	440	495	555	610	
92.4	215	275	295	370	435	495	550	605	
88.4	235	275	285	344	410	465	520	580	
85.4	315	370	396	470	530	565	605	650	
107.4	220	270	280	360	445	490	540	605	90
102.4	210	235	250	315	350	435	510	570	
97.4	210	221	235	295	365	420	490	560	
95.4	185	250	265	350	410	460	530	595	
92.4	170	245	270	345	410	470	535	595	
88.4	205	250	260	315	386	440	500	570	
85.4	260	325	350	410	490	550	590	640	
107.4	190	260	260	345	410	460	530	590	75
102.4	175	210	230	290	360	420	480	555	
97.4	180	200	215	280	350	405	470	560	
95.4	170	225	245	325	400	450	510	585	
92.4	201	225	240	315	390	450	510	580	
88.4	180	210	235	290	365	450	489	630	
85.4	230	325	350	390	470	560	570	625	
107.4	210	250	290	340	410	455	525	590	60
102.4	205	215	235	275	360	405	470	570	
97.4	200	202	205	275	340	390	460	560	
95.4	190	245	255	355	415	450	505	575	
92.4	170	220	250	330	390	435	490	570	
88.4	210	225	230	302	360	412	490	570	
85.4	215	300	310	385	450	505	550	610	

Table VI.2. The Suction Pressure (P_s) at Different Nozzle Setting with Respect to the Diffuser Throat for Ejector (E2).

The Distance from the Nozzle Outlet to Diffuser Throat L (mm)	The Mass of Air Entrained by The Motive Steam m_a (kg/hr.)								Motive Steam Pressure P_m (psig.)
	1.72	6.88	8.60	15.48	22.36	27.52	34.40	43.00	
	The Suction Pressure P_s (mm Hg. Abs.)								
83.4	450	510	538	590	655	680	695	720	
78.4	305	410	450	535	590	645	680	700	
73.4	270	350	360	485	560	600	640	680	105
71.4	205	290	330	460	550	590	630	670	
69.9	330	425	450	545	605	645	670	700	
83.4	390	475	485	555	630	665	687	710	
78.4	280	360	385	500	575	610	650	690	
73.4	230	330	335	450	530	580	595	670	90
71.4	190	280	305	430	520	570	580	670	
69.9	290	390	418	528	570	613	655	690	
83.4	385	435	450	520	600	640	670	700	
78.4	310	385	410	480	540	630	660	690	
73.4	245	330	370	435	520	560	620	680	75
71.4	180	305	325	430	500	550	600	660	
69.9	305	390	425	505	565	600	650	695	
83.4	560	580	590	610	630	650	665	700	
78.4	470	570	580	600	620	635	656	690	
73.4	450	470	560	590	620	630	650	670	60
71.4	400	420	450	520	600	640	650	670	
69.9	440	485	545	573	610	630	660	690	

Table VI.3. The Suction Pressure (P_s) at Different Nozzle Setting with Respect to the Diffuser Throat for Ejector (E3).

The Distance from the Nozzle Outlet to Diffuser Throat L (mm)	The Mass of Air Entrained by The Motive Steam m_a (kg/hr.)								Motive Steam Pressure P_m (psig.)
	1.72	6.88	8.60	15.48	22.36	27.52	34.40	43.00	
	The Suction Pressure P_s (mm Hg. Abs.)								
85.4	285	385	430	555	610	650	690	715	
80.4	280	380	390	510	590	620	660	690	
73.4	240	330	360	470	570	620	660	695	105
71.4	135	173	202	325	480	560	615	655	
70.4	290	370	415	510	615	650	665	700	
85.4	275	350	420	520	585	635	665	695	
80.4	220	340	350	460	570	620	645	680	
73.4	195	290	340	445	550	610	650	672	90
71.4	120	167	190	320	485	530	590	655	
70.4	245	350	375	465	570	610	650	690	
85.4	355	420	460	510	570	615	650	685	
80.4	190	365	370	475	550	590	630	670	
73.4	195	330	365	470	535	590	620	665	75
71.4	100	160	195	375	485	545	580	635	
70.4	255	330	350	490	550	590	630	670	
85.4	505	545	550	570	600	630	655	680	
80.4	480	530	535	555	590	630	650	675	
73.4	470	490	495	555	590	610	635	670	60
71.4	445	460	465	498	550	575	605	640	
70.4	450	470	475	530	575	610	635	675	

Table VI.4. The Suction Pressure (P_s) at Different Nozzle Setting with Respect to the Diffuser Throat for Ejector (E4).

The Distance from the Nozzle Outlet to Diffuser Throat L (mm)	The Mass of Air Entrained by The Motive Steam m_a (kg/hr.)								Motive Steam Pressure Pm (psig.)
	1.72	6.88	8.60	15.48	22.36	27.52	34.40	43.00	
	The Suction Pressure Ps (mm Hg. Abs.)								
82.1	200	260	270	355	410	460	520	580	
77.1	250	300	310	385	445	490	535	590	
75.1	245	190	305	375	430	480	530	590	
72.1	240	280	290	360	410	465	515	580	105
69.1	210	265	345	345	405	455	510	575	
66.1	155	230	250	310	380	435	505	570	
63.1	180	265	280	335	410	465	520	580	
82.1	210	305	285	350	410	450	500	575	
77.1	250	295	375	430	465	515	520	585	
75.1	240	290	310	360	415	455	510	575	
72.1	240	280	300	350	405	440	495	570	90
69.1	210	250	265	330	395	440	500	575	
66.1	130	220	235	305	365	420	485	570	
63.1	180	250	260	330	390	445	500	570	
82.1	320	380	385	425	460	490	525	570	
77.1	295	340	365	410	450	485	525	580	
75.1	290	335	355	400	445	474	520	575	
72.1	285	360	395	435	470	510	570	580	75
69.1	295	330	340	390	440	460	515	570	
66.1	250	280	285	375	415	460	505	565	
63.1	255	290	310	380	425	470	510	575	
82.1	530	545	550	550	560	575	590	615	
77.1	520	530	535	550	565	575	590	615	
75.1	510	530	535	550	565	575	590	615	
72.1	530	550	555	565	580	590	600	610	60
69.1	530	550	555	570	590	590	600	620	
66.1	505	530	530	550	565	570	585	610	
63.1	510	530	540	555	570	580	590	620	

Table VI.5. The Suction Pressure (P_s) at Different Nozzle Setting with Respect to the Diffuser Throat for Ejector (E5).

The Distance from the Nozzle Outlet to Diffuser Throat L (mm)	The Mass of Air Entrained by The Motive Steam m_a (kg/hr.)								Motive Steam Pressure Pm (psig.)
	1.72	6.88	8.60	15.48	22.36	27.52	34.40	43.00	
	The Suction Pressure Ps (mm Hg. Abs.)								
96.1	240	290	315	365	415	455	500	560	105
91.1	230	270	290	350	405	435	485	545	
89.1	240	285	295	360	455	450	495	555	
83.1	230	250	255	300	355	490	440	510	
86.1	225	250	260	310	360	400	450	510	
80.1	230	255	265	325	380	420	465	530	
96.1	210	250	265	340	490	425	470	540	90
91.1	200	235	260	325	370	420	465	520	
89.1	215	260	270	280	385	420	470	540	
83.1	195	225	230	280	280	370	425	490	
86.1	195	220	240	290	335	375	430	490	
80.1	190	220	250	295	360	390	440	520	
96.1	210	250	265	315	365	405	455	520	75
91.1	190	230	250	300	350	490	440	505	
89.1	195	245	255	315	365	400	450	520	
83.1	200	205	210	260	310	350	405	470	
86.1	200	215	225	270	320	410	475	480	
80.1	185	210	245	300	345	380	435	500	
96.1	270	315	330	365	410	440	470	520	60
91.1	300	290	300	355	395	430	465	505	
89.1	280	445	355	405	440	475	520	530	
83.1	310	315	320	330	350	375	415	480	
86.1	295	295	300	330	360	390	430	490	
80.1	280	290	300	345	385	425	465	515	

Table VI.6. The Suction Pressure (P_s) at Different Nozzle Setting with Respect to the Diffuser Throat for Ejector (E6).

The Distance from the Nozzle Outlet to Diffuser Throat L (mm)	The Mass of Air Entrained by The Motive Steam m_a (kg/hr.)								Motive Steam Pressure Pm (psig.)
	1.72	6.88	8.60	15.48	22.36	27.52	34.40	43.00	
	The Suction Pressure P_s (mm Hg. Abs.)								
87.1	200	265	275	350	425	470	535	590	
82.1	200	255	270	350	430	470	535	590	
77.1	175	250	265	350	420	465	525	590	
75.1	210	270	280	370	435	480	540	590	105
72.1	120	205	225	305	395	455	510	580	
69.1	155	240	250	320	385	434	510	585	
66.1	220	275	290	350	420	460	510	575	
87.1	240	285	310	370	425	470	515	575	
82.1	215	270	290	365	420	465	510	575	
77.1	220	270	290	355	410	455	505	570	
75.1	240	290	310	365	425	465	515	575	90
72.1	110	215	230	330	410	445	500	565	
69.1	210	250	260	365	425	500	520	565	
66.1	190	290	305	360	410	445	490	555	
87.1	390	410	410	440	465	495	470	585	
82.1	370	395	400	430	460	485	530	575	
77.1	360	390	400	425	455	480	525	570	
75.1	360	390	400	430	460	490	525	560	75
72.1	375	400	405	430	455	495	530	575	
69.1	400	425	430	445	460	480	520	570	
66.1	330	370	380	410	440	465	510	620	
87.1	590	610	615	625	630	635	640	650	
82.1	580	600	610	615	620	625	630	635	
77.1	475	505	517	610	630	635	645	655	
75.1	480	510	520	615	630	650	660	665	60
72.1	550	565	570	595	605	620	630	630	
69.1	535	550	555	560	580	590	610	605	
66.1	540	555	560	565	590	605	620	640	

Table VI.7. The Suction Pressure (P_s) at Different Nozzle Setting with Respect to the Diffuser Throat for Ejector (E7).

The Distance from the Nozzle Outlet to Diffuser Throat L (mm)	The Mass of Air Entrained by The Motive Steam m_a (kg/hr.)								Motive Steam Pressure Pm (psig.)
	1.72	6.88	8.60	15.48	22.36	27.52	34.40	43.00	
	The Suction Pressure P_s (mm Hg. Abs.)								
82.1	235	290	310	395	510	520	560	610	
77.1	205	265	280	368	440	500	552	605	
75.1	210	260	280	350	430	485	540	600	
72.1	185	260	275	345	420	480	535	600	105
69.1	165	230	250	335	415	465	530	595	
66.1	180	270	285	350	425	470	535	600	
62.1	175	250	270	345	420	470	530	595	
82.1	220	285	300	375	440	485	535	595	
77.1	210	275	285	353	435	480	530	590	
75.1	220	265	275	345	420	460	520	580	
72.1	220	265	275	335	420	465	520	590	90
69.1	155	230	245	320	400	450	520	590	
66.1	210	270	285	355	410	455	525	595	
62.1	155	255	270	335	410	455	515	580	
82.1	410	425	450	470	505	545	585	645	
77.1	365	410	415	425	460	485	530	575	
75.1	400	415	420	430	460	495	540	575	
72.1	380	395	400	420	455	480	530	575	75
69.1	365	375	380	420	455	460	520	575	
66.1	290	330	345	410	450	465	520	580	
62.1	290	330	345	410	450	465	520	580	
82.1	535	550	555	560	565	570	590	640	
77.1	360	420	420	440	470	495	540	580	
75.1	520	545	545	550	560	565	582	615	
72.1	460	530	530	542	560	565	580	610	60
69.1	495	506	525	534	560	565	580	605	
66.1	480	490	495	515	540	565	575	610	
62.1	480	505	515	530	555	565	580	610	

Table VI.8. The Suction Pressure (P_s) at Different Nozzle Setting with Respect to the Diffuser Throat for Ejector (E8).

The Distance from the Nozzle Outlet to Diffuser Throat L (mm)	The Mass of Air Entrained by The Motive Steam m_a (kg/hr.)								Motive Steam Pressure Pm (psig.)
	1.72	6.88	8.60	15.48	22.36	27.52	34.40	43.00	
	The Suction Pressure P_s (mm Hg. Abs.)								
83.8	220	245	280	340	390	430	480	535	
76.8	220	270	280	335	390	430	470	530	
73.8	150	215	210	275	335	370	430	505	
71.8	150	215	240	295	345	380	440	500	105
68.8	135	195	220	285	330	365	420	490	
65.8	140	195	215	275	325	360	420	490	
63.8	165	230	255	315	360	400	440	510	
83.8	250	290	315	355	400	430	465	530	
76.8	230	280	290	350	397	425	460	520	
73.8	130	190	200	255	310	360	415	500	
71.8	150	220	240	300	345	375	425	485	90
68.8	130	210	230	285	330	360	425	485	
65.8	130	200	210	265	315	355	410	475	
63.8	145	235	250	300	350	375	425	485	
83.8	390	410	425	445	470	490	515	550	
76.8	465	395	410	430	450	490	505	550	
73.8	380	410	420	455	470	480	505	540	
71.8	360	380	390	400	435	465	490	510	75
68.8	350	375	385	410	425	445	480	500	
65.8	350	355	360	385	410	430	475	520	
63.8	360	355	365	390	420	435	475	525	
83.8	530	550	555	565	570	585	595	610	
76.8	460	540	545	550	560	570	585	605	
73.8	515	530	535	550	565	570	585	605	
71.8	535	545	550	555	565	575	590	600	60
68.8	510	530	540	550	565	570	585	600	
65.8	515	530	535	550	565	570	580	595	
63.8	540	555	560	570	575	590	600	615	

Table VI.9. The Suction Pressure (P_s) at Different Nozzle Setting with Respect to the Diffuser Throat for Ejector (E9).

The Distance from the Nozzle Outlet to Diffuser Throat L (mm)	The Mass of Air Entrained by The Motive Steam m_a (kg/hr.)								Motive Steam Pressure Pm (psig.)
	1.72	6.88	8.60	15.48	22.36	27.52	34.40	43.00	
	The Suction Pressure Ps (mm Hg. Abs.)								
92.8	190	260	265	310	350	395	450	495	105
87.8	200	240	270	330	375	410	455	520	
85.8	205	235	265	330	370	400	458	530	
82.8	180	202	210	255	300	340	390	460	
80.8	170	198	205	255	300	333	385	450	
77.8	255	310	325	375	410	458	495	550	
92.8	160	220	225	290	335	365	415	488	90
87.8	155	215	240	298	340	380	430	500	
85.8	170	210	240	300	340	380	390	492	
82.8	150	180	192	240	285	325	370	450	
80.8	155	180	200	230	280	323	375	440	
77.8	220	275	290	350	400	430	470	525	
92.8	190	230	250	300	350	380	425	485	75
87.8	205	240	270	310	345	370	420	490	
85.8	160	170	180	230	270	305	360	430	
82.8	150	165	175	235	275	302	360	430	
80.8	490	470	460	415	362	305	270	240	
77.8	270	290	300	345	398	455	490	520	
92.8	205	240	250	300	370	380	422	490	60
87.8	290	320	340	370	410	450	485	520	
85.8	292	330	340	380	430	440	490	520	
82.8	265	280	280	290	325	350	390	460	
80.8	265	335	275	300	380	415	460	470	
77.8	310	335	350	390	460	480	500	538	

Table VI.10. The Suction Pressure (P_s) at Different Nozzle Setting with Respect to the Diffuser Throat for Ejector (E10).

The Distance from the Nozzle Outlet to Diffuser Throat L (mm)	The Mass of Air Entrained by The Motive Steam m_a (kg/hr.)								Motive Steam Pressure Pm (psig.)
	1.72	6.88	8.60	15.48	22.36	27.52	34.40	43.00	
	The Suction Pressure P_s (mm Hg. Abs.)								
90.8	130	150	175	200	260	310	410	535	
83.8	100	120	140	150	240	270	355	480	
79.8	90	100	105	150	225	280	345	450	105
76.8	95	100	140	175	250	280	350	435	
73.8	100	110	160	205	270	315	385	475	
90.8	180	200	250	310	370	400	470	530	
83.8	140	160	180	190	310	390	450	505	
79.8	130	135	140	170	250	320	420	470	90
76.8	130	135	160	180	260	280	355	445	
73.8	115	120	170	215	290	350	430	480	
90.8	490	505	510	520	535	550	560	585	
83.8	460	470	475	480	500	510	540	565	
79.8	420	430	440	470	485	495	510	550	75
76.8	425	435	445	455	475	490	525	550	
73.8	410	425	435	445	470	480	500	550	
90.8	580	590	590	600	610	620	625	640	
83.8	575	590	600	610	615	620	625	640	
79.8	540	560	565	580	590	595	605	620	60
76.8	550	560	565	570	575	590	600	615	
73.8	525	550	550	560	585	600	605	620	

Table VI.11. The Suction Pressure (P_s) at Different Nozzle Setting with Respect to the Diffuser Throat for Ejector (E11).

The Distance from the Nozzle Outlet to Diffuser Throat L (mm)	The Mass of Air Entrained by The Motive Steam m_a (kg/hr.)								Motive Steam Pressure Pm (psig.)
	1.72	6.88	8.60	15.48	22.36	27.52	34.40	43.00	
	The Suction Pressure P_s (mm Hg. Abs.)								
83.8	140	200	215	300	340	380	445	530	
78.8	145	235	250	315	370	395	450	525	
73.8	150	245	255	310	355	453	455	525	105
71.8	150	230	250	320	370	390	450	525	
68.8	170	250	270	330	360	400	450	460	
83.8	200	220	230	300	370	395	450	510	
78.8	225	260	270	315	370	430	465	510	
73.8	155	250	260	310	360	405	455	505	90
71.8	150	240	250	305	370	420	455	500	
68.8	210	255	265	325	390	420	455	505	
83.8	425	440	450	455	470	475	510	545	
78.8	390	405	410	420	435	465	495	475	
73.8	360	370	380	410	435	455	485	530	75
71.8	350	360	370	400	430	450	475	520	
68.8	350	360	365	390	420	455	490	525	
83.8	520	535	545	555	560	570	580	595	
78.8	525	535	540	545	550	555	565	590	
73.8	500	510	525	535	545	550	565	585	60
71.8	495	505	415	435	545	550	565	580	
68.8	510	515	520	520	545	550	560	590	

Table VI.12. The Suction Pressure (P_s) at Different Nozzle Setting with Respect to the Diffuser Throat for Ejector (E12).

The Distance from the Nozzle Outlet to Diffuser Throat L (mm)	The Mass of Air Entrained by The Motive Steam m_a (kg/hr.)								Motive Steam Pressure Pm (psig.)
	1.72	6.88	8.60	15.48	22.36	27.52	34.40	43.00	
	The Suction Pressure Ps (mm Hg. Abs.)								
89.7	305	325	330	390	405	410	440	490	105
84.7	295	325	330	350	385	405	440	480	
82.7	280	325	325	350	375	385	420	465	
79.7	230	260	270	300	330	365	400	440	
76.7	310	320	330	345	375	390	430	460	
74.7	320	340	345	365	390	420	450	480	
89.7	330	350	355	390	420	435	460	505	90
84.7	305	335	345	375	405	425	450	490	
82.7	305	335	345	375	405	425	450	490	
79.7	250	340	300	330	370	405	430	465	
76.7	287	310	315	355	395	410	435	480	
74.7	325	345	350	370	400	425	450	480	
89.7	445	460	465	480	495	510	525	550	75
84.7	440	460	465	485	500	520	525	550	
82.7	430	440	445	455	470	485	500	535	
79.7	450	470	475	480	495	510	520	540	
76.7	450	465	470	475	490	500	515	540	
74.7	450	455	455	470	486	490	500	540	
89.7	555	560	565	570	575	580	590	610	60
84.7	555	560	560	560	575	570	590	605	
82.7	560	570	575	580	585	590	590	600	
79.7	570	575	580	585	590	595	600	615	
76.7	565	570	570	575	580	585	595	605	
74.7	560	565	570	575	570	590	595	605	

Table VI.13. The Suction Pressure (P_s) at Different Nozzle Setting with Respect to the Diffuser Throat for Ejector (E13).

The Distance from the Nozzle Outlet to Diffuser Throat L (mm)	The Mass of Air Entrained by The Motive Steam m_a (kg/hr.)								Motive Steam Pressure Pm (psig.)
	1.72	6.88	8.60	15.48	22.36	27.52	34.40	43.00	
	The Suction Pressure Ps (mm Hg. Abs.)								
109.7	350	365	370	390	425	455	480	515	105
104.7	300	330	340	370	400	420	460	520	
102.7	285	325	340	365	390	415	460	510	
99.7	275	305	315	355	380	400	445	500	
95.7	205	240	245	290	330	360	390	441	
91.7	200	225	230	270	303	340	382	425	
109.7	295	320	340	360	390	440	465	495	90
104.7	280	315	335	365	375	395	435	495	
102.7	270	325	330	350	375	410	455	460	
99.7	245	265	275	325	350	370	410	480	
95.7	195	325	230	270	315	333	365	427	
91.7	190	217	220	260	301	320	360	425	
109.7	355	360	365	385	435	445	465	505	75
104.7	315	340	350	375	405	430	455	490	
102.7	290	325	330	365	395	425	455	510	
99.7	280	290	295	330	365	390	425	490	
95.7	255	260	268	295	320	360	393	430	
91.7	249	255	265	295	315	348	395	448	
109.7	400	420	420	440	455	465	470	530	60
104.7	400	415	420	440	460	460	505	530	
102.7	385	415	420	430	445	460	485	530	
99.7	380	385	390	415	435	440	465	500	
95.7	365	370	375	390	460	412	438	475	
91.7	360	370	373	380	410	425	450	490	

Table VI.14. The Suction Pressure (P_s) at Different Nozzle Setting with Respect to the Diffuser Throat for Ejector (E14).

The Distance from the Nozzle Outlet to Diffuser Throat L (mm)	The Mass of Air Entrained by The Motive Steam m_a (kg/hr.)								Motive Steam Pressure Pm (psig.)
	1.72	6.88	8.60	15.48	22.36	27.52	34.40	43.00	
	The Suction Pressure P_s (mm Hg. Abs.)								
102.7	315	345	350	375	420	435	465	525	
92.7	310	325	345	370	400	430	455	495	
89.7	199	223	230	290	325	380	422	465	105
85.7	255	290	310	325	370	410	435	480	
82.7	315	330	350	365	415	420	450	540	
102.7	385	405	415	450	465	490	510	530	
92.7	365	375	385	440	455	460	490	520	
89.7	305	350	355	380	405	450	470	495	90
85.7	310	330	355	385	420	445	480	505	
82.7	340	378	380	410	435	455	490	520	
102.7	480	500	510	520	540	550	560	590	
92.7	455	475	480	495	515	530	545	565	
89.7	460	465	470	485	500	535	550	555	75
85.7	465	470	475	480	500	510	530	555	
82.7	450	455	465	480	495	520	540	555	
102.7	610	620	620	625	630	630	635	650	
92.7	590	600	605	610	610	625	640	655	
89.7	590	595	600	610	625	630	635	640	60
85.7	610	610	620	625	630	640	640	645	
82.7	620	630	630	635	635	638	640	645	

Table VI.15. The Suction Pressure (P_s) at Different Nozzle Setting with Respect to the Diffuser Throat for Ejector (E15).

The Distance from the Nozzle Outlet to Diffuser Throat L (mm)	The Mass of Air Entrained by The Motive Steam m_a (kg/hr.)								Motive Steam Pressure Pm (psig.)
	1.72	6.88	8.60	15.48	22.36	27.52	34.40	43.00	
	The Suction Pressure P_s (mm Hg. Abs.)								
97.7	320	345	365	390	422	465	490	530	105
92.7	340	350	355	390	445	455	490	545	
87.7	330	340	345	390	435	465	490	545	
86.7	140	145	150	190	250	290	330	410	
85.7	238	250	275	310	340	375	410	460	
82.7	250	285	275	325	350	375	410	480	
79.7	240	265	280	330	365	390	435	490	
97.7	368	402	410	433	455	470	508	545	90
92.7	360	390	405	425	455	470	505	535	
87.7	345	375	380	420	450	470	495	545	
86.7	360	370	370	400	415	420	430	460	
85.7	260	278	305	360	390	410	460	490	
82.7	270	330	340	365	405	420	450	500	
79.7	260	310	350	365	405	420	445	490	
97.7	460	470	475	510	515	520	540	560	75
92.7	455	460	470	485	505	525	540	560	
87.7	450	455	460	480	500	510	530	560	
86.7	480	495	500	505	515	525	535	550	
85.7	460	468	473	477	490	505	515	545	
82.7	465	465	475	480	490	470	510	540	
79.7	455	470	475	533	495	500	510	540	
97.7	558	565	570	570	578	585	595	615	60
92.7	565	565	565	573	585	590	600	615	
87.7	560	565	570	573	580	580	600	610	
86.7	560	565	570	580	590	600	610	615	
85.7	557	573	573	585	585	590	602	610	
82.7	565	570	570	580	585	590	595	605	
79.7	555	570	570	573	580	590	595	615	

Table VI.16. The Suction Pressure (P_s) at Different Nozzle Setting with Respect to the Diffuser Throat for Ejector (E16).

The Distance from the Nozzle Outlet to Diffuser Throat L (mm)	The Mass of Air Entrained by The Motive Steam m_a (kg/hr.)												Motive Steam Pressure P_m (psig.)
	0.00	1.72	6.88	8.60	15.48	17.20	22.36	27.52	34.40	43.00	49.88	58.48	
	The Suction Pressure P_s (mm Hg. Abs.)												
107.6	116	130	155	163	195	202	225	261	294	330	356	404	60
114.6	107	122	149	157	187	195	217	250	289	340	355	398	
121.6	107	122	151	159	193	199	219	250	290	329	354	396	
128.6	106	119	151	161	196	202	222	252	292	332	358	399	
135.6	96	109	149	159	194	199	218	246	289	330	353	399	
138.6	91	106	145	156	191	199	218	241	286	327	353	393	
142.6	78	94	137	149	183	192	213	233	278	318	348	382	
149.6	66	79	134	144	183	190	211	231	276	317	343	378	
156.6	61	74	114	133	176	185	204	226	263	312	336	368	
163.6	52	64	114	129	173	179	204	223	256	309	336	368	
170.6	58	73	118	137	178	185	206	226	265	313	338	370	
107.6	134	147	168	174	212	219	251	275	304	338	373	410	75
114.6	126	137	163	171	198	217	251	274	301	336	378	416	
121.6	124	138	160	166	202	212	244	270	296	333	369	409	
128.6	123	136	163	169	206	217	250	274	302	338	374	414	
135.6	113	135	161	169	206	218	251	275	302	338	375	413	
138.6	104	122	156	163	198	209	244	270	298	335	370	409	
142.6	99	116	148	157	193	198	234	262	294	329	356	398	
149.6	79	99	140	151	187	196	226	257	290	322	352	395	
156.6	69	86	123	136	176	183	208	236	276	314	340	383	
163.6	56	77	128	140	183	191	214	244	279	318	344	386	
170.6	60	83	134	145	183	191	214	241	279	317	344	385	

Table V.17. The Suction Pressure (P_s) at Different Nozzle Setting with Respect to the Diffuser Throat for Ejector (E17), at the two Motive Steam Pressure (P_m=60 and 75 psig.).

The Distance from the Nozzle Outlet to Diffuser Throat L (mm)	The Mass of Air Entrained by The Motive Steam m_a (kg/hr.)												Motive Steam Pressure P_m (psig.)
	0.00	1.72	6.88	8.60	15.48	17.20	22.36	27.52	34.40	43.00	49.88	58.48	
	The Suction Pressure P_s (mm Hg. Abs.)												
107.6	141	154	176	182	229	239	261	283	309	359	389	430	90
114.6	141	154	178	189	234	242	262	283	316	365	392	433	
121.6	136	148	161	179	229	229	256	279	308	350	383	419	
128.6	134	146	173	182	230	238	264	288	311	361	391	430	
135.6	119	138	173	183	232	242	269	290	315	365	394	443	
138.6	115	131	161	173	225	234	258	282	310	355	384	421	
142.6	108	121	151	159	206	218	249	273	299	339	374	410	
149.6	93	104	138	151	196	211	245	269	296	334	370	405	
156.6	76	93	122	131	174	184	223	251	283	318	351	391	
163.6	68	84	121	136	185	198	235	260	292	325	358	398	
170.6	73	90	131	142	185	198	231	258	289	322	356	395	
107.6	150	161	195	204	238	246	269	291	325	372	402	443	105
114.6	151	163	197	206	240	251	272	290	333	377	410	449	
121.6	143	156	185	194	231	239	262	286	314	365	394	436	
128.6	143	157	190	198	239	250	272	294	333	375	411	452	
135.6	126	141	190	199	240	249	272	295	334	375	408	451	
138.6	121	135	178	190	233	240	265	290	320	368	398	441	
142.6	112	124	154	171	219	228	252	267	306	359	388	430	
149.6	96	106	137	149	216	226	252	274	302	352	383	419	
156.6	78	94	119	129	183	196	231	256	284	331	364	403	
163.6	70	79	115	125	199	214	242	268	296	336	372	408	
170.6	76	95	126	138	193	214	242	262	292	336	368	406	

Table V.18. The Suction Pressure (P_s) at Different Nozzle Setting with Respect to the Diffuser Throat for Ejector (E17), at the two Motive Steam Pressure (P_m=90 and 105 psig.).

The Distance from the Nozzle Outlet to Diffuser Throat L (mm)	The Mass of Air Entrained by The Motive Steam m_a (kg/hr.)												Motive Steam Pressure P_m (psig.)
	0.00	1.72	6.88	8.60	15.48	17.20	22.36	27.52	34.40	43.00	49.88	58.48	
	The Suction Pressure P_s (mm Hg. Abs.)												
100.6	38	50	79	89	124	132	163	188	217	255	302	340	60
107.6	33	42	70	80	115	124	154	175	207	247	291	331	
114.6	35	47	76	86	121	129	160	185	214	252	299	337	
121.6	38	47	79	90	123	134	165	190	218	258	300	335	
128.6	38	50	85	93	130	141	171	194	218	265	305	341	
135.6	29	39	84	91	126	138	171	194	219	259	304	341	
138.6	34	47	85	94	130	140	172	194	221	263	306	341	
142.6	34	49	72	82	120	127	165	189	220	258	301	339	
149.6	43	55	90	99	139	151	179	202	229	272	314	344	
156.6	39	51	87	100	128	137	172	197	224	262	304	341	
163.6	33	41	82	88	127	130	167	192	220	259	301	338	
170.6	40	49	84	92	129	134	170	193	220	260	302	340	
100.6	41	50	77	87	136	144	164	185	215	267	304	338	75
107.6	35	45	70	75	130	138	158	175	205	257	293	331	
114.6	38	47	74	84	133	141	161	182	212	264	301	335	
121.6	38	48	75	87	140	148	166	190	218	274	307	339	
128.6	38	47	78	91	143	150	172	192	218	274	307	343	
135.6	37	50	84	94	142	151	172	194	224	279	310	343	
138.6	35	47	85	91	143	151	173	194	226	281	312	346	
142.6	31	40	68	80	131	142	168	191	220	272	306	342	
149.6	41	52	84	100	152	160	182	204	231	289	319	351	
156.6	27	36	82	94	142	151	176	199	224	280	314	344	
163.6	30	42	71	83	136	146	171	194	223	276	308	341	
170.6	32	42	79	90	141	150	175	199	224	279	312	342	

Table V.19. The Suction Pressure (P_s) at Different Nozzle Setting with Respect to the Diffuser Throat for Ejector (E18), at the two Motive Steam Pressure (P_m=60 and 75 psig.).

The Distance from the Nozzle Outlet to Diffuser Throat L (mm)	The Mass of Air Entrained by The Motive Steam m_a (kg/hr.)												Motive Steam Pressure P_m (psig.)
	0.00	1.72	6.88	8.60	15.48	17.20	22.36	27.52	34.40	43.00	49.88	58.48	
	The Suction Pressure P_s (mm Hg. Abs.)												
100.6	42	52	79	94	138	147	167	186	215	273	302	336	90
107.6	35	45	58	70	131	138	161	174	202	258	289	317	
114.6	38	48	75	90	134	143	164	182	211	269	298	332	
121.6	38	47	80	93	140	150	171	187	215	272	305	335	
128.6	38	47	84	97	145	153	171	190	230	278	306	342	
135.6	34	49	86	99	145	154	172	192	232	282	310	342	
138.6	36	48	82	96	147	154	174	194	232	285	313	345	
142.6	32	41	66	79	134	144	168	188	221	275	306	335	
149.6	37	36	85	105	156	162	182	204	241	293	320	357	
156.6	21	45	74	108	150	157	178	199	236	287	314	344	
163.6	28	28	65	75	144	152	174	194	224	281	310	342	
170.6	27	36	64	82	148	154	179	199	230	283	314	344	
100.6	46	57	87	98	138	144	168	188	224	272	299	337	105
107.6	35	40	60	75	121	131	154	174	207	251	282	317	
114.6	39	50	80	91	131	137	161	181	217	265	292	330	
121.6	42	53	86	95	138	145	170	187	230	274	304	345	
128.6	39	50	87	96	139	148	171	191	234	275	306	352	
135.6	35	50	90	99	143	151	173	194	234	278	309	349	
138.6	36	49	84	96	145	152	175	199	240	285	312	351	
142.6	33	47	79	92	134	145	171	190	231	275	306	340	
149.6	37	45	88	105	153	161	183	204	248	290	320	360	
156.6	18	25	81	95	148	158	180	200	243	288	313	355	
163.6	28	35	69	79	142	148	175	195	233	282	310	344	
170.6	23	29	75	88	149	159	179	200	240	285	315	352	

Table V.20. The Suction Pressure (P_s) at Different Nozzle Setting with Respect to the Diffuser Throat for Ejector (E18), at the two Motive Steam Pressure (P_m=90 and 105 psig.).

The Distance from the Nozzle Outlet to Diffuser Throat L (mm)	The Mass of Air Entrained by The Motive Steam m_a (kg/hr.)												Motive Steam Pressure P_m (psig.)
	0.00	1.72	6.88	8.60	15.48	17.20	22.36	27.52	34.40	43.00	49.88	58.48	
	The Suction Pressure P_s (mm Hg. Abs.)												
107.6	45	56	83	90	135	146	175	197	228	276	304	337	60
114.6	44	54	85	92	139	148	179	198	228	283	304	335	
121.6	46	57	86	96	138	148	185	206	237	279	304	341	
128.6	57	68	98	106	158	168	192	214	244	281	307	333	
135.6	53	68	105	118	173	180	204	224	254	275	299	330	
138.6	52	61	94	105	162	171	196	216	245	278	303	334	
142.6	47	58	93	99	156	164	191	211	239	276	311	338	
149.6	58	68	110	127	176	183	206	228	253	289	313	342	
156.6	64	82	114	121	175	184	205	225	252	290	311	338	
163.6	46	59	96	106	158	168	194	215	242	285	300	333	
170.6	51	62	98	108	158	168	194	215	239	280	299	333	
107.6	46	56	86	93	139	146	168	193	225	292	314	342	75
114.6	49	63	93	103	144	152	176	200	238	286	308	342	
121.6	45	55	98	108	148	157	187	206	236	294	320	344	
128.6	64	73	116	127	160	168	195	219	260	306	335	348	
135.6	54	74	124	136	177	184	211	235	276	317	333	365	
138.6	54	64	111	122	163	172	199	221	264	311	324	352	
142.6	52	61	98	116	158	166	196	216	256	304	319	348	
149.6	59	75	127	138	179	189	211	234	275	318	328	358	
156.6	39	51	132	143	184	191	214	234	274	306	331	353	
163.6	46	55	94	119	167	176	199	221	254	306	319	352	
170.6	59	71	96	117	166	176	199	219	254	304	318	351	

Table V.21. The Suction Pressure (P_s) at Different Nozzle Setting with Respect to the Diffuser Throat for Ejector (E19), at the two Motive Steam Pressure (P_m=60 and 75 psig.).

The Distance from the Nozzle Outlet to Diffuser Throat L (mm)	The Mass of Air Entrained by The Motive Steam m_a (kg/hr.)												Motive Steam Pressure P_m (psig.)
	0.00	1.72	6.88	8.60	15.48	17.20	22.36	27.52	34.40	43.00	49.88	58.48	
	The Suction Pressure P_s (mm Hg. Abs.)												
107.6	47	58	90	103	138	145	167	189	236	281	308	348	90
114.6	52	65	100	108	145	163	170	198	248	288	319	353	
121.6	53	67	101	109	151	159	181	209	260	301	329	368	
128.6	74	88	123	132	167	172	196	229	268	310	337	381	
135.6	64	86	133	139	173	183	216	250	283	322	349	381	
138.6	59	74	111	122	161	169	197	232	273	311	336	371	
142.6	54	69	105	117	158	164	191	222	267	310	336	375	
149.6	75	97	134	142	173	183	214	248	282	316	345	376	
156.6	35	46	142	151	184	194	218	254	289	325	351	382	
163.6	37	50	114	134	165	175	201	226	270	309	336	374	
170.6	65	79	114	130	167	176	198	224	271	311	334	371	
107.6	54	65	102	110	145	152	176	202	249	291	314	365	105
114.6	55	66	98	107	141	148	173	199	241	285	309	360	
121.6	56	68	100	110	146	154	188	214	255	296	325	374	
128.6	86	94	126	134	169	179	211	239	274	310	346	386	
135.6	68	82	116	131	177	191	226	255	286	323	358	399	
138.6	70	82	114	125	162	173	207	244	278	315	353	395	
142.6	60	74	105	116	158	166	196	234	273	308	338	384	
149.6	78	100	117	129	174	181	218	255	286	322	355	396	
156.6	51	63	142	155	188	197	236	266	295	331	362	403	
163.6	52	65	103	117	167	175	199	244	279	315	339	390	
170.6	66	78	107	121	169	177	204	244	277	315	339	383	

Table V.22. The Suction Pressure (P_s) at Different Nozzle Setting with Respect to the Diffuser Throat for Ejector (E19), at the two Motive Steam Pressure (P_m=90 and 105 psig.).

The Distance from the Nozzle Outlet to Diffuser Throat L (mm)	The Mass of Air Entrained by The Motive Steam m_a (kg/hr.)												Motive Steam Pressure P_m (psig.)
	0.00	1.72	6.88	8.60	15.48	17.20	22.36	27.52	34.40	43.00	49.88	58.48	
	The Suction Pressure P_s (mm Hg. Abs.)												
114.6	105	126	159	168	203	212	235	257	299	344	371	407	60
121.6	80	91	123	134	174	183	207	227	260	308	340	371	
128.6	73	88	107	117	165	172	195	215	244	295	325	359	
135.6	77	87	113	121	163	170	197	217	242	295	322	356	
138.6	78	90	115	120	166	174	196	217	243	297	323	357	
142.6	80	93	120	130	168	174	196	215	245	298	322	356	
149.6	78	89	114	120	162	169	194	214	242	295	322	358	
156.6	72	83	103	116	160	168	194	213	241	293	320	356	
163.6	82	94	118	122	164	175	198	216	242	298	323	358	
170.6	69	81	105	114	156	164	187	208	235	282	315	349	
114.6	128	147	173	182	214	223	250	281	316	355	382	425	75
121.6	84	104	137	145	182	187	211	242	279	316	344	384	
128.6	83	93	128	138	171	180	203	225	265	305	331	373	
135.6	82	98	132	143	175	181	202	226	265	307	333	363	
138.6	87	100	138	147	178	183	203	228	269	309	334	370	
142.6	82	100	138	146	175	182	202	225	265	306	333	368	
149.6	88	101	135	145	178	182	202	222	269	308	333	362	
156.6	78	91	123	134	170	178	199	220	260	303	329	360	
163.6	88	100	135	143	179	183	205	222	265	309	335	367	
170.6	70	82	109	120	164	170	192	211	240	292	319	351	

Table V.23. The Suction Pressure (P_s) at Different Nozzle Setting with Respect to the Diffuser Throat for Ejector (E20), at the two Motive Steam Pressure (P_m=60 and 75 psig.).

The Distance from the Nozzle Outlet to Diffuser Throat L (mm)	The Mass of Air Entrained by The Motive Steam m_a (kg/hr.)												Motive Steam Pressure P_m (psig.)
	0.00	1.72	6.88	8.60	15.48	17.20	22.36	27.52	34.40	43.00	49.88	58.48	
	The Suction Pressure P_s (mm Hg. Abs.)												
114.6	145	163	185	195	229	242	268	298	328	369	405	443	90
121.6	105	122	147	155	185	195	225	255	285	322	351	395	
128.6	105	121	143	149	178	188	214	243	275	309	343	383	
135.6	102	121	146	152	182	190	210	242	278	314	338	380	
138.6	108	122	143	154	183	190	212	245	279	315	342	386	
142.6	116	124	148	156	182	188	214	243	275	313	340	381	
149.6	105	120	148	157	182	190	211	240	276	314	338	382	
156.6	83	108	135	143	177	182	206	238	272	312	337	380	
163.6	95	112	139	148	179	185	206	233	269	308	335	376	
170.6	71	87	123	134	167	174	195	217	257	297	322	360	
114.6	160	172	199	209	250	260	287	308	339	386	422	462	105
121.6	121	131	156	164	193	203	233	262	289	326	364	404	
128.6	119	128	149	156	187	198	227	251	275	312	350	388	
135.6	109	128	153	158	188	198	224	254	282	318	353	392	
138.6	120	135	155	162	193	204	235	257	286	319	357	395	
142.6	120	132	153	160	188	203	233	255	282	317	354	400	
149.6	120	129	153	159	188	200	229	252	280	315	348	388	
156.6	101	118	142	150	182	193	222	250	282	315	350	392	
163.6	108	122	145	155	184	189	220	248	280	313	348	387	
170.6	82	100	128	137	166	171	195	222	257	295	318	363	

Table V.24. The Suction Pressure (P_s) at Different Nozzle Setting with Respect to the Diffuser Throat for Ejector (E20), at the two Motive Steam Pressure (P_m=90 and 105 psig.).

APPENDIX VII

AN EQUATION FOR THE PREDICTION OF STEAM FLOWRATE REQUIRED IN THE DESIGN OF EJECTORS

Peter Rice and Jaber Dandachi
Loughborough University of Technology, Loughborough

INTRODUCTION

In the design of steam ejectors entraining ambient air, the steam required for a given suction load will depend on the steam pressure, the suction pressure and the discharge pressure.

HEI standards for ejectors[1] give methods for correcting for entrained fluids, other than air, as equivalent air flow. Also, they give methods, for making corrections for temperatures other than ambient.

Estimation of the steam required relies on data gathered from previous experience or experiment. This is, usually, commercially confidencial information and is not openly available. However, Vil'der[2], based upon Russian experience, provides a graph giving the steam required in the form of an injection coefficient U against expansion ratio E and compression ratio C such that :

$$U = \frac{m_a}{m_m} \quad ; \quad E = \frac{P_m}{P_s} \quad \text{and} \quad C = \frac{P_d}{P_s}$$

The theory we present leads to an equation which relates U to E and C. Due to friction and mixing losses which can not be estimated there are still constants which need to be found. This has been done with data extracted from the graph Vil'der[2] presents using a standard NAG library curve fitting routine.

We present an example of an ejector, designed using this equation to estimate the steam required and, for comparison, the experimental results obtained when the ejector was tested over a range of air loads.

THEORY

We consider an ejector in which steam is the motive fluid and air, at ambient temperature, is the entrained fluid. If we assume constant pressure mixing as the most effective as proposed by Keenan et al[3], a simple momentum balance gives :

$$(m_a + f_1 m_m) V_d = f_2 (m_m V_m)$$

where the contribution to the momentum of the entrained flow at inlet is small in comparison to the steam momentum and is ignored. The flowrate at the outlet of the nozzle is some fraction f_1 of the steam flowrate at inlet to the nozzle and represents the 'loss' due to condensation, as the flow in the nozzle is considered isentropic. f_2 is some fraction (of the steam nozzle outlet momentum) and represents losses due to condensation, mixing and friction.

Rearranging

$$\frac{m_a}{m_m} + f_1 = f_2\left[\frac{V_m}{V_d}\right]$$

so that :

$$U = \frac{m_a}{m_m} = f_2\left[\frac{V_m}{V_d}\right] - f_1 \qquad (1)$$

We assume the steam nozzle is supersonic. Likewise, we treat mixing tube and diffuser as a supersonic diffuser, Dowson[4]. We can write using compressible flow equations, Cheers[5], for the steam nozzle, putting

$$Y_m = \frac{\gamma_m - 1}{\gamma_m}$$

$$V_m = \sqrt{\frac{2}{Y_m}\left(\frac{P_m}{\rho_m}\right)\left[1 - \left(\frac{P_m}{P_s}\right)^{-Y_m}\right]}$$

where the steam velocity prior to the steam nozzle is negligibly small.

For the mixing tube, putting

$$Y_d = \frac{\gamma_d - 1}{\gamma_d}$$

$$V_d = \sqrt{\frac{2}{Y_d}\left(\frac{P_d}{\rho_d}\right)\left[1 - \left(\frac{P_d}{P_s}\right)^{-Y_d}\right]}$$

Again, we have assumed the steam air discharge velocity is small in comparison with the supersonic velocity in the mixing tube and can be ignored. Over a large range of values P/ρ varies very little, 1.95 to 2.0 for steam over a pressure range of 6 bar to 14 bars. Also, we assume $(\gamma_m - 1/\gamma_m)$ and $(\gamma_d - 1/\gamma_d)$ are constant so that :

$$V_m = \sqrt{K\left[1 - \left(\frac{P_m}{P_s}\right)^K\right]} = \sqrt{K(1 - E^K)}$$

and

$$V_d = \sqrt{K\left[1 - \left(\frac{P_d}{P_s}\right)^K\right]} = \sqrt{K(1 - C^K)}$$

where K's represents various constants.

Substituting for V_m and V_d in equation (1) we get :

$$U = f_2\sqrt{\frac{K(1 - E^K)}{K(1 - C^K)}} - f_1$$

or

$$U = K\sqrt{\frac{1 - E^K}{1 - C^K}} - K$$

again K's are various constants.

Numbering the K's we can write this as :

$$U = K_1 \sqrt{\frac{1 - E^{K_2}}{1 - C^{K_3}}} - K_4 \qquad (2)$$

The constants K_1 to K_4 have to be found.

Using 107 data points extracted from Vil'der's[2] graph covering the complete range of variables [E, 10-4000 and C, 1.4-10 giving U 0.04-2.0] and using the multi regression NAG routine E04 FDF the constants K_1 to K_4 have been evaluated. The routine is a least square fit and minimises the error $(U_a - U_{pred})$.

To obtain a better fit, since fitting extra constants entails no extra work, we have written, also,

$$U = K_1 \sqrt{\frac{K_2 - E^{K_3}}{K_4 - C^{K_5}}} - K_6 \qquad (3)$$

and proceeded as above.

RESULTS

The constants obtained from the curve fitting routine are :

Equation (2)	Equation (3)
K_1=2.2062	K_1=1.9539
K_2=-0.356	K_2=0.9825
K_3=-0.5886	K_3=-0.3154
K_4=2.2173	K_4=0.9694

K_5=-0.57

K_6=1.914

RMS=0.096 RMS=0.028

where RMS is defined as :

$$RMS = \sqrt{\frac{\sum_{1}^{N}(U_a - U_{pred})^2}{N}}$$

so that the injection coefficient U is :

$$U = 2.2062 \sqrt{\frac{1 - E^{-0.356}}{1 - C^{-0.5886}}} - 2.2173 \qquad (4)$$

or

$$U = 1.9539 \sqrt{\frac{0.9825 - E^{-0.3154}}{0.9694 - C^{-0.57}}} - 1.914 \qquad (5)$$

DISCUSSION

The indices of E and C are both negative and fractional corresponding to $-(\gamma-1/\gamma)$ but greater than the values expected for steam or air i.e. 0.2 and 0.29 respectively. This is due in part to the equations used for compressible flow applying to an ideal gas which cools when it expands. With steam, however as already noted, condensation occurs in the nozzle with the production of a water mist which then evaporates in the mixing tube on compression i.e. the mass flow of steam is continually changing. We note how equation (4) and (5) are very similar.

In fig.1 the 107 data points are shown compared to the equation (5). The excellent fit justifies, also, the square root predicted from the analysis.

A DESIGN EXAMPLE

As a demonstration of the application of the equation we present an ejector design and the results from testing an ejector fabricated to the calculated values.

The ejector was required to handle an air load of 10 kg/hr at a suction pressure of 13.54 kPa abs using dry or slightly saturated steam at 6.8 bar (100 psig).

An outlet pressure from the ejector of 1.02 bar was assumed to allow for back pressure due to an outlet condenser or ducting pressure loss.

We have then : E = 58.4 and C = 7.64. From equation (5) U=0.113 so that the steam flowrate is 10/0.113=88.7 kg/hr.

This gives a steam nozzle throat diameter of 5.4 mm and a steam outlet diameter of 15.8 mm, to give slight underexpansion, Vil'der[2]. The mixing tube throat diameter was then calculated as 15.6 mm.

The mixing tube was made with axial dimensions of 92 mm inlet converging, 61 mm parallel throat and 92 mm outlet diverging

sections i.e. 6D, 4D, 6D where D is the mixing tube throat diameter[6]. The inlet converging angle is 7.2° and the outlet diverging angle is 12.2°.

The steam nozzle and mixing tube were turned from steel bar and then assembled in the cross arm of a 50.8 mm (2") standard steam pipe 'T' to form the ejector. All the calculations were made using a computer program[7].

RESULTS AND DISCUSSION

The experimental results for the ejector are presented in fig.2. The slightly better than required performance must be due to the curves in Vil'der[2] being liberal in their estimation. Note, however, the 'break point' (loss of vacuum) is only just beyond 10 kg/hr.

However, it is our experience that industrial users are happy if the ejector gives the design performance (or slightly better) in contrast to if it does not meet performance figures causing delay and loss of production.

CONCLUDING REMARKS

The equation can be used in multi-stage ejector design. For instance, in a two stage ejector after the choice of a suitable intermediate pressure (P_i say) then each stage can be treated independently so that for the first stage $E=P_m/P_s$, $C=P_i/P_s$ and for the second stage $E=P_m/P_i$, $C=P_d/P_i$.

The load to the second stage will be the sum of the ejector load plus the steam to the first stage if the ejector set has no interstage condenser. However if an intercondenser is fitted the load to the second stage will be the non condensables plus vapour carryover calculated using Dalton's law at the temperature of the load. This temperature is typically 3-5°C above the cooling water inlet temperature when operating in counter current mode.

A good starting value for P_i is

$$P_i = \sqrt{P_s P_d} \qquad \text{for a two stage ejector}$$

and

$$P_{i_1} = \sqrt{P_s^2 P_d} \quad \text{and} \quad P_{i_2} = \sqrt{P_i P_d^2} \quad \text{for a three stage ejector}$$

and so on for more stages.

This means that C is the same for all stages. Note, however, that the steam has more effect expanding to the lower pressures.

NOMENCLATURE

C	Ratio of discharge to suction pressure
E	Ratio of steam to suction pressure
f_1	Fraction loss of momentum due to condensation, mixing etc.
f_2	Fraction 'loss' of steam flowrate
K	Constant
m_a	Suction load mass flowrate
m_m	Motive steam flowrate

N Number of data points

P_d Steam air mixture discharge pressure

P_m Motive steam pressure

P_s Suction pressure

U Injection coefficient - ratio of suction to motive steam flowrates (suffix a is actual; suffix pred is predicted)

V_d Velocity of steam air mixture in mixing tube

V_m Velocity of steam at nozzle outlet

Y_d $(\gamma_d - 1)/\gamma_d$

Y_m $(\gamma_m - 1)/\gamma_m$

γ_d Ratio of specific heats steam air mixture

γ_m Ratio of specific heats steam

ρ_d Density of steam air mixture

ρ_m Density of steam

REFERENCES

1. "Standards for steam jet ejectors", 1956, 3rd edition, Heat Exchanger Institute, New York.

2. Vil'der S. I. , 1964, Int. Chem Engg., 4, 88.

3. Keenan J. H., E. P. Neumann and F. Lustwerk, 1950, J. of App. Mech., 17, 299.

4. Dowson R., 1937, The Engineer, Dec. 650 and 680.

5. Cheers F., 1963, Elements of Compressible Flow, J. Wiley and Sons, London.

6. Shklover G. G., A. Z. Rosenskii and A. V. Gerasinov, 1966, Teplioenergetika, 13, 42.

7. Beresford R. H. and P. Rice, 1983, Inst. Chem. Engrs. Conference, Manchester, Paper 1.3.1.

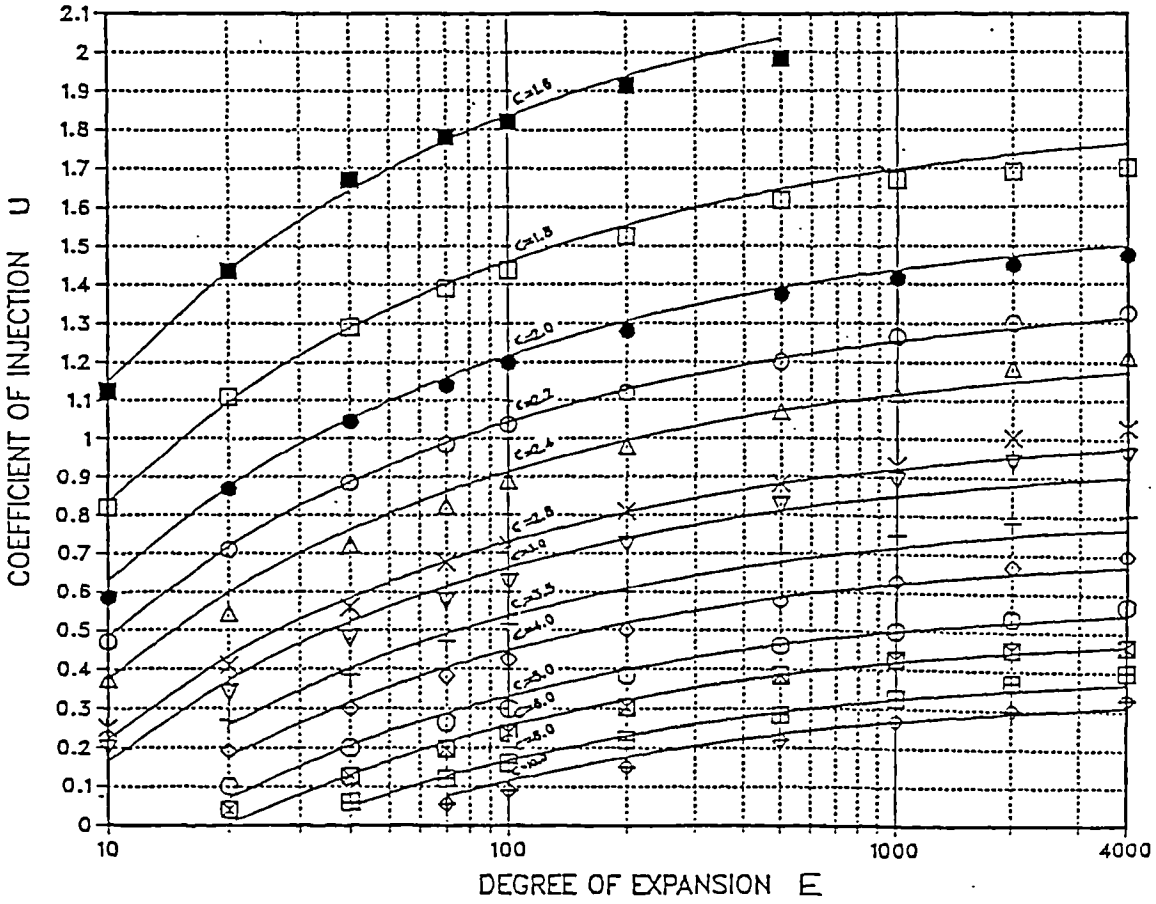

Figure VII.1. Comparison of derived equation with data from ref.1.

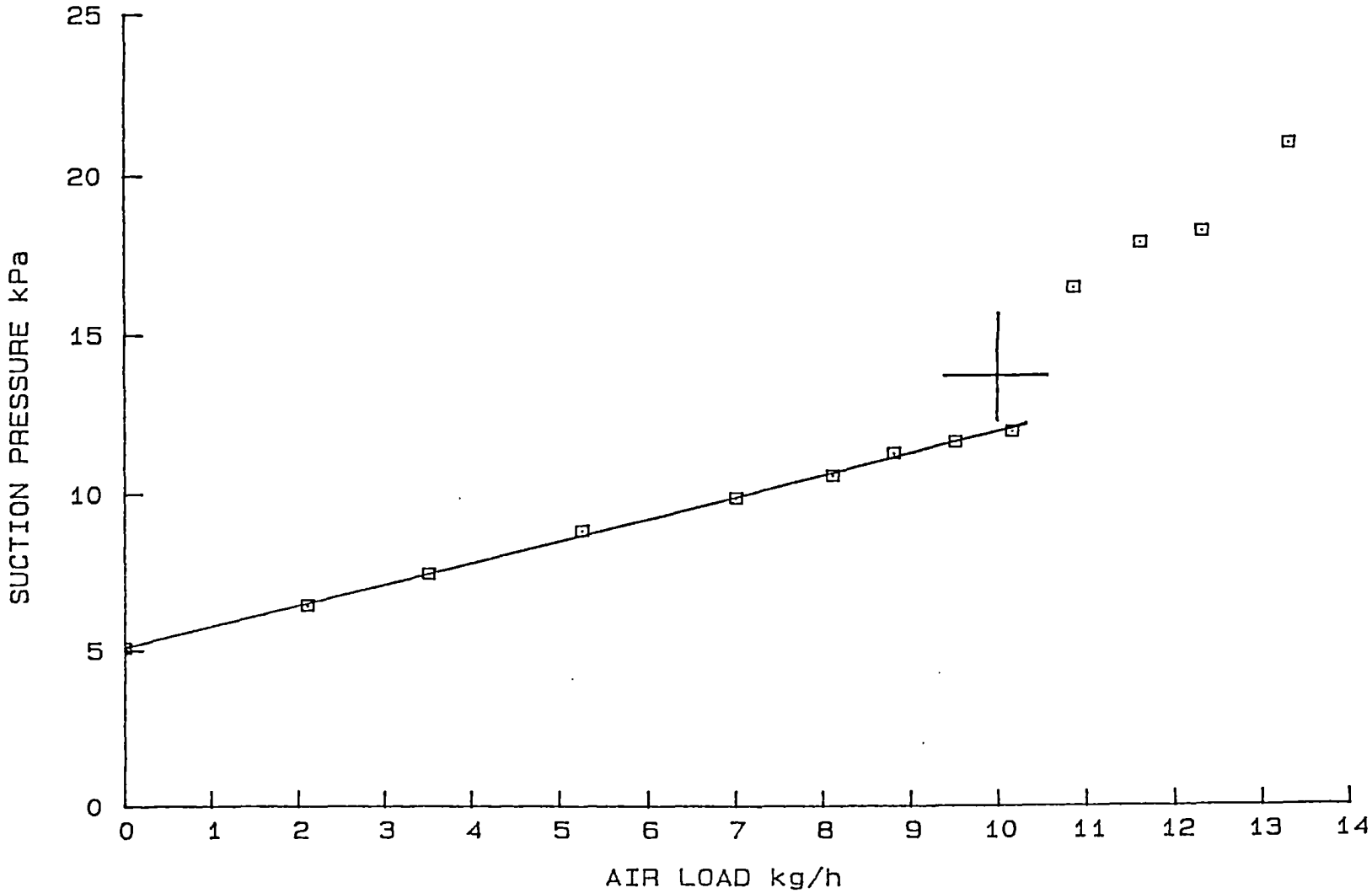

Figure VII.2. Performance of the ejector given as an example of the use of the derived equation.

LIST OF REFERENCES

- Antsupov A. V., Properties of Underexpanded and Overexpanded Supersonic Gas Jets, Sov. Phys. Tech. Phys., (August 1974), Vol. 19, No. 2, 234-238.

- Abramovich G. N., The Theory of Turbulent Jets, The Massachusetts Institute of Technology, 1963.

- Adamson T. C. and Nicholls J. A., On the Structure of Jets from Highly Underexpanded NOzzles into Still Air, Journal of the Aero/Space Sciences, (January 1959), 16-24.

- Barrere M., Rocket Propulsion, Elsevier Publishing Company, 1960.

- Benson R. S. and Eustace V. A., A Study of Two-Dimensional Supersonic Air Ejector Systems, Proc. Instn. of Mech. Engrs., (1973), Vol. 187 60/73, 733-743.

- Che^-haing Chiang, Axially Symmetric Supersonic Turbulent Jets Discharged from a Nozzle with Underexpansion, Turbulent Jets of Air, Plasms, and Real Gases (Edited by G. N. Abramovich), (1968), Consultants Bureau, NewYork,111-137.

- Chow W. L. and Addy A. L., Interaction between Primary and Secondary Streams of Supersonic Ejector Systems and their Performance Characteristics, A.I.A.A., (April 1964), Vol. 2, No. 4.

- Cunningham R. G., Jet-Pump Theory and Performance with Fluids of High Viscosity, Transactions of the ASME, (November 1957), 1807-1820.

- Dowson R., Performance of Single-Stage Steam Jet Operated Ejectors, The Engineer, (10 December 1937), No. 1, 650-652.

- Dowson R., Performance of Single-Stage Steam Jet Operated Ejectors, The Engineer, (17 December 1937), No. 2, 680-681.

_ Dutton J. C. and Carroll B. F., Limitation of Ejector Performance Due to Exit Chocking, Journal of Fluids Engineering, (March 1988), Vol. 110, 91-93.

_ Engdahl R. B. and Holton W. C., Overfire Air Jets, Transactions of the ASME, Vol. 65,(1943), 741-754.

_ ESDU, Ejectors and Jet Pumps Design for Steam Driven Flow, (November 1986), Item Number 86030.

_ Eastop T. D. and McConkey A., Applied Thermodynamics for Engineering Technologists, 1981, Longman Group Limited.

_ Frumerman R., Steam Jet Ejectors, Chemical Engineering, (June 1956), 196-201.

_ Harris L. S. and Fischer A. S., Characteristics of the Steam-Jet Vacuum Pump, Transactions of the ASME, (November 1964), Vol. 84, Series B, 358-364.

_ Heat Exchanger Institute, Standards for Steam Jet Ejectors, Third Edition, New York, 1967.

_ Hickman K. E. et al, Analysis and Testing of High Entrainement Single-Nozzle Jet Pump with Variable-Area Mixing Tube, NASA CR-2067, (June 1972).

_ Irvine T. F. and Liley P. E., Steam & Gas Tables with Computer Equations, 1983.

_ Johannesen N. H., Ejector Theory and Experiments, Danish Accademic of Tech. Sci., Transactions of the ATS, (1951), No. 1, Copenhagen.

_ Kastner L. J. and Spooner J. R., An Investigation of the Performance and Design of the Air Ejector Employing Low-Pressure Air as the Driving Fluid, Proc. of the Inst. of Mech. Eng., (1950), Vol. 162, 149-159.

_ Keenan J. H. et al, An Investigation of Ejector Design by Analysis and Experiment, Transactions of the ASME, J. APP. MECH.,(1950), Vol. 72, 299-309.

_ Keenan J. H. and Neumann E. P., A Simple Air Ejector, Journal of Applied Mechanics, (June 1942), A75-A81.

_ Keown J. E., Letters to the Editor, The Engineer, (31 December 1937), 747.

_ Kroll A. E., The Design of Jet Pumps, Chemical Engineering Progress, (February 1947), Vol. 1, No. 2, 21-24.

_ Kuznestor Yu. M. and Uspenskii V. A., Selection of the Axial Dimensions of Steam Jet Ejector, Izo. Uyss. Ucheb. Energ., (March 1967), Vol. 10, No. 3, 110-113, (In Russian).

_ Love E. S. et al, Experimental and Theoretical Studies of Axisymmetric Free Jets, NASA Tech. Report, (1959), R-6.

_ Medici M., The Design of Jet Ejectors, Abriged Translation Engrs., (February 1953), Dig. 14, No. 2, 51-53.

_ Mellanby A. L., Fluid Jets and their Practical Applications, Transactions- Institution of Chemical Engineers, (October 1928), 66-84.

_ Matsuo K. et al, Studies of Condensation Shock Waves, (Part 1, Mechanism of their Formation), Bulletin of JSME, (July 1985), Vol. 28, No. 241, 1416-1422.

_ Matsuo K. et al, Studies of Condensation Shock Waves, (2nd Report, Relation between Condensation Shock Wave and Condensation Zone), Bulletin of JSME, (February 1986), Vol. 29, No. 248, 1416-1422.

_ Plapp J. E., Engineering Fluid Mechanics, 1968, Prentice-Hall International.

_ Power R. B., Steam Jet Air Ejectors : Specification, Evaluation, and Operation, An ASME, Paper No. (63-WA-143), (1964).

_ Prandtl M., Fluid Dynamics, (1952), Blakie.

_ Putilov M. I., Calculating the Optimal Distance of the Nozzle from the Mixing Chamber in Injectors, Thermal Engineering, (1967(a)), Vol. 14(b), No. 7, 94-101.

_ Putilov M. I., Selecting the Distance between the Nozzle and the Mixing Chamber of Ejectors, Thermal Engineering, (1967(b)), Vol. 14(b), No. 12, 92-95.

_ Ramskill P. K., A Study of Axisymmetric Underexpanded Gas Jets, United Kingdom Atomic Energy Authority, (March 1985), SRD-R-302.

_ Robozev A. H., Applications of Nomograms for Circulation of Multi-Stage Ejectors, Energomashinostroe, (1965), Vol. 8, 21-26.

_ Rogers G. F. C. and Mayhew Y. R., Thermodynamics and Transport Properties of Fluids, 1983, Basil Blackwell.

_ Royds R. and Johnson E., The Fundamental Principles of the Steam Ejector, Inst. Mech. Eng. Proc., (1941), Vol. 145, 193-209.

_ Saad M. A., Compressible Fluid Flow, (1985), Prentice-Hall, Inc.

_ Sokolov E. Ya., Ibid, (1948), No. 11.

_ Shapiro A. H., The Dynamics and Thermodynamics of Compressible FLuid Flow, (1953), Vol. 1, The Ronald Press Company.

_ Shapiro A. H. and Hawthorne W. R., The Mechanics and Thermodynamics of Steady One-Dimensional Gas Flow, Journal of Applied Mechanics, (December 1947), A317-A336.

- Shklover G. C. et al, Dimensionless Characteristics of KTZ Steam-Jet Ejectors, Thermal Engineering, (1966), Vol. 13, No. 3, 54-61.

- Third A. D., The Air Ejector, Journal of the Royal Tech. College, (December 1927), 84-103.

- Vil'der S. I., A Simplified Method of Calculating Steam-Jet Ejector Vacuum Pumps, International Chemical Engineering, (January 1964), Vol. 4, No. 1, 88-92.

- Watanabe I, Experimental Investigation Concerning Pneumatic Ejectors, with Special Reference to the Effect of Dimensional Parameters on Performance Characteristics, Symposium on Jet Pumps and Ejectors, (November 1972), No. 7, 97-120.

- Watson F. R. B., The Production of a Vacuum in an Air Tank by Means of a Steam Jet, Inst. Mech. Eng. Proc., (1933), Vol. 124, 231-300.

- Zinger N. M., Calculation of Steam Jet Ejectors for Vacuum Deaerators, Thermal Engineering, (1968), Vol. 15, No. 2, 125-129.